THE UNIVERSITY
of EDINBURGH

The role of endothelin-1 in the renal handling of salt in early Type 1 diabetes mellitus

Geoff J. Culshaw

Submitted for the degree of Doctor of Philosophy

The University of Edinburgh 2018

Declaration

I declare that this thesis is solely my own work. It has not been submitted, in whole or in part, in any previous application for a degree. Except where stated otherwise by reference or acknowledgement, the work presented is entirely my own.

Acknowledgements

I wish to thank my supervisors Professor David J. Webb, Dr. Patrick W. F. Hadoke and Professor Matthew A. Bailey, all of whom have displayed an immense degree of tolerance and patience. David afforded me the opportunity to begin my PhD studies, and has guided me through a rigorous but fair overhaul of my critical thinking. His ability to pull out the key features from a sea of data is outstanding and inspiring. Paddy has instilled in me a scientific, methodical approach based on answering key questions, and he has tutored me extensively on how to present my data. Matt's enthusiasm for data acquisition and analysis has been infectious. He has taught me the finer points of renal physiology, and his friendly, approachable demeanour has helped me through the darkest times.

I wish to thank Professor Jeremy Hughes for allowing me to operate under his Project Licence and Dr. Bryan Conway for his help in establishing a rat model of early Type 1 diabetes mellitus. Both are nephrologists and have been very friendly towards this veterinary cardiologist.

I have benefitted from technical assistance provided by Gill Brooker who helped me hone my surgical skills, and Dave Binnie whose rat husbandry skills were outstanding. Dave also assisted in the blinding process and performed some of the urinary assays. Carolynn Cairns patiently taught me qPCR while Neil Johnston helped establish me within the laboratory and provided technical assistance with laboratory equipment.

I must acknowledge my clinical colleagues in the Cardiopulmonary Service of the Royal (Dick) School of Veterinary Studies, Professor Brendan Corcoran and Yolanda Martinez, because they have taken on additional clinical and administrative roles during my absence from clinics.

Pilot data for this study was possible through funding from the Moray Endowment Fund of The University of Edinburgh, and The Roslin Institute. All other funding for this study has been through a research project grant (RP2/2014) from Kidney Research UK, who have been flexible in their deadlines and have generously accommodated requests to meet unforeseen costs. All work was performed in facilities funded by the British Heart Foundation Centre of Research Excellence (RE/08/001/23904). Endothelin receptor antagonists were kindly donated by AbbVie Ltd.

Finally, I wish to thank my wife, Katrina, and my son, James, who have given me the love, patience and understanding to see me through one of the most challenging periods of my life. I could not have done this without you.

Abstract

Tight control of blood glucose and blood pressure (BP) reduces cardiovascular risk in early Type 1 diabetes mellitus (T1DM). Increased BP normally increases renal medullary perfusion and sodium excretion. This is called acute pressure natriuresis. Inadequate acute pressure natriuresis disrupts circadian regulation of BP, which predicts hypertension. The peptide, endothelin-1 (ET-1), regulates BP via ET_A and ET_B receptors. ET_A receptor antagonists reduce BP and restore its circadian rhythm. Two hypotheses were investigated. First, that acute pressure natriuresis is impaired in early T1DM, prior to established nephropathy, and this is associated with elevated BP. Second, that the mechanism is an ET_A receptor-mediated blunting of medullary perfusion which can be reversed with insulin and ET_A receptor antagonism.

Experimental acute pressure natriuresis was induced in young, early T1DM (2-3 weeks post streptozotocin) Sprague Dawley rats and healthy controls. Despite maintaining glomerular filtration rate, early T1DM suppressed urinary flow (UV, 22.9±2.9 v. 93.7±11.1µl/min/gkw) and sodium excretion (UNaV, 3.2±0.7 v. 22.7±3.3µmol/min/gkw) rates by >80%, and reduced gradients of pressure diuresis (linear, 1.9 to 0.3) and natriuresis (non-linear k, 0.05 to 0.01) curves. Insulin treatment lowered blood glucose (16.8±1.8 to 9.3±0.6mmol/l) and restored gradients of the responses. Tissue and urine analyses did not suggest structural nephropathy.

In early T1DM rats, changes in BP on radiotelemetry were consistent with impaired circadian regulation of BP and precursors of hypertension: 24–hour diastolic BP rose

(92.3±0.4 to 97.1±0.5mmHg), and the circadian dip in diastolic BP fell (6±1 to 2±1%). Atrasentan (ET_A receptor antagonist, 5mg/kg/day orally) reduced diastolic dipping in early T1DM (3±1 to 1±1%) while additional ET_B receptor antagonism (A-192621, 10mg/kg/day orally) reversed this, suggesting that ET_A, and not ET_B receptors, mediate impairment of acute pressure natriuresis. To address this, renal blood flow was measured during experimental acute pressure natriuresis and ET receptor antagonism. Early T1DM suppressed the normal rise in medullary perfusion (flux, 227.2±26.7 v. 115.4±10.3%) by ~90%. Suppressed medullary flux was unaffected by insulin (112.2±6.8%), despite restoration of UV and UNaV. In controls, atrasentan reduced UV (15.7±4.9 v. 38.6±6.2µl/min/gkw), UNaV (1.7±0.5 v. 16.7±1.4µmol/min/gkw), FENa (3.4±1.4 v. 15.0±2.4%) and medullary flux (122.2±26.7%) by 60 to 90% of control values, while A-192621 increased UNaV (26.6±6.9µmol/min/gkw) and FENa (21.6±3.4%), but not medullary flux, by ~50%. ET receptor antagonism did not modify early T1DM+/-insulin effects. Diabetic status had no effect on renal ET-1 and ET receptor expression.

These results support the first hypothesis but disprove the second. Early T1DM blunts medullary perfusion and acute pressure natriuresis, and increases diastolic BP. Insulin restores natriuresis but not medullary flow. Therefore, targeting medullary perfusion may reduce cardiovascular risk in early T1DM, but this is not achievable with selective ET_A receptor antagonists. Novel natriuretic (ET_A) and anti-natriuretic (ET_B) roles for ET receptors, which are not apparent in early T1DM during severe, experimental rises in BP, appear to contribute to daily regulation of BP, and may preclude the use of selective ET_A receptor antagonists in T1DM prior to nephropathy.

Lay summary

People with Type 1 diabetes (high blood sugar due to lack of insulin) have a higher risk of cardiovascular disease such as heart attacks, stroke and kidney failure, even when their blood glucose is lowered with insulin. Cardiovascular risk can be monitored by measuring blood pressure (BP), which is regulated by the kidneys. It is thought that high BP, especially at night, indicates greater cardiovascular risk, and results from reduced blood flow through the kidneys causing sodium and water retention. A new class of medicine, called endothelin A (ET_A) blockers, can correct abnormal BP and reduce kidney damage. These effects are countered by ET_B blockers. So, this thesis investigated whether rats with diabetes retain salt and water because of abnormal kidney blood flow, and also whether ET_A blockers and insulin, but not ET_B blockers, can reverse these effects and restore normal BP.

BP in experimental rats was artificially increased by tying major abdominal arteries using a technique that had been perfected beforehand. During this procedure, the kidneys of diabetic rats filtered blood normally but salt and water retention increased by 80% and central kidney blood flow decreased by around 90%. Insulin restored normal salt and water excretion in diabetic rats, although central kidney blood flow remained decreased. Analysis of tissue and urine showed that these effects had occurred before the kidneys had developed structural damage from the diabetes.

To find out if salt and water retention in diabetes affects BP, surgically-implanted radiotransmitters were used to measure BP in rats over several days. Diabetic rats had similar BP measurements to those in people with higher cardiovascular risk- BP

was higher overall and failed to drop when the rats were resting. Surprisingly, this was made worse by an ET_A blocker but improved with an ET_B blocker, suggesting that the ET_A blocker was causing rather than correcting the salt and water retention in diabetic rats. This theory was tested by repeating the first set of experiments but this time rats were injected with ET_A and ET_B blockers. In normal rats, the ET_A blocker halved central kidney blood flow and increased salt and water retention by up to 90%, while the ET_B blocker reduced salt and water retention without changing kidney blood flow. Despite these effects, none of these changes was observed in diabetic rats.

In summary, these experiments in diabetic rats confirm that diabetes causes salt and water retention by reducing central kidney blood flow, and that this is associated with increased BP. However, although insulin reduces salt and water retention, it doesn't do this by increasing central kidney blood flow but by another mechanism, not yet identified. This means that further reductions in cardiovascular risk might be achieved in diabetics by using new medicines that increase central kidney blood flow. However, ET_A blockers will not be the agents to do this. They unexpectedly reduced central kidney blood flow and increased salt and water retention in healthy rats. Although this did not occur immediately in diabetic rats, the changes in BP that the ET_A blockers caused in the diabetics over several days were consistent with this effect. Therefore, although ET_A blockers are used to reduce BP, they cause salt and water retention.

Table of contents

List of figures

List of tables

List of abbreviations

A	Adenine
Acro	Acrophase
Amp	Amplitude
ACE	Angiotensin converting enzyme
AM	Amplitude modulation
AMI	Acute myocardial infarction
AngI	Angiotensin I
AngII	Angiotensin II
AngIIR	Angiotensin II receptor
ANCOVA	Analysis of covariance
ANOVA	Analysis of variance
AQP2	Aquaporin-2
ASCEND	Avosentan on doubling of serum creatinine, end-stage renal disease and death in diabetic nephropathy
ATP	Adenosine triphosphate
BOLD	Blood oxygen level-dependent
BP	Blood pressure
bpm	Beats per minute
BSA	Bovine serum albumin
C	Cytosine
ºC	Degrees Celsius
CD	Cluster of differentiation
coeff.	Coefficient

col	Collagen
cDNA	Complementary deoxyribonucleic acid
CKD	Chronic kidney disease
cos	Cosine function
CT	Computed tomography
C_T	Cycle threshold
CVD	Cardiovascular disease
DCCT	Diabetes control and complications trial
DCT	Distal convoluted tubule
ΔC_T	Change in cycle threshold
DM	Diabetes mellitus
DNA	Deoxyribonucleic acid
DOCA	Deoxycorticosterone acetate
DRP	Diabetes Recording Period
DSR	Dahl salt-resistant
DSS	Dahl salt-sensitive
ECE	Endothelin-converting enzyme
ECM	Extracellular matrix
EDIC	Epidemiology of diabetes interventions and complications
EDTA	Ethylenediaminetetraacetic acid
EGFR-TK	Epidermal growth factor receptor-tyrosine kinase
ELISA	Enzyme-linked immunosorbent assay
ENaC	Epithelial sodium channel
ESRD	End-stage renal disease

ET	Endothelin
ET_A	Endothelin A
ET_B	Endothelin B
ET-1	Endothelin-1
ET-2	Endothelin-2
ET-3	Endothelin-3
FAM	Fluorescein amidite
FDA	Food and Drug Administration
FENa	Fractional excretion of sodium
fg	Femtogrammes
fmol	Femtomoles
Fig.	Figure
FITC	Fluorescein isothiocyanate
fmol	Femtomoles
FSGS	Focal and segmental glomerulosclerosis
G	Guanine
g	Gramme
GAPDH	glyceraldehyde 3-phosphate dehydrogenase
gbw	Gramme bodyweight
gDNA	Genomic deoxyribonucleic acid
GBM	Glomerular basement membrane
GFR	Glomerular filtration rate
H&E	haematoxylin and eosin
HbA1c	Glycosylated haemoglobin

HCl	Hydrochloric acid
Hz	Hertz
ICAM-1	Intercellular adhesion molecule-1
IgG	Immunoglobulin-G
IL-1b	Interleukin-1b
IL-6	Interleukin-6
ip.	Intraperitoneal
IU	International units
iv.	Intravenous
JG	Juxtaglomerular
k	Growth constant
kHz	Kilohertz
kg	Kilogramme
KIM-1	Kidney injury molecule-1
KO	Knockout
kw	Kidney weight
l	Litres
LDS	Laser Doppler spectroscopy
L-NAME	N-nitro L-arginine methyl ester
Ltd.	Limited company
nm	Nanometres
M	Molar
mg	Milligrammes
µg	Microgrammes

MCP-1	Monocyte chemoattractant protein-1
min	Minute
ml	Millilitres
µl	Microlitres
mM	Millimolar
mmHg	Millimetres of mercury
µm	Micrometres
mmol	Millimoles
µmol	Micromoles
MMP-2	Matrix metallopeptidase-2
MMP-9	Matrix metallopeptidase-9
mRNA	Messenger ribonucleic acid
MRI	Magnetic resonance imaging
Na	Sodium
NADPH	nicotinamide adenine dinucleotide phosphate
NCC	Sodium-chloride co-transporter
NF-κB	Nuclear factor kappa B
ng	Nanogrammes
NHS	National Health Service
NHE3	Sodium-hydrogen exchanger-3
NKCC2	Sodium-potassium-chloride co-transporter-2
NO	Nitric oxide
NOS	Nitric oxide synthase
O-GlcNAcase	O-linked β-N-acetyl glucosaminyl hydrolase

P	Period
PBS	Phosphate buffered saline
PCT	Proximal convoluted tubule
PET	Positron emission tomography
PFA	Paraformaldehyde
PGE_2	Prostaglandin E_2
pH	Potential of hydrogen
P2	Purinergic-2
Q_p	24-hour periodicity
qPCR	Semi-quantitative polymerase chain reaction
r	Coefficient of correlation
R^2	Coefficient of determination
RAAS	Renin-angiotensin-aldosterone system
RNA	Ribonucleic acid
ROS	Reactive oxygen species
rpm	Revolutions per minute
RRP	Randomisation Recording Period
sc.	Subcutaneous
SEM	Standard error of the mean
SGLT2	Sodium-glucose transporter-2
SHR	Spontaneously hypertensive rat
sin	Sine function
SONAR	Study Of diabetic Nephropathy with AtRasentan
STZ	Streptozotocin

T	Thymine
TATA	thymine-adenine-thymine-adenine
TBE	Tris borate ethylenediaminetetraacetic acid
TBP	thymine-adenine-thymine-adenine box binding protein
TGF	Tubuloglomerular feedback
TGF-β1	Transforming growth factor-beta-1
Θ	Acrophase
TIF	Tagged image format
TK	Tyrosine kinase
TNF-α	Tumour necrosis factor-alpha
T1DM	Type 1 diabetes mellitus
TPU	Tissue perfusion units
T2DM	Type 2 diabetes mellitus
UET-1	Urinary endothelin-1
UET-1V	Urinary endothelin-1 excretion rate
UK	United Kingdom
UNaV	Urinary sodium excretion rate
US	United States
UV	Urine flow rate
V	Volts
v	Versus
V2	Vasopressin-2
VSMC	Vascular smooth muscle cell
WT	Wild-type

1 Introduction

Type 1 diabetes mellitus (T1DM), a chronic disease in which an absolute lack of insulin results in persistent hyperglycaemia [1,2], could hardly be described as an emerging disease, since it has accompanied mankind through the rise and fall of civilisations. It was recognised as a separate disease entity in Ancient Egypt and was first named *diabetes* meaning "passing through" by the Ancient Greeks [2]. The term *mellitus*, meaning "sweet or honeylike", was coined in 17th century England by Thomas Willis, although the sugary urine that sufferers produced, and which attracted ants, had already been recognised in ancient India and medieval Persia [3]. From antiquity up until the early 20th century, T1DM was almost always lethal as a consequence of ketoacidosis, and it was not until the latter half of the 19th century that significant advances were made in identifying the aetiology of the disease. Following the discovery by Langerhans of the eponymous pancreatic islets, von Mering and Minkowsky successfully induced and reversed hyperglycaemia in experimental dogs by removing and then regrafting the pancreas [4]. The mysterious pancreatic agent responsible for regulating blood glucose was named *insulin* by the Belgian physicist de Mayer, in reference to Langerhans's islets or *insulae* [3]. Once isolated, insulin was famously used therapeutically for the first time in 1922, when Frederick Banting and colleagues successfully treated a sick, ketotic, 14-year-old boy, Leonard Thomson [5,6], who then lived for a further 13 years. Banting received the Nobel Prize for medicine, in recognition of a scientific breakthrough in a disease prevalent within the general, and in particular the younger, population.

To this day, T1DM remains one of the most common chronic diseases in children and adolescents [7]. The other form of DM, Type 2, in which hyperglycaemia results

from insulin resistance, is usually associated with obesity, and has, in modern times, attained greater notoriety as an epidemic of the Western world, affecting more than 400 million people worldwide [8]. Yet T1DM still accounts for 10% of all cases of DM, affecting one in every 500 children under the age of 16 in the United Kingdom (UK) [9]. Furthermore, its incidence is increasing by approximately 3.5% per year, with the highest prevalence in northern European countries [10,11]. The reason for this increase is not known, but such a prevalent, incurable and lifelong condition exerts an ever-increasing strain on health services. Currently, T1DM consumes more than £1bn (1%) of the annual budget of the National Health Service (NHS) [12], with an additional estimated yearly cost to the UK economy of £1bn, in the form of social and productivity costs [12].

Despite the historical and economic importance of T1DM, many of the pathological features of the disease have not been fully explained. It is known that it is an immune-mediated condition, in which insulin-producing pancreatic islet β cells are attacked early in life by autoantibodies [13] and destroyed by infiltrating T cells [14], but the triggering stimulus to this process remains unknown. Furthermore, despite instigating insulin replacement therapy to successfully reduce blood glucose, life expectancy for people with T1DM, who are in their early twenties, is reduced by 11-13 years [15], and devastating long-term complications still occur, usually in the form of cardiovascular disease (CVD) [7]. Therefore, there is a great unmet need to identify novel therapeutic targets that combat the additional cardiovascular risk of T1DM.

This introduction will firstly consider the cardiovascular complications of T1DM and the risk factors for their development, namely, hyperglycaemia, nephropathy and hypertension. Thereafter, pre-clinical and clinical studies of T1DM, including those that support therapeutic intervention with the endothelin (ET) receptor antagonists, will be discussed.

1.1 Cardiovascular complications of T1DM

1.1.1 Macro- and microvascular disease

The risk of CVD is four to ten times greater in patients with T1DM than the general population [16,17], and macro- and microvascular complications contribute significantly to morbidity and mortality. Macrovascular disease can lead to angina and myocardial infarction [18], limb ischaemia often necessitating amputation [19], and cerebrovascular disease resulting in stroke [20]. Microvascular complications include loss of vision from retinopathy [21], loss of limb sensation, limb ulceration and gastroparesis from neuropathy [22], and the development of nephropathy. In diabetic nephropathy, early glomerular damage, defined as microalbuminuria (≥40mg/24hours), can progress to macroalbuminuria (>300mg/24hours) and end-stage renal failure requiring dialysis or transplant [23].

Although these complications do not usually occur in T1DM patients until later in life [24], functional and structural abnormalities in the cardiovascular system develop very early in the course of the disease [25,26]. T1DM is most frequently diagnosed in patients between five and seven years of age, and at puberty [27], so treatment

strategies to reduce CVD risk must also be suitable for use in younger patients. This poses a significant therapeutic challenge.

1.2 Cardiovascular risk and blood glucose

1.2.1 Longitudinal studies assessing cardiovascular risk

When replacement insulin therapy was first introduced, it successfully met the therapeutic goals of preventing ketoacidosis and alleviating polyuria, polydipsia, lethargy and weight loss. This strategy limited glycosuria by lowering blood glucose below the renal threshold of maximal capacity for glucose reabsorption [28] but blood glucose still exceeded physiological levels of 4.0-6.0 mmol/l [24]. Seventy years after Banting's breakthrough, two clinical studies set out to determine whether macro- and microvascular complications of T1DM could be reduced by more intensive insulin therapy that maintained blood glucose close to physiological parameters.

The Diabetes Control and Complications Trial (DCCT) [29] was a controlled clinical trial in which 1,441 normotensive patients with T1DM were recruited over six years with a minimum follow-up of 6.5 years. Approximately half of the patients were randomised to conventional management with insulin. The other half was intensively managed with either three daily insulin injections or insulin infusion pump therapy, according to self-monitored blood glucose levels and monthly glycated haemoglobin (HbA1c, a marker of the mean glucose over the previous two to three months) [30]. Interim analysis discovered that intensively managed patients had a lower HbA1c (7% versus 9%) and a 35-76% reduction in the development or progression of retinopathy, neuropathy and macro- and microalbuminuria. This

striking reduction in microvascular risk led to the premature termination of the study. All DCCT patients were then invited to take part in the follow-on Epidemiology of Diabetes Interventions and Complications (EDIC) study [24]. Unlike DCCT, EDIC was only observational but all patients, including those previously managed conventionally, were now under an intensive management regimen that removed the glycaemic separation between the two original DCCT cohorts (HbA1c=8% in both cohorts). Surprisingly, though, the difference in microvascular risk between cohorts continued to widen. The ongoing EDIC study continues to demonstrate long-term improvement in CVD risk in the intensively managed DCCT patients [31], who have reduced carotid intima thickness [32], reduced computed tomography (CT)-measured coronary artery calcification [33] and a 58% reduction in CVD events after ~18 years of follow-up [24]. However, these landmark studies also show that maximal reductions in macro- and microvascular risk are only achievable in the long term when intensive insulin therapy is instigated at an early stage.

1.2.2 Difficulties arising from intensive blood glucose management

The clinical need to lower blood glucose in T1DM has to be offset against the threefold increased risk of potentially life-threatening hypoglycaemia that occurs with intensive management [34], the practical difficulties of tight blood glucose control and monitoring in young patients, and the development of resistance to neuroglycopaenia (unawareness of hypoglycaemia) [35]. Furthermore, despite clear benefits from a lower blood glucose, 6% of intensively managed patients in the DCCT still experienced a cardiovascular event (non-fatal stroke, acute myocardial infarction (AMI), angina, the need for limb or coronary revascularisation) within

18 years, 90% had retinopathy, 19% had some form of nephropathy, and 24% demonstrated signs of clinical neuropathy [31]. Thus, it can be concluded that alternative treatment strategies, which complement insulin therapy, are required to remove cardiovascular risk in T1DM. Suitable therapeutic targets are nephropathy and hypertension, both risk factors for CVD.

1.3 Diabetic nephropathy

1.3.1 The worldwide importance of chronic kidney disease

Chronic kidney disease (CKD) is defined as renal damage leading to abnormal urinary excretion of albumin, or a reduction in measured or estimated glomerular filtration rate (GFR <60ml/min per 1.73m^2), that persists for a period of at least three months [36]. CKD is a major clinical and financial burden worldwide. This is partly because of its high prevalence (~11%) within the United States (US) and Western Europe [37,38] but also because of the high morbidity and mortality associated with it. Patients with advanced CKD are most likely to die from CVD [39]. Indeed, CKD is so strongly associated with CVD [40] that the US Kidney Foundation Task Force on CVD in CKD recommends that patients with CKD should be considered in the highest risk group for subsequent cardiovascular events [41]. Dialysis and renal transplantation in patients, who do not succumb to CVD prior to end-stage renal disease (ESRD), consumes around 2% of the NHS's annual budget [42].

DM is the single most common cause of CKD, and is responsible for ~25% of all cases of renal failure in the UK [43]. Diabetic nephropathy is similar in T1DM and T2DM. Its progression is typical of glomerulopathy and has been well characterised,

consisting of five stages: renal hypertrophy with glomerular hyperfiltration, mesangial expansion, microalbuminuria, macroalbuminuria, and ESRD [44].

GFR is usually kept constant, or autoregulated, despite fluctuation in arterial blood pressure (BP) [45]. Autoregulation is a consequence of an endogenous myogenic response within the afferent and efferent arterioles of every glomerulus. The myogenic response is modified by ligands, such as angiotensin II (AngII), and by the *macula densa* in response to changes in luminal sodium concentration called tubuloglomerular feedback (TGF) [46]. Impaired autoregulation of GFR increases the risk of hyperfiltration and injury to the glomerular filtration barrier of podocytes, endothelial cells and glomerular basement membrane (GBM) [47]. Once the glomerular filtration barrier is breached, small plasma proteins, including albumin, leak into the tubule and initiate a vicious cycle of neutrophil and macrophage infiltration, progressive glomerulosclerosis, and mesangial cell hyperplasia and migration [48] . The consequences are ever greater perfusion and hyperfiltration of neighbouring glomeruli, and their subsequent injury [48]. Tubulointerstitial ischaemia and fibrosis ensue because peritubular blood supply is downstream of the glomerulus and impaired by glomerular destruction [49,50]. Therefore, hyperfiltration is a suitable therapeutic target for reducing glomerular injury and functional nephron destruction in T1DM, and albuminuria is an independent predictor of ESRD and cardiovascular mortality [51]. In many of the pre-clinical and clinical studies of diabetic nephropathy that are mentioned in this introduction, reduced albuminuria is used as an end-point.

1.3.2 Hyperfiltration and the salt paradox

Studies in rats have demonstrated that hyperfiltration in T1DM is a consequence of increased activity of the sodium/glucose co-transporter in the proximal convoluted tubule (PCT) which lowers the concentration of sodium in luminal fluid at the *macula densa*, reducing TGF and increasing GFR [52]. In T1DM, increasing oral salt intake paradoxically reduces GFR because sodium reabsorption in the PCT is reduced and TGF is increased [53]. The opposite effect is achieved with a low salt diet [54]. The mechanistic basis to the bidirectional changes in sodium reabsorption that underpin the "salt paradox" has not been fully resolved but translation to a clinical setting has demonstrated that renal handling of dietary salt may be crucial to nephroprotection in people with T1DM [55,56] . However, restricting dietary salt as a therapeutic strategy in T1DM remains controversial [57]. For example, in the two-kidney one-clip Goldblatt rat model of T1DM renal injury, in which one renal artery is clipped to induce unilateral renal ischaemia, high salt intakes do not reduce susceptibility to injury in the unclipped, hyperfiltering kidney [58]. Furthermore, clinical outcomes in people with T1DM do not have a linear relationship with urinary sodium excretion. Rather, the relationship is U-shaped, with increased mortality occurring with salt intakes at opposite ends of the spectrum [59]. Because CVD risk rises with salt intake [60], there is currently no consensus on increasing dietary salt to delay or prevent diabetic nephropathy in T1DM [57]. Instead, medical management of hyperfiltration in T1DM focuses on targeting the renin-angiotensin-aldosterone system (RAAS).

1.3.3 Hyperfiltration and the renin-angiotensin-aldosterone system

AngII and aldosterone, individual components of RAAS, play a vital role in the regulation of BP by controlling extracellular volume and sodium concentrations, and peripheral vascular resistance [61]. Sympathetic stimulation and exposure of the *macula densa* to reduced luminal concentrations of sodium stimulate release of renin from the juxtaglomerular (JG) cells of the afferent arteriole. Renin converts circulatory angiotensinogen to AngI, which in turn is converted to AngII by angiotensin converting enzyme (ACE). AngII, a potent vasoconstrictor, stimulates release of aldosterone from the adrenal cortex, which promotes sodium and water retention from the renal collecting duct by increasing activity of the epithelial sodium channel (ENaC).

Once ACE inhibition had demonstrated a direct role for AngII in hyperfiltration, glomerular injury and proteinuria in T1DM Munich-Wistar rats [62], the ACE inhibitor captopril was trialled clinically. It reduced the risk of doubling of serum creatinine (a marker of impairment to GFR), renal transplantation and death in >200 T1DM patients compared to placebo [63]. This landmark study showed that blocking RAAS to reduce hyperfiltration could significantly reduce the risk of developing ESRD. The effects were observed in patients already receiving medication to control hypertension, suggesting that the benefits of ACE inhibition stemmed from modulation of afferent and efferent arteriolar tone [64], in addition to lowering BP. The success of ACE inhibition also challenged the hypothesis that hyperfiltration due to hypertension was the source of nephropathy. Further doubt was cast by the different time courses to nephropathy in the two forms of DM. In T2DM, by the

time albuminuria is first detected, hypertension is already present [65]. In T1DM, however, albuminuria precedes the development of hypertension, suggesting that in T1DM, hypertension is a consequence of nephropathy rather than its cause. It made sense, therefore, that ACE inhibitors would be most beneficial after albuminuria had developed rather than before. ACE inhibitors are also known to possess potent anti-inflammatory and anti-fibrotic properties [66] and they remain the mainstay of treatment of nephropathy in T1DM, with a significant cost:benefit ratio if instigated once microalbuminuria has developed [67].

1.3.4 Hypertension and initiation of nephropathy

Despite the renoprotective benefits of ACE inhibition [63], creatinine clearance still declines by >10% over three years [63]. In the EDIC study, ACE inhibition failed to narrow the gap in macro- and microvascular complication rates between the DCCT intensively- and conventionally-treated cohorts [24]. This raised the possibility of hypertension playing an important role in hyperfiltration at an earlier stage of T1DM than previously imagined.

Hypertension, defined as systolic BP ≥140mmHg and/or diastolic BP ≥90mmHg, [68] is the single largest contributor to the global disease burden [69]. Hypertensive nephrosclerosis constitutes approximately 30% of all cases of ESRD [70] and hypertension exacerbates all forms of CKD by driving further glomerular injury [71]. The importance of hypertension to the development of diabetic nephropathy is supported by pre-clinical studies which show that rodent models are particularly

resistant to developing nephropathy unless they are hypertension-prone or hypertension is induced [72,73].

In another landmark study, designed to investigate the discrepancy between onset of hypertension and appearance of microalbuminuria in T1DM and T2DM, Lurbe *et al.* recorded ambulatory BP and 24-hour urinary albumin excretion in 61 normalbuminuric T1DM patients over a mean follow-up period of 63 months [74]. By the end of the study, 19% of the patients had developed microalbuminuria. Interestingly, a rise in nocturnal systolic BP of ~5mmHg had preceded microalbuminuria by at least three years. By contrast, the 81% of patients whose nocturnal systolic BP had not been elevated, were still not microalbuminuric by the end of the study. Comparison of nocturnal with diurnal systolic BP gave additional insight into the relationship between BP and albuminuria. A 10% or more dip in BP at night was associated with a 70% reduction in the risk of developing microalbuminuria. Therefore, not only was increased risk of diabetic nephropathy associated with increased BP, but changes to BP, which would be undetected by a single "in office" measurement, preceded nephropathy. Furthermore, a subgroup of patients, whose glycaemic control was suboptimal, but whose systolic BP dipped by 10% or more at night, still failed to develop microalbuminuria. Thus, the importance of elevated nocturnal BP, as well as hyperglycaemia, to the development of diabetic nephropathy, early in the course of the disease, was established. To understand why nocturnal BP rather than diurnal BP might be elevated in early T1DM, prior to microalbuminuria, it is necessary to understand how BP is regulated.

1.4 Regulation of BP

1.4.1 Short-term regulation of blood pressure

Arterial BP is generated by the expulsion of stroke volume by the left ventricle against the resistance of the arterial tree. It is tightly regulated in the short term by the autonomic nervous system [75], which, in response to central inputs and peripheral baroreceptors, modifies heart rate, cardiac contractility, and arteriolar tone. This ensures adequate perfusion of the vital organs (heart, brain and kidneys) as well as meeting metabolic or survival requirements such as "fight or flight". Perfusion of organs can be further modified by fluctuations in endothelium- and non-endothelium-dependent arteriolar tone and pre-capillary constriction by pericytes. These are usually in response to autocrine and paracrine agents released as metabolic by-products or inflammatory mediators, and following autonomic stimulation and changes in vascular wall stress [76,77]. Usually, acute rises and falls in BP are short-lived, whereas, in the state of hypertension, BP is inappropriately elevated over the long-term.

1.4.2 Long-term regulation of blood pressure

Central to the long-term regulation of BP are the kidneys, which control plasma volume by controlling sodium balance [78]. This has been confirmed through a series of renal transplantation experiments in several rodent models of hypertension.

BP in nephrectomised Dahl salt-sensitive (DSS) rats normalises following transplantation of a single kidney from a Dahl salt-resistant (DSR) donor. Similarly, nephrectomised DSR rats become hypertensive following transplantation of a single

kidney from a DSS rat donor [79-81]. Thus, the BP phenotype follows the genotype of the kidney donor rather than the genotype of the recipient. Similar results have been reproduced in other hypertensive rodent models, such as the spontaneous hypertensive rat (SHR), and in studies with very young hypertensive rat donors whose kidneys show no evidence of structural injury [82,83]. When recipient rats develop hypertension, they also rapidly retain sodium [84] but do not have vascular dysfunction or elevated afterload due to RAAS [85,86]. This indicates that the kidneys regulate BP by regulating sodium excretion to control plasma volume.

Renal handling of sodium can be influenced by external factors. Nephrectomised wild-type (WT) mice, transplanted with a kidney from an AngII receptor knockout (AngIIR KO) donor mouse, are protected from hypertension during chronic infusion of AngII [87]. Conversely, nephrectomised AngIIR KO mice develop hypertension during AngII infusion when grafted with a WT mouse kidney. Not only does this reaffirm the importance of the kidney to the regulation of BP, it also shows that renally-derived components of RAAS modify its role [88]. Combined with the clinical studies of Lewis *et al.* [63] and Lurbe *et al.,* [74] which demonstrate the importance of hyperfiltration and BP, it is concluded that sodium balance is crucial to limiting progression of diabetic nephropathy. The intrinsic ability of the kidneys to maintain sodium balance is called acute pressure natriuresis.

1.5 Acute pressure natriuresis

1.5.1 Regulation of sodium and blood pressure by acute pressure natriuresis

Crucial to the kidney's role in the long-term regulation of BP is its ability to modify excretion of sodium and water in response to short-term fluctuations in BP. The mammalian kidney is incapable of actively secreting sodium into urine, and so urinary sodium and water excretion is dependent on a process of large-scale filtration followed by selective reabsorption. The relationship between renal perfusion pressure (a surrogate marker of arterial BP) and urinary sodium excretion is a sigmoidal one. However, with Western diets, which exceed maintenance salt requirements, the relationship is linear, so that increases in BP lead to corresponding increases in sodium excretion [78]. This physiological phenomenon is called acute pressure natriuresis and the relationship between BP and urinary sodium excretion, the acute pressure natriuresis curve [78]. The mechanism is vasculotubular and activated following ingestion of a meal [89]. Rapid sodium reabsorption from the gastrointestinal tract leads to an abrupt rise in plasma osmolality. This stimulates neural osmoreceptors leading to the sensation of thirst, the ingestion of water, and dilution of the plasma osmolality at the expense of increased plasma volume [90]. The peritubular blood supply of the kidney is in series with, and downstream of, the glomeruli. Autoregulation of GFR, therefore, transmits increased renal perfusion to the renal medulla. The renal medulla is highly vascular, containing an extensive capillary network called the *vasa recta*. Increased perfusion through this network increases medullary hydrostatic pressure and, through Starling's forces, inhibits tubular sodium and water reabsorption [91], principally from the PCT [92]. Distal sodium transporters such as the sodium-potassium-chloride co-transporter (NKCC2),

sodium-chloride co-transporter (NCC) and ENaC may also be inhibited by paracrine agents such as nitric oxide (NO), endothelin-1 (ET-1) and adenosine triphosphate (ATP) [93-96]. The result is a diuresis/natriuresis appropriate for the degree of sodium and water ingestion, and that is self-limiting once an appropriate plasma volume has been restored [78].

Consistent with the AngIIR KO renal transplant model [87], the acute pressure natriuresis curve can be modified by external influences such as RAAS activation, which shifts the acute pressure natriuresis curve to the right and decreases its gradient [78,93]. This response, though, can be overridden. For example, in the phenomenon of "aldosterone escape", sustained hypertension from hyperaldosteronism is prevented by compensatory adaptations to the tubular phase of acute pressure natriuresis that increase its sensitivity to BP and increases in BP [97]. This is thought to result from downregulation [98] and inhibition of sodium transport [99].

Many consider acute pressure natriuresis to be so important to the long-term regulation of BP, that in order for the state of hypertension to exist, acute pressure natriuresis must also be impaired [89].

1.5.2 Nocturnal dipping

Acute pressure natriuresis is activated soon after salt ingestion. Salt ingestion varies over a 24-hour period, suggesting that an intact acute pressure natriuresis response is vital to maintaining a circadian rhythm in BP [100]. In populations with a high prevalence of salt-sensitive hypertension, reduced daytime urinary sodium excretion

is tightly linked to increased nocturnal BP and reduced dipping in BP [101]. A similar failure of BP to dip in people with T1DM [74] suggests that daytime acute pressure natriuresis is also impaired in T1DM and has to be maintained during the night at the expense of increased BP [100].

In essential hypertension, loss of nocturnal dipping is associated with a higher risk of target organ damage [102-104], suggesting that nocturnal dipping may be necessary for organ recovery from the haemodynamic stresses of the daytime systemic arterial load. In the kidney, which is highly perfused and receives approximately 25% of cardiac output, elevated nocturnal BP could induce a form of hyperfiltration that initiates glomerular injury. Thus, there are potential benefits from therapeutic targeting of hypertension to re-establish nocturnal dipping as well as simply lowering BP. This is the rationale behind the recommendation by the American Diabetes Association to dose anti-hypertensive medication at bedtime [105] and there is already evidence that this may reduce cardiovascular risk [106]. Alternatively, acute pressure natriuresis could be targeted directly. Protocols for inducing acute pressure natriuresis in animal models have been developed to identify the mechanistic basis to acute pressure natriuresis and potential therapeutic targets.

1.5.3 Induction of acute pressure natriuresis through volume expansion

Rapid expansion of the vascular compartment induces acute pressure natriuresis. This can be achieved through water immersion [107] or more usually, in animal models, by rapid intravenous (iv.) administration of isotonic saline. Both approaches increase cardiac preload which, in turn, increases cardiac output by the Frank-Starling

mechanism, and renal perfusion. Either technique is simple and mimics the stimulus to acute pressure natriuresis following salt and water ingestion. In experimental animals, the main disadvantage is the unpredictability of fluid distribution within the vascular compartment. This makes it difficult to maintain BP and renal perfusion pressure within the narrow, predictable range required to facilitate comparisons between experimental cohorts. Nevertheless, saline infusion, at levels far exceeding maintenance requirements, has induced sodium and water excretion rates in T1DM Sprague Dawley rats that only reach ~20% of those measured in controls [108,109]. Interestingly, diuresis and natriuresis recover when T1DM rats are treated with insulin [108]. Since excretion of sodium following water immersion is halved in T1DM patients [110], this raises the possibility that the results of DCCT [24] might be linked to reversal of impaired acute pressure natriuresis.

1.5.4 Pharmacological induction of acute pressure natriuresis

Acute pressure natriuresis can be induced by increasing BP acutely through peripheral vasoconstriction. In Sprague Dawley rats, adrenaline (at iv. infusion rates of 0.5-1.7µg/min) increases BP, and hence renal perfusion pressure, by 35-45mmHg up to a maximum of 147mmHg for 20-25 minutes [111]. Although glomerular autoregulation is maintained with this technique, systemic and renal effects of adrenaline due, in part, to activation of RAAS, make this protocol unsuitable for investigating the relationship between renal regulation of sodium balance and BP.

1.5.5 Ligature-induced acute pressure natriuresis

This protocol is the current "gold standard" technique for inducing acute pressure natriuresis since it leads to more predictable, controllable and reversible increases in renal perfusion pressure which can be achieved in a stepwise manner. This is advantageous because it permits multiple time points for sampling and hence more opportunity for comparing experimental cohorts [112]. Its major disadvantage is that it is surgically invasive, requiring laparotomy. In rodents, there is the potential for significant and rapid hypothermia and hypotension because the surgical preparation is time consuming, and involves manipulation of the abdominal contents, which promotes extravasation of fluid into the abdomen. However, a skilled, experienced operator can reduce surgical time and minimise extravasation of fluid.

In ligature-induced pressure natriuresis, the major conducting arteries are acutely compressed by tightening pre-placed ligatures or inflating peri-arterial cuffs [112]. The volume of the vascular tree is immediately reduced. Plasma volume is maintained because capillary beds, whose arterial supply has been removed, gradually drain into systemic veins. As long as there is adequate myocardial function to overcome the acute increase in afterload, BP and renal perfusion pressure rise acutely. The original technique, developed by Dresser *et al.* [113], combined bilateral carotid artery occlusion with vagotomy. However, changes in autonomic outflow, in response to vagotomy and acute reductions in intracranial blood flow, mean that this technique has been superseded by ligation of alternative major conducting arteries.

Ligature-induced methods are now usually based on the protocol that Roman and Cowley developed [112] to demonstrate autoregulation of GFR and renal artery and cortical blood flow , and simultaneous increases in medullary blood flow and urinary sodium excretion during acute pressure natriuresis. Their protocol included two stepwise increases in BP by, firstly, simultaneous ligation of the coeliac and cranial mesenteric arteries, and at a later time point, the aorta distal to the left kidney. Intravenous isotonic crystalloid fluids were supplemented with 1% BSA to increase plasma oncotic pressure, thereby reducing fluid extravasation. A high iv. infusion rate (100µl/min) was double the rate typically used for renal clearance studies, and ensured replacement of fluid loss due to extravasation while, itself, inducing natriuresis.

Since its publication, Roman and Cowley's protocol has been applied to many rodent models of human disease with only minor adaptations. Adjustments to the duration of equilibration and collection periods are made according to operator skill and the health status of the animal being studied. Sympathetic innervation of the kidney promotes sodium and water retention, and Roman and Cowley demonstrated that renal sympathetic neurectomy shifted the pressure natriuresis curve approximately 20mmHg to the left [112], allowing them to induce acute pressure natriuresis at lower BPs with a proximal aortic cuff. Neurectomy has not been undertaken in other studies as it requires further organ manipulation and increases the duration of surgical preparation time. Also, it is not required to induce the crucially important increase in renal interstitial hydrostatic pressure that underpins the acute pressure

natriuresis response [114]. Neurectomy may, in some instances, actually shift the pressure natriuresis curve to the right [115].

Attempts to minimise external endocrine effects include acute adrenalectomy, immediately prior to inducing acute pressure natriuresis, and infusion of a "hormone cocktail" of noradrenaline, aldosterone, hydrocortisone and vasopressin to maintain steady serum levels of these hormones [112]. However, "hormone cocktails" are often not employed as they can introduce additional confounding factors and result in serum levels that differ significantly from reference ranges [112].

Acute pressure natriuresis can be induced in uninephrectomised rats and rats with both kidneys intact, with no appreciable differences in GFR, renal blood flow, natriuretic or diuretic responses on a per gramme kidney weight basis.

1.5.6 Molecular pathways of acute pressure natriuresis identified by the ligature-induced protocol

The ligature-induced protocol has been used to establish impaired acute pressure natriuresis as a source of salt sensitivity in DSS rats [116] and deoxycorticosterone acetate (DOCA)-salt-sensitive mice [117], and to probe for potential underlying mechanisms. One important mechanism involves renal NO signalling.

NO is a gaseous vasodilatory molecule synthesised by one of three isoforms of the enzyme nitric oxide synthase (NOS), and released from the endothelium in response to increased blood flow [118,119]. Its importance to acute pressure natriuresis is

demonstrated when NOS is inhibited with N-nitro L-arginine methyl ester (L-NAME) in Sprague Dawley rats, leading to a rightward shift in the acute pressure natriuresis curve [120]. Although this effect could, in part be explained by haemodynamic effects such as efferent arteriolar vasoconstriction and reduced medullary perfusion, it now appears that acute pressure natriuresis is dependent on NOS1 and NOS3 isoforms that are highly expressed in the inner medullary collecting duct [121], at levels which correlate with dietary salt intake [122]. Tubular NO has now been shown to modify sodium reabsorption, according to salt intake, at several sites along the nephron [96]. In the inner medullary collecting duct, NOS co-localises at high concentrations with ENaC where NO, in combination with the peptide ET-1, plays an important role in inhibiting sodium reabsorption. Again, the acute pressure natriuresis curve shifts to the right when this relationship is disrupted genetically or pharmacologically, and the ligation-induced protocol is applied [122]. Thus, ligature-induced acute pressure natriuresis has been instrumental in probing the complexity of the interplay between renal haemodynamics, glomerular autoregulation and tubular function, and has identified novel pathways that modulate sodium excretion.

The technique has also identified a link between susceptibility to hypertensive renal injury in Fischer F344 rats and impaired acute pressure natriuresis prior to the onset of hypertension [123]. This would be consistent with impaired acute pressure natriuresis underpinning the loss of nocturnal dipping [124] and the development of microalbuminuria recorded by Lurbe *et al.* [74]. Despite this, the ligature-induced protocol has, somewhat surprisingly, never before been applied to either a T1DM or T2DM rodent model. This represents a significant deficiency in our understanding

of the interplay between nephropathy, renal regulation of BP and CVD risk in T1DM, particularly since the ligature-induced acute pressure natriuresis protocol could be adapted to a suitable T1DM model.

1.6 Pre-clinical studies on T1DM

1.6.1 The streptozotocin-induced model of Type 1 diabetes mellitus

Animal models of disease should have consistent, well-defined functional and pathological phenotypes that are good representations of some or all of the components of the corresponding human disease. They should be amenable to pharmacological, molecular and genetic manipulation and probing without compromising animal welfare.

The greatest contributions to understanding the aetiopathogenesis of T1DM have been made using spontaneous mutation [125, 126] and genetically engineered [127] rodent models. However, such models are costly to develop and maintain, and onset of T1DM can be variable. In T2DM, the cardiovascular complications are related to multiple factors such as dyslipidaemia and pro-inflammatory and pro-coagulant states [128]. However, in T1DM, the long term macro- and microvascular complications are a direct consequence of hyperglycaemia, hypoinsulinaemia and nephropathy. These can be modelled simply and cheaply by destroying pancreatic β cells with a pharmacological agent [129]. Since rodent models of T1DM only develop nephropathy after several months of hyperglycaemia [130], pharmacological models of T1DM provide a large window of opportunity within which to investigate functional changes that contribute to cardiovascular risk before the confounding effects of

nephropathy. This is of direct clinical relevance since reductions in cardiovascular risk in DCCT were obtained very early in the course of T1DM [29].

The pharmacological agent most commonly used to induce T1DM is streptozotocin (STZ), an analogue of N-acetyl glucosamine. It is selectively toxic against pancreatic β cells because it selectively inhibits β-cell O-linked β-N-acetyl glucosaminyl hydrolase (O-GlcNAcase). This leads to irreversible O-glycosylation of intracellular proteins and β cell apoptosis [131]. Following iv. or intraperitoneal (ip.) injection, there is a transient phase of hyperinsulinaemia for which oral sucrose supplementation in the drinking water is required [129]. The degree of hyperglycaemia attained is related to the degree of β cell destruction. Several dosing protocols exist including low dose injections for five consecutive days, medium-dose injections 24-48 hours apart and high-dose single injections with additional increments as required [129].

Most of what is known about how T1DM affects acute pressure natriuresis through promoting vascular dysfunction, tubular sodium reabsorption and hypertension and hyperfiltration has been learned from the STZ-induced T1DM rodent model.

1.6.2 Changes to renal vascular function in Type 1 diabetes mellitus

Vascular function describes the balance between local vasodilatory and vasoconstrictive effects that are mediated by autocrine and paracrine agents. Myographic studies of arteries from STZ-induced T1DM rodents have shown that reactive oxygen species, generated by nicotinamide adenine dinucleotide phosphate

(NADPH)-oxidase in response to hyperglycaemia, uncouple NOS3 and reduce vasodilatory NO bioavailability [132]. At the same time, increased epidermal growth factor receptor-tyrosine kinase (EGFR-TK)-mediated signalling raises intracellular calcium levels, increasing vasoconstrictive responses to norepinephrine, ET-1 and AngII [133]. Thus, the STZ model demonstrates both impaired vasodilation and increased vasoconstriction. Alternative compensatory vasodilatory pathways are overwhelmed [134] and a shift towards increased vasoreactivity is observed at multiple points along the arterial tree [132,134] including the renal artery [133].

Myographic studies are limited by vessel size but reduced urinary excretion of NO metabolites [135] and increased generation of renal reactive oxygen species (ROS) [136] in STZ-induced T1DM rats suggest that vascular dysfunction also occurs distal to the renal artery. However, the overall consequences for medullary perfusion and the rise that initiates acute pressure natriuresis are not clear. Medullary blood supply is downstream of the glomeruli, and despite the trend towards reduced overall NO production within the kidney, NO levels within the glomerulus can increase rather than decrease and, thus, contribute to hyperfiltration [137]. This paradox, a consequence of increased glomerular NOS1 expression, varies with the degree and duration of hyperglycaemia [137]. Furthermore, medullary perfusion is not only dependent on the resistance of the medullary vascular bed but also the cortical vascular bed [138] and the distribution of flow between cortical and juxtamedullary glomeruli [139]. Therefore, to determine the overall contribution of vascular dysfunction to changes in acute pressure natriuresis in T1DM, renal artery and cortical and medullary blood flow should be measured simultaneously following

acute rises in BP. This could be achieved in an STZ-induced T1DM rat since rats are large enough to accommodate several probes for measuring renal blood flow while, at the same, allowing access to major abdominal arteries for ligature-induced acute pressure natriuresis.

1.6.3 Changes to renal tubular sodium reabsorption in Type 1 diabetes mellitus

STZ models have provided conflicting evidence for the effect of T1DM on renal sodium reabsorption. Microperfusion studies in rats have shown that sodium-glucose transport within the PCT progressively increases with rises in luminal glucose concentration [140]. It has been proposed that this response is the mechanism for glomerular hyperfiltration in T1DM [52], and it is the target for sodium-glucose transporter-2 (SGLT2) inhibitors [141,142]. By contrast, *in vitro* studies have demonstrated reduced sodium-glucose transport across renal microvilli [143] and downregulation of expression of SGLT2, the principal renal sodium-glucose transporter, within three days of STZ injection [144]. Increased abundance of sodium-hydrogen exchanger-3 (NHE3), NCC and ENaC subunits α, β and γ [145] suggest that sodium reabsorption, independent of glucose transport, is increased along the nephron. Overall, the amount of sodium reabsorbed in T1DM is dependent on the severity and duration of hyperglycaemia [140], hypoinsulinaemia [146] and oral sodium intake [53]. Unsurprisingly, therefore, the degree that acute pressure natriuresis is modified by T1DM for given increases in BP and medullary perfusion is not known but could be determined by ligature-induced acute pressure natriuresis.

1.6.4 Consequences of hypertension and hyperfiltration in Type 1 diabetes mellitus

Susceptibility to nephropathy, following development of T1DM, varies between rodent species and strains. The C57Bl6/J mouse, on which background most KO models are constructed, appears to be particularly resistant [147]. The STZ-induced T1DM rodent model can be adapted to promote hyperfiltration by performing nephrectomy [148], or by using rodents that develop hypertension spontaneously [73,149] or inducibly [72]. These techniques accelerate the development of nephropathy and illustrate the importance of hyperfiltration and hypertension to its development in T1DM. For example, the NOS3 KO mouse combines hypertension with endothelial dysfunction, and the glomerular changes that develop are probably the most similar to those observed in diabetic patients [130,149]. Also, the Cyp1a1mRen2 rat, in which hypertension is induced by upregulating renin expression through dietary manipulation, is probably the best model for diabetes-induced tubulointerstitial fibrosis. Its renal transcriptomic profile compares favourably with that from human T1DM [72] and is in agreement with the BP-independent role for RAAS in promoting diabetic nephropathy proposed by Lewis *et al.* [63].

Once nephropathy develops, the renal and histopathological changes in STZ-induced rodents are similar to those in people. In the glomeruli, there is sclerosis and hyalinosis, dilation and cast formation [150], and reduced numbers of podocytes and nephrin [150]. This is accompanied by mesangial expansion [150], inflammation [151,152] and tubulointerstitial fibrosis [150,153]. The point at which these changes begin can be determined by expression of kidney injury molecule-1 (KIM-1), and pro-fibrotic genes such as collagen 1a1 (col1a1) and col3a1 [72,153]. *In vivo* it can be easily

detected by increased urinary protein excretion although the onset and severity of proteinuria can vary from 500mg/day only six weeks after STZ injection [154] to 60mg/day after four months [150]. Therefore, the time course of T1DM following STZ injection can be divided into distinct, well-defined pre-nephropathy and nephropathy phases, offering the possibility of translating to clinical T1DM functional changes in sodium excretion that precede albuminuria and expression of renal injury markers.

1.6.5 The relevance of the nephropathy phase to pre-nephropathy investigation

The nephropathy phase in STZ-induced T1DM has demonstrated that RAAS has a key pro-inflammatory and pro-fibrotic role [155,156] and induces mesangial expansion, podocyte damage and apoptosis [157], and generation of ROS [158]. Reductions in pathological glomerular remodelling with ACE inhibition [150] have been translated into treatment of clinical T1DM nephropathy. Similarly, the failure of ACE inhibitors to reverse glomerulosclerosis [150] agrees with the clinical findings of Lewis *et al.* [63], and emphasises the importance of intervention prior to the onset of nephropathy. However ACE inhibitors also fail to prevent nephropathy from developing in both STZ-induced T1DM rats and in non-albuminuric T1DM patients [159-161]. This lack of success probably reflects the large number of signalling pathways that contribute to T1DM nephropathy, and changes in the degree to which individual pathways contribute over time. These factors likely apply to most therapies. As a consequence, the development of novel therapeutic agents, such as SGLT2 inhibitors, seeks to complement rather than replace ACE inhibitor therapy.

In 2009, Gagliardini *et al.* [150] adopted this strategy by administering the ACE inhibitor lisinopril and the selective ET_A receptor antagonist avosentan to STZ-induced T1DM rats in the post-nephropathy phase. Not only did this combination reduce glomerular pathology and albuminuria, glomerular remodelling was, for the first time, reversed. Just four years after the publication of this paper, a Phase 3 clinical trial of the selective ET_A receptor antagonist, atrasentan, began in patients with T2DM diabetic nephropathy (SONAR) [162]. To determine whether the benefits of ET_A receptor antagonists extend to a much earlier stage of T1DM, this thesis will investigate the role of the renal endothelin system in the pre-nephropathy phase and its contribution to the risk of nephropathy and CVD.

1.7 The endothelin system

1.7.1 Endothelin-1

ET-1 was first identified in 1988 as an extremely potent vasoconstrictor released by endothelial cells [163]. The concept that maintenance of vascular tone was endothelium-dependent was not new at the time [118]. However, ET-1 was the first endothelium-derived vasoconstrictor to be identified. Since its discovery, it has naturally attracted a great deal of interest as a major player in CVD and hypertension. Initially considered as universally deleterious, it is now clear that ET-1 is important in homeostasis and organogenesis as well as in pathological states. Although first identified as a vasoactive peptide released by endothelial cells, it likely plays a crucial role in long-term regulation of BP through its effects within the renal collecting duct [77]. ET signalling also plays a pivotal role in glomerular injury and remodelling, and the subsequent development of CKD in both diabetic and non-

diabetic states. For this reason, ET receptors are now considered a viable therapeutic target, along with RAAS, in the long-term management of diabetic nephropathy.

1.7.2 Physiology of the endothelins

The ETs exist as three peptides– ET-1, ET-2 and ET-3. Each is 21 amino acids long [164]. ET-1 is the predominant ET expressed in the vasculature [163] and although ET-2 and ET-3 are also present within the renal microvasculature and can regulate afferent and efferent arteriolar tone, ET-1 is the most potent [165,166]. The majority of publications on the role of ET in diabetic nephropathy relate to ET-1, so the remainder of this thesis will focus on this isoform.

ET-1 is generated by a series of peptidase-mediated conversions of a prepropeptide. The immediate precursor, big ET-1, is an inactive 38 amino acid peptide that is rapidly converted into the smaller active peptide, ET-1 [167], by endothelin converting enzymes (ECEs), chymase or neutral endopeptidase. Any overspill of big ET-1 into the circulation is largely inactive with only 10% of ET-1's biological activity [168]. Although newly formed ET-1 can be stored temporarily in intracellular vesicles [169], it is more usually secreted immediately after translation. The circulating half-life of ET-1 is limited to ~one minute [170] because of rapid clearance by pulmonary, splanchnic and renal circulations [171-173] and local degradation by neutral endopeptidase [172]. Thus, ET-1 is generally considered as an autocrine or paracrine mediator rather than a systemic hormone.

1.7.3 Endothelin receptors

ET receptors have been intensively researched and, despite alternatives to blocking the effects of ET-1, such as ECE inhibition [174], ET receptors currently remain the most investigated therapeutic target for manipulation of the ET system. ET-1 binds to two G-protein-coupled receptors, ET_A and ET_B, which often mediate opposing effects. This is exemplified by the biphasic change in BP after iv. bolus injection of ET-1 first observed by Yanagisawa *et al.* in anaesthetised rats [163]. A transient depressor response occurs as ET-1 binds to ET_B receptors on endothelial cells, triggering local release of vasodilatory NO and prostacyclin [77]. This is followed by a prolonged hypertensive response due to ET-1 binding to ET_A receptors (or less frequently ET_B receptors) on vascular smooth muscle cells (VSMCs), inducing inositol trisphosphate-dependent contraction [77]. Webb and Haynes showed that potent ET-1/ET_A receptor-mediated vasoconstriction plays an important homeostatic role in maintaining basal vascular tone when they demonstrated vasodilation and up to 64% increased blood flow in the forearm after infusing an ET_A receptor antagonist into the brachial artery of healthy subjects [168]. ET-1/ET_B receptor-mediated vasodilation serves to dampen this effect.

Crucially, if attempting to determine whether renal ET-1 is important in initiating T1DM nephropathy, it is necessary to understand that the source of ET-1 that regulates BP is not simply the endothelium (Fig.1.1). For example, transgenic mouse models over-expressing ET-1 do not develop hypertension, even when plasma ET-1 is elevated, and develop only moderate salt-sensitive hypertension [175,176]. It has emerged that ET-1 regulates BP from the renal collecting duct but can also modify

both the vascular and tubular components of acute pressure natriuresis from multiple sites within the kidney.

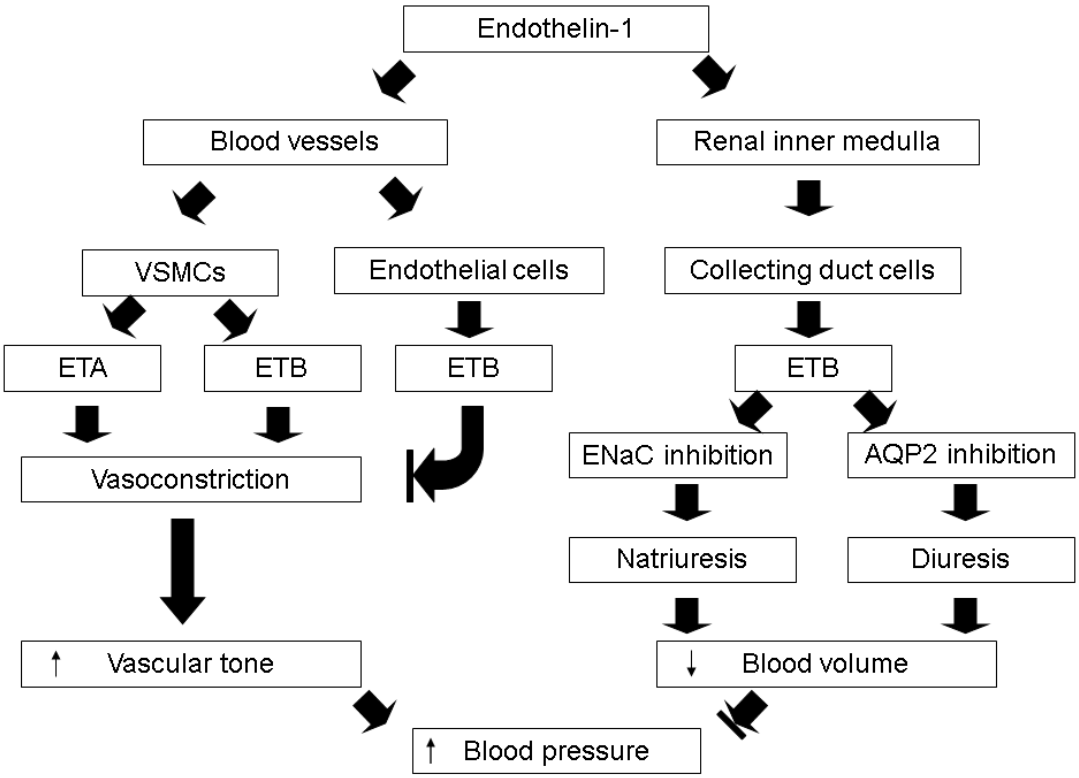

Fig. 1.1. The role of vascular and renal endothelin-1 (ET-1) and its receptors in blood pressure (BP) homeostasis

ET-1 regulates BP through its effects on vascular tone, and on sodium and water balance by regulating epithelial sodium channel (ENaC) and aquaporin-2 (AQP2) activity. Lines blocking arrows represent inhibition.

1.7.4 Regulation of blood pressure by collecting duct endothelin-1

Since its initial discovery in the vasculature, expression of ET-1 and its receptors has been identified ubiquitously within the body [77]. However, ET-1 is most highly expressed within the inner medullary collecting duct of the kidney [177] where it co-localises with ET_B receptors [178,179]. Transgenic mouse models have provided the best

evidence to date of the importance of ET-1/ET_B receptor signalling to BP homeostasis (Fig. 1.1). Collecting duct-specific ET-1 or ET_B KO mice develop salt-sensitive hypertension that can be rescued by selective inhibition of ENaC [180,181]. This means that ET-1 regulates BP by controlling activity of a sodium transporter known to be modified in T1DM. Thus, T1DM has the potential to modify the tubular sodium reabsorption phase of acute pressure natriuresis by modifying regulation of ENaC by ET-1.

1.7.5 Endothelin-1 in the renal vasa recta

The majority of studies on renal ET-1 have focused on the inner medullary collecting duct, where there is the greatest expression of ET-1, and the glomerulus, the obvious site of pathology in early diabetic nephropathy. More recently, there has been additional interest in the medullary zone between these two sites, which contains the *vasa recta* and the thick ascending limb of the loop of Henle. Each *vas rectum* is a single endothelial cell thick and supplies blood through the renal medulla. Best known for contributing to the counter current exchange mechanism that establishes medullary hypertonicity, the *vasa recta* are also conduits of the increased medullary blood flow that initiates acute pressure natriuresis.

Blood flow through the *vasa recta* is regulated at regular intervals along their length by contractile pericytes [182]. These mesenchymal cells respond to a variety of vasoactive peptides, including ET-1, by acting on ET_A receptors [183]. Their responsiveness can be modified by factors released from the thick ascending limb (tubulovascular crosstalk) [184], allowing the *vasa recta* to autoregulate their flow [185]

and contribute to the shifts in cortico-medullary blood flow that precede acute pressure natriuresis [138]. The exact relationships between *vasa recta*, tubules and pericytes have not been fully defined but, clearly, regulation of pericyte constriction by ET-1/ET_A has the potential to influence the acute pressure natriuresis response by reducing medullary blood flow.

1.7.6 Endothelin-1 in the glomerulus

ET-1 and its receptors are expressed by endothelial cells, podocytes and mesangial cells within the glomerulus. Studies in juxtamedullary nephrons have identified ET_A, and endothelial and VSMC ET_B receptors within afferent and efferent arterioles. This suggests not only an important role in glomerular autoregulation [165,166,186], but also regulation of medullary perfusion, acute pressure natriuresis and subsequently, BP [187].

1.7.7 Glomerular endothelin-1 and Type 1 diabetic nephropathy

There is now a wealth of additional *in vivo* and *in vitro* evidence that glomerular, and subsequently tubular, ET-1 contributes heavily to progressive loss of renal function in T1DM by mediating cellular injury, inflammation [154,188-195], mesangial expansion and fibrosis [50,196-198] as well as through synergism with RAAS [199-203].

In STZ-induced T1DM rats, glomerular expression of ET-1 increases as nephropathy develops [204] and urinary ET-1 excretion is increased by six weeks after STZ injection. Increased glomerular ET-1 expression by podocytes, endothelial cells [205] or inflammatory cells [206-208] leads to glomerulosclerosis and interstitial fibrosis [176].

Since urinary ET-1 is entirely renally derived [209], measurement of urinary ET-1 can be used, in addition to albuminuria, to mark when the pre-nephropathy phase of T1DM ends and the nephropathy phase begins.

1.7.8 Endothelin-1 in Type 1 diabetic rodent models

The wide-ranging effects of renal ET-1 during the nephropathy phase of T1DM are summarised in Fig. 1.2 but are beyond the scope of this thesis. However, selective ET receptor antagonism in non-diabetic and T1DM rodent models suggests that most of the deleterious effects of ET-1 on renal function are mediated by ET_A rather than ET_B receptors. In STZ-induced T1DM rodents, both ET_A and ET_B receptors mediate podocyte injury in T1DM [210] but only selective ET_A receptor antagonists have anti-inflammatory and anti-fibrotic effects. They attenuate severe urinary protein loss, expression of inflammatory markers intercellular adhesion molecule-1 (ICAM-1) and monocyte chemotactic protein-1 (MCP-1), macrophage infiltration, and urinary excretion of markers of transforming growth factor-β-1 (TGF-β1, pro-fibrotic) and prostaglandin E_2 (PGE_2, pro-inflammatory) expression [154].

Gagliardini *et al.* combined a selective ET_A receptor antagonist with an ACE inhibitor in their landmark study [150] because earlier work had shown that ACE inhibition halved the rise in glomerular ET-1 messenger ribonucleic acid (mRNA) by 24 weeks after STZ injection [211]. Two years after simultaneous ACE inhibition and ET_A receptor antagonism had been shown to completely reverse proteinuria and glomerulosclerosis, and restore renal blood flow in STZ-induced T1DM Sprague Dawley rats [150], Saleh *et al*. demonstrated that more severe urinary protein loss in

early STZ-induced T1DM could be attenuated by selective ET_A or non-selective ET receptor antagonism without ACE inhibition [154]. Ironically, having firmly established these effects by antagonising the most potent vasoconstrictor known, and justifying progression to clinical studies, the haemodynamic contribution to reversal of diabetic nephropathy following endothelial ET receptor antagonism remains unknown.

1.7.9 The potential for endothelin receptor antagonists to prevent nephropathy in Type 1 diabetes mellitus: pre-clinical evidence

DCCT/EDIC has demonstrated the importance of early intervention in T1DM to reduce cardiovascular risk. Albuminuria is a significant risk factor for CVD in T1DM, so any therapeutic agent that can reduce albuminuria clinically is likely to be trialled at earlier and earlier stages of T1DM nephropathy. The SONAR study [162] has been investigating the clinical benefits of the selective ET_A receptor antagonist, atrasentan, in patients with T2DM. The study was recently stopped, as a consequence of study design rather than an adverse effect of atrasentan. However, even if reductions in albuminuria and cardiovascular risk can be demonstrated, the synergy between RAAS and ET-1 [211], and the failure of ACE inhibitors to prevent the development of nephropathy in T1DM patients [159-161], suggest that ET receptor antagonists are unlikely to lower CVD risk or prevent progression of very early nephropathy unless ET-1 plays a key role in hyperfiltration. Based on studies that demonstrate loss of nocturnal dipping prior to nephropathy, this means that ET_A receptor antagonists would have to promote acute pressure natriuresis.

In most rodent models of renal hyperfiltration, with or without hypertension, ET_A receptor antagonism does not appear to minimise renal injury by modifying GFR. Although proteinuria, glomerular hyalinisation and glomerulosclerosis are reduced in association with reductions in BP in DSS rats [212], podocyte injury is still observed in DSS rats when BP is reduced with hydralazine [213]. Furthermore, glomerular injury and inflammation, and interstitial fibrosis can be prevented by ET_A receptor antagonists without reductions in BP, even when ET-1 is infused or overexpressed [176,214-216]. The conclusion from these models is that ET_A receptor antagonists minimise renal injury by anti-inflammatory and anti-fibrotic effects and not by modifying hyperfiltration.

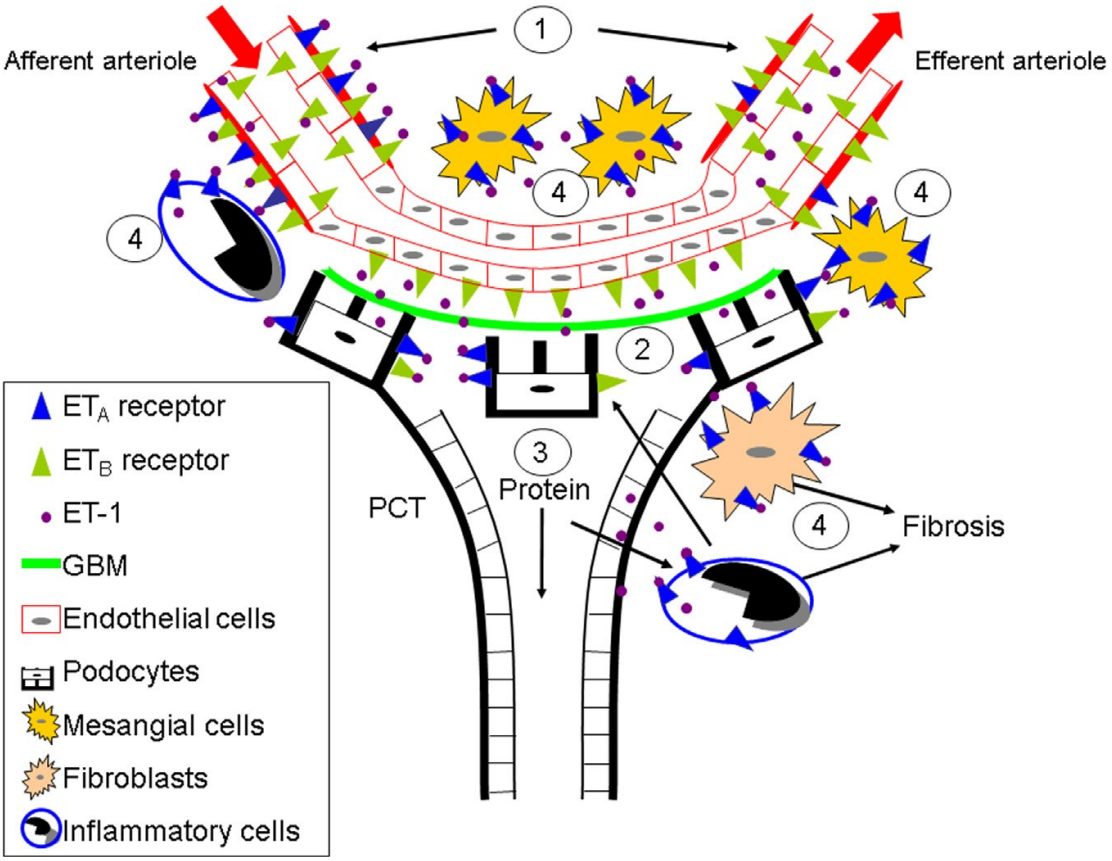

Fig. 1.2. Schematic diagram of the pathogenesis of nephropathy in Type 1 diabetes mellitus (T1DM) and the potential role of endothelin-1 (ET-1) and its receptors

(1) In hyperfiltration, glomerular autoregulation fails to protect the glomerulus from the systemic vascular load. In this diagram, ET-1–mediated afferent arteriolar constriction and efferent arteriolar dilatation are inadequate.

(2) Components of the glomerular filter, such as the glomerular basement membrane (GBM), are injured by hyperfiltration and inflammation. Podocyte injury is mediated by ET_A receptors but also ET_B receptors, and allows proteins to leak into the proximal convoluted tubule (PCT).

(3) Proteins in the PCT initiate an inflammatory cycle mediated by ET_A receptors, which leads to further podocyte damage.

(4) The inflammatory response with activated mesangial cells and interstitial fibroblasts leads to deposition of matrix proteins and fibrosis.

1.7.10 The potential for endothelin receptor antagonists to prevent nephropathy in Type 1 diabetes mellitus: clinical evidence

Results from clinical studies of ET receptor antagonists in diabetic nephropathy mirror much of the pre-clinical data. They demonstrate reductions in urinary albumin excretion, suggesting that glomerular injury and remodelling are slowed or reversed [217-219]. The majority of trials have recruited only patients with T2DM. However, in the first Phase 2 clinical study, approximately half of 286 diabetic patients had T1DM [220]. Despite no effect on creatinine clearance and BP, the higher doses of avosentan used in this study were associated with a 12% incidence of peripheral oedema.

Although hepatotoxicity has been reported in small numbers of patients receiving sulphonamide-based ET receptor antagonists [221], sodium and water retention, resulting in oedema has consistently proved problematic to their clinical development [222], and has even led to premature termination of a Phase 3 clinical trial [223]. The degree of salt and water retention that occurs appears to be dose-related [220,224] but has been sufficient to postpone clinical development of the drug class in heart failure, in which patients are already prone to oedema.

The most frequently cited explanations for sodium and water retention are inadequate ET_A:ET_B receptor selectivity and inappropriately high dose rates that lead to off-target antagonism of ET_B receptors in the collecting duct and loss of inhibition of ENaC [181,222]. This mechanism would profoundly impair acute pressure natriuresis [225]. Unsurprisingly, therefore, when the highly selective ET_A receptor antagonist,

sitaxentan (ET_A:ET_B selectivity ~6,000:1) was used in a randomised, three-way, double-blind crossover study in patients with non-diabetic CKD, sodium and water retention was not observed. What was not expected was that nocturnal dipping in BP also recovered with sitaxentan but not with the calcium channel blocker, nifedipine [226]. This suggested that sitaxentan did not achieve its effect by lowering vascular resistance but rather by enhancing acute pressure natriuresis. Furthermore, it means that the pre-clinical studies mentioned above (in which podocyte injury is not reduced by arteriodilation [213], and renal injury is prevented by ET_A receptor antagonists without apparently reducing BP [176,214-216]) are not valid predictors of the effect of ET_A receptor antagonists on regulation of BP and hyperfiltration. This conflict between pre-clinical and clinical data illustrates the clear need to measure the effect of selective ET_A receptor antagonists on acute pressure natriuresis in both diabetic and non-diabetic states.

The clinical development of novel classes of drug is costly and, with various setbacks at an advanced stage, including the recent early termination of SONAR, development of ET receptor antagonists has proved no exception. Despite extensive, encouraging pre-clinical and clinical data, Phase 3 clinical trials have failed to lead to approval from the US Food and Drug Administration (FDA) for use of these agents in patients with hypertension or diabetic nephropathy. As well as issues with study design, one of the principal reasons for this has been the sodium and water retention they can cause. To date, the FDA only approves the use of ET receptor antagonists for scleroderma digital ulcers and pulmonary arterial hypertension [227]. In the case of the latter, ET receptor antagonism has a higher cost:benefit ratio than the use of

phosphodiesterase-5 inhibitors [228], and with many ET_A receptor antagonists close to losing their patent protection [227], the financial incentive to pharmaceutical companies to invest in further costly clinical trials is rapidly waning. Measuring the effect of selective ET_A receptor antagonism on acute pressure natriuresis is likely to make a significant contribution to understanding, and therefore, combatting, sodium and water retention, and determining the potential of this drug class to prevent T1DM nephropathy and reduce cardiovascular risk. Without this information, and with the limitations to what can be gleaned from SONAR, it will be difficult to assess whether savings made from reduced CVD risk and ESRD will offset the costs of additional clinical development of ET_A receptor antagonists in T1DM, their prolonged use from an early stage of T1DM, and the treatment of associated sodium and water retention.

1.8 Summary

Cardiovascular risk is increased in T1DM. Tight control of blood glucose increases the risk of life-threatening hypoglycaemia and does not eliminate increased cardiovascular risk, so alternative therapies are required that target risk factors for CVD.

Nephropathy and hypertension are major risk factors for CVD in T1DM and are intimately linked. Failure of BP to dip at night is a precursor to nephropathy and implicates impaired acute pressure natriuresis, yet the effect of T1DM on acute pressure natriuresis has not been fully determined in T1DM animal models.

ACE inhibitors have important beneficial anti-inflammatory and anti-fibrotic effects that reduce but do not reverse progression of diabetic nephropathy, and they have limited ability to modify acute pressure natriuresis. A relatively new class of agent, the ET receptor antagonists, exerts similar remodelling effects. When given with ACE inhibitors, they can reverse renal fibrosis in animal models, but when administered clinically, reductions in proteinuria can be offset by sodium and water retention.

ET-1 induces profound vasoconstriction via ET_A receptors but the consequences of ET_A receptor antagonism on acute pressure natriuresis are unknown. Understanding the effect of T1DM and ET receptor antagonists on acute pressure natriuresis is paramount to combatting sodium and water retention and determining whether ET_A receptor antagonists might reduce the risk of CVD and nephropathy during the crucial period of early T1DM, at a significant cost:benefit ratio.

1.9 Hypotheses and aims

1.9.1 Hypotheses

1) Pressure natriuresis is impaired in early T1DM, prior to the onset of established nephropathy, and is associated with elevated BP.
2) The mechanism underlying this impairment is an ET_A-receptor-mediated blunting of medullary perfusion which can be reversed with insulin and ET_A receptor antagonism.

1.9.2 Aims

1) To adapt a protocol for measuring acute pressure natriuresis so that it can be applied to an STZ-induced rat model of early T1DM
2) Using this protocol, to measure the effect of early T1DM on acute pressure natriuresis and determine whether it can be reversed with insulin.
3) To determine whether changes in acute pressure natriuresis due to T1DM are reflected in changes in BP and its circadian rhythm
4) To identify the role of ET-1 in acute pressure natriuresis, the receptors that mediate this role, and determine whether it is modified by early T1DM and insulin.

2 Methods

2.1 Generation of a rat model of T1DM

2.1.1 Animals

All animal experiments were performed in adult male Sprague Dawley rats. Following purchase and transfer from Charles River Laboratories, Tranent, United Kingdom (UK), rats (250-300g) were acclimatised for a minimum of six days. They were housed under a 12-hour light cycle (lights 7am-7pm), at 21±1ºC and 50% humidity, within Phase 2 of the University of Edinburgh Biomedical Research Facility, Little France, Edinburgh, UK. Standard chow (0.25% sodium) and water were offered *ad libitum*.

All procedures, assays and measurements were performed single-blind under a UK Home Office licence, following local approval by a University of Edinburgh veterinary surgeon. Euthanasia was performed by a Schedule one technique, either exposure to a rising concentration of carbon dioxide gas followed by cervical dislocation, or overdose of general anaesthetic followed by confirmation of cessation of circulation.

2.1.2 Induction of Type 1 diabetes mellitus

Type 1 diabetes mellitus (T1DM, blood glucose >12mmol/l) was induced with one (30mg/kg) or two (additional 15mg/kg 48 hours later) intraperitoneal (ip.) injections of streptozotocin (STZ, 50mg/mL in 0.1M fresh, chilled citrate buffer [129]; Sigma-Aldrich Company Ltd, Gillingham, UK). Blood glucose was measured by a test strip and glucometer (Accu-Chek; Roche Diagnostics Ltd. (Limited), Burgess Hill, UK) 48 hours after the first STZ injection (Fig. 2.1). Rats only received a

second injection of STZ if the blood glucose was <12mmol/l. To confirm diabetic status throughout, blood glucose was measured again seven days after the first STZ injection and at the end of the experimental procedure. Rats, in which normoglycaemia was re-established, were euthanased (Chapter 2.1, page 46) and not included in data analysis.

2.1.3 Control rats

Non-diabetic control rats received a single ip. injection of citrate vehicle. Blood glucose was measured 48 hours later (Fig. 2.1) and at the end of the experimental procedure.

2.1.4 Insulin-treated diabetic rats

Selected experiments included a third cohort of insulin-treated T1DM rats (T1DM+insulin). One slow-releasing insulin pellet (LinShin, Toronto, Canada) was implanted subcutaneously (sc.) into T1DM rats under brief general anaesthesia with isoflurane (IsoFlo; Zoetis Animal Health Ltd, Sandwich, UK), seven days after the first STZ injection (Fig. 2.1). Blood glucose <12mmol/l from a tail nick sample two and four days after implantation confirmed an appropriate response to insulin. Rats whose blood glucose was >12mmol/l by four days after implantation were euthanased (Chapter 2.1, page 46).

.

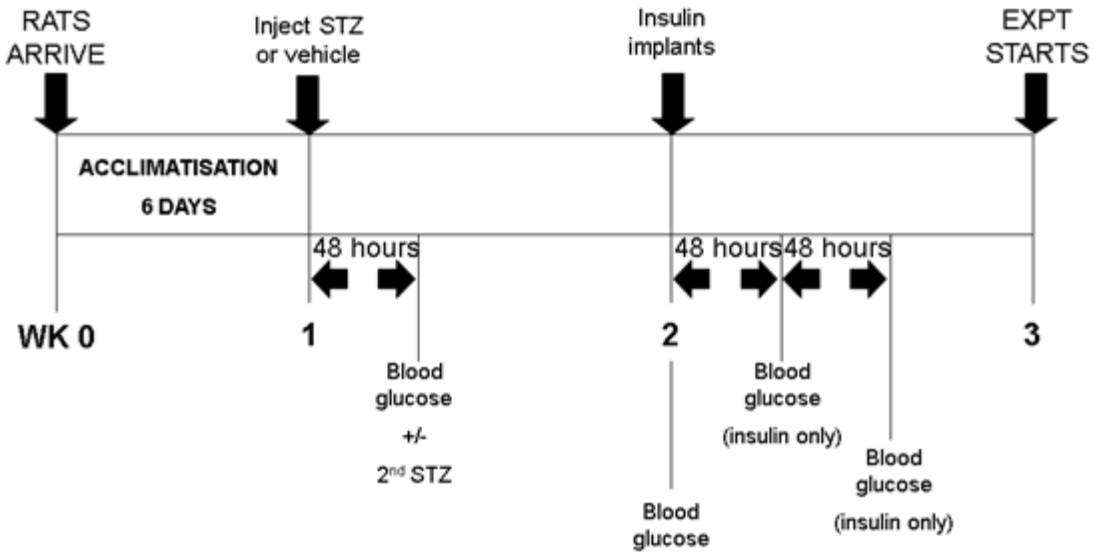

Fig. 2.1. Timeline for generation of control, diabetic and insulin-treated diabetic rats

Time points for streptozotocin (STZ) injections, inserting insulin implants and measuring blood glucose are shown, WK=week, EXPT=experiment.

2.2 *In vitro* studies: collection of urine and renal tissue

2.2.1 Urine collection

Control, T1DM and T1DM+insulin rats were removed from normal housing to metabolic cages for 24 hours. Every metabolic cage consisted of a wire mesh floor with *ad libitum* access to food and water, a collection system to prevent contamination of urine with spillage from the drinking water, and separate urine and faecal collecting tubes. After 24 hours, rats were returned to standard cages. Volumes of water consumption and urine production were recorded. Urine was frozen at -80ºC for future analysis.

2.2.2 Renal tissue collection

Whole animal perfusion-fixation was performed within 72 hours of rats returning from metabolic cages.

Each rat was anaesthetised with ip. thiopental (50mg/ml, 50mg/kg; Archimedes Pharma, Reading, UK) and maintained with inhalational isoflurane (IsoFlo; Zoetis Animal Health Ltd) administered via face mask (Fig. 2.2A, B). The rat was placed in dorsal recumbency onto a heat pad, with the head pointing away from the operator (Fig. 2.2B). A digital rectal thermometer was inserted and body temperature maintained at 38-39ºC by manually adjusting the power output of the heat pad. The ventrum was clipped and the abdomen entered by a midline coeliotomy from the costal arch to just cranial to the pubis (Fig. 2.2B).

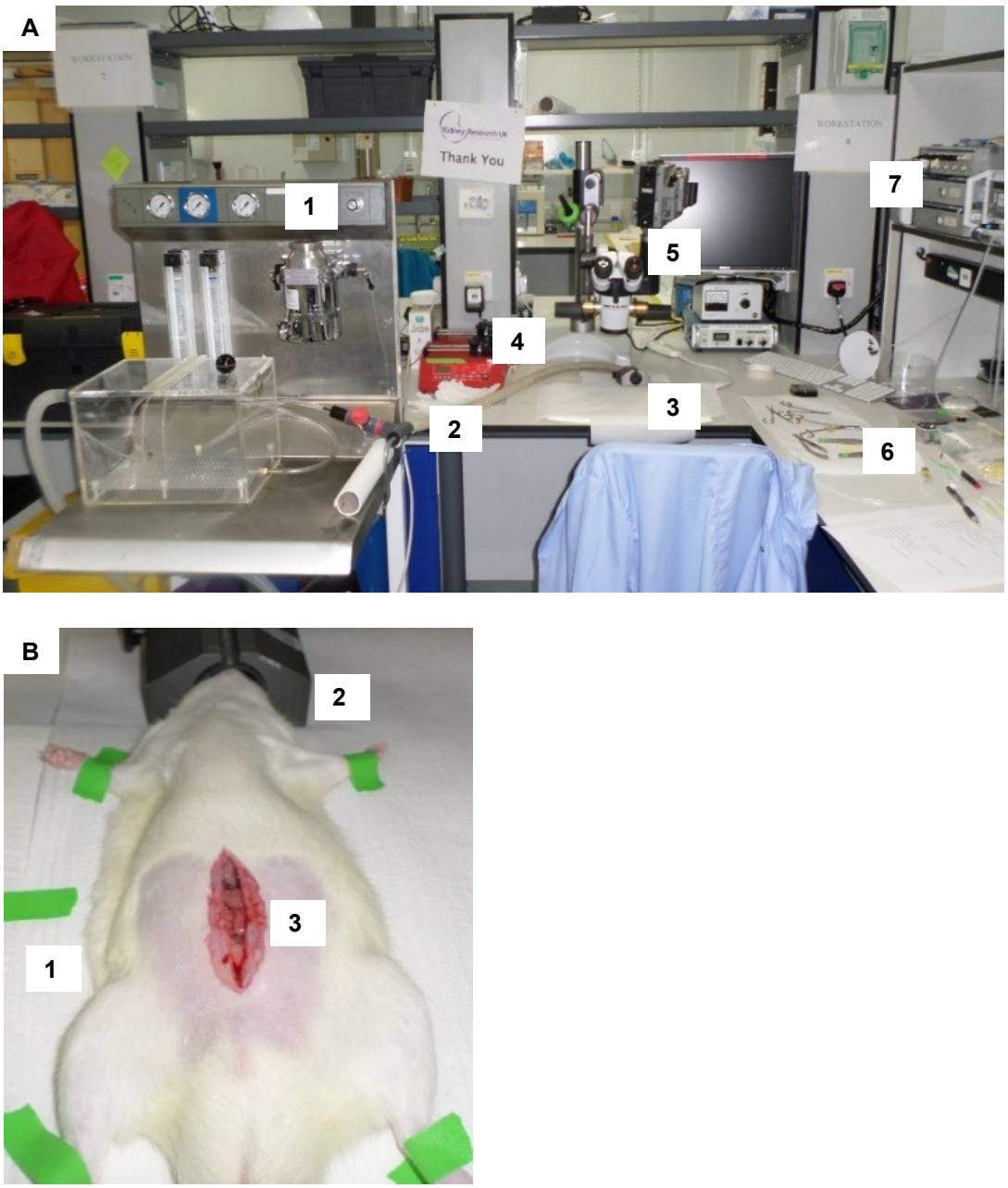

Fig. 2.2. Equipment set-up and animal positioning

A) Anaesthetic machine (1) and circuit (2), heat pad (3), syringe drivers (4), dissecting microscope (5), instruments (6) and data acquisition system (7)

B) The rat is taped to paper towel on a heat pad (1), with its head in a weighted anaesthetic mask (2). Abdominal contents are just visible through a midline coeliotomy (3).

The abdominal contents were gently displaced manually and the left kidney exposed through gentle, blunt dissection. The renal artery and vein were simultaneously ligated with 0.17mm silk suture thread (4/0; Interfocus, Linton, UK; Fig. 2.3A). The left kidney was removed without delay (Fig. 2.3B) and placed onto a tile kept cold by dry ice. The kidney immediately adhered to the tile and was sectioned sagittally, the uppermost half then being flipped onto the cold tile (Fig.2.3C). With both halves of the left kidney now adhered to the tile, the cortex of each half was identified and sectioned with a scalpel blade using three straight cuts (Figs. 2.3D, E). Following additional trimming to minimise the amount of residual cortex, the medulla of each half was sectioned approximately sagittally in a single cut (Fig.2.3F). All tissues were immediately wrapped into tin foil, placed into 2ml Eppendorfs, snap-frozen in dry ice and transferred to a freezer for storage at -80ºC.

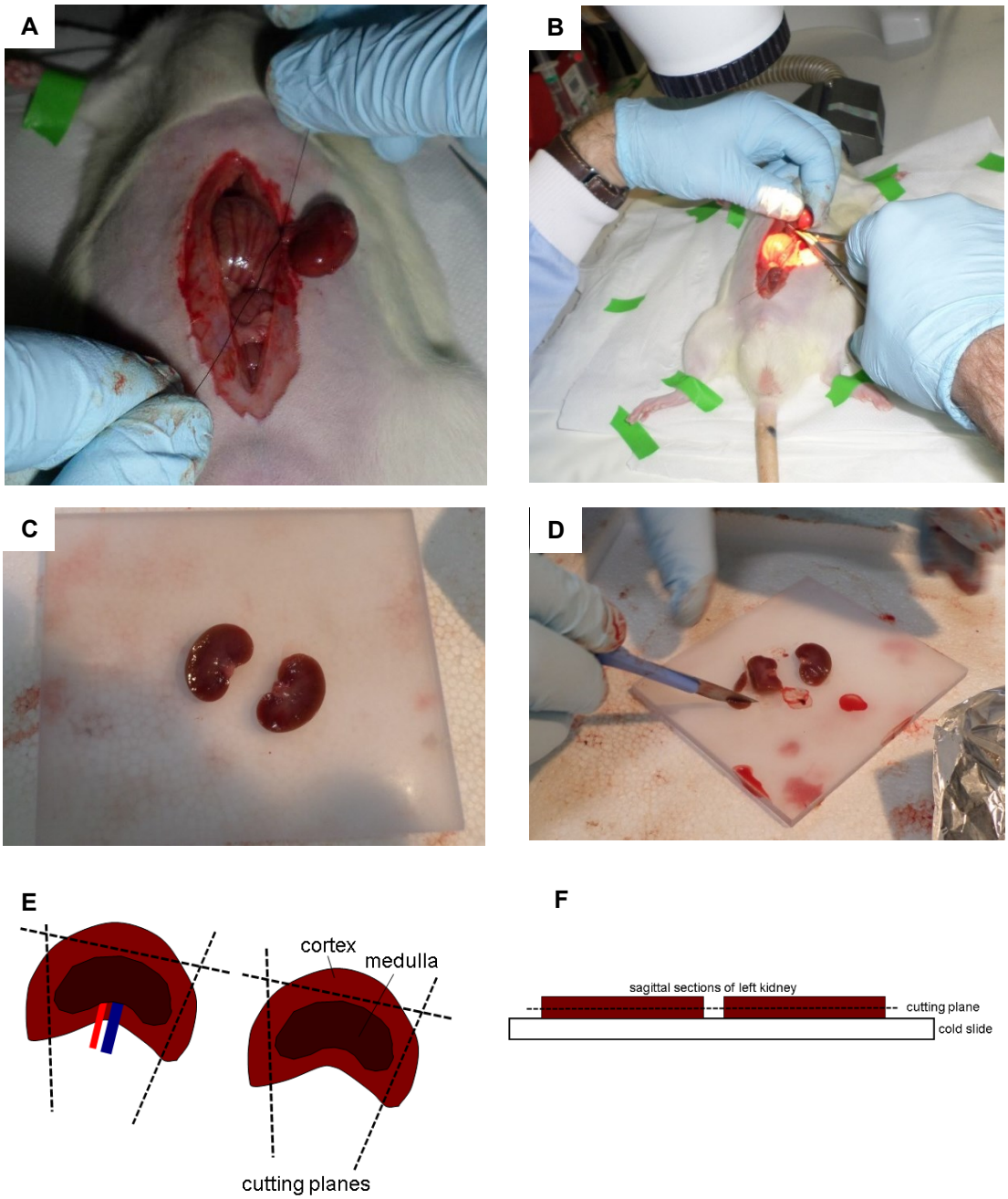

Fig. 2.3. Removal and preservation of the left kidney

A) The kidney was exposed and the renal artery and vein ligated.

B) The renal artery and vein were clamped distal to the ligature and the kidney removed.

C) The kidney was sectioned sagittally on a cold tile.

D) Samples of cortex and medulla were removed.

E) Schematic diagram showing cutting planes for removal of cortex

F) Schematic diagram showing cutting planes for removal of medulla

The distal aorta was identified and carefully dissected away from the caudal vena cava just cranial to the trifurcation, using straight DeBakey forceps and cotton buds. Once freed, the distal aorta was ligated with silk with the free ends of the ligature kept long. A straight vessel clip (1.5 x 8mm, World Precision Instruments, Hitchin, UK) was placed across the aorta approximately 1cm cranial to the ligature, and a second ligature placed in between but not tightened. The aorta was then penetrated between the two ligatures by a bent 23-gauge needle. Polythene tubing, 0.86mm internal diameter and 1.27mm outer diameter (P90; Smiths Medical, Ashford, Kent), with a closed three-way tap on one end, was inserted through the arteriotomy into the aortic lumen and advanced up to the clamp (Fig. 2.4A). The cranial ligature was now tightened around the aorta (and tubing) and the long ends of the first ligature tightened around the tubing (Fig. 2.4B). The clamp was then released slowly, ensuring there was no haemorrhage.

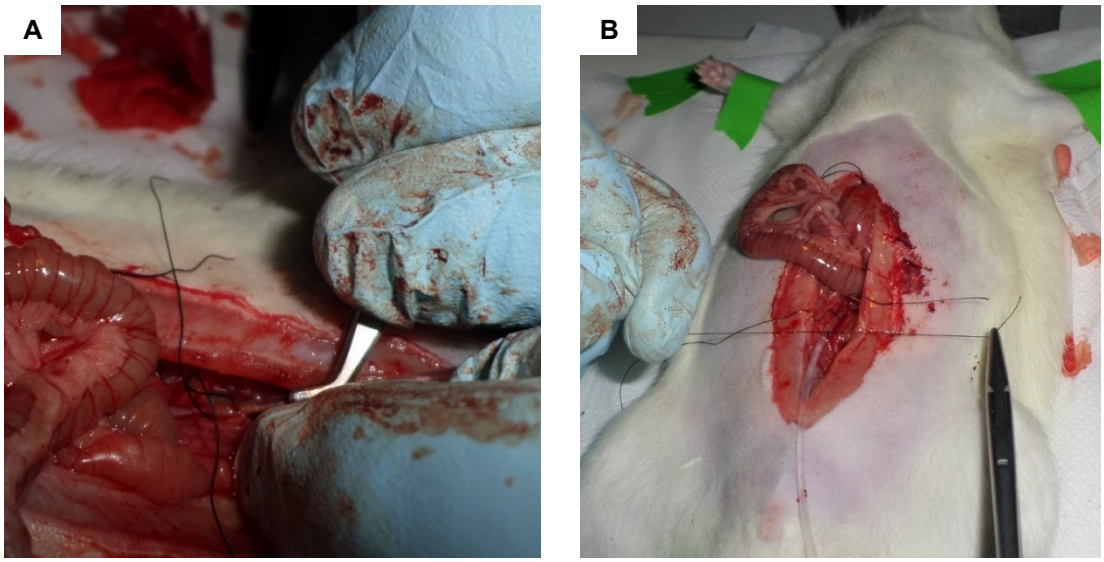

Fig. 2.4. Cannulating the distal aorta

A) The polythene tubing was inserted into the aorta with cannulation forceps.

B) The tubing was secured by two ligatures.

Immediately following aortic cannulation, the rat was transferred to a fume cupboard (Fig. 2.5A), where anaesthesia was maintained. A 500ml bag of medical 0.9% saline (Aqupharm Number 1; Animalcare Ltd, York, UK; Fig. 2.5B) was then connected to the three-way tap through a standard intravenous (iv.) giving set (Aqupharm). At the instant this was connected, the caudal vena cava was cut and saline forced through the iv. line by a blood pressure (BP) cuff and sphygmomanometer placed around the saline bag and inflated to 180mmHg [229]. Blood was swabbed with paper towel as the rat exsanguinated into its abdomen. The time to the liver turning clear (target within three minutes) was recorded. After exactly three minutes, 4% paraformaldehyde (PFA) was forced through a separate iv. line connected to the same three-way tap, as described for the saline. The time to fixation tremors (target within one minute) was recorded. After an additional three minutes, the rat was checked for rigidity, and the PFA infusion was stopped. The right kidney was then removed (Fig. 2.5C), sectioned sagittally (Fig. 2.5D) and stored in fresh 4% PFA, which was changed after 24 hours. After an additional 72 hours, the kidney was transferred to 70% ethanol and stored at 4ºC until histological processing.

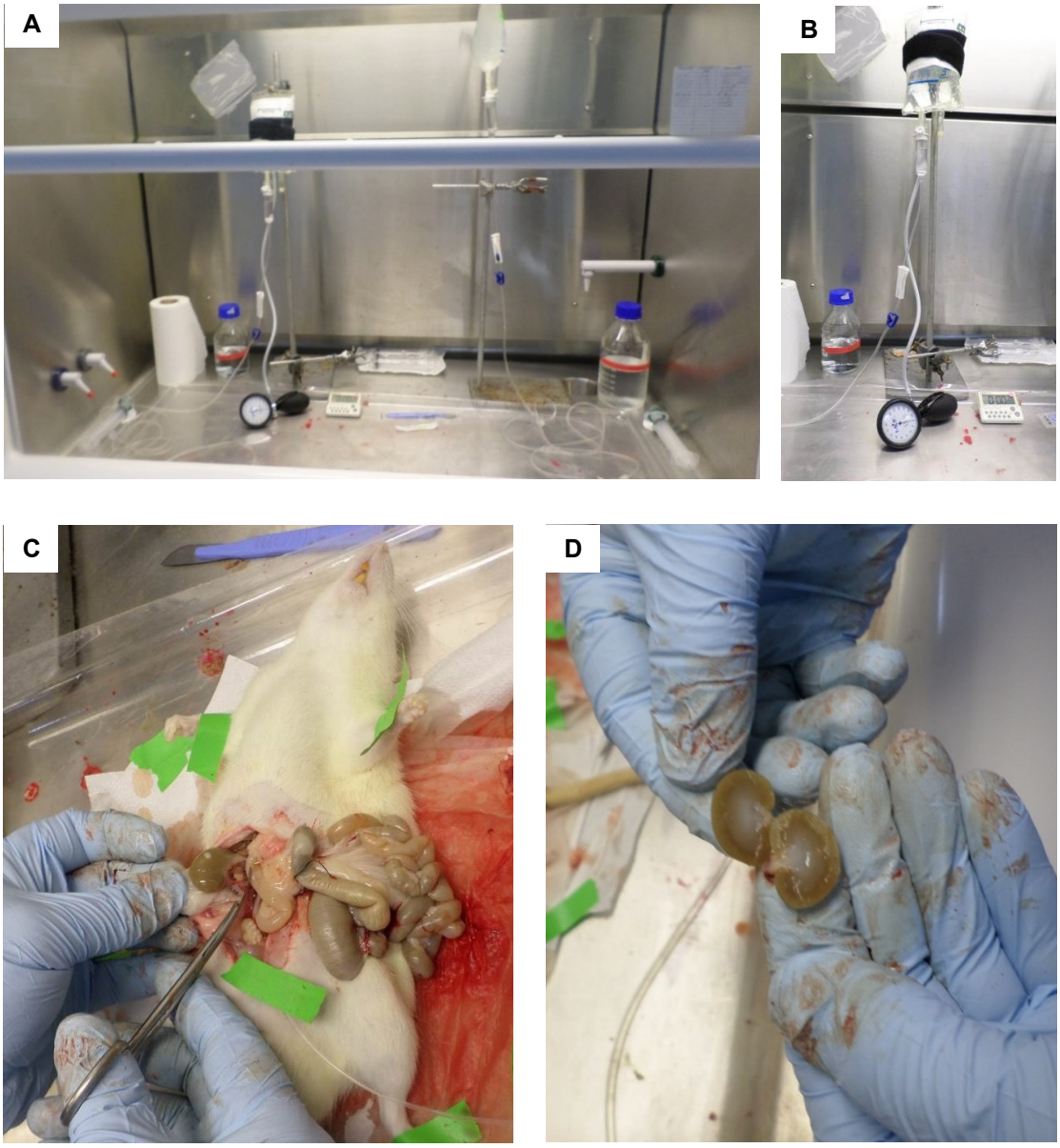

Fig. 2.5. Whole animal perfusion-fixation with paraformaldehyde (PFA)

A) The rat was transferred to a fume cupboard.

B) Pressure for PFA infusion through a giving set came from a blood pressure cuff around a fluid bag.

C) After exsanguination and fixation, the pale right kidney was removed.

D) The right kidney was sectioned sagittally, prior to immersion in PFA.

2.3 *In vitro* studies: urine assays

2.3.1 Urine biochemistry

To determine glomerular integrity in relation to glomerular filtration rate (GFR), urinary albumin and creatinine concentrations were measured by Dr. Forbes Howie, University of Edinburgh, on a Cobas Fara centrifugal analyser (Roche Diagnostics Ltd.) using adapted commercial kits based on immunoturbidimetric (Microalbumin Kit; Olympus Diagnostics Ltd, Watford, UK) and creatininase/creatinase specific [230] enzymatic (Alpha Laboratories Ltd., Eastleigh, UK) methods. Albumin was indexed to creatinine.

2.3.2 Aldosterone assay

Activity of the renin-angiotensin-aldosterone system (RAAS) was determined from urinary aldosterone concentrations measured by Dr. Christopher Kenyon, University of Edinburgh, with an in-house enzyme-linked immunosorbent assay (ELISA) [231]. Aldosterone was indexed to urinary creatinine.

2.3.3 Endothelin-1 assay

Urinary endothelin-1 (ET-1) concentrations were measured by a sandwich ELISA (Biomedica Medizinprodukte, Vienna, Austria). Samples were added to wells pre-coated with mouse anti-ET-1 detection antibody. Additional detection antibody was added, followed by an anti-mouse immunoglobulin G (IgG)-horse radish peroxidase conjugate and then a chromogenic substrate which turned the solution yellow. Using a monochromator-based microplate reader (Infinite M1000 Pro; Tecan Group Ltd., Männedorf, Switzerland), absorbance of light of wavelength 450nm was measured

for each sample and referenced to 630nm. ET-1 concentrations were calculated from the equation of a contemporaneous standard curve of absorbance against six standard solutions of known concentrations of ET-1 ranging from 0-10 fmol/l (R^2>0.9) and provided by the manufacturer. All measurements were performed in duplicate.

2.4 *In vitro* studies: quantitative real-time polymerase chain reaction

2.4.1 Total ribonucleic acid extraction

Snap-frozen renal cortex and medulla were placed on a Petri dish mounted on a bed of dry ice. Samples approximately 2mm^3 in size were cut using a scalpel blade cooled in dry ice. Harvested tissue was placed into 2ml nuclease free tubes containing 5mm stainless steel beads (Qiagen, Manchester, UK) and a lysis buffer (RLT plus buffer; Qiagen) before being pulverised for two minutes at 30Hz in a mixer mill (MM301; Retsch UK Limited, Hope, UK). Ribonucleic acid (RNA) was then extracted using a commercial kit (RNA Easy Plus Mini Kit; Qiagen) in which genomic deoxyribonucleic acid (gDNA) was removed with an extractor column and RNA was isolated with an ethanol-based protocol, according to manufacturer's instructions.

The yield of total RNA was determined from absorbance of 260nm during spectrophotometry (Fig. 2.6A; Nanodrop 1000; Thermo Scientific, Wilmington, United States (US)) and the purity by the ratio of 260:230nm absorbance (>1.8 of acceptable purity; Fig. 2.6B).

Samples were assessed for RNA degradation by the ribosomal RNA 28S:18S ratio. 2µl RNA were mixed with 2µl cyanine dye (SYBR safe; ThermoFisher Scientific Inc, Glasgow, UK) and 8µl RNAse-free water (ThermoFisher Scientific Inc) and separated through a trisaminomethane (Tris) borate EDTA gel by electrophoresis (90V for 30 minutes). Gels were inspected under ultraviolet light and the 18S and 28S bands assessed subjectively, with a ratio of intensity of around 2:1 being acceptable. Extracted RNA was stored at -80ºC before further processing.

2.4.2 Reverse transcription

Stored RNA samples were thawed on ice. 1000ng of RNA were pipetted into nuclease free Eppendorfs. The volume required for each sample was calculated according to the following equation and made up to 12µl with RNAse-free water:

$$\text{Volume RNA (µl)} = \frac{1000}{\text{concentration of RNA (ng/ml)}}$$

gDNA was eliminated by incubation with a DNAse at 42ºC for two minutes before transfer back to ice. First-strand complementary DNA (cDNA) was reverse transcribed with a buffered reverse transcriptase-random primer mastermix (Quantitect; Qiagen). cDNA was stored at -20ºC before further processing.

A

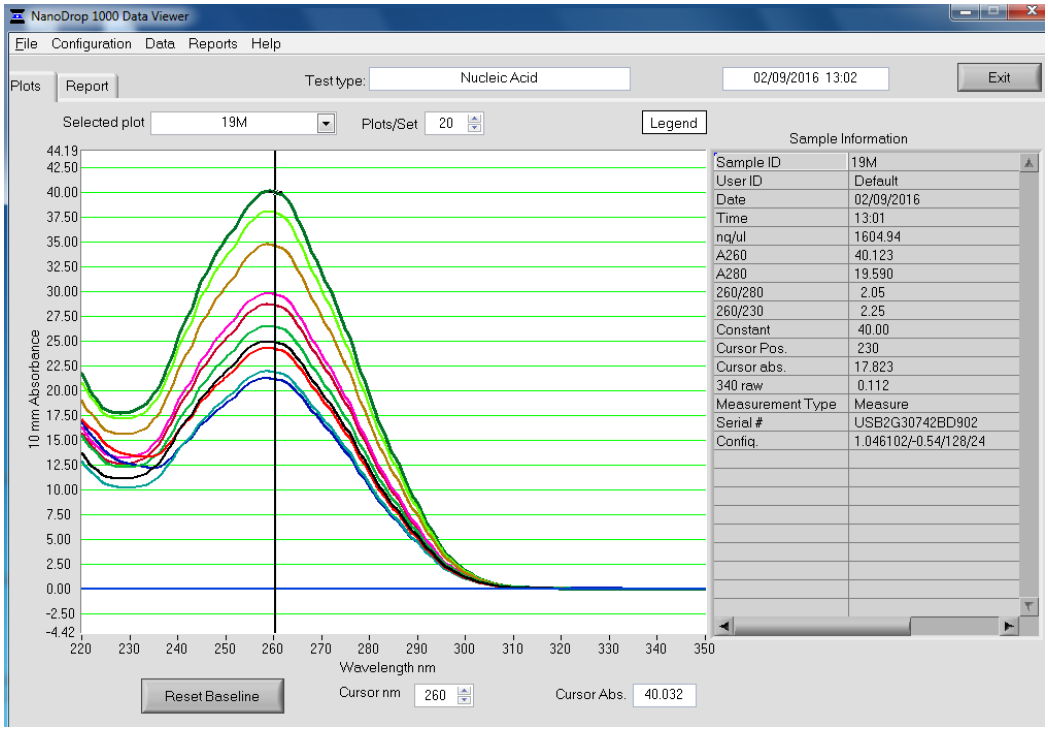

B

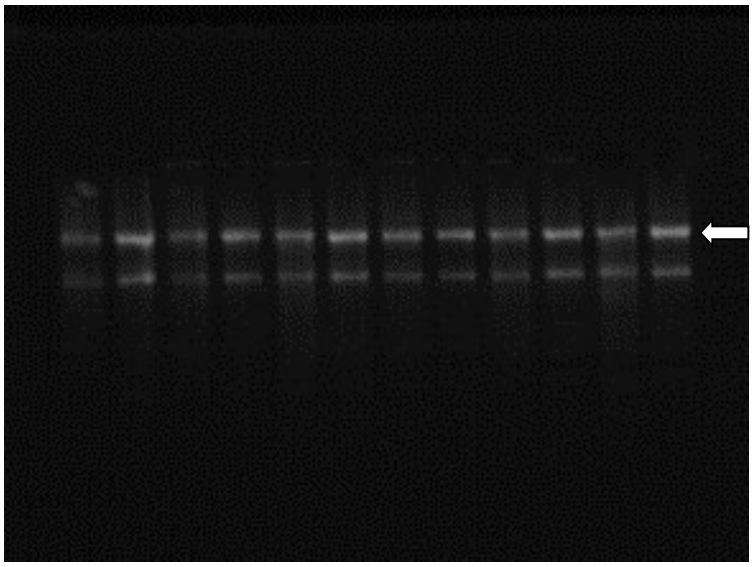

Fig. 2.6. Yield, purity and degradation of messenger ribonucleic acid (mRNA) isolated from tissue samples

A) Spectrophotometry of mRNA from 10 tissue samples, the data in the column on the right-hand side refers to sample "19M", containing 1604.95ng/µl of mRNA. The ratio of 260:230nm absorbance is 2.25.

B) Gel electrophoresis of RNA from 12 tissue samples viewed under UV light, there is separation of brighter 28S (arrow) and 18S ribosomal RNA subunits.

2.4.3 Semi-quantitative polymerase chain reaction

Samples of cDNA were slowly thawed on ice and loaded onto multiwell plates. To each well was added a mastermix of DNA polymerase, deoxynucelotide triphosphates (Perfecta qPCR Fastmix II; VWR International Ltd, Lutterworth, UK) and appropriate, exon-spanning, unlabelled, rat-specific primers mixed with a fluorescein amidite (FAM) dye-labelled Taqman probe (ThermoFisher Scientific Inc). Plates were subjected to 50 cycles of 10 seconds at 95ºC and 30 seconds at 60ºC, to amplify DNA. After each cycle, fluorescence of the FAM probes was measured (Lightcycler 480; Roche Diagnostics Ltd.).

Concentrations of mRNA were calculated from the equation of a contemporaneous standard curve of the points at which the threshold of background fluorescence was exceeded (C_T) in serial dilutions (1:8 to 1:512) of a mix of all cDNA samples. R^2>0.9 was considered acceptable.

C_T values for renal cortical and medullary reference (housekeeper) genes, glyceraldehyde 3-phosphate dehydrogenase (GAPDH) and thymine-adenine-thymine-adenine (TATA) box binding protein (TBP) [232], were compared between cohorts to confirm they were unchanged by diabetic status. After subtracting C_T values for genes of interest from C_T values for reference genes, delta C_T (ΔC_T) values were compared between cohorts (Chapter 2.8). Where significant differences were observed, the fold change was calculated from the difference in mean ΔC_T between cohorts ($\Delta\Delta$CT) [233] by the formula, fold change = $2^{-\Delta\Delta C_T}$.

2.5 *In vitro* studies: histology

2.5.1 Sectioning and mounting

Fixed tissues were processed and stained by the histology department of the shared university research facilities (SuRF), University of Edinburgh, using standard protocols. Briefly, tissues were paraffin-embedded and cut into 4µm-thick sections with a microtome (RM2235; Leica Biosystems Limited, Milton Keynes, UK), mounted onto glass microscope slides (VWR International Ltd) and dried overnight at 37ºC. Sections were stained with haematoxylin and eosin (H&E), and the pan-collagen marker, picrosirius red.

2.5.2 Staining with haematoxylin and eosin

In a fume cupboard, renal tissue sections were dewaxed in xylene (five minutes twice), rehydrated through a series of graded alcohols (100%, 95%, 90% and 70%, five minutes in each) and immersed in distilled water (five minutes). The sections were then immersed in the following solutions: Mayer's haematoxylin (Sigma-Aldrich Company Ltd.) for five minutes, distilled water for 30 seconds, 1% hydrochloric acid (HCl) in 70% ethanol for 30 seconds, distilled water for 30 seconds, aqueous eosin stain (Eosin Y; Sigma-Aldrich Company Ltd) for three minutes and finally distilled water for 30 seconds. Slides were then dehydrated through graded alcohols and xylene before being mounted in a xylene-based medium (DePeX; Gurr-BDH Chemicals Ltd, Poole, UK).

2.5.3 Staining with picrosirius red

Picrosirius red staining solution was prepared by dissolving a polyazo dye (Direct Red 80; Sigma-Aldrich Company Ltd) and a plasma counter-stain consisting of sea green triarylmethane food dye (Fast Green FCF; Sigma-Aldrich Company Ltd) in saturated aqueous picric acid (Sigma-Aldrich Company Ltd) according to manufacturer's instructions, giving a 1% solution of both agents.

In a fume cupboard, renal tissue sections were dewaxed in xylene (five minutes twice), rehydrated through a series of graded alcohols (100%, 95%, 90% and 70%, five minutes in each) and then immersed in distilled water (five minutes). Following an additional immersion in picrosirius red solution for two hours, slides were rinsed in distilled water (30 seconds) and then dehydrated through graded alcohols and xylene before being mounted in a xylene-based medium (DePeX; Gurr-BDH Chemicals Ltd).

2.5.4 Objective assessment of renal sections

Stained sections were viewed single-blind under a 20x objective lens (Carl Zeiss Ltd., Cambridge, UK) connected to a desktop computer using specialist imaging software (MCID Basic; Interfocus) and, where appropriate, images were saved as tagged image format (TIF) files.

For each rat, the glomerulosclerosis index was calculated from all glomeruli in one sagittal section of kidney stained with H&E [234].

The percentage of picrosirius red positive staining in 20 randomly selected TIF files (10 cortical, 10 medullary) was determined using Photoshop software (Adobe Systems Incorporate, San Jose, US). A reference level of positive staining was defined by selecting an area of collagen-dense connective tissue with a colour sampler tool. Positive pixels were identified within the reference area as superimposed flashing white areas. The width of the reference scale was then adjusted manually to modify the sensitivity of detection. This ensured detection of positively stained areas but not negatively stained areas, such as the lumens of blood vessels. The rest of every section was then analysed automatically and the number of positive pixels recorded. For every additional section, the reference level of staining was reset and a new reference defined.

2.6 In vivo studies: surgical techniques and sample collection

2.6.1 Jugular vein cannulation

The right jugular vein was exposed by cutdown and cannulated by introducing fine bore polythene tubing of internal diameter 0.58mm, external diameter 0.96mm (P50; Smiths Medical International Ltd, Hythe, Kent, UK) through a venotomy made with a bent 23 gauge needle (Fig. 2.7A, B). Using a syringe driver (World Precision Instruments), the rat was infused intravenously through this line with a balanced electrolyte solution, pH7.4 (0.01ml/gbw/hour; Chapter 2.8) containing 2% bovine serum albumin (BSA, Sigma-Aldrich Company Ltd) and 0.25% fluorescein isothiocyanate (FITC)-inulin (Sigma-Aldrich Company Ltd) for measurement of GFR. General anaesthesia was also maintained through this iv. line by small bolus

injections of sodium thiopental solution (0.02-0.03ml of 50mg/ml; Archimedes Pharma).

2.6.2 Tracheotomy and carotid artery cannulation

The trachea was exposed through a midline cervical incision and supported by a 2.5cm long piece of polythene tubing, 0.58mm internal diameter, 0.96mm outer diameter (P90; Smiths Medical International Ltd.), inserted under its dorsal aspect. A small tracheotomy was made with electrocautery (Fig. 2.7C).

The right carotid artery was exposed through careful dissection (Fig. 2.7D). It was elevated with 0.17mm silk suture thread (4/0; Interfocus) and separated from the vagosympathetic trunk by passing DeBakey forceps between the structures and pulling the silk through the small gap (Fig. 2.7E). The silk was then advanced along the carotid artery to its most cranial point which was then ligated. A straight vessel clip (1.5 x 8mm, World Precision Instruments) was applied to the most caudal point of the carotid artery (Fig. 2.7F) and a loose silk ligature placed in between. The carotid artery was penetrated with a bent 23 gauge needle and cannulated with polythene tubing (P50; Smiths Medical International Ltd) that was pre-flushed with heparinised saline (50IU/ml) and connected to a closed three-way tap. Once the free end of the tubing had been advanced to the level of the straight vessel clip, it was held in place by tightening the caudal pre-placed ligature (Fig. 2.7G), and the free ends of the cranial ligature (Fig.2.7H). The straight vessel clip was then released and haemostasis confirmed.

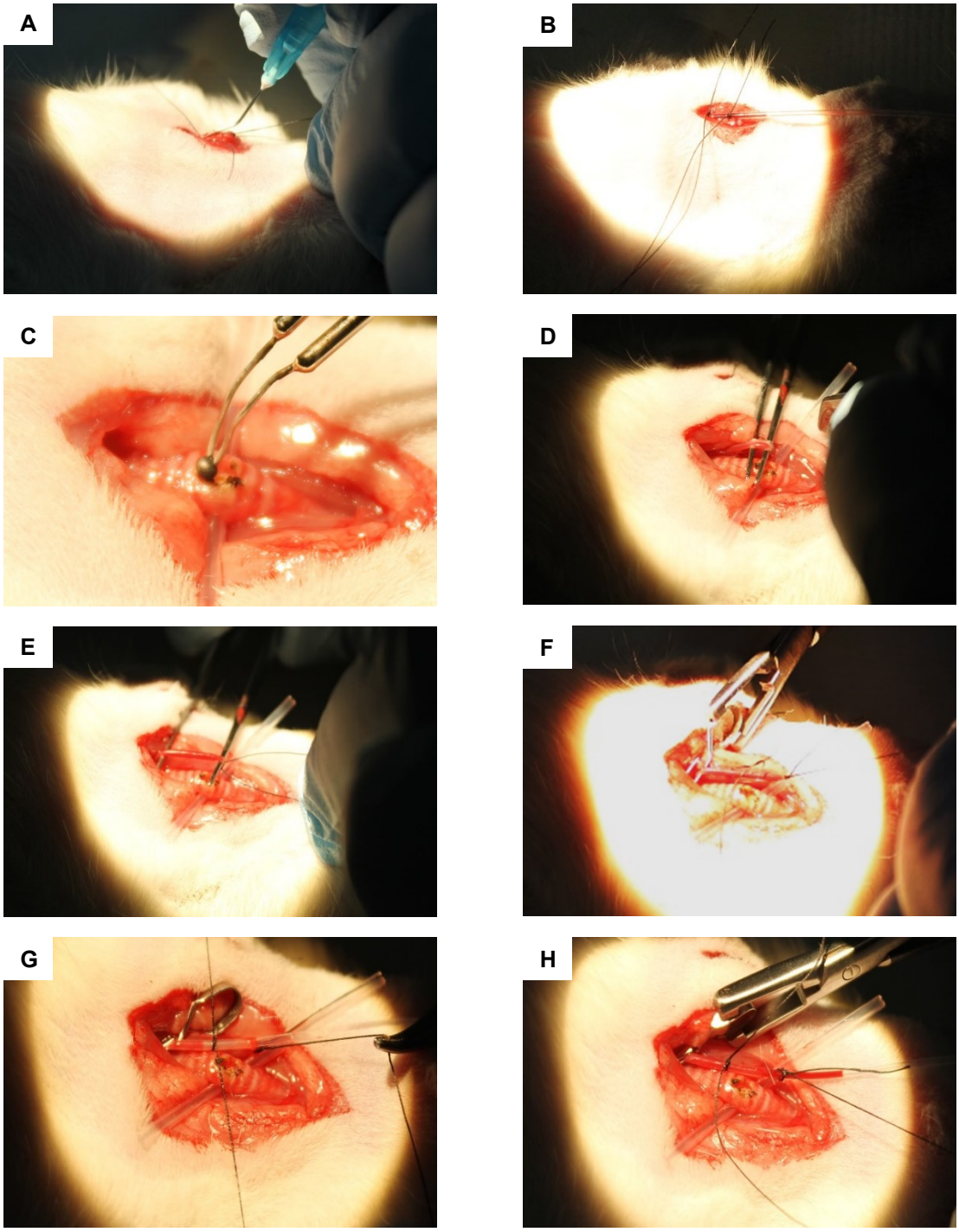

Fig. 2.7. Cannulating the jugular vein and carotid artery

A) and B). The right jugular vein is cannulated.

C) A tracheotomy is performed using electrocautery.

D) and E) The right carotid artery is exposed and separated from the vagosympathetic trunk.

F) A straight vessel clip occludes the carotid artery prior to arteriotomy

G) and H) Tubing is secured within the carotid artery with silk ligatures.

2.6.3 Real-time blood pressure measurement

Following arterial cannulation, the polythene tubing was clamped, removed from its connection to the three-way tap and transferred via additional heparinised tubing to a pressure transducer (ADInstruments, Oxford, UK) that had previously been calibrated manually with a sphygmomanometer, bulb pump and valve. The transducer was connected to a multi-channel data acquisition system (Powerlab; ADInstruments). The clamp was removed and all lines flushed with heparinised saline. Real-time BP was measured through this arterial line. Signal quality was considered optimal when oscillations between systolic and diastolic BP were clearly visible. Mean BP was recorded, post acquisition.

2.6.4 Arterial blood sampling and haematocrit measurement

Arterial blood was collected from the carotid arterial line. The polythene tubing was flushed with 0.2ml heparinised saline, clamped and separated from the connection to the pressure transducer. The clamp was partially released and blood allowed to flow slowly along to the end of the tube where five drops were blotted onto a paper towel. If the haematocrit was being measured, the end of the tubing was inserted into two haematocrit tubes which were filled by slightly releasing the clamp. For blood collection, the end of the tubing was inserted into a 0.3ml heparinised collection tube (Microvette CB300; Sarstedt, Numbrecht, Germany) and the clamp released further until the tube was full. Where appropriate, three additional collection tubes were filled. Following blood collection, the tube was fully clamped, re-connected to the pressure transducer and then flushed with 0.2ml heparinised saline after clamp release.

Blood samples were centrifuged at 1250rpm for five minutes. Plasma was decanted into 0.5ml Eppendorfs. Samples were refrigerated immediately at 4ºC and then stored at -80ºC.

2.6.5 Tube cystotomy and urine collection

Following coeliotomy, the bladder was identified, exteriorised and passed through a hole made in the centre of a small piece of paper towel. This held the bladder in position. A pre-formed loose ligature of 17mm silk (4/0; Interfocus) was placed over the cranial pole of the bladder (Fig. 2.8A). Holding the cranial pole with DeBakey forceps, a small cystotomy was performed through the loop of the ligature using electrocautery. Urine spillage was absorbed by the paper towel. A 15cm length of P90 polythene tubing (Smiths Medical International Ltd), with the end pre-softened by the flame of a cigarette lighter, was passed into the bladder lumen. The pre-placed ligature was then tightened, taking care to include bladder wall as well as tubing to form a tight seal (Fig. 2.8B). The free end of the cystotomy tube was allowed to drip onto a paper towel so that patency could be monitored.

Urine was collected from the tube cystotomy into pre-weighed 1.5ml Eppendorfs containing a spot of mineral oil. Samples were refrigerated immediately at 4ºC and then stored at -80ºC.

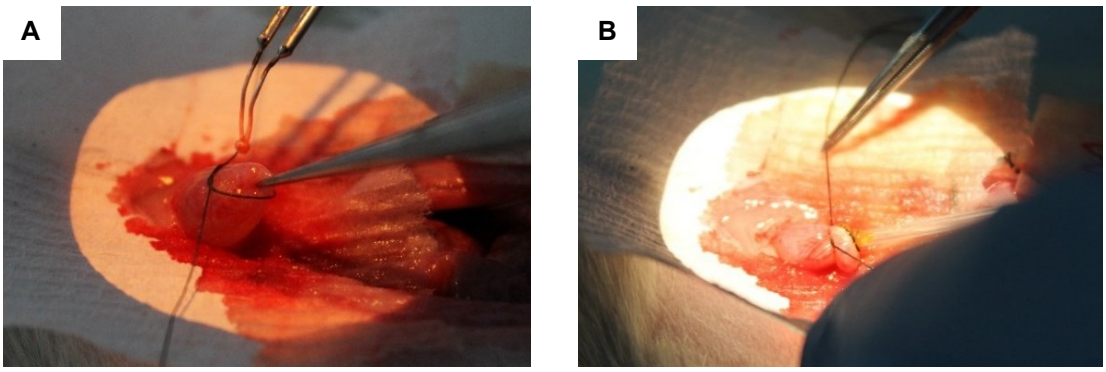

Fig. 2.8. Tube cystotomy

A) The bladder is exteriorised and a loose silk suture is placed

B) Following cystotomy with electrocautery, a cystotomy tube is tied in place.

2.6.6 Exposure of the left kidney and renal artery

Following coeliotomy, gentle pressure was placed on the left abdominal wall while simultaneously retracting the left abdominal wound margin. This exposed the left kidney which was freed from its retroperitoneal site and completely exteriorised by blunt dissection with DeBakey forceps, while gently retracting loose fragments of perirenal fat (Fig. 2.9A).

With gentle retraction on the kidney that was not sufficient to cause blanching, the left renal artery and vein were identified, the vein being dorsal and the artery ventral. The mesenteric fat ventral to the artery was carefully stripped away with DeBakey forceps. Small 2cm x 2cm square paper towel swabs absorbed abdominal fluid and were inserted into the abdomen to keep intestines away from the site of interest. The artery was freed from the tightly apposed vein by gentle dissection involving downward pressure along the dorsal border of the artery with closed DeBakey forceps, and then allowing the forceps to spring open (Fig. 2.9B). The artery frequently bifurcated prior to entering the renal hilus. When this occurred, dissection

was always started proximal to this. Once the artery was freed, further manipulation ceased, to allow time for any iatrogenic vasoconstriction to resolve.

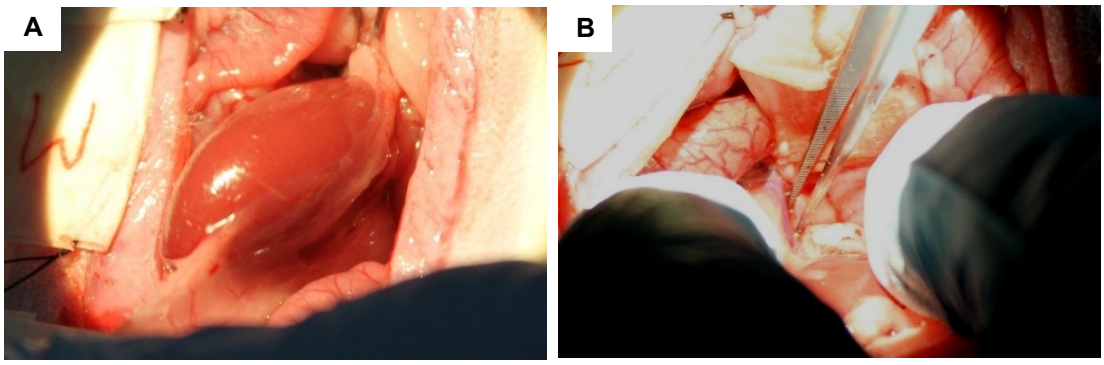

Fig. 2.9. Exposure of the left kidney

A) The left kidney is freed from perirenal fat and is exteriorised.

B) The left renal artery and vein are carefully separated with forceps.

2.6.7 Cannulation of the left ureter

Following coeliotomy and exposure of the left kidney (Fig. 2.10A), the left ureter just cranial to the bladder was identified within the mesenteric fat by a combination of peristalsis and the greenish hue from inulin-coloured urine within it. The ureter was undermined and a 0.17mm silk ligature (4/0; Interfocus) with long free ends was placed around it as close as possible to the bladder. The ureter was then cut distal to this ligature. Quickly, a second silk ligature was loosely placed around the ureter and advanced proximally. An ureterotomy was performed close to the cut end, using the first ligature for caudal traction, and taking care not to penetrate the opposite luminal wall. A 10cm length of thin polythene tubing of internal diameter 0.28mm, external diameter 0.61mm (P10; Smiths Medical International Ltd.) with a slightly sharpened tip was then inserted through the ureterotomy and advanced slowly proximally within the ureteral lumen (Fig. 2.10B). Patency was confirmed by the presence of pulsatile flow of inulin-coloured urine along the tubing. Sometimes this

did not occur until the second ligature had been tightened and the free ends of the first ligature had been tied around the tubing to hold it in position. If pulsatile flow was still not observed, the tubing was either re-positioned or a fresh ureterotomy was performed. The free end of the tubing was placed on tissue paper when urine was not being collected so that patency could be monitored.

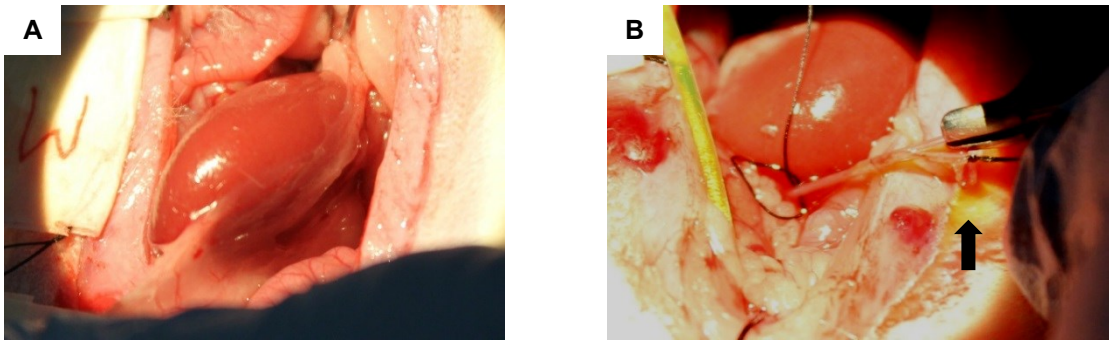

Fig. 2.10. Measurement of left renal urine output and blood flow

A) The left kidney is exposed.

B) The left ureter is cannulated. Urine spillage (arrow) is stained with inulin.

2.6.8 Measurement of left renal artery flow

Renal artery flow was measured in ml/min by a Doppler ultrasound flow probe (Transonic, Ithaca, United States (US)) placed around the freed left renal artery (Fig. 2.11A). Acoustic coupling was completed by copious application of ultrasound gel between and around the probe and artery using a 5ml syringe attached to a blunt and bent 23-gauge needle (Fig. 2.11B). At time of placement, the probe was gently manipulated to give maximal flow readings, and then held in position by the abdominal viscera.

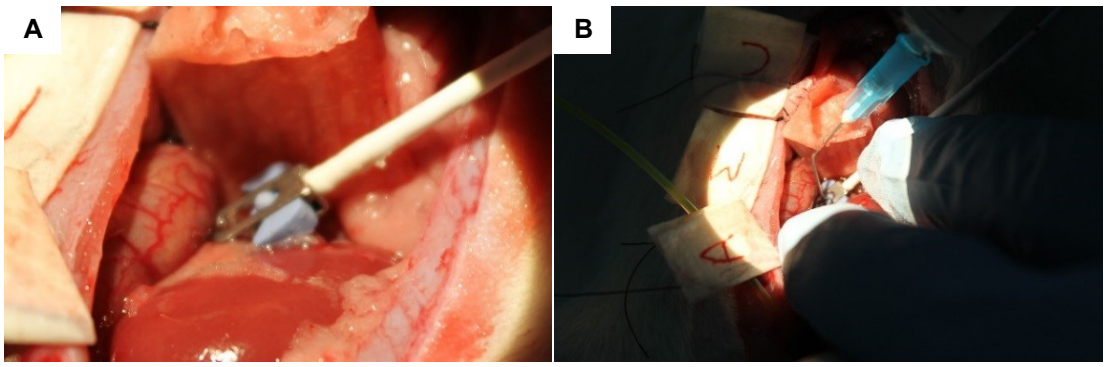

Fig. 2.11. Measurement of left renal artery flow

A) The ultrasonic flow probe is in place around the left renal artery.

B) Ultrasound gel is applied through a blunt, bent needle to improve acoustic coupling.

2.6.9 Measurement of intrarenal blood flow

Renal cortical blood flow and medullary blood flow were measured separately by laser Doppler spectroscopy (LDS; Fig. 2.12). This technique follows the same principle as Doppler ultrasonography, but instead, laser light of a set frequency is reflected by moving red blood cells to its source at a higher or lower frequency, according to whether the red blood cells are moving towards or away from it [235]. This shift in frequency (Doppler shift) is proportional to the velocity of the red blood cells and the cosine of the angle of the red blood cells to the laser beam, and is maximised when the laser beam and the direction of the red blood cells are parallel. Because of the varying concentrations of red blood cells at the exact point of interrogation within the kidney, and because the relative contributions of small blood vessels at different angles to the probe are not known, an absolute flow velocity is not determined [236]. Instead, the laser Doppler signal is described as *flux*, and measured in a relative unitary scale (tissue perfusion units, TPU). Therefore, changes in flux are expressed as a percentage of a baseline value.

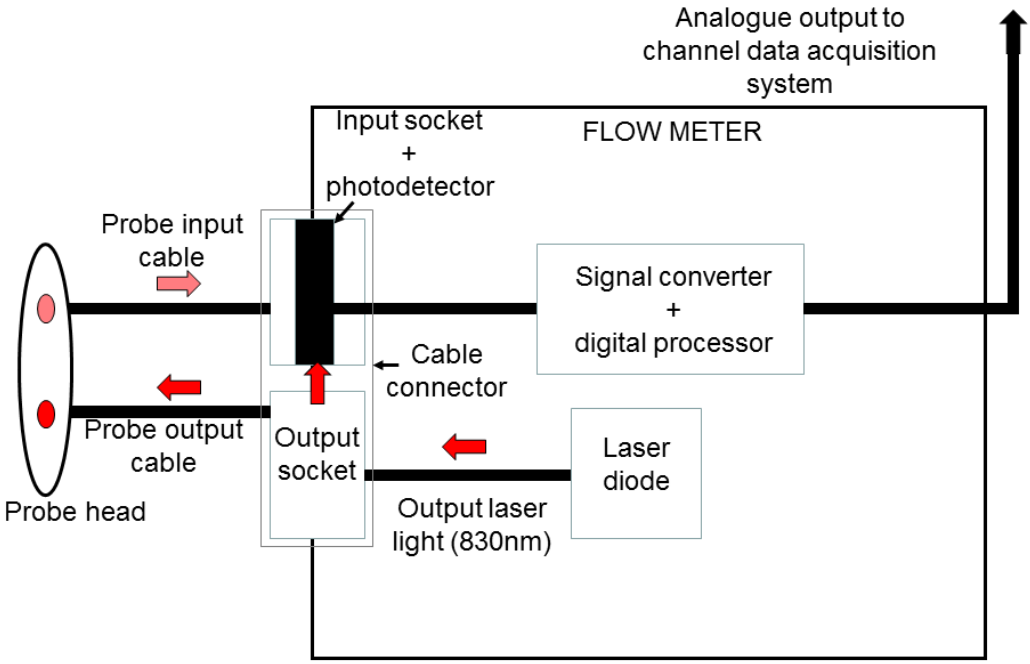

Fig. 2.12. Schematic diagram of a laser Doppler probe and flow meter.

Laser light is generated by a laser diode, and is split to the output cable and the photodetector. The photodetector compares reflected light with the incident beam through optical beating. The electrical signal generated enters a digital processor which calculates the Doppler shift and the number of tissue perfusion units (TPUs). The resultant analogue signal is sent to the channel data acquisition system. Red arrows indicate output laser light. Pink arrows indicate reflected (scattered) laser light.

Renal cortical flux was measured by a surface laser Doppler flow probe (ADInstruments). An adhesive patch with a central hole was placed over the detecting surface of the probe with the hole over the central laser beam source (Fig. 2.13A). Tissue glue (Vetbond; 3M, Bracknell, UK) was applied sparingly around the rim of the adhesive patch, far away from the central hole so as not to affect readings, and the probe was then applied to the dorsal renal capsule (the

surface closer to the table). Gentle pressure was applied for around 30 seconds, the time taken for the glue to set.

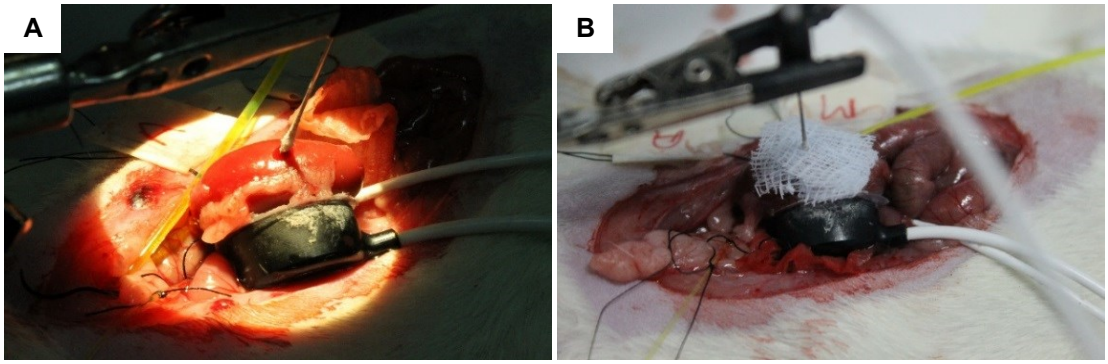

Fig. 2.13. Placement of laser Doppler probes to measure intrarenal flux

A) The surface probe, for measuring cortical flux, adheres to the dorsal renal surface. The needle probe, for measuring medullary flux, is inserted through the anti-mesenteric border of the kidney.

B) The needle probe is stabilised with gauze swabs, tissue glue and a micromanipulator.

Renal medullary flux was measured by a needle laser Doppler probe (ADInstruments). A 25-gauge needle was inserted 5mm through the renal capsule at the midpoint of the anti-mesenteric border and then removed. Following haemostasis, the needle probe was inserted 5mm through the hole pointing in the direction of the hilus (Fig. 2.13A). The probe was stabilised with a micromanipulator but additional stabilisation was required in order to minimise movement artefact associated with respiration. This was obtained by gluing the probe to the kidney without allowing glue to enter the puncture, since this could flow down into the kidney and occlude the tip of the probe. The technique was as follows: two small squares, each with a slit on one side that formed a "V" shape (Fig. 2.13B) were cut from a piece of gauze swab. Using DeBakey forceps, the "V" of one piece of swab was placed around the probe, with the arms of the "V" pointing away from

the operator. This was followed by application of the second piece of swab with the arms of the "V" pointing towards the operator. Both pieces of swab were then stuck to the renal capsule with tissue glue. As the glue spread towards the probe, it dried and stabilised the probe, without entering the puncture site and affecting the area being sampled. While the glue was setting, minor adjustments were made to the position of the needle probe to maximise the reading. The combination of rigidly fixed cortical and medullary probes was sufficient to dampen movement artefact created by respiration.

2.6.10 Calculation of urine flow rate

The volume of urine in each sample was calculated by subtracting the weight of the Eppendorf + mineral oil from the final weight of the Eppendorf + mineral oil + urine.

Urine flow rate (UV) was calculated as follows:

$$\text{UV (µl/min/gkw)} = \frac{\text{urine volume (ml) x 1000}}{\text{kidney weight (g) x duration of collection period (minutes)}}$$

2.6.11 Calculation of urinary sodium excretion rate and fractional excretion of sodium

Sodium concentrations in urine and plasma were measured by ion-selective electrode (9180 Electrolyte Analyzer; Roche Diagnostics Ltd.) calibrated to known concentrations of sodium ions, provided by the manufacturer. Urine was diluted by a ratio of 1:5 in distilled water and added to 120mM sodium chloride. The value measured by the analyser was then multiplied by the appropriate dilution factor (five)

to give the sodium concentration in mmol/l. Sodium concentrations in plasma were measured without dilution.

Urinary sodium excretion rate (UNaV) was calculated as follows:

$$\text{UNaV (µmol/min/gkw)} = \frac{\text{UV (µl/min/gkw) x sodium concentration in urine (mmol/l)}}{1000}$$

Fractional excretion of sodium (FENa), the proportion of renally filtered sodium that is not reabsorbed, was calculated as follows:

$$\text{FENa (\%)} = \frac{\text{UNaV (µmol/min/gkw) x 100}}{\text{Sodium concentration in plasma (mmol/l) x GFR (ml/min/gkw)}}$$

2.6.12 Calculation of glomerular filtration rate

Using a monochromator-based microplate reader (Infinite M1000 Pro; Tecan Group Ltd.), diluted concentrations of FITC-inulin in urine (1:4000) and plasma (1:40) samples were determined by FITC-fluorescence at a wavelength of 538nm following excitation at 485nm. Diluted concentrations were calculated from the equation of a contemporaneous standard curve of fluorescence against six standard solutions of known concentrations of FITC-inulin ranging from 0-1mg/ml (R^2>0.9). The original concentrations of FITC-inulin were calculated after multiplying by the appropriate dilution factor (400 for urine, 40 for plasma). All measurements were performed in triplicate.

GFR for every urine collection period was calculated using the equation:

$$\text{GFR} = \frac{\text{inulin concentration in urine (mg/ml) x UV (ml/min)}}{\text{inulin concentration in plasma (mg/ml)}}$$

where inulin concentration in plasma was the mean of the concentrations in the plasma samples obtained at the beginning and end of the urine collection period. The GFR was then divided by combined renal mass (tube cystotomy only) or the mass of the left kidney (tube ureterostomy only) to give GFR in ml/min/gkw.

2.6.13 Calculation of urinary endothelin-1 excretion rate

Urinary ET-1 excretion rate (UET-1V) was calculated for every collection period as follows:

UET-1V (fg/min/gkw) = UET-1 concentration (fmol/ml) x UV (µl/min/gkw) x 2.49

2.7 *In vivo* studies: radiotelemetry

2.7.1 Housing and radiotelemetry units

Rats were housed individually in a room dedicated to radiotelemetry studies for 48 hours. Every radiotelemetry unit (TA11-CA P40; Data Sciences International, 's-Hertogenbosch, Netherlands) was re-conditioned by the manufacturer and contained a pressure transducer. Differences to zero pressure were recorded for each unit pre- and post explantation. Every implanted unit could be switched on and off by a strong magnet placed over the skin.

2.7.2 Implantation of radiotelemetry units

Strict asepsis was observed during surgical implantation. Anaesthesia was induced with inhalational isoflurane (IsoFlo; Zoetis Animal Health Ltd.) in an anaesthetic chamber, and maintained with isoflurane by mask. 10ml of warmed saline was injected sc. The ventral abdominal wall was clipped and surgically prepared and the

rat positioned in dorsal recumbency on a thermostatically controlled heat pad (38ºC) with its head facing away from the operator. Bubble wrap was placed over the thorax for insulation. Following a midline coeliotomy from the umbilicus to the pubis, the abdominal cavity was exposed and the abdominal contents displaced to either side using retractors and swabs soaked in warmed, sterile saline. The distal aorta was identified and, using DeBakey forceps and a cotton bud, was carefully dissected free from the caudal vena cava from just cranial to the aortic trifurcation for a length of 1-2cm, to just caudal to the left renal vein. Straight vessel clips (1.5 x 8mm, World Precision Instruments) were applied across the distal aorta, first cranially, then caudally, and a timer was started. Following penetration of the aorta caudally with a 23 gauge bent needle, the sensory catheter of a radiotelemetry unit was inserted into the aorta using vessel cannulation forceps, and advanced to the cranial vessel clip. The arteriotomy site was closed and secured around the catheter with two small cellulose patches (Data Sciences International) with a "V" cut on one free edge. One patch was advanced between the catheter and the aorta along the "V" up to the point at which the catheter entered the aorta. The other patch was orientated in the opposite direction and overlaid the aorta and catheter. Each patch was secured separately with tissue glue (Vetbond; 3M). The vessel clips were removed, ensuring that no haemorrhage occurred. If haemorrhage did occur, the vessel clips were re-applied, the cellulose patches were removed and new ones applied. If the final clamp removal was more than 15 minutes after aortic occlusion, euthanasia was performed by barbiturate overdose. If less than 15 minutes but more than 10 minutes, rats were subsequently monitored closely to ensure that hind limb

paresis was only temporary (less than three hours). Hind limb paresis longer than three hours resulted in euthanasia (Chapter 2.1, page 46).

The radiotelemetry unit was secured to the peritoneal aspect of the transversus abdominis muscle with 2 metric polyglactin 910 (Vicryl; Ethicon, Livingston, UK). The abdominal wound was closed in two layers with simple interrupted and continuous coated 2 metric polyglactin 910 (Vicryl; Ethicon) sutures. The skin was closed with staples. Transmission from the radiotelemetry unit was confirmed, following activation of the unit with a strong magnet, by detection of a high frequency noise from an amplitude modulation (AM) transistor radio placed over the body wall. Rats recovered from anaesthesia in a recovery box containing insulating substrate and heated by warm air flow. Following recovery, they were transferred back to individual cages in the radiotelemetry room. They received buprenorphine (Buprecare; Animalcare, York, UK) at 0.5mg/kg/day sc. every 12 hours for three days during which time they were fed a mash of standard chow. Ten days after unit implantation, they were briefly anaesthetised with isoflurane (IsoFlo; Zoetis Animal Health Ltd.) for staple removal. They received 10ml of warmed saline sc. to aid recovery in a heated chamber.

Transmission from the radiotelemetry units was monitored as soon as the units were fitted. Units transmitted to a receiver pad under each cage, which was connected to a central acquisition system (Data Sciences International) attached to a desktop computer. During the immediate post-operative period, units were only switched on intermittently, to check unit function while preserving battery life.

Euthanasia was performed (Chapter 2.1, page 46) if any of the following major complications occurred: complete wound breakdown, generalised severe wound infection requiring antibiosis, loss of signal due to catheter migration, damage or occlusion of the catheter tip with a thrombus, and failure of post-operative paresis to resolve.

2.7.3 Measurement and calculation of blood pressure and heart rate.

During recording, systolic and diastolic BP and heart rate were acquired continually at 1kHz for one minute in every hour. However, BP and heart rate could be monitored at any time using a remote desktop connection.

In individual rats, data acquired over one minute were averaged. Data from every four hours were then combined, so that every light and dark period (12 hours) contained three data sets for every parameter. Circadian variation in BP and heart rate was calculated using three different methods.

2.7.4 Calculation of circadian variation in blood pressure: diurnal dipping

Diurnal dipping was defined as the percentage reduction in BP as rats entered a light (resting) period from a dark (active) period. The mean dip in BP in a cohort was the mean of every dip for every rat in that cohort.

2.7.5 Calculation of circadian variation in blood pressure: 24-hour-periodicity

Chi-square analysis was used to generate a Qp statistic according to the formula:

$$Q_p = \frac{KN\Sigma_{h=1}^{P}(M_h - M)^2}{\Sigma_{i=1}^{N}(x_i - M)^2}$$

where K= number of blocks that period P can be folded into, M_h= is the mean of K values under each time unit, and M is the mean of all N values [237].

Q_p represents the degree to which periodic variations in BP of duration tau hours are present within the data. For example, for a standard circadian rhythm, Q_p is at its highest value when tau=24.

2.7.6 Calculation of circadian variation in blood pressure: cosinor analysis

Sinusoidal variation in heart rate and BP was determined from multiple linear regression, using sine function least squares regression [237]. Starting from the first hour of the first dark period, and assuming a 24-hourly variation, mesor values from every rat were calculated from the equation:

Y= mesor + (cos coeff.cos time) – (sin coeff.sin time)

where cos time = $\frac{\cos 2\pi t}{T}$ and sin time = $\frac{\sin 2\pi t}{T}$

where t = 1- to 24-hourly and T=24 hours.

Amplitude (Amp) was calculated from the equation:

Amp = $\sqrt{(\text{cos coeff.}^2 + \text{sin coeff.}^2)}$

Acrophase (θ) was calculated from the equation:

$$\theta = \text{Arctan}\left[\frac{\text{sin coeff.}}{\text{cos coeff.}}\right]$$

2.8 Statistical analysis

All data were expressed as mean ± standard error of the mean (SEM) and analysed with Minitab 17 (Minitab Ltd, Coventry, UK) and GraphPad Prism 6.0 (GraphPad Software, La Jolla, US). Cohort sizes for experiments were calculated to achieve a minimum of 80% power (Minitab 17) based on expected results.

Normal distribution of data within cohorts was determined by the Anderson-Darling test. If data were not distributed normally, they were transformed to permit the use of parametric tests. If transformation was not possible, appropriate non-parametric tests were used.

Independent and dependent variables were compared between two cohorts by two-sample Student's *t* tests (normal) or Mann-Whitney *U* tests (non-normal). If experiments included more than two cohorts, one-way or two-way analysis of variance (ANOVA) or Kruskal-Wallis tests were used, according to normality and equality of variance of residuals, with Tukey's (normal) or Dunn's (non-normal) *post hoc* tests.

Correlations were calculated by Pearson's (normal) or Spearman's rank (non-normal) tests. Where dependent variables were plotted against an independent variable, regression lines were compared by analysis of covariance (ANCOVA) with Tukey's *post hoc* tests (linear) and extra sum of squares F-tests (non-linear).

For all tests, statistical significance was set at $P<0.05$.

2.9 Reagents and solutions

The following reagents were prepared:

Balanced electrolyte solution for in vivo *studies*

0.25g FITC-inulin (Sigma-Aldrich Company Ltd), 0.58g sodium chloride, 0.13g sodium hydrogen carbonate, 0.04g potassium chloride, in 100ml distilled water;

pH to 7.4 at room temperature.

0.5M ethylenediaminetetraacetic acid

186.1g disodium EDTA.$2H_2O$, in 800ml distilled water (vigorous stirring);

pH to 8.0 with 10M sodium hydroxide

4% paraformaldehyde

40g PFA powder, in 500ml distilled water (fume cupboard, stirred on a hot plate at 60-65ºC), 10ml 1M sodium hydroxide to clear solution, 100ml 10 x phosphate buffered saline (PBS);

pH to 7.4 at room temperature, adjust volume to 1 litre with distilled water

Phosphate buffered saline

80g sodium chloride, 2.0g potassium chloride, 14.4g disodiumhydrogenphosphate, 2.4g potassiumdihydrogenphosphate, in 800ml distilled water;

pH to 7.4, adjust volume to 1 litre with distilled water

0.9% saline solution

9g sodium chloride, in 1l distilled water;

pH to 7.4

Sodium citrate buffer

1.47g sodium citrate (enzyme grade), in 50ml distilled water;

pH to 4.5 with citric acid solution

10 x Tris borate ethylenediaminetetraacetic acid

56g tris base, 57.5g boric acid, in 20ml 0.5M EDTA pH8.0 and 500ml distilled water

Tris borate ethylenediaminetetraacetic acid running buffer and gel

Dilute 10 x tris borate EDTA (TBE) diluted 1:20 with distilled water (0.5xTBE), for running buffer

1.20g agarose (Seakem LE Agarose; Lonza, Rockland, US) in 100ml 0.5xTBE; microwave at full power for two minutes, for gel

3 Method development: optimisation of ligature-induced acute pressure natriuresis

3.1 Introduction.

Acute pressure natriuresis is the process by which increases in arterial blood pressure (BP) lead to corresponding increases in urinary sodium and water excretion while glomerular filtration rate (GFR) is autoregulated [89,112]. To investigate the hypothesis, acute pressure natriuresis will be induced by arterial ligation in a rat model of early Type 1 diabetes mellitus (T1DM). In healthy rats, this technique produces consistent, marked step-ups in BP and urinary sodium and water excretion [112] that allow deficiencies in acute pressure natriuresis to be identified. Unfortunately, it is also surgically invasive, and requires prolonged general anaesthesia, so the protocol has to be adapted to meet the experimental requirements of unhealthy animal models. In this chapter, experiments investigated cardiovascular and renal stability during prolonged general anaesthesia in a rat model of early T1DM. They also determined the adaptations to the protocol for inducing acute pressure natriuresis that will suit the needs of the model and optimise increases in BP and urinary sodium and water excretion.

There are several different techniques for inducing acute pressure natriuresis. Of these, expansion of the vascular compartment through water immersion, and rapid intravenous (iv.) infusion of isotonic fluids have been applied previously to diabetic patients [107] and models of T1DM [108,109]. While these techniques successfully induce diuresis/natriuresis, the increases in BP, urinary sodium excretion rate (UNaV) and urine flow rate (UV) are gradual and variable [108,109], making it difficult to establish the relationships between them, and to make comparisons between cohorts.

Ligature-induced acute pressure natriuresis is the technique that has been selected for this thesis because it is the current "gold standard". Sequential ligation of major arteries generates marked stepwise increases in BP at fixed time points. These do not prevent maintenance of glomerular filtration rate (GFR) but still induce corresponding rapid rises in sodium and water excretion [112]. This permits generation and comparison of pressure diuresis/natriuresis curves [112,116]. Ligature-induced acute pressure natriuresis has never been applied to a rodent model of T1DM, and so it is not known whether the model can tolerate the procedure. If the model cannot maintain BP and GFRs during prolonged general anaesthesia and surgical intervention, and if glycosuria increases baseline urinary sodium and water excretion [238], comparisons between T1DM rats and healthy controls during acute pressure natriuresis will not be possible.

One method of adapting the protocol to meet the needs of early T1DM rats is to shorten the duration of the experiment. Surgical preparation time and surgical trauma can be reduced if the operator is sufficiently skilled and experienced. Shorter urine collection periods after arterial ligation (clearance periods) reduce the risk of avascular necrosis of abdominal viscera supplied by ligated arteries, and allow step-ups in BP despite rapid onset compensatory diuretic/natriuretic responses [112]. However, if clearance periods are too short, time, rather than a treatment or disease effect, becomes the major limiting factor for diuresis/natriuresis, and a larger number of animals is required to demonstrate differences between cohorts. Therefore, optimising the duration of clearance periods maximises rises in BP, UV and UNaV and minimises experimental mortality in early T1DM rats, preventing wastage of

time and resource, and the generation of incomplete data sets of questionable reliability.

In this chapter, two series of experiments were undertaken to address the proposal that ligature-induced acute pressure natriuresis can be successfully adapted for use in a sufficiently robust model of early T1DM. In the first series, baseline renal clearance of early T1DM rats was compared with healthy controls. BP, GFR, UV and UNaV were measured, and their stability during prolonged general anaesthesia determined. In the second series, the optimal protocol for ligature-induced acute pressure natriuresis in healthy rats was determined. The magnitude and duration of increases in BP following arterial ligation, the subsequent diuretic/natriuretic responses and the changes in GFR were recorded.

3.2 Methods

3.2.1 Animals

Experiments were performed, single-blinded, in two groups of adult male Sprague Dawley rats: early T1DM (blood glucose >12mmol/l induced with one or two intraperitoneal (ip.) injections of streptozotocin (STZ); Chapter 2.1, page 46) and healthy control rats (ip. citrate buffer). Experiments were performed two-to-three weeks after the first ip. injection.

3.2.2 Anaesthesia, preparation and vascular cannulation

Rats were anaesthetised with ip. sodium thiopental solution (50mg/kg, 50mg/ml; Archimedes Pharma, Reading, UK). The ventrum, ventral midline neck and right

jugular furrow were clipped and the rat placed in dorsal recumbency onto a heat pad, with the rat's head pointing towards the operator. A rectal thermometer was inserted, and body temperature maintained at 38-39ºC by manually adjusting the power output of the heat pad.

Following jugular vein cannulation (Chapter 2.6, page 63), the rats were infused intravenously (iv.) with a balanced electrolyte solution, pH7.4, (0.01ml/gbw/hour; Chapter 2.6, page 63) containing 2% bovine serum albumin (BSA, Sigma-Aldrich Company Limited (Ltd.), Gillingham, UK) and 0.25% fluorescein isothiocyanate (FITC)-inulin (Sigma-Aldrich Company Ltd.) for measurement of GFR. General anaesthesia was also maintained through this iv. line by small bolus injections of sodium thiopental solution (0.02-0.03ml of 50mg/ml; Archimedes Pharma). Following tracheotomy, systolic and diastolic BP were recorded continuously through an arterial line into the right carotid artery and mean BP was calculated post acquisition (Chapter 2.6, pages 64-66).

3.2.3 Baseline renal clearance

Twelve healthy, control rats, and eight early T1DM rats were selected. Following induction of anaesthesia and vascular cannulation, a caudal abdominal laparotomy was performed and urine was collected via a tube cystotomy (Chapter 2.6, page 67).

Following a 60-minute equilibration period, 0.3ml of blood was collected through the arterial line (Chapter 2.6, page 66) at the beginning and end of three consecutive 60-minute clearance periods (Clearance 1, Clearance 2, Clearance 3; Fig. 3.1). Every clearance period was subdivided into two urine collection periods, each lasting 30 minutes. Mean BP was recorded continuously (Chapter 2.6, page 66) and the average value for every 30 minutes was calculated. After the final blood collection, every rat was euthanased by an iv. overdose of sodium thiopental. The kidneys were removed and weighed. The rat carcase was incinerated as clinical waste.

Urinary sodium concentrations were measured. GFR, UV, UNaV and FENa for every 30 minutes were calculated (Chapter 2.6, pages 74-76).

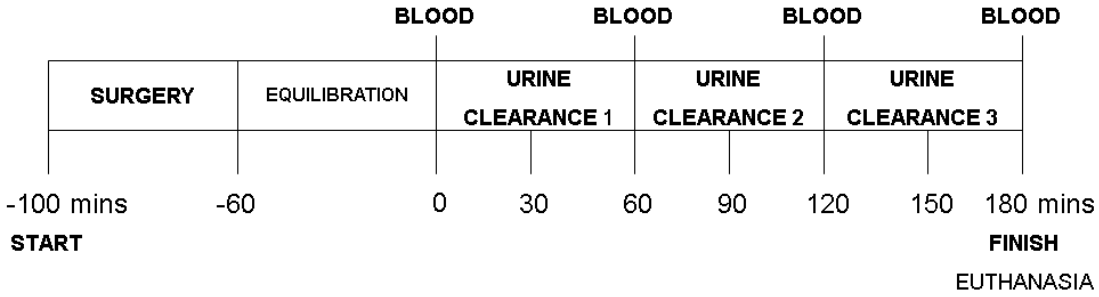

Fig. 3.1. Timeline for determining baseline renal clearance

Blood samples were taken at the beginning and end of every urine clearance period, mins=minutes.

3.2.4 Acute pressure natriuresis: ligature placement and tube cystotomy

The protocol proposed by Roman and Cowley [112] was adapted and applied to 12 healthy rats, without controlling neural and hormonal influences on the kidney (Fig. 3.2).

A midline coeliotomy was performed from the costal arch to the pubis, taking care not to cut through large subcutaneous blood vessels or lacerate the liver and bladder. Mean BP was monitored closely during this process. If mean BP fell acutely, surgery was stopped for two-to-three minutes to allow mean BP to recover.

The omentum and intestines were displaced to the left hemiabdomen, exposing the coeliac and cranial mesenteric arteries. Following blunt dissection with DeBakey forceps through the mesentery, ligatures of 0.17mm silk (4/0; Interfocus, Linton, UK) with long free ends were pre-placed around each of these vessels but not tightened. The free ends of each ligature were then labelled with tape and placed to the right of the rat, out of the surgical field (Figs. 3.3A-C). Fluctuations in BP, associated with manipulation of the arteries, were then allowed two-to-three minutes to stabilise.

The aorta distal to the left kidney was identified. Using DeBakey forceps and cotton buds, it was carefully dissected away from the caudal vena cava as close to the left kidney as possible. There was frequent variation in the branching of the aorta and caudal vena cava into the left hemi-abdomen, and in the degree of mesenteric fat, so care had to be taken not to rupture concealed large blood vessels. Once freed, a 0.17mm silk ligature with long ends was placed around the aorta and labelled with

tape (Figs. 3.3D,E). Again, there was a pause of two-to-three minutes to allow BP to stabilise.

A tube cystotomy was performed, allowing the free end of the cystotomy tube to drip onto a paper towel, so that patency could be monitored (Chapter 2.5, page 67; Fig. 3.3F). The iv. infusion rate was increased to (0.02ml/gbw/hour). The surgical preparation time (approximately 60 minutes) was noted and an equilibration period of 30 minutes was started (Fig. 3.4).

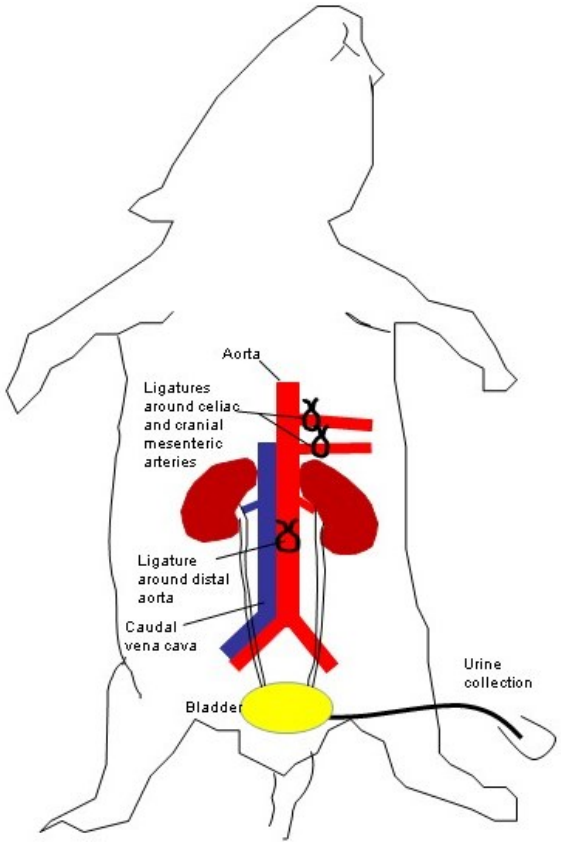

Fig. 3.2. Schematic diagram of the method for ligature-induced acute pressure natriuresis

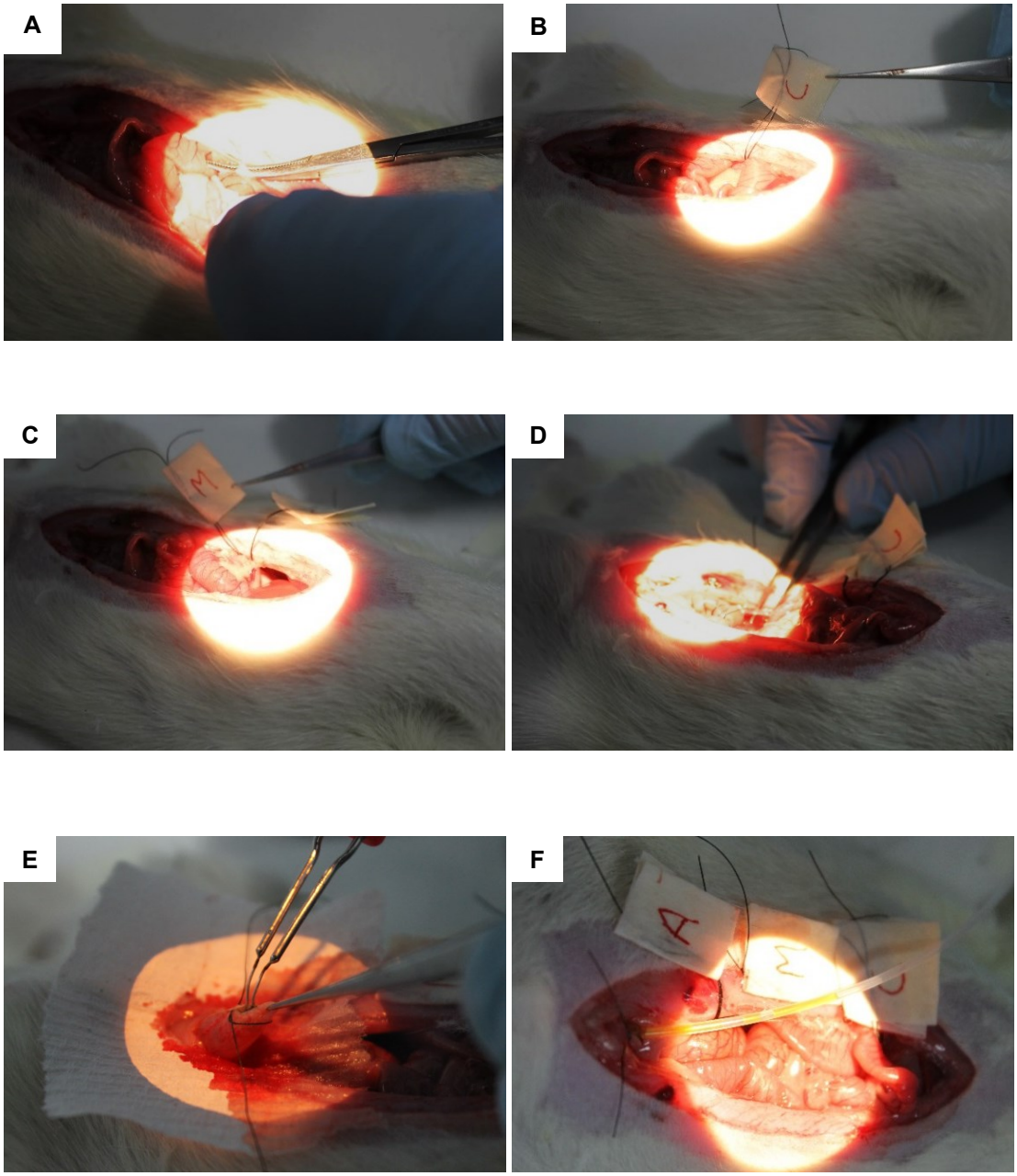

Fig. 3.3. Pre-placement of arterial ligatures and cystotomy

A) The coeliac artery is isolated.

B) A loose ligature is placed around the coeliac artery and labelled C.

C) A loose, labelled ligature (M) is placed around the cranial mesenteric artery.

D) A loose, labelled ligature (A) is placed around the distal aorta.

E) Cystotomy is performed by electrocautery.

F) Urine flows along the cystotomy tube, past the three labelled pre-placed ligatures.

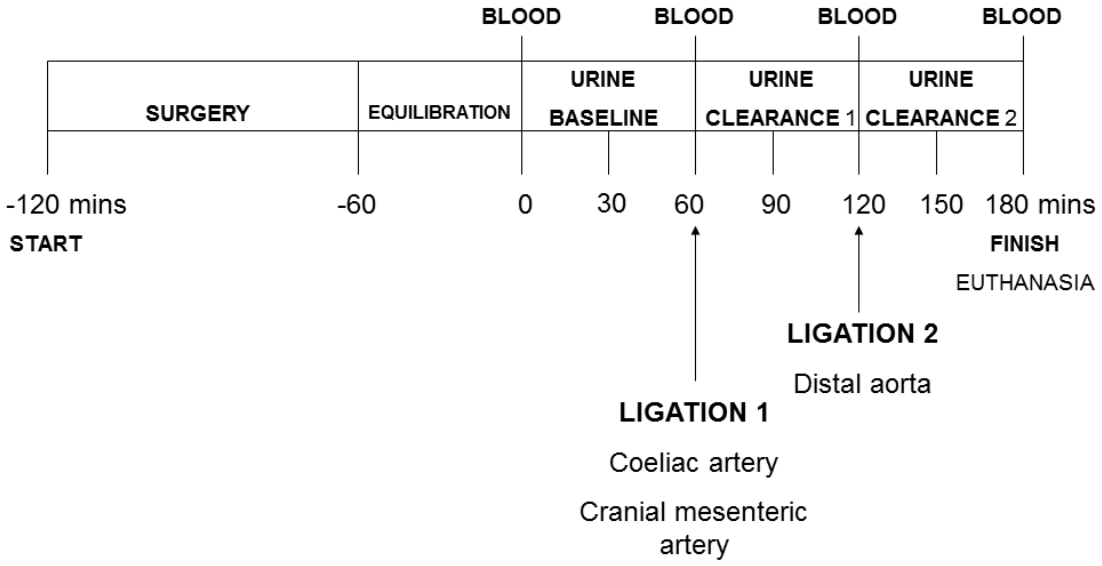

Fig. 3.4. Timeline for ligature-induced acute pressure natriuresis

mins=minutes

3.2.5 Acute pressure natriuresis: arterial ligation and urine and plasma collection

Following equilibration, 0.3ml of blood was collected through the arterial line at the beginning and end of three consecutive 60-minute clearance periods (Baseline, Clearance 1, Clearance 2; Fig. 3.4). Every clearance period was divided into two urine collection periods, each lasting 30 minutes. Mean BP was recorded continuously, and the average value for every five minutes after arterial ligation was calculated. After the final blood collection, every rat was euthanased by iv. overdose of sodium thiopental (Archimedes Pharma). The kidneys were removed and weighed. The rat carcase was incinerated as clinical waste.

Urinary sodium concentrations were measured. GFR, UV, UNaV and FENa for every 30 minutes were calculated (Chapter 2.6, pages 74-76).

3.2.6 Statistical analysis

Data were expressed as mean ± standard error of the mean (SEM) and analysed with Minitab 17 (Minitab Ltd, Coventry, UK) and GraphPad Prism 6.0 (GraphPad Software, La Jolla, US).

For baseline renal clearance, two-way analysis of variance (ANOVA) with Sidak's *post hoc* tests were used for between-cohort comparisons of independent (mean BP) and dependent variables (GFR, UV and UNaV) during individual urine collection periods, and to compare every urine collection period with the same-cohort first urine collection period. Data were subjected to log or square-root transformation according to normality and equality of variance of residuals. Interaction between diabetic status and clearance period was calculated.

For the acute pressure natriuresis studies, independent (mean BP) and dependent variables (UV, UNaV and FENa) during Clearances 1 and 2 were compared to Baseline values by one-way ANOVA with Tukey's *post hoc* tests.

For all tests, statistical significance was set at $P<0.05$.

3.3 Results

3.3.1 Baseline renal clearance and mortality

Three control and three early T1DM rats did not complete the study (30% mortality rate). Of these, two early T1DM rats were euthanased because of excessive weight loss (>20% starting bodyweight). The other rats developed severe hypotension during baseline renal clearance and died or were euthanased.

Mean BP did not vary during the study and was similar in control (126.9±4.7mmHg) and early T1DM (132.0±3.8mmHg) rats (Fig. 3.5A; Table 3.1). Overall, GFR rose ($P=0.04$, interaction $P=0.32$) and had doubled in controls by the end of Clearance 2 ($P=0.03$; Fig. 3.5B; Table 3.1). Though the effect was less in early T1DM rats (mean GFR 0.8±0.1ml/min/gkw) than in controls (1.3±0.1ml/min/gkw, $P<0.01$), GFR did not differ between cohorts during individual clearance or urine collection periods (Fig. 3.5B).

Overall, fluid perfusion induced a mild diuresis ($P=0.02$, interaction $P=0.25$) and mild natriuresis ($P<0.01$, interaction $P=0.96$). The increases in UV in control rats during Clearances 2 ($P=0.02$) and 3 ($P=0.04$; Fig. 3.6A; Table 3.1) were not observed in early T1DM rats. By contrast, UNaV ($P<0.01$) and FENa ($P<0.01$, interaction $P=0.85$) increased overall in only early T1DM rats (Figs. 3.6B,C; Table 3.1). Despite these small differences, UV, UNaV and FENa remained unaffected by early T1DM during individual clearance and urine collection periods (Figs. 3.6A-C).

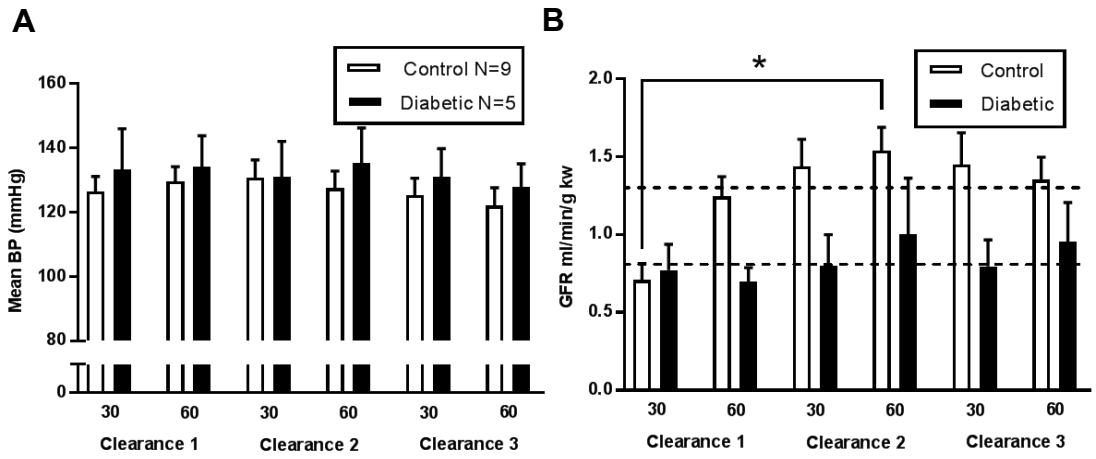

Fig. 3.5. Mean blood pressure (BP) and glomerular filtration rate (GFR) during baseline renal clearance in control and diabetic rats

A) Similar values for mean BP were maintained in controls and diabetic rats.

B) An increase in GFR during Clearance 2 was not observed in diabetic rats. The dashed lines represent mean values of GFR in male Sprague Dawley rats during general anaesthesia, prior to intervention [225,239].

Columns show mean ± standard error of the mean (SEM), *=P<0.05 compared with first 30-minute urine collection period in same cohort. All comparisons made with two-way analysis of variance (ANOVA) with Sidak's *post hoc* tests, 30 and 60=minutes

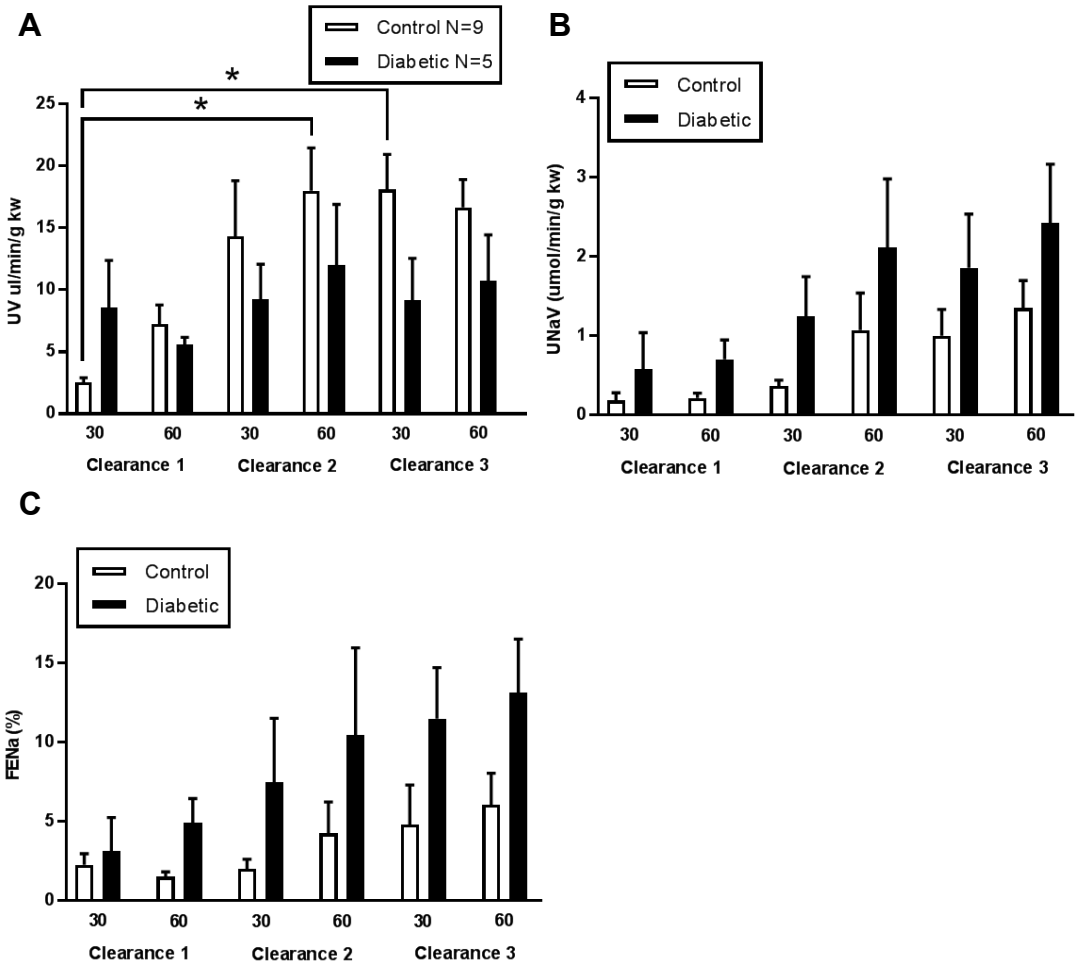

Fig. 3.6. Urine flow rate (UV), urinary sodium excretion rate (UNaV) and fractional excretion of sodium (FENa) during baseline renal clearance in control and diabetic rats

A) A small diuretic effect during Clearances 2 and 3 was not observed in diabetic rats.

B) Sodium excretion during individual clearance periods did not vary between cohorts.

C) FENa during individual clearance periods did not vary between cohorts.

Columns show mean ± standard error of the mean (SEM), *=P<0.05 compared with first 30-minute urine collection period in same cohort. All comparisons made with two-way analysis of variance (ANOVA) with Sidak's *post hoc* tests, 30 and 60=minutes.

	Clearance 1				Clearance 2				Clearance 3			
Minutes	**30**		**60**		**30**		**60**		**30**		**60**	
	Control	**Diabetic**	**Control**	**Diabetic**	**Control**	**Diabetic**	**Control**	**Diabetic**	**Control**	**Diabetic**	**Control**	**Diabetic**
Weight (g)	367.0±18.1	353.4±7.4										
Mean BP (mmHg)	126.4±4.7	133.2±12.7	129.6±4.5	134.1±9.7	130.8±5.5	130.9±11.1	127.5±5.4	135.2±10.9	125.3±5.3	130.9±8.9	122.1±5.5	127.9±7.1
GFR (ml/min/gkw)	0.7±0.1	0.8±0.2	1.20±0.1	0.7±0.1	1.4±0.2	0.8±0.2	**1.5±0.2***	1.0±0.4	1.5±0.2	0.8±0.2	1.4±0.2	1.0±0.3
UV (µl/min/gkw)	2.5±0.4	8.6±3.8	7.2±1.5	5.6±0.6	14.3±4.5	9.2±2.8	**18.0±3.5***	12.0±4.9	**18.1±2.9***	9.2±3.4	16.7±2.3	10.7±3.7
UNaV (µmol/min/gkw)	0.18±0.1	0.6±0.5	0.2±0.1	0.7±0.2	0.4±0.1	1.2±0.5	1.1±0.5	2.1±0.9	1.0±0.3	1.9±0.7	1.4±0.3	2.4±0.7
FENa (%)	1.8±0.1	3.1±0.2	1.2±0.1	4.9±1.5	1.9±0.5	7.4±4.1	4.2±1.5	10.5±5.5	4.6±1.9	11.5±3.2	6.6±1.6	13.2±3.4

Table 3.1. Weight, urine flow rate (UV), urinary sodium excretion rate (UNaV), fractional excretion of sodium (FENa), glomerular filtration rate (GFR) and blood glucose (BG) in control and diabetic rats during baseline renal clearance

***=P<0.05 compared with first 30-minute urine collection period in same cohort. All comparisons made with two-way analysis of variance (ANOVA) with Sidak's *post hoc* tests.**

3.3.2 Acute pressure natriuresis

Six rats completed the study (50% mortality rate). Two rats died prematurely due to haemorrhage caused by laceration of one of the major abdominal arteries. A severe abdominal effusion developed during Clearance 2 in three rats, accompanied by pallor and odour from the jejunal loops, and hypotension. This was consistent with avascular necrosis and endotoxaemic shock that necessitated immediate euthanasia. One rat developed severe bradycardia and hypotension degenerating into death, immediately following cystotomy.

Following sequential arterial ligation, Baseline mean BP rose overall by ~10mmHg from 142.5±3.3mmHg to 152.8±1.4mmHg but there was marked variation in mean BP during Clearances 1 and 2 (Fig. 3.7A; Table 3.2). Following an initial rise of ~20mmHg, mean BP decreased during the second half of Clearance 1 to Baseline levels. Although mean BP increased again following the second arterial ligation, it did not exceed the maximum mean BP obtained during Clearance 1. Variance in mean BP increased during Clearance 2 after ~25 minutes.

GFR (1.20 ml/min/gkw) was maintained within values obtained during the previous experiment on baseline renal clearance (Fig. 3.7B; Table 3.2). There was a significant pressure diuresis and natriuresis. UV rose during Clearance 1 from 1.48±0.21 to 2.54±0.34 µl/min/gkw (P=0.02; Fig. 3.7C; Table 3.2), and was maintained during Clearance 2 (P=0.04). However, although UNaV rose from 4.07±1.22 to 9.43±2.47µmol/min/gkw (P=0.045; Fig. 3.4D; Table 3.2) during Clearance 1, it decreased towards Baseline levels during Clearance 2. Similarly,

FENa increased from 4.7±1.1% to 8.7±1.1% (P=0.03) during Clearance 1 but decreased to 7.5±0.7% during Clearance 2 (Fig.3.7E; Table 3.2).

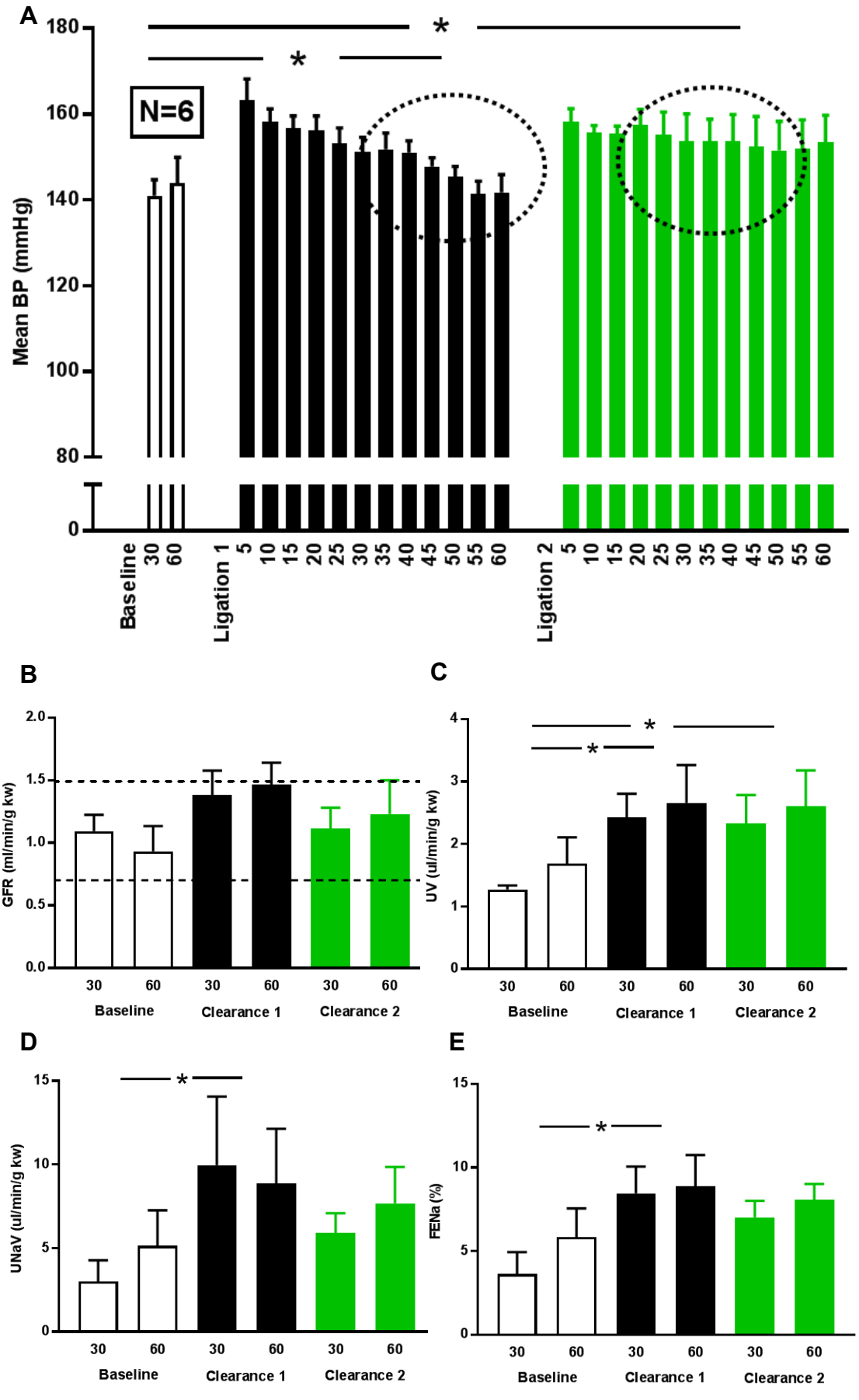
A
N=6
Mean BP (mmHg)
180
160
140
120
100
80
0
*
*
Baseline
Ligation 1
Ligation 2
30
60
5
10
15
20
25
30
35
40
45
50
55
60
B
GFR (ml/min/g kw)
2.0
1.5
1.0
0.5
0.0
C
UV (ul/min/g kw)
4
3
2
1
0
D
UNaV (ul/min/g kw)
15
10
5
0
E
FENa (%)
Baseline
Clearance 1
Clearance 2

Fig. 3.7. (page opposite) Ligature-induced acute pressure natriuresis in healthy rats

A) Rises in mean blood pressure (BP) following arterial ligation, the dashed circles show where BP falls during Clearance 1 and where variance in BP is increased during Clearance 2.

B) Mean glomerular filtration rates (GFR) remained within the range of maximum and minimum mean values obtained during baseline renal clearance, represented by the dashed lines.

C) Urine flow rate (UV) increased during Clearance 1 and was maintained during Clearance 2.

D) Urinary sodium excretion rate (UNaV) increased during Clearance 1 but fell to Baseline levels during Clearance 2.

E) Fractional excretion of sodium (FENa) also increased during Clearance 1 and fell to Baseline levels during Clearance 2.

Columns show mean ± standard error of the mean (SEM), *=P<0.05 compared with 60-minute Baseline values. All comparisons made with one-way analysis of variance (ANOVA) with Tukey's *post hoc* tests, 30 and 60=minutes.

	Baseline		Clearance 1		Clearance 2	
Minutes	**30**	**60**	**30**	**60**	**30**	**60**
Weight (g)	310.6±10.9					
Mean BP (mmHg)	141.0±3.8	143.9±6.0	156.5±1.5	146.5±1.4	156.0±1.5	152.8±2.3
GFR (ml/min/gkw)	1.1±0.1	0.9±0.2	1.4±0.2	1.5±0.2	1.1±0.2	1.2±034
UV (µl/min/gkw)	1.3±0.1	1.7±0.4	**2.4±0.4***	**2.7±0.6***	**2.3±0.5***	**2.6±0.6***
UNaV (µmol/min/gkw)	3.0±1.3	3.2±1.1	**10.0±4.1***	5.9±1.7	5.9±1.2	6.5±2.6
FENa (%)	3.6±1.3	5.3±2.1	8.5±1.6	8.9±1.3	7.9±1.3	7.5±0.7

Table 3.2. Weight, mean blood pressure (BP), glomerular filtration rate (GFR), urine flow rate (UV), urinary sodium excretion rate (UNaV) and fractional excretion of sodium (FENa) in healthy rats during Baseline and Clearances 1 and 2

***=P<0.05 compared with first Baseline 30-minute urine collection period using one-way analysis of variance (ANOVA) with Tukey's *post hoc* tests, 30 and 60=minutes**

3.4 Discussion

The experiments in this chapter investigated the suitability of a rat model for studying the effects of early T1DM on renal sodium handling, and then modified a protocol for inducing acute pressure natriuresis.

For an early T1DM rat model to be suitable, it must be sufficiently robust to survive general anaesthesia and surgery, and baseline determinants of renal sodium and water excretion must be similar to those in healthy controls. This can be facilitated by adapting experimental procedures so that they suit the model's needs. In the first series of experiments, general anaesthesia was as well tolerated in the model as in healthy controls, and early T1DM exerted only minor influences on BP, GFR and sodium and water excretion. In the second series of experiments, a protocol for inducing acute pressure natriuresis, based on the work of Roman and Cowley [112], successfully increased diuresis and natriuresis in healthy rats. However, elevated BPs and levels of sodium and water excretion were not sustained for more than 30 minutes, and experimental mortality, to which avascular necrosis contributed the most, was too high. This suggests that the experimental timeline should be shortened not only to suit the requirements of early T1DM rats, but also to maximise the degree of diuresis/natriuresis while minimising experimental mortality.

From these experiments, it is concluded that, following arterial ligation, clearance periods limited to 30 minutes will be sufficient to demonstrate impairment to acute pressure natriuresis in a rat model of early T1DM, as discussed further below.

3.4.1 Baseline renal clearance was similar between healthy control and diabetic rats.

Uncontrolled T1DM causes glycosuria that can increase urinary sodium and water excretion and modify the stability of BP and GFR [238]. Variations in BP and GFR confound comparisons with healthy controls because acute pressure natriuresis is induced by increased BP while GFR is autoregulated [89,112]. Therefore, before proceeding to experiments on acute pressure natriuresis, baseline BP, GFR and urinary sodium and water excretion were measured in healthy and early T1DM rats during prolonged general anaesthesia.

Following induction of anaesthesia, mean BP remained stable and was unaffected by early T1DM. Despite a lower overall GFR in early T1DM rats, and increases in BP that were only observed in controls, GFR in both cohorts remained within ranges previously published for this rat strain during general anaesthesia [225,239]. This suggested that autoregulation of GFR was maintained in both healthy and diabetic states. There was a small influence of early T1DM on UV, UNaV and FENa, but none of these parameters differed from control values during individual clearance periods. These results are significant. The similarity and stability in baseline BP mean that subsequent acute pressure natriuresis studies will not require placement of a cuff around the proximal aorta in order to equalise renal perfusion pressures [112]. The similar baseline levels of sodium and water excretion will permit comparisons between cohorts in response to changes in BP. Together, the data demonstrate that the early T1DM rat model is a suitable choice for studying acute pressure natriuresis.

These studies on baseline renal clearance were not performed single-blind. This was so that requirements specific to early T1DM rats could be determined and incorporated into the protocols of subsequent studies that require general anaesthesia and surgery. These adaptations concerned anaesthetic dosing and frequency of dosing to minimise the effect on BP, and included pauses during laparotomy and manipulation of viscera to allow BP sufficient time to recover. Identifying these requirements may have contributed to maintaining an acceptably low mortality rate. There was a subjective increase in surgical skill over the months that these studies were conducted. The effect this had on outcome was minimised by use of contemporaneous controls and random selection of rats.

3.4.2 Acute pressure natriuresis was successfully induced in healthy rats.

The second series of experiments optimised a technique for inducing acute pressure natriuresis through ligation of abdominal arteries [112]. In acute pressure natriuresis, rises in BP increase urinary sodium and water excretion because of reduced tubular sodium reabsorption and not because of increased GFR, which is autoregulated [89,112]. Therefore, to induce acute pressure natriuresis experimentally, step-ups in BP must be of sufficient magnitude and duration to induce diuresis and natriuresis, and a stable GFR must be maintained [112]. In Roman and Cowley's original protocol in healthy rats, clearance periods of 40 minutes followed a five-minute equilibration period [112], whereas in their follow-up study in unhealthy, hypertensive rats, shorter clearance periods of 15 and 30 minutes were employed [116]. Several published studies have also adapted the original protocol [114,115,120,240-246], using clearance periods as short as 10 minutes and as long as 50 minutes, and equilibration periods after surgery

and arterial ligation ranging from five minutes to one hour. The reasons for these adaptations are not clear. One could speculate that as well as reflecting variable susceptibility of unhealthy animal models to prolonged general anaesthesia and surgical manipulation, they might also have been modified according to operators' skill, and the differences in UV and UNaV required between cohorts to achieve adequate power.

To determine whether similar adaptations in experimental time could be applied in this thesis, dependent and independent variables were sampled frequently during prolonged periods of renal clearance after arterial ligation. An equilibration period of 30 minutes was sufficient for BP, UV and UNaV to recover after surgery, and to exceed levels recorded during the preceding baseline renal clearance studies. These elevated levels may have been a consequence of the higher rate of iv. fluid infusion that was used, and could also be attributed to adequate surgical skill, and the shorter surgical preparation time afforded by not having to place a cuff around the proximal aorta.

Following arterial ligation, increments in BP stabilised within two-to-three minutes, and diuresis and natriuresis were rapidly induced, suggesting longer post-ligation equilibration periods were unnecessary. Rises in BP were sufficient to double UV and UNaV during clearance periods of one hour. This diuretic/natriuretic response could not be explained by increases in GFR, which remained within the range of GFRs recorded during the previous baseline renal clearance studies. By contrast, increases in FENa were similar to those observed for UV and UNaV, and

demonstrated that sodium and water excretion had increased because of decreased tubular sodium reabsorption. Together, these data show that acute pressure diuresis/natriuresis can be induced in the healthy Sprague Dawley rat.

3.4.3 Thirty-minute clearance periods are sufficient and suitable for inducing acute pressure natriuresis.

Following the first of two arterial ligations, the compensatory diuretic/natriuretic response was so marked, that it rapidly offset the rise in BP. As a consequence, after one hour of clearance time, the second arterial ligation did not achieve an additional step-up in BP even higher than the first, and additional increases in UV and UNaV were limited. This contributed to an overall diuretic/natriuretic effect that was less than that achieved in healthy rats following rapid expansion of circulatory volume with iv. saline [109]. However, the data also identified how this deficit could be corrected. Limiting clearance periods in future experiments to 30 minutes, will lead to further increases in BP, UV and UNaV because they will not have had adequate time to return to Baseline levels. The data also suggest an additional benefit of using 30-minute clearance periods. One of the advantages of ligature-induced acute pressure natriuresis over natriuresis through volume expansion is that variance in BP is reduced within cohorts [112]. With acute volume expansion, there is variability in distribution of fluid within the vascular compartment, and the resulting increases in BP are less reproducible. It was therefore important to demonstrate in these studies that there was a low level of variance in BP following arterial ligation. Variance was low throughout Clearance 1, but after 30 minutes of Clearance 2, the BP decreased in some rats and not in others. Therefore, restricting clearance periods to 30 minutes,

will minimise this potentially confounding effect and facilitate inter-cohort comparisons.

3.5 Conclusions

The experiments in this chapter demonstrated that the rat model of early T1DM will meet the requirements of future experiments on acute pressure natriuresis and allow the hypothesis of this thesis to be explored. The model is sufficiently robust to maintain BPs and GFRs similar to those in healthy controls rats, over prolonged periods of general anaesthesia. Baseline UV and UNaV are also similar to control values, facilitating future comparisons between cohorts. A suitable protocol for ligature-induced acute pressure natriuresis has also been determined. Shorter equilibration and clearance periods than originally described for this technique will provide predictable and reproducible increases in BP. These will be adequate for studying differences in UV and UNaV that are independent of GFR, while also reducing the risk of experimental mortality. It is intended to test the new protocol for the first time in early T1DM rats in the following chapter, when investigating the effect of early T1DM on acute pressure natriuresis.

4 The effects of early Type 1 diabetes mellitus and insulin on acute pressure natriuresis

4.1 Introduction

Hypertension and nephropathy are major risk factors for cardiovascular disease (CVD) in Type 1 diabetes mellitus (T1DM) [247-250]. Hypertension and hyperglycaemia are key to the development of diabetic nephropathy [72] and when either blood pressure (BP) or blood glucose is tightly controlled in early T1DM, the risk of nephropathy and CVD is much reduced [31,251]. However, lowering blood glucose increases the risk of potentially life-threatening hypoglycemia [29]. Thus, BP and its regulation in early T1DM are attractive therapeutic targets to complement control of blood glucose.

The kidneys are central to regulation of BP. As BP rises, there is a corresponding increase in renal medullary blood flow [138] that induces a compensatory diuresis and natriuresis in a process called acute pressure natriuresis [89]. Excretion of sodium and water is reduced when BP subsequently falls. Hyperglycaemic T1DM patients and animal models are unable to excrete an acute sodium and water load rapidly [109,110,252], suggesting that they have impaired acute pressure natriuresis, although this has not been confirmed experimentally. Such dysfunction in renal sodium handling is important because it has been implicated in the rise in nocturnal BP that predicts hypertension and nephropathy in T1DM patients [74,124]. Increased nocturnal BP has now become a therapeutic target for reducing cardiovascular risk [106], and night-time dosing of anti-hypertensive medication is recommended by the American Diabetes Association to reduce cardiovascular risk [253]. However, conventional anti-hypertensive medication may not always reduce nocturnal BP [226], and, therefore,

an alternative strategy to restore the dip in BP at night, and reduce cardiovascular risk, might be to manipulate acute pressure natriuresis directly.

The paracrine peptide endothelin-1 (ET-1) may be a suitable therapeutic target for three reasons. First, it regulates vascular and tubular components of acute pressure natriuresis [89] via its two receptor subtypes. ET_A receptor-mediated vasoconstriction can reduce renal medullary blood flow [182,184] and suppress acute pressure natriuresis, whereas ET_B receptor-mediated vasodilation [77] and suppression of tubular sodium reabsorption through the epithelial sodium channel (ENaC) [181] have the opposite effect. Second, T1DM is known to have profound effects on ET-1 signalling that are implicated in impaired regulation of BP. Hyperglycaemia increases transcription and release of ET-1 from endothelial cells [205,254], and plasma levels of ET-1 are elevated in STZ-induced T1DM rats [255] and in patients with T1DM and hypertension [256]. There is a shift towards increased vasoconstriction from enhanced ET_A receptor signalling [257,258] and impaired vasodilation via nitric oxide (NO) [259], the mediator of both ET_B receptor-mediated vasodilation and inhibition of ENaC [122,260]. Third, and finally, selective ET_A receptor antagonists are already at an advanced stage of clinical development. They reduce BP and proteinuria in clinical diabetic nephropathy [217], and re-establish nocturnal dipping in non-diabetic chronic kidney disease (CKD) [226], suggestive of restored acute pressure natriuresis.

4.1.1 Hypotheses

1) Acute pressure natriuresis is impaired in early T1DM before the development of established nephropathy.
2) This impairment is reversed by insulin and mediated by renal ET-1.

4.1.2 Aims

To investigate these hypotheses, a rat model of early T1DM was used to answer the following questions:

1) Does early T1DM impair acute pressure natriuresis prior to overt nephropathy?
2) Is this reversed by lowering blood glucose with insulin?
3) Does urinary ET-1 (UET-1) excretion correlate with urinary sodium and water excretion during acute pressure natriuresis?
4) How are these relationships modified in early T1DM?

4.2 Methods

4.2.1 Animals

Experiments were performed, single-blinded, in two groups of adult male Sprague Dawley rats: early T1DM (blood glucose >12mmol/l induced with one or two intraperitoneal (ip.) injections of streptozotocin (STZ); Chapter 2.1, page 46) and healthy control rats (ip. citrate buffer). Experiments were performed two-to-three weeks after the first ip. injection.

Selected experiments included a third cohort of early T1DM rats that had received a subcutaneous (sc.) insulin implant (T1DM+insulin) seven days after the first injection of STZ (Chapter 2.1, page 47).

4.2.2 Effects of Type 1 diabetes mellitus on acute pressure natriuresis

Acute pressure natriuresis was induced by arterial ligation in anaesthetised control and early T1DM rats (Table 4.1), using a protocol developed by Roman and Cowley [112], and modified in Chapter 3 (Fig. 4.1). Briefly, after a 30-minute baseline clearance period (Baseline), urine was collected, at higher mean BPs, during two subsequent 30-minute clearance periods (Clearance 1 and 2) that followed sequential arterial ligation. Systolic and diastolic BP were recorded continuously and mean BP was calculated post acquisition (Chapter 2.6, page 66). Arterial blood samples (0.3µl) were obtained at the beginning and end of every clearance period. Urinary sodium concentrations were measured (Chapter 2.6, page 74). Urine flow rate (UV), urinary sodium excretion rate (UNaV), glomerular filtration rate (GFR), and

fractional excretion of sodium (FENa) were calculated (Chapter 2.6, pages 74-76). Where appropriate, measurements were indexed to kidney weight (gkw).

	Control	Diabetic
Number	8	7
Weight (g)	360±6	354±7
BG (mmol/l)	4.7±0.6	**27.0±1.6****

Table 4.1 Number, weight and blood glucose (BG) of control and diabetic rats, immediately prior to general anaesthesia for ligature-induced acute pressure natriuresis

Data are mean ± standard error of the mean (SEM), **=P<0.05 compared with diabetics. All comparisons made with two-sample Student's *t*-tests.

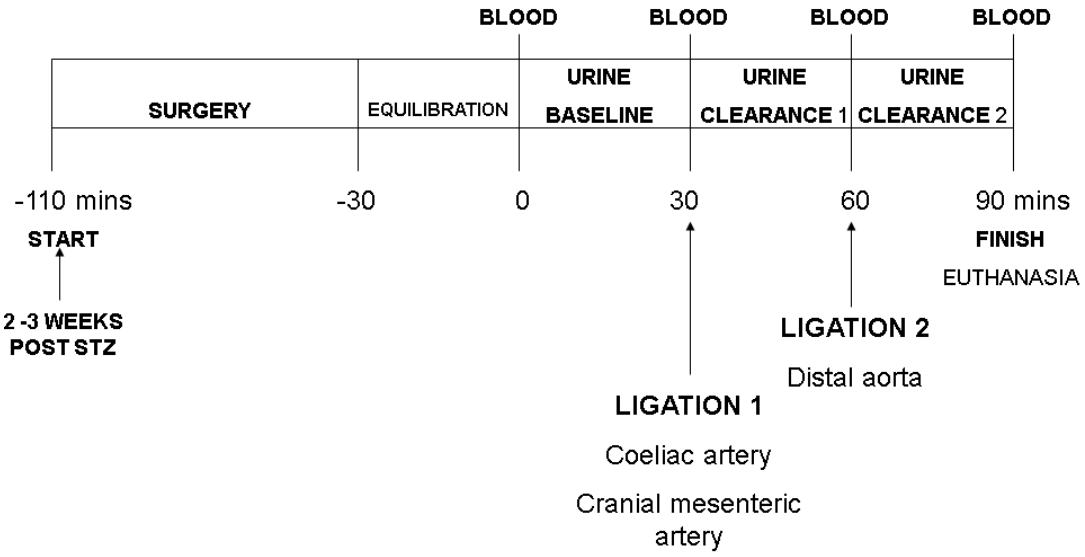

Fig. 4.1 Timeline for ligature-induced acute pressure natriuresis

Blood and urine collection time points are shown, STZ=streptozotocin, mins=minutes

4.2.3 Effect of insulin treatment on acute pressure natriuresis in diabetic rats

In a second series of experiments, ligature-induced acute pressure natriuresis was repeated but with an additional cohort of T1DM+insulin rats (Table 4.2). Concentrations of UET-1, a marker of renal ET-1 activity [209], were also measured by commercial enzyme-linked immunosorbent assay (ELISA; Chapter 2.3, page 56). UET-1 excretion rate (UET-1V) was calculated (Chapter 2.6, page 76).

	Control	**Diabetic**	**Insulin**
Number	9	7	8
Weight (g)	399.5±12.9	**338.3±18.5****	362.7±9.1
BG (mmol/l)	4.8±0.2	**16.8±1.8****	**9.3±0.6***

Table 4.2 Number, weight, and blood glucose (BG) in control, diabetic and insulin-treated diabetic rats, immediately prior to general anaesthesia for ligature-induced acute pressure natriuresis

Data are mean ± standard error of the mean (SEM),*=P<0.05 compared with diabetics, **=P<0.05 compared with controls. All comparisons made with one-way analysis of variance (ANOVA) with Tukey's *post hoc* tests.

4.2.4 Biochemical and molecular assessment of renal injury and activation of the renin-angiotensin-aldosterone system

Urine was collected for 24 hours from eight control, eight early T1DM and eight T1DM+insulin rats placed in metabolic cages (Chapter 2.2, page 48; Table 4.3). To determine glomerular integrity in relation to GFR, urinary albumin and creatinine

concentrations were measured with adapted commercial kits (Chapter 2.3, page 56). Activity of the renin-angiotensin-aldosterone system (RAAS) was determined from urinary aldosterone concentrations measured by an in-house ELISA (Chapter 2.3, page 56). Albumin and aldosterone were both indexed to creatinine. Twenty-four-hourly UET-1 excretion, a marker of diabetic renal injury [261], was calculated by multiplying 24-hourly urinary volume by urinary ET-1 concentration as determined by commercial ELISA. The value was indexed to kidney weight.

	Control	Diabetic	Insulin
Number	8	8	8
Weight (g)	383.8±7.7	359.5±12.4	372.7±13.0
BG (mmol/l)	6.8±0.3	**22.0±3.0****	**10.5±0.9***

Table 4.3 Number, weight and blood glucose (BG) in control, diabetic and insulin-treated diabetic rats during a metabolic cage study, prior to tissue collection

Data are mean ± standard error of the mean (SEM), *=P<0.05 compared with diabetics, **=P<0.05 compared with controls. All comparisons made with one-way analysis of variance (ANOVA) with Tukey's *post hoc* tests.

Following removal from the metabolic cages, rats were anaesthetised for tissue collection (Chapter 2.2, pages 49-55). The left kidney was removed, and sections of cortex and medulla were snap-frozen separately on dry ice for subsequent extraction of messenger ribonucleic acid (mRNA). Tissues were then perfusion-fixed with 4% paraformaldehyde (PFA) [229], the right kidney was removed, paraffin-embedded, and sectioned (4μm; Chapter 2.5, page 61).

Semi-quantitative polymerase chain reaction (qPCR) of renal tissue (Chapter 2.4, pages 57-60) measured expression of markers of renal injury, inflammation and fibrosis. Total RNA was extracted from pulverised snap-frozen renal cortex and medulla from control, early T1DM and T1DM+insulin rats. First-strand complementary deoxyribonucleic acid (cDNA) was reverse transcribed and amplified (qPCR) with exon-spanning, unlabelled, rat-specific primers for renal injury and fibrosis (kidney injury molecule-1 (KIM-1), collagen (Col) 1a1, Col3a1 and cluster of differentiation 68 (CD68)) mixed with a fluorescein amidite (FAM) dye-labelled Taqman probe (ThermoFisher Scientific Inc, Glasgow, UK; Table 4.4). Using the change in cycle threshold (ΔC_T) method, fluorescence of the FAM probes was compared to reference genes 3-phophate dehydrogenase (GAPDH) and thymine-adenine-thymine-adenine (TATA) box binding protein (TBP) [232], which had been previously compared between cohorts to confirm they were unchanged by diabetic status. Where differences were identified, the fold-difference was calculated using the $\Delta\Delta C_T$ method [233].

Glomerulosclerosis and renal fibrosis were assessed histologically. Fixed, sectioned renal tissue, from control and early T1DM rats only, was stained with haematoxylin and eosin (H&E), and the pancollagen marker picrosirius red, using standard protocols (Chapter 2.5, pages 61-62). For each rat, the glomerulosclerosis index was calculated from all glomeruli in one sagittal section of kidney stained with H&E, and viewed, single-blind, under a 20x objective lens (Chapter 2.5, pages 62-63). The percentage of picrosirius red positive staining in 20 randomly selected fields

(10 cortical, 10 medullary) was determined using Photoshop software (Adobe Systems Incorporate, San Jose, United States (US)) [72].

Gene	Marker	Manufacturer reference	Exon boundary	Location	Length	Approximate probe sequence
KIM-1	Renal injury	Rn00597703_m1	5-6	1264	60	5'TAATCACACTGTAAGAATCCCTTTGAG3'
Col1a1	Renal fibrosis	Rn01463848_m1	1-2	189	115	5'GCCAAGAAGACATCCCTGAAGTCAGCT3'
Col3a1	Renal fibrosis	Rn01437681_m1	48-490	3921	71	5'ACTCAAGAGCGGAGAATACTGGGTTGA3'
CD68	Macrophage	Rn01495634_g1	5-6	911	62	5'TTCGGGCCATGCTTCTCTTGCGCCAGT3'
GAPDH	Reference gene	Rn01775763_g1	8-8	1153	174	5'GAGGAGTCCCCATCCCAACTCAGCCCC3'
TBP	Reference gene	Rn01455646_m1	4-5	791	75	5'TAATCCCAAGCGGTTTGCTGCAGTCAT3'

Table 4.4 Semi-quantitative polymerase chain reaction (qPCR) probes selected for determining renal injury

The probe sequence is not released by the manufacturer (ThermoFisher Scientific). The approximate probe sequence within the amplicon is derived from adding 13 nucleotides upstream and downstream of the assay location, using the Reference Sequence Database of the National Center for Biotechnology Information (NCBI, Bethesda, United States (US)), KIM-1=kidney injury molecule-1, Col=collagen, CD=cluster of differentiation, GAPDH= glyceraldehyde 3-phosphate dehydrogenase, TBP=TATA (thymine-adenine-thymine-adenine) box binding protein, A=adenine, C=cytosine, G=guanine, T=thymine.

4.2.5 Statistical analysis

Studies were designed to obtain a power >80% if cohort sizes were six rats and UNaV in diabetic rats was 50±25% [262] of the expected value in controls [112]. Additional rats were included to account for an expected dropout rate of 25% based on experimental mortality in Chapter 3, and to ensure controls were contemporaneous.

Data were expressed as mean ± standard error of the mean (SEM) and analysed with Minitab 17 (Minitab Ltd, Coventry, UK) and GraphPad Prism 6.0 (GraphPad Software, La Jolla, US).

Single comparisons (weight, blood glucose and renal injury) between two cohorts were made with two-sample Student's *t*-tests (normal) or Mann Whitney *U*-tests (non-normal) according to normality (Anderson-Darling test), while multiple comparisons between three cohorts employed one-way analysis of variance (ANOVA) with Tukey's *post hoc* tests (normal) or Kruskal Wallis with Dunn's *post hoc* tests (non-normal). Data for all ANOVAs were transformed by log or square-root transformation according to normality and equality of variance of residuals.

For acute pressure natriuresis, two-way ANOVA with Sidak's (two cohorts) or Tukey's (three cohorts) *post hoc* tests confirmed similar Baseline mean BP and increments (independent variable) between cohorts. Dependent variables were

similarly compared, and interaction between diabetic status and clearance period was calculated.

As additional analyses, dependent variables were plotted against BP and regression lines compared by analysis of covariance (ANCOVA) with Tukey's *post hoc* tests (linear) and extra sum of squares F-tests (non-linear). Correlations between dependent variables used Pearson's (normal) or Spearman's rank (non-normal) tests.

For all tests, statistical significance was set at $P<0.05$.

4.3 Results

4.3.1 Effects of Type 1 diabetes mellitus on acute pressure natriuresis

Two control rats died prior to inducing acute pressure natriuresis- one died immediately after induction of anaesthesia, and the other developed severe hypotension following cystotomy. One early T1DM rat was euthanased (Chapter 2.1, page 46) because of excessive weight loss. None of these rats is included in the data presented.

Baseline mean BP (aggregated mean 136±3mmHg) and the increase in mean BP following sequential arterial ligation (~25mmHg) did not differ between early T1DM and control rats (Fig. 4.2A, Table 4.5). GFR rose as mean BP rose ($P<0.01$; Figs. 4.2B,C; Table 4.5), independently of diabetic status (interaction $P=0.13$). Overall, GFR was lower in early T1DM rats than control rats (1.4±0.1ml/min/gkw

versus 1.6±0.1ml/min/gkw, P=0.011) but did not differ from controls during individual clearance periods (Table 4.5).

There were a significant pressure diuresis (P<0.01; Figs. 4.3A,B) and natriuresis (P<0.01; Fig. 4.3C,D), largely reflecting inhibition of tubular sodium reabsorption, since FENa also increased as mean BP rose (P<0.01; Figs. 4.3E,F; Table 4.5). Early T1DM substantially suppressed both the pressure diuresis and natriuresis relationships (both P<0.01, interactions P<0.01 (UV) and P=0.05 (UNaV)). During Clearance 2, UV reached only 24% (P<0.01; Figs. 4.3A,B; Table 4.5) and UNaV only 14% (P<0.01; Figs. 4.3C,D; Table 4.5) of the values obtained in controls, despite similar increases in mean BP. There was a linear relationship between UV and mean BP in both cohorts (both P<0.01; Fig. 4.3B) but the slope of the pressure diuresis response was markedly reduced in early T1DM (P<0.01). UNaV and FENa increased in a nonlinear manner in both cohorts (Figs. 4.3D,F) but the rate of increase was less in early T1DM (both P<0.01).

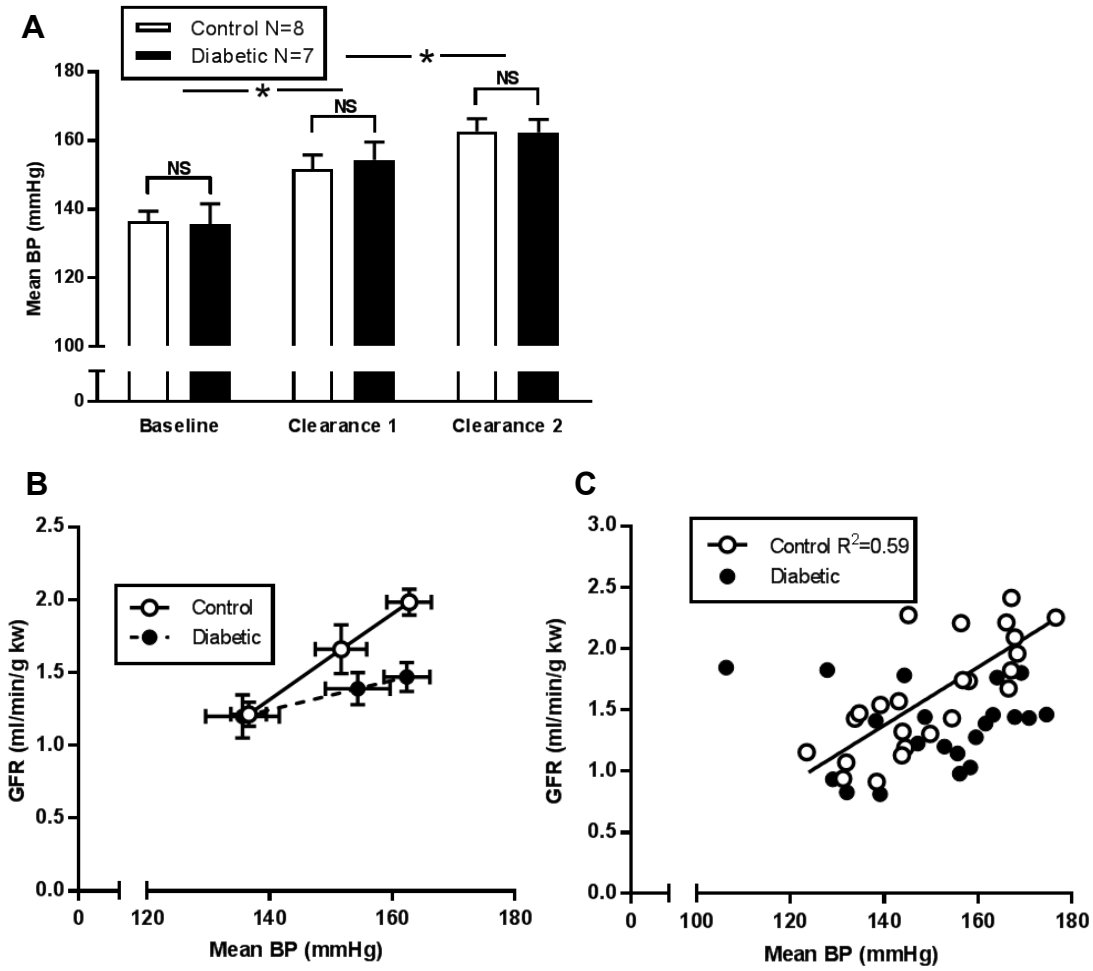

Fig. 4.2. Mean blood pressure (BP) and glomerular filtration rate (GFR) during ligature-induced acute pressure natriuresis in control and diabetic rats

A) Baseline mean BP and increments were not significantly different between cohorts, columns show mean ± standard error of the mean (SEM), *=P<0.05 compared with mean BP in previous period, NS=not significant. All comparisons made with two-way analysis of variance (ANOVA) with Sidak's *post hoc* tests.

B) GFRs were similar between cohorts during every clearance period. Every data point is the mean value of the dependent variable plotted against mean BP±SEM of both variables, and corresponds to one of three clearance periods.

C) GFR increased in a linear manner in control rats only, R^2=coefficient of determination.

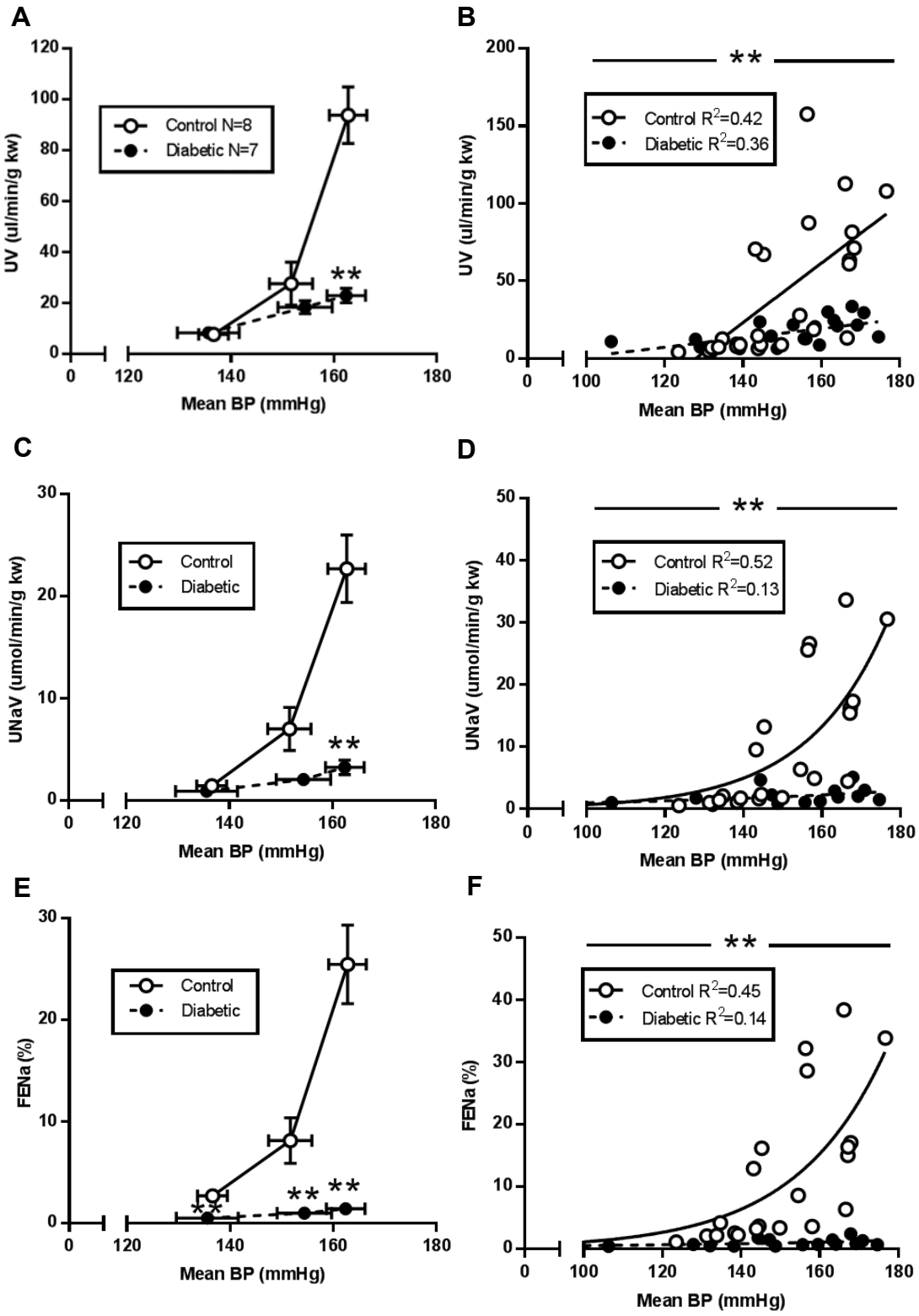
A
B
C
D
E
F
UV (ul/min/g kw)
Mean BP (mmHg)
Control N=8
Diabetic N=7
Control R2=0.42
Diabetic R2=0.36
UNaV (umol/min/g kw)
Control
Diabetic
Control R2=0.52
Diabetic R2=0.13
FENa (%)
Control R2=0.45
Diabetic R2=0.14
**

Fig. 4.3. (page opposite) Ligature-induced acute pressure natriuresis in control and diabetic rats

A) Pressure diuresis responses, with reduced urine flow rate (UV) in diabetic rats during Clearance 2

B) Pressure diuresis responses, with reduced gradient of the regression line for UV in diabetic rats (0.11-0.49, 95% confidence) compared with controls (0.9-2.9)

C) Pressure natriuresis responses, with reduced urinary sodium excretion rate (UNaV) in diabetic rats during Clearance 2

D) Pressure natriuresis responses, with reduced nonlinear rise in UNaV in diabetic rats (growth constant (k) =0.01) compared with controls (k=0.05)

E) Reduced fractional excretion of sodium (FENa) in diabetic rats during all three clearance periods

F) Reduced nonlinear rise in FENa in diabetic rats (k=0.01) compared with controls (k=0.04)

For A), C) and E), every data point is the mean value of the dependent variable plotted against mean blood pressure (BP) ± standard error of the mean (SEM) of both variables, and corresponds to one of three clearance periods, **=P<0.05 compared with controls. All comparisons made with two-way analysis of variance (ANOVA) with Sidak's *post hoc* tests.

For B), D) and F), R^2=coefficient of determination

	Baseline		Clearance 1		Clearance 2	
	Control	**Diabetic**	**Control**	**Diabetic**	**Control**	**Diabetic**
BP (mmHg)	136.6±2.9	135.6±6.0	152.7±4.2	154.4±5.3	162.8±3.6	162.4±3.8
GFR (ml/min/gkw)	1.2±0.1	1.2±0.1	1.7±0.2	1.4±0.1	2.0±0.1	1.5±0.1
UV (µl/min/gkw)	7.6±0.9	8.3±1.1	27.6±8.5	18.4±2.6	93.7±11.1	**22.9±2.9****
UNaV (µmol/min/gkw)	1.4±0.2	0.9±0.1	7.0±2.1	2.0±0.3	22.7±3.3	**3.2±0.7****
FENa (%)	2.7±0.4	**0.5±0.1****	8.1±2.2	**1.0±0.2****	25.4±3.9	**1.4±0.3****

Table 4.5 Mean blood pressure (BP), glomerular filtration rate (GFR), urine flow rate (UV), urinary sodium excretion rate (UNaV) and fractional excretion of sodium (FENa) in control and diabetic rats during Baseline and Clearances 1 and 2

****=P<0.05 compared with controls. All comparisons made with two-way analysis of variance (ANOVA) with Sidak's *post hoc* tests.**

4.3.2 Effects of insulin treatment of Type 1 diabetes mellitus on acute pressure natriuresis

One early T1DM rat was euthanased (Chapter 2.1, page 46) because of excessive weight loss. This rat is not included in the data presented.

Baseline mean BP (aggregated mean 110±2mmHg) and GFR (aggregated mean 0.4±0.1ml/min/gkw) did not differ between the three cohorts (Table 4.6). Sequential arterial ligation induced significant increases in mean BP of ~35mmHg (P<0.01; Fig. 4.4A) that did not differ between cohorts. GFR (Figs. 4.4B,C) rose as mean BP rose (P<0.01), in a linear manner (P<0.01), and independently of diabetic status (interaction P=0.09). GFR was less in early T1DM rats than controls only during

Clearance 2, by~0.7±0.2ml/min/gkw (P=0.01; Fig. 4.4B; Table 4.6) but did not differ from GFR in the insulin-treated cohort.

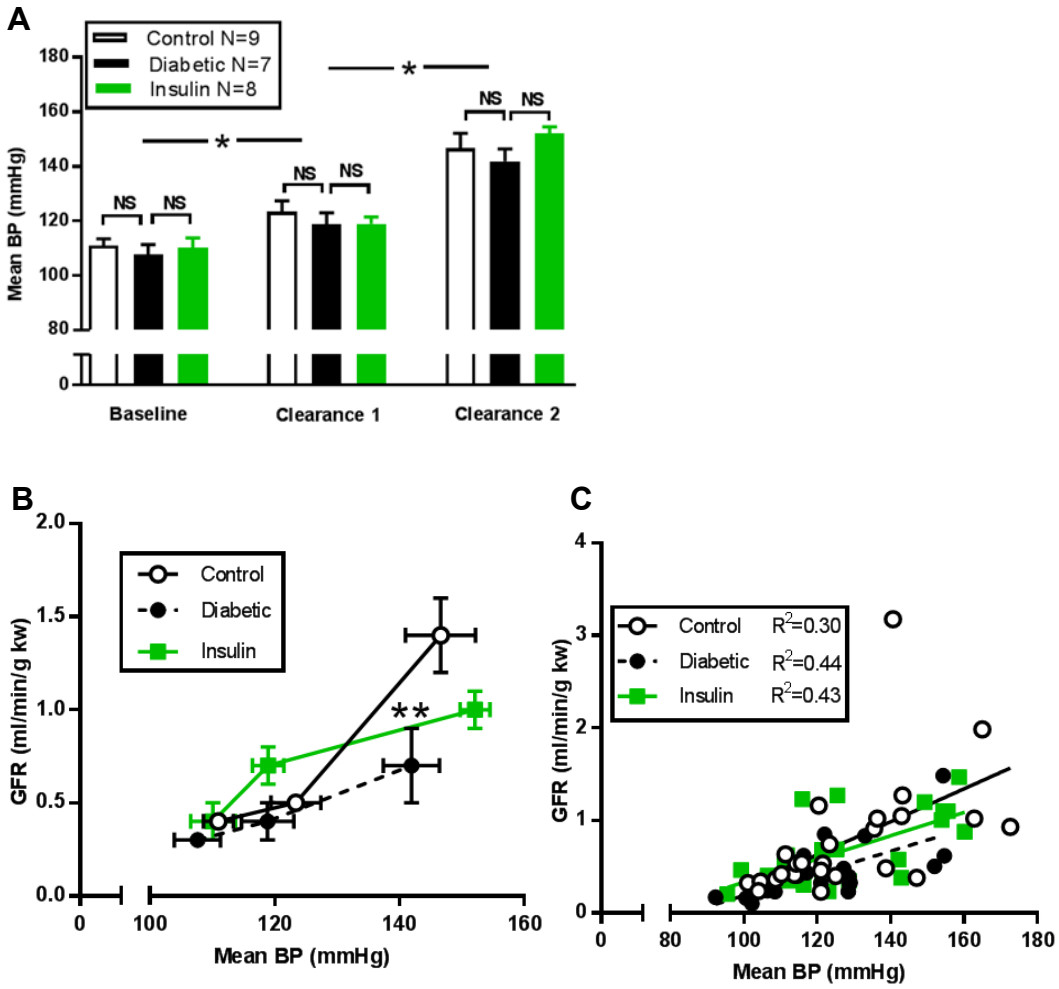

Fig. 4.4. Mean blood pressure (BP) and glomerular filtration rate (GFR) during ligature-induced acute pressure natriuresis in control, diabetic and insulin-treated diabetic rats

A) There were similar Baseline mean BP and increments after ligation in all three cohorts. Columns show mean ± standard error of the mean (SEM), *=P<0.05 compared with mean BP in previous period, NS=not significant.

B) GFR was lower in diabetic rats than in controls during Clearance 2. Every data point is the mean value of the dependent variable plotted against mean BP±SEM of both variables, and corresponds to one of three clearance periods, **=P<0.05 compared with controls.

C) GFR increased in the same linear manner in all three cohorts, R^2=coefficient of determination.

For A) and B), all comparisons made with two-way analysis of variance (ANOVA) with Tukey's *post hoc* tests.

Pressure diuresis (Figs. 4.5A,B) and natriuresis (Figs. 4.5C,D) were again induced by increasing mean BP (both $P<0.01$) and suppressed overall by early T1DM (both $P<0.01$, interactions $P<0.01$ (UV) and $P=0.03$ (UNaV)), particularly during Clearance 2 ($P<0.01$ (UV) and $P=0.02$ (UNaV); Table 4.6). This effect was associated with a reduction in FENa ($P<0.01$, interaction $P=0.02$; Figs. 4.5E,F), most noticeable during Clearance 2 ($P=0.02$; Table 4.6), that suggested differences in UV and UNaV could not be ascribed to differences in GFR. By contrast, suppression of UV ($P<0.01$ versus early T1DM), UNaV and FENa ($P=0.02$ versus early T1DM; Table 4.6) was not observed in insulin-treated diabetic rats: the slopes of these linear relationships were comparable to controls (Figs. 4.5B,D and F); both were significantly steeper than in rats with untreated early T1DM (all $P<0.01$).

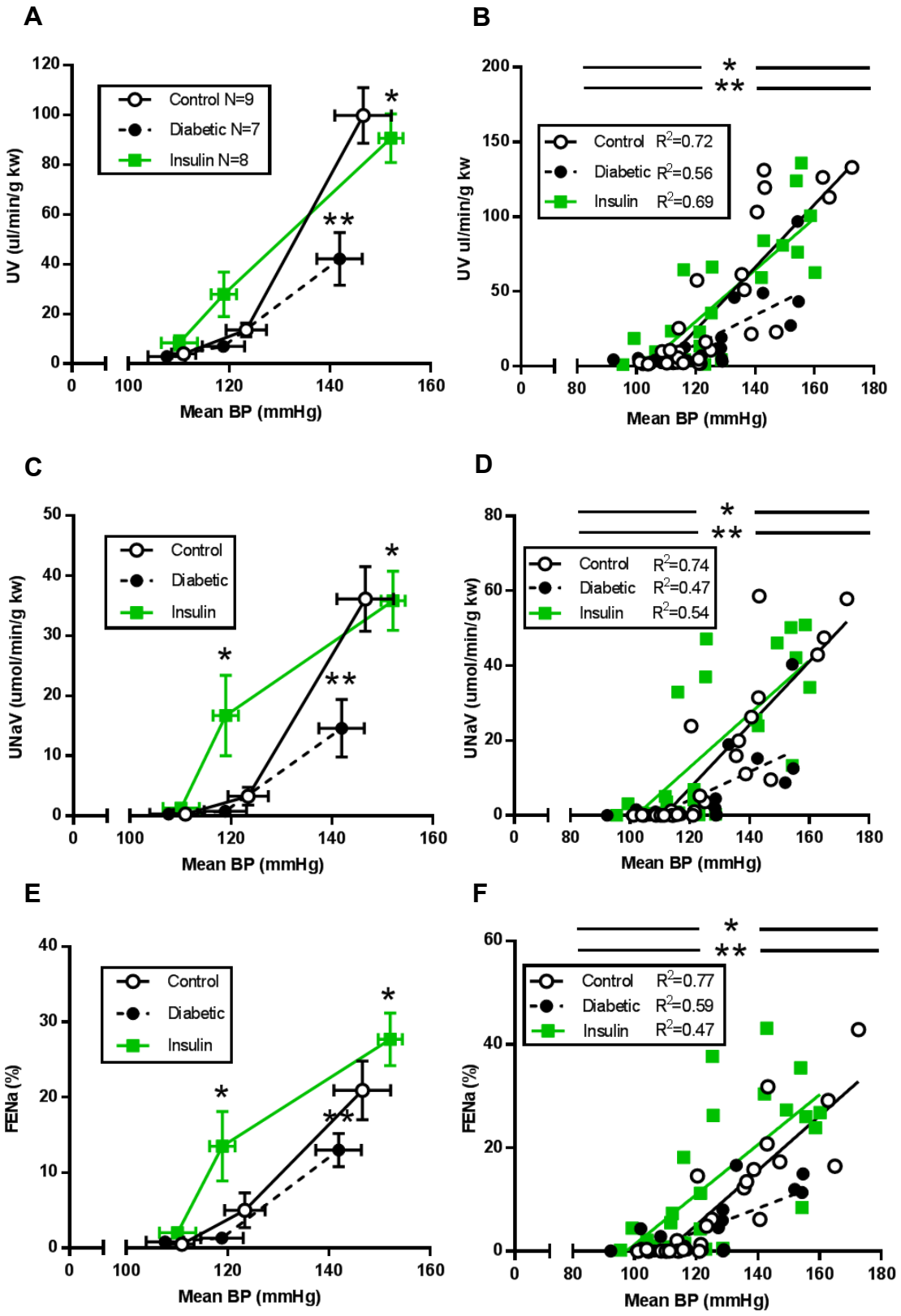
A
B
C
D
E
F
Control N=9
Diabetic N=7
Insulin N=8
UV (ul/min/g kw)
Mean BP (mmHg)
Control R2=0.72
Diabetic R2=0.56
Insulin R2=0.69
UV ul/min/g kw
Control
Diabetic
Insulin
UNaV (umol/min/g kw)
Control R2=0.74
Diabetic R2=0.47
Insulin R2=0.54
FENa (%)
Control R2=0.77
Diabetic R2=0.59
Insulin R2=0.47

Fig. 4.5. (page opposite) Ligature-induced acute pressure natriuresis in control, diabetic and insulin-treated diabetic rats

A) Pressure diuresis responses, with lower urine flow rate (UV) in diabetic rats than insulin-treated diabetic rats and controls during Clearance 2

B) Pressure diuresis responses, with reduced gradient of the regression line for UV in diabetic rats (0.6-1.4, 95% confidence) compared with insulin-treated diabetic rats (1.2-2.2) and controls (0.9-2.9)

C) Pressure natriuresis responses, with lower urinary sodium excretion rate (UNaV) in diabetic rats than insulin-treated diabetic rats during Clearances 1 and 2, and compared with controls during Clearance 2

D) Pressure natriuresis responses, with reduced gradient of the regression line for UNaV in diabetic rats (0.2-0.6, 95% confidence) compared with insulin-treated diabetic rats (0.4-1.0) and controls (0.6-1.1)

E) Lower fractional excretion of sodium (FENa) in diabetic rats compared with insulin-treated diabetic rats during Clearances 1 and 2, and compared with controls during Clearance 2

F) FENa responses, with reduced gradient of the regression line in diabetic rats (0.1-0.3, 95% confidence) compared with insulin-treated diabetic rats (0.3-0.7) and controls (0.4-0.6)

For A, C) and E), every data point is the mean value of the dependent variable plotted against mean blood pressure (BP) ± standard error of the mean (SEM) of both variables, and corresponds to one of three clearance periods, **=P<0.05 compared with controls, *=P<0.05 compared with diabetics. All comparisons made with two-way analysis of variance (ANOVA) with Tukey's *post hoc* tests, R^2=coefficient of determination.

	Baseline			Clearance 1			Clearance 2		
	Control	**Diabetic**	**Insulin**	**Control**	**Diabetic**	**Insulin**	**Control**	**Diabetic**	**Insulin**
BP (mmHg)	111.0±2.4	107.7±3.8	110.2±3.6	123.4±4.0	118.9±4.2	119.0±2.5	146.6±5.6	141.9±4.5	152.1±2.4
GFR (ml/min/gkw)	0.4±0.0	0.3±0.0	0.4±0.1	0.5±0.0	0.4±0.1	0.7±0.1	1.4±0.2	**0.7±0.2****	1.0±0.1
UV (µl/min/gkw)	4.0±1.1	2.9±0.5	8.4±2.9	13.6±2.8	7.0±1.5	27.9±9.0	99.7±11.2	**42.1±10.6****	**90.6±9.8***
UNaV (µmol/min/gkw)	0.3±0.2	0.3±0.0	1.3±0.5	3.3±1.5	0.8±0.4	**16.7±6.7***	36.1±5.4	**14.6±4.8****	**35.8±4.9***
FENa (%)	0.5±0.2	0.8±0.6	**2.0±0.6***	5.0±2.3	1.3±0.7	**13.5±4.6***	20.9±3.9	**13.0±2.2****	**27.7±3.5***
UET-1V (fg/min/gkw)	3.8±0.8	4.3±1.0	**6.3**±2.5	7.6±1.6	4.8±1.1	10.6±4.1	37.6±6.4	**13.4±3.9****	28.9±7.1

Table 4.6 Mean blood pressure (BP), glomerular filtration rate (GFR), urine flow rate (UV), urinary sodium excretion rate (UNaV), fractional excretion of sodium (FENa) and urinary endothelin-1 excretion rate (UET-1V) in control, diabetic and insulin-treated diabetic rats during Baseline and Clearances 1 and 2

***=P<0.05 compared with diabetics, **=P<0.05 compared with controls. All comparisons made with two-way analysis of variance (ANOVA) with Tukey's *post hoc* tests**

4.3.3 Relationships of renal endothelin-1 with mean blood pressure, urinary sodium and water excretion and diabetic status

UET-1V increased with mean BP (P=0.02, interaction P=0.05; Figs. 4.6A,B; Table 4.5). By the end of Clearance 2, the increase in UET-1V by ~30fg/min/gkw was suppressed by early T1DM by ~25fg/min/gkw (P<0.01; Fig. 4.6A; Table 4.6) but recovered with insulin (P=1.0 and 0.05 versus control and early T1DM rats respectively). The rise in UET-1V was linear in all three cohorts (control P<0.01; diabetic P<0.01; insulin-treated diabetic P<0.01; Fig. 4.6B) and correlated strongly with UV and UNaV, regardless of diabetic status (all P<0.01; Figs. 4.6C,D).

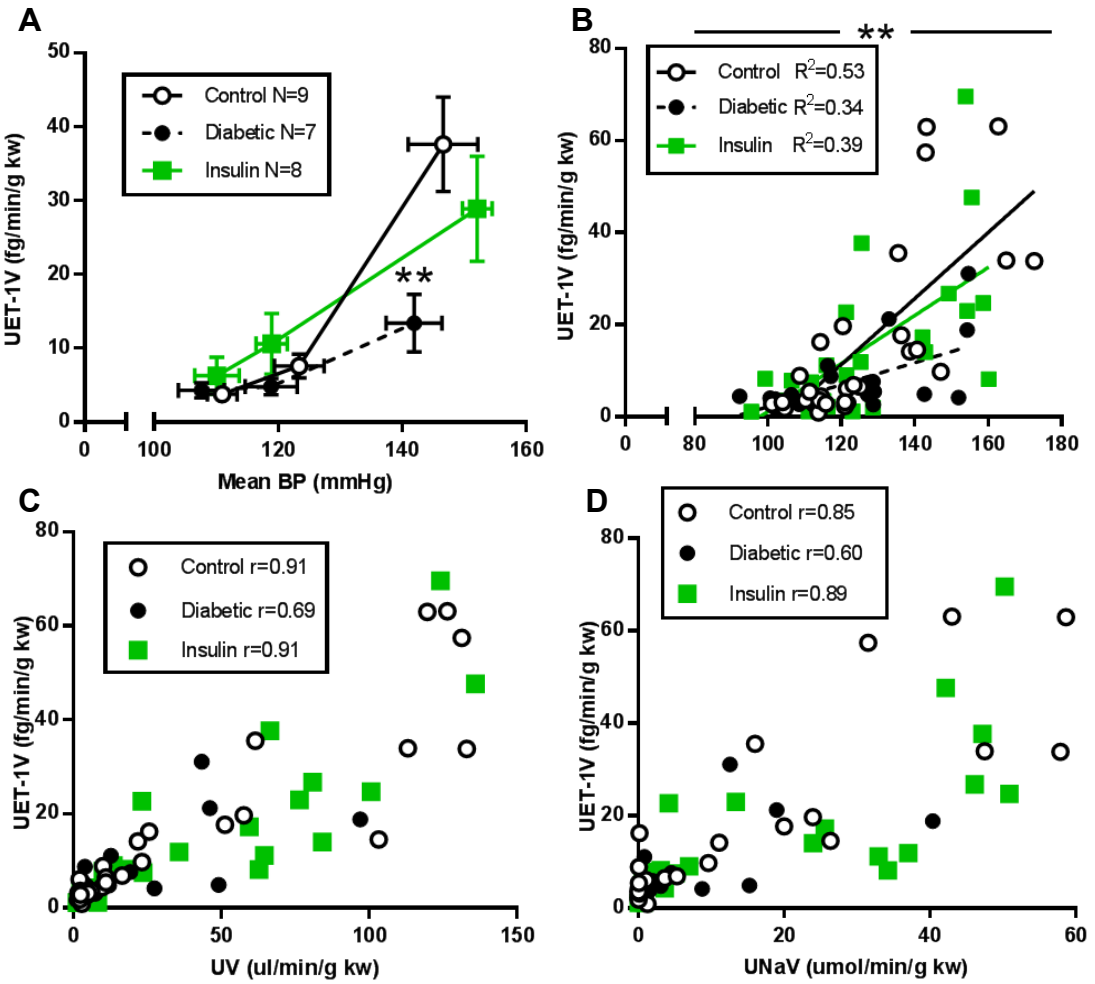

Fig. 4.6. Relationships of urinary endothelin-1 excretion rate (UET-1V) with mean blood pressure (BP), urine flow rate (UV) and urinary sodium excretion rate (UNaV) in control, diabetic and insulin-treated diabetic rats

A) Lower UET-1V in diabetic rats than controls during Clearance 2, every data point is the mean value of the dependent variable plotted against mean BP ± standard error of the mean (SEM) of both variables, and corresponds to one of three clearance periods, **=P<0.05 compared with controls, all comparisons made with two-way analysis of variance (ANOVA) with Tukey's *post hoc* tests.

B) Changes in UET-1 V with mean BP, with reduced gradient of the regression line in diabetic rats (0.07-0.40, 95% confidence) compared with insulin-treated diabetics (0.23-0.81) and controls (0.44-0.99), **=P<0.05 compared with controls, R^2=coefficient of determination

C) Strong correlations between UET-1V and UV regardless of diabetic status

D) Strong correlations between UET-1V and UNaV regardless of diabetic status

Correlations made by Pearson's and Spearman's rank tests, r=coefficient of correlation.

4.3.4 Biochemical, histological and molecular assessment of renal injury

All of the rats that entered these experiments, completed them. The urinary albumin:creatinine ratio was slightly higher in early T1DM rats than controls by ~0.17mg/mg (P=0.02; Fig. 4.7A; Table 4.7) but no different in T1DM+insulin rats.

Aldosterone:creatinine ratios (aggregated mean 0.76±0.32ng/mg) and 24-hourly UET-1 excretion (aggregated mean 39.4±10.6pg/day) were not different between cohorts (Figs. 4.7B,C). Similarly, the cortical (Fig. 4.8A) and medullary (Fig. 4.8B) expressions of mRNA of all the renal injury markers tested were unchanged in early T1DM and T1DM+insulin rats (Table 4.7).

Glomerulosclerosis was not observed on any H&E stained sections (Figs. 4.9A,B). Cortical (Figs. 4.9C,D) and medullary staining (Figs. 4.9E,F) with picrosirius red did not differ over 160 fields (x20 objective) in control and early T1DM cohorts (Table 4.7).

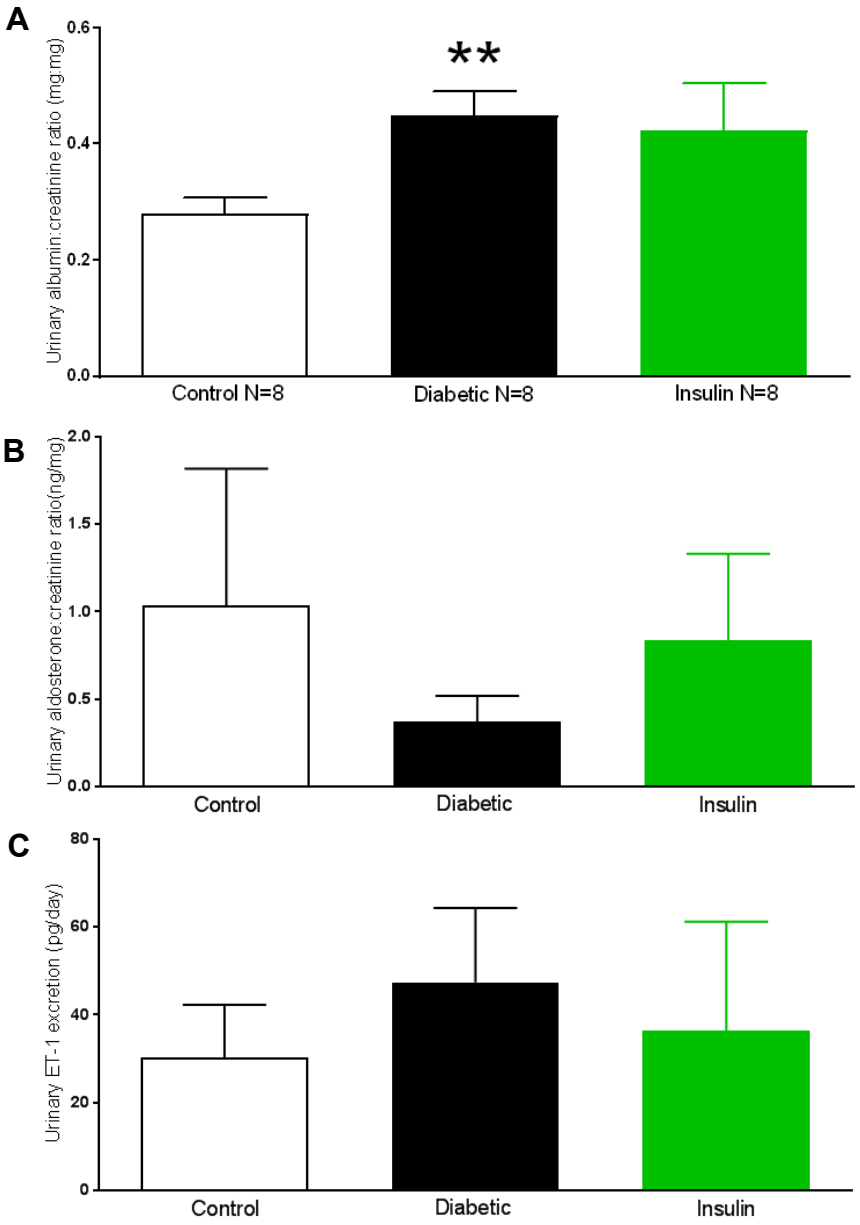

Fig. 4.7. Urinary markers of renal injury and activation of the renin-angiotensin-aldosterone system (RAAS) in control, diabetic and insulin-treated diabetic rats

A) Urinary albumin:creatinine was higher in diabetic rats than controls. Although statistically significant, the difference was not physiologically significant.

B) Urinary aldosterone:creatinine did not differ between cohorts.

C) Twenty-four-hourly urinary endothelin-1 (ET-1) excretion did not differ between cohorts.

Columns show mean ± standard error of the mean (SEM), **=P<0.05 compared with controls. All comparisons made with one-way analysis of variance (ANOVA) or Kruskal Wallis with Tukey's or Dunn's *post hoc* tests.

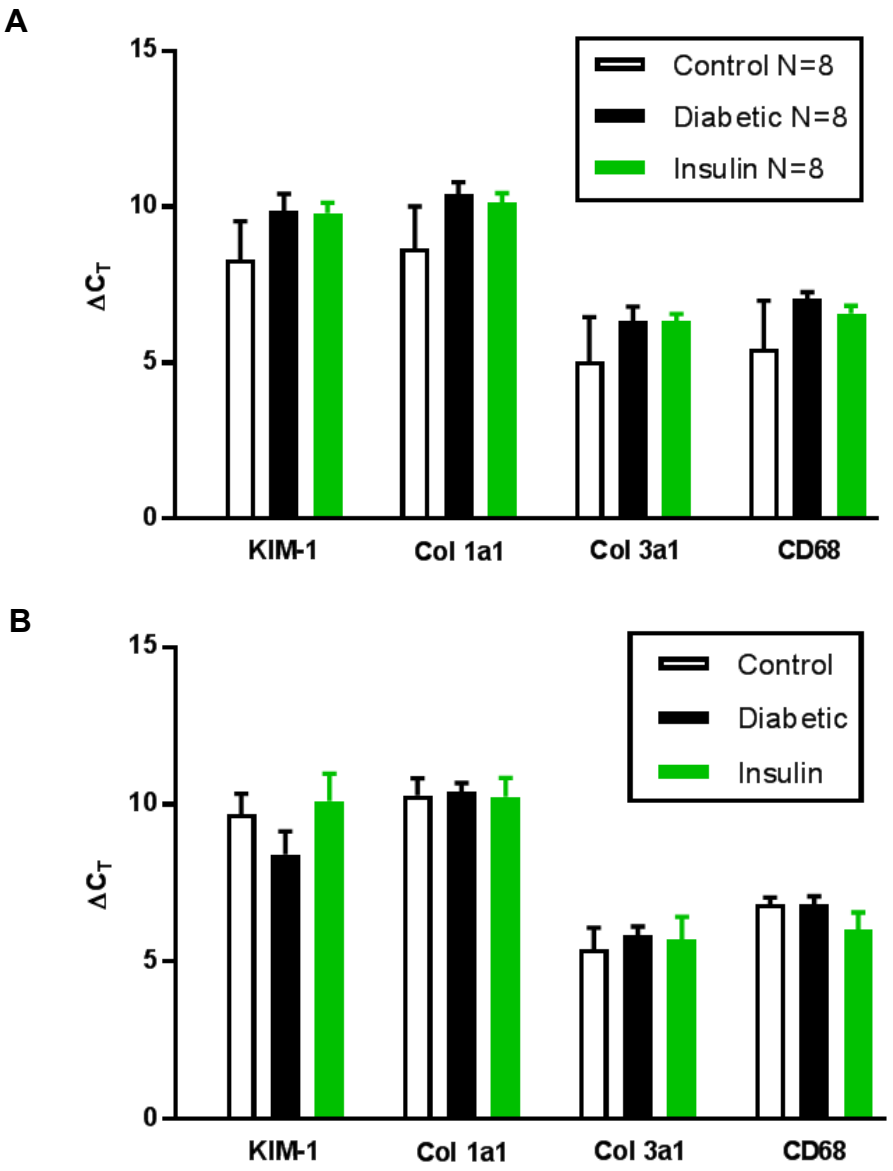

Fig. 4.8. Expression of markers of renal injury in control, diabetic and insulin-treated diabetic rats

A) Expression of kidney injury molecule-1 (KIM-1), collagen (Col) 1a1, Col3a1, and cluster of differentiation (CD) 68 in the renal cortex did not differ between cohorts.

B) Expression of KIM-1, Col1a1, Col3a1, and CD68 in the renal medulla did not differ between cohorts.

ΔC_T refers to the cycle threshold referenced to glyceraldehyde 3-phosphate dehydrogenase (GAPDH). Columns show mean ± standard error of the mean (SEM). All comparisons made with one-way analysis of variance (ANOVA) or Kruskal Wallis with Tukey's or Dunn's *post hoc* tests.

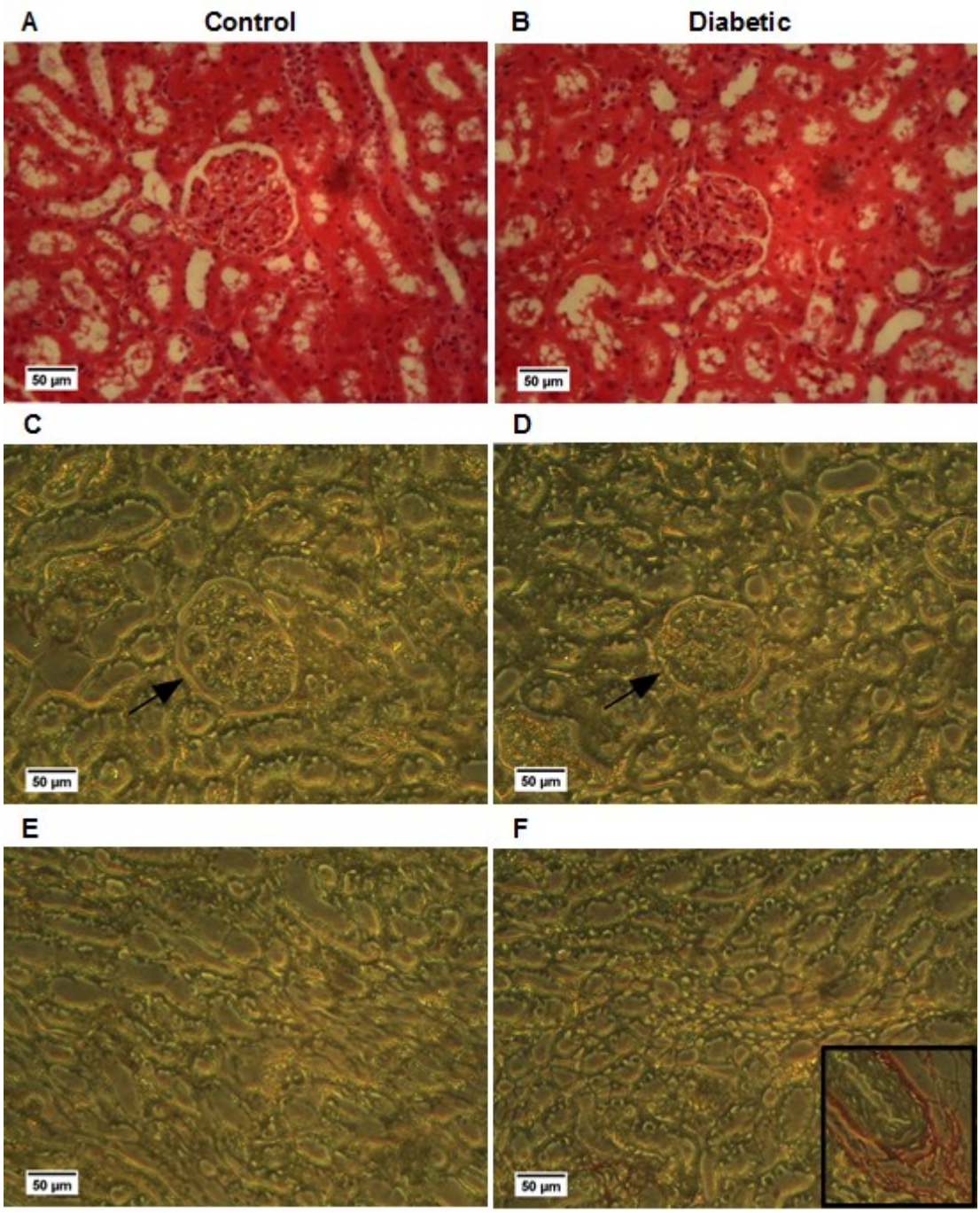

Fig. 4.9. Renal histopathology in control and diabetic rats

A) and B) Glomerulosclerosis was absent on haematoxylin and eosin staining, as demonstrated in the central glomerulus.

C) and D) Picrosirius red staining for collagen in the cortex (arrows indicate glomeruli) did not identify fibrosis.

E) and F) Picrosirius red staining for collagen in the medulla did not identify fibrosis. Positive staining of collagen in normal connective tissue is shown for reference as an inset in F).

	Control		Diabetic		Insulin	
Albumin:creatinine (mg/mg)	0.28±0.03		**0.45±0.04****		0.43±0.08	
Aldosterone:creatinine (ng/mg)	0.83±0.78		0.37±0.15		0.83±0.50	
ET-1 excretion (pg/day)	30.25±12.01		47.38±10.32		36.26±24.93	
	Cortex	**Medulla**	**Cortex**	**Medulla**	**Cortex**	**Medulla**
C_T GAPDH	25.2±1.5	23.1±0.4	22.6±0.2	22.9±0.2	23.2±0.2	22.9±0.5
C_T TBP	32.2±0.3	31.2±0.4	31.7±0.2	31.7±0.2	32.2±0.2	31.8±0.5
ΔC_T KIM-1	8.3±1.2	9.7±0.7	9.9±0.6	8.4±0.7	9.8±0.3	10.1±0.9
ΔC_T Col1a1	8.7±1.4	10.3±0.5	10.4±0.4	10.4±0.3	10.1±0.3	10.2±0.6
ΔC_T Col3a1	5.1±1.4	5.4±0.7	6.4±0.5	5.8±0.3	6.3±0.2	5.7±0.7
ΔC_T CD68	5.5±1.5	6.8±0.2	7.0±0.2	6.8±0.3	6.6±0.3	6.0±0.6
Picrosirius staining	0.41±0.02	0.52±0.08	0.36±0.03	0.29±0.03	-	-

Table 4.7 Markers of renal injury

All data are mean ± standard error of the mean (SEM), **=P<0.05 compared with controls. All comparisons made with one-way analysis of variance (ANOVA) or Kruskal Wallis with Tukey's or Dunn's *post hoc* tests, ΔC_T refers to the threshold cycle referenced to glyceraldehyde 3-phosphate dehydrogenase (GAPDH). ET-1=endothelin-1, TBP= thymine-adenine-thymine-adenine (TATA) box binding protein, KIM-1=kidney injury molecule-1, Col =collagen, CD68=cluster of differentiation 68

4.4 Discussion

This chapter describes the first direct assessment of acute pressure natriuresis in early T1DM rats. It demonstrates that acute pressure natriuresis is severely impaired within three weeks of inducing T1DM, before clear evidence of renal injury and fibrosis has developed. The effect can be reversed with insulin, and is associated with changes in UET-1 excretion. Acute pressure natriuresis stabilises BP, so it is concluded that functional changes that may contribute to cardiovascular risk are present at an early stage of T1DM, prior to the onset of nephropathy.

4.4.1 Type 1 diabetes mellitus severely blunts acute pressure natriuresis by increasing tubular sodium reabsorption.

After adopting renal clearance times derived from Chapter 3, sequential arterial ligation gave predictable rises in BP, generating a robust and controllable experimental protocol. This permitted statistically rigorous comparisons between cohorts, and investigation of a potential causative mechanism. Attenuation of UV and UNaV at higher BPs in the early T1DM rats was accompanied by a striking reduction in FENa, showing that excessive sodium reabsorption made a greater contribution than a slightly lowered GFR to reduced sodium excretion.

A smaller FENa might have been expected in the early T1DM rats because T1DM increases sodium reabsorption in the proximal convoluted tubule (PCT) [263]. However, this would have increased rather than decreased GFR by reducing tubuloglomerular feedback (TGF) and increasing afferent arteriolar flow [263]. The resulting hyperfiltration is a key step in the development of diabetic nephropathy [44]

and, importantly, increased GFR and renal blood flow would have been confounding variables in this study. A rat model of early T1DM, only two-to-three weeks after STZ injection, was deliberately selected because STZ-induced T1DM rats take several weeks to develop hyperfiltration [72], and even Dahl salt-sensitive rats take nine weeks to demonstrate increased GFR and increased renal blood flow [264]. The GFR of the model had already been shown to match GFR in healthy controls under prolonged anaesthesia (Chapter 3), and there was no biochemical, histological or molecular evidence of renal pathology or RAAS activation. Although urinary albumin levels were slightly higher in the earlyT1DM rats, the levels were not consistent with significantly increased glomerular permeability [72]. Therefore, it was concluded that impaired acute pressure natriuresis precedes hyperfiltration in early T1DM rats and cannot be explained by reduced TGF, RAAS activation or structural nephropathy.

Acute pressure natriuresis is a renal vasculotubular response to increases in BP. Medullary blood flow, which, unlike cortical flow and GFR, is not autoregulated, rises in line with BP [138]. Medullary hydrostatic pressures also rise, and there is a reduction in sodium reabsorption, principally from the PCT [91], although the overall natriuretic effect is also dependent on sodium transport activity in the more distal nephron [186,265]. Impaired excretion of sodium and water has been identified previously in T1DM rats [108,109,266] but this study shows that it results from either reduced medullary blood flow or increased tubular sodium transport.

4.4.2 Impairment of acute pressure natriuresis is reversed with insulin.

In these experiments, impairment of acute pressure natriuresis by early T1DM was reversed when blood glucose was reduced with insulin. Whether this was a consequence of lowering blood glucose or a direct effect of insulin was not determined, but the latter is a possibility since the effects of insulin on sodium reabsorption are well documented [238]. Insulin stimulates ENaC as well as other renal transporters [267], and in hyperinsulinaemia due to Type 2 diabetes mellitus (T2DM), sodium-glucose transporter-2 (SGLT2) inhibitors combat hypertension from enhanced sodium reabsorption [268]. However, insulin also promotes sodium excretion, which is more consistent with the recovery of acute pressure natriuresis in this study. This occurs through the actions of the vasodilator, NO [146,269], which also mediates the vasodilatory effects of ET-1, and its pro-natriuretic effects at ENaC [122], raising the possibility that insulin could modify acute pressure natriuresis via vascular or tubular renal ET-1.

4.4.3 Urinary endothelin-1 excretion rate varies with urine flow rate and urinary sodium excretion rate, regardless of diabetic status.

All ET-1 in urine is renally derived [77] so UET-1 excretion was used in these experiments as a surrogate marker of renal ET-1 activity [209]. Twenty-four-hourly UET-1 excretion failed to demonstrate increased chronic renal ET-1 signalling in the early T1DM model, but this probably reflected the absence of overt glomerular remodelling [261]. By contrast, during acute pressure natriuresis, UET-1V increased abruptly, and matched marked increases in UV and UNaV in control and T1DM+insulin rats and even the relatively suppressed increases in UV and UNaV in

T1DM rats. UET-1V and UNaV are both a function of flow rate, and so the data demonstrate that the urinary concentrations of ET-1 and sodium were maintained, even at higher urine flow rates. This is consistent with release of ET-1 from the collecting duct in response to urine flow and sodium [270,271], suggesting that the increase in UET-1V in control and T1DM+insulin rats, and the decrease in UET-1V in early T1DM rats may have been more a consequence rather than a cause of changes to UV and UNaV. However, although collecting duct ET-1 is a component of a negative feedback loop of ENaC activity that includes nitric oxide synthase 1 (NOS1) [272], a negative feedback loop of ET-1 release has not been identified. Collecting duct ET-1 is an autocrine/paracrine agent that promotes natriuresis, so, in the absence of negative feedback, there is the potential for it to mediate a runaway natriuresis during pre-existing polyuria, as in glycosuria in untreated T1DM. This clearly did not take place during acute pressure natriuresis in the early T1DM rats, so an alternative explanation for the suppression of UET-1V, UV and UNaV in T1DM is required.

Collecting duct ET-1 expression and ET_B receptor activity can be modified by many intrarenal regulatory mechanisms but because of their complex, conflicting interactions with ET-1 and ET_B receptors, how these might restrict increases in collecting duct ET-1 in T1DM is not apparent. For example, vasopressin and angiotensin II (AngII) can reduce collecting duct ET_B receptor activity [273,274]. Equally, though, ET_B receptor activity reduces collecting duct vasopressin-2 (V2) receptor activity [275], and, in these experiments, RAAS activation in the early T1DM rats was not identified. Similarly, adenosine triphosphate (ATP) reduces ET-1

expression in collecting duct cells [276] but activation of purinergic-2 (P2) receptors in the renal medulla promotes ET-dependent natriuresis [277].

An alternative source of UET-1 may provide additional insight. Studies in collecting duct ET-1 knockout (KO) mice [180] and with ET_B receptor antagonists [209] suggest that approximately half of UET-1 is an overspill from the collecting duct, and the other half is from the renal interstitium, the site of the medullary *vasa recta* where acute pressure natriuresis is initiated by an increase in BP. ET-1 regulates flow through the *vasa recta* by constriction (ET_A) [182] or relaxation (ET_B) [278] of surrounding vascular pericytes, and endothelial ET_B receptors clear locally produced ET-1 from the circulation [77]. T1DM is already known to increase vascular ET_A receptor-mediated constriction [257,258], reduce endothelial ET_B receptor activity [255] and promote activity of ENaC [265]. This means that the reductions in UET-1, UV and UNaV observed in the early T1DM rats may reflect an increase in medullary vascular ET_A receptor activity or a decrease in medullary vascular and/or collecting duct ET_B receptor activity (Fig. 4.10). This is an attractive theory because it links the renal vascular and tubular functions of ET-1 with the vascular and tubular stages of acute pressure natriuresis. It also links UET-1 with BP to prevent a runaway collecting duct ET-1-mediated natriuresis, and offers potential mechanisms by which these might be modified by early T1DM.

The possibility that early T1DM impairs acute pressure natriuresis through increased vascular ET_A receptor activity is important because it could be amenable clinically to selective ET_A receptor antagonism. If a link between impaired acute pressure

natriuresis and cardiovascular risk can be demonstrated in the same rat model of early T1DM, then further investigation of the causal role of ET-1 and its receptors in the suppression of acute pressure natriuresis in early T1DM, and its recovery with insulin would be indicated.

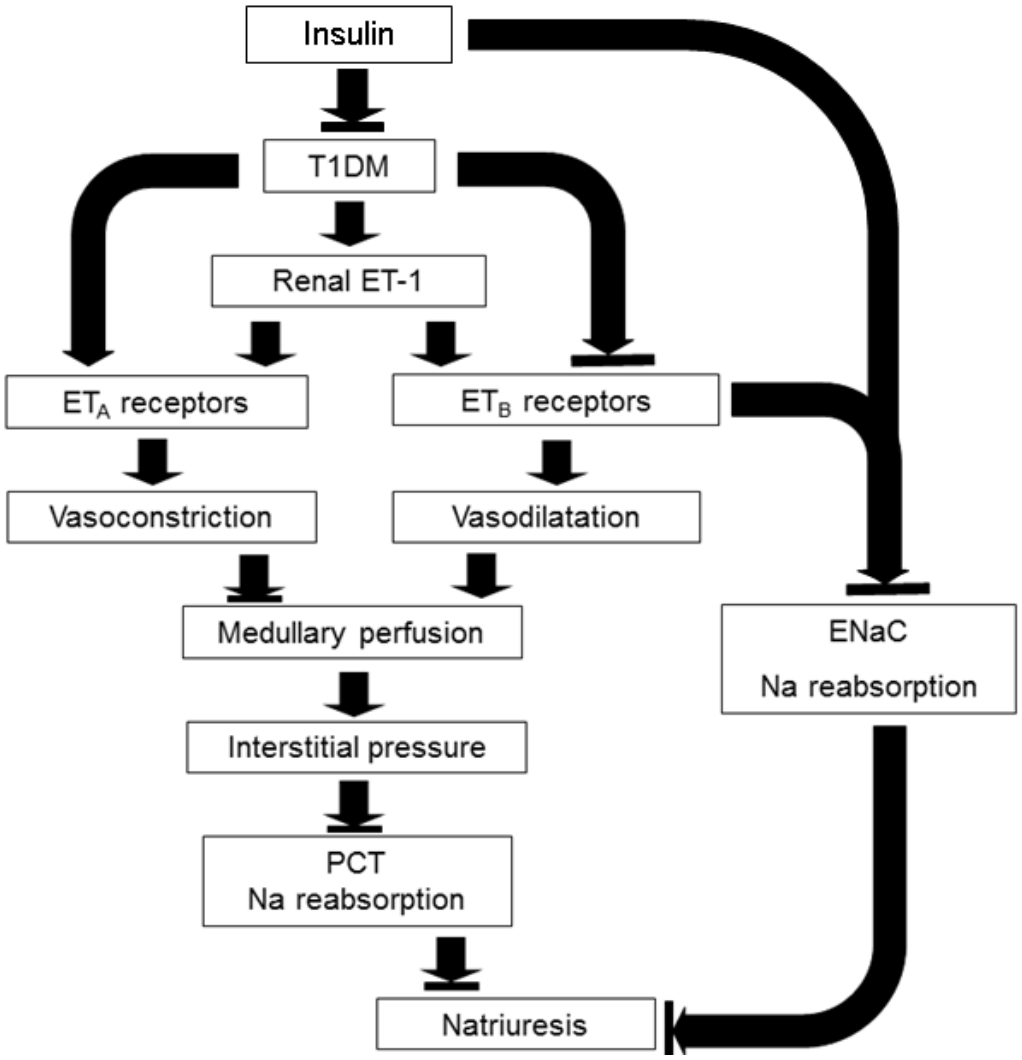

Fig. 4.10 Algorithm proposing mechanisms by which early Type 1 diabetes mellitus (T1DM) and insulin modify regulation of acute pressure natriuresis by endothelin-1 (ET-1).

Lines blocking arrows represent inhibition.

PCT=proximal convoluted tubule, ENaC=epithelial sodium channel

4.5 Conclusions

Impairment to acute pressure natriuresis, a precursor to hypertension and nephropathy, occurs at a very early stage of experimental T1DM, prior to structural nephropathy. The response is reversed with insulin and is associated with changes in renal ET-1 signalling.

This study is relevant to the development of CVD risk in T1DM patients. By successfully re-establishing acute pressure natriuresis in an early T1DM rat model with insulin, these pre-clinical data support the findings of DCCT/EDIC [24,29] that cardiovascular risk is tightly linked to blood glucose control. They also suggest that acute pressure natriuresis may be a therapeutic target where tight blood glucose control cannot be achieved. Existing drugs, such as the selective ET_A receptor antagonists, might achieve this.

4.5.1 Follow-on work

The full implications from these data towards reducing cardiovascular risk in T1DM, should be determined. The following chapter will assess the impact of such profound suppression of acute pressure natriuresis on BP control, and whether control of BP is restored by manipulating ET-1 signalling.

5 The effect of Type 1 diabetes mellitus on blood pressure, and the response to endothelin receptor antagonists

5.1 Introduction

Acute pressure natriuresis plays a key role in regulating blood pressure (BP) by increasing sodium excretion when BP increases [89]. In the previous chapter, Type 1 diabetes mellitus (T1DM) was shown to impair acute pressure natriuresis severely. Such impairment has clinical relevance because it would be expected to increase BP. However, in the previous chapter, mean BP was not increased in either of the two untreated early T1DM cohorts in which acute pressure natriuresis was induced. All BP measurements were obtained under general anaesthesia, following laparotomy, and it may be that this reduced BP more in diabetic rats than controls. This thesis is investigating factors that contribute to increased cardiovascular risk in early T1DM and, because increased BP is a major risk factor for cardiovascular disease (CVD) [247-250], it is necessary to determine unequivocally whether impaired acute pressure natriuresis in early T1DM is associated with increased BP, before proceeding to experiments that investigate a causative mechanism. Consequently, the experiments in this chapter are designed to measure systolic and diastolic BP in conscious rats with early T1DM.

In people, acute pressure natriuresis is more active during the day, when most salt intake occurs, and less active at night, when there is less salt intake. As a result, sodium excretion, and hence BP, follow a circadian pattern [100]. Both vary in a sinusoidal manner [237] with peak levels during the day, and trough levels during the night [100,101]. Disruption to the circadian rhythm in BP is associated with increased risk of CVD [102-104], and in patients with T1DM, occurs several years in advance of diabetic nephropathy, itself a major risk factor for CVD [74]. Importantly, this loss of

circadian rhythm also precedes elevated BP, as recorded in the clinic (office hypertension) [74]. Therefore, to identify the potential full influence of impaired acute pressure natriuresis on BP, continuous 24-hourly BP measurements rather than single, daily BP measurements are performed in this chapter. This allows the peak and trough levels of BP to be recorded and the sinusoidal variation between these values to be determined [237].

Also in the previous chapter, a link between renal endothelin-1 (ET-1) and impaired acute pressure natriuresis was established: urinary ET-1 excretion was suppressed when urinary sodium excretion was suppressed. Renal ET-1 is of interest because it is highly expressed within the kidney by endothelial cells, vascular smooth muscle cells (VSMCs) and renal tubular cells [77], all of which contribute to acute pressure natriuresis [89]. T1DM increases expression and secretion of ET-1 [205,254], enhances ET_A receptor signalling [257,258] and reduces endothelial ET_B receptor-mediated vasodilation [259]. These effects promote vasoconstriction [77], and renal injury [154] which would be expected to impair acute pressure natriuresis [89]. This is supported by clinical studies with ET_A receptor antagonists, which re-establish circadian variation in BP in non-diabetic chronic kidney disease (CKD) [226], and reduce proteinuria and BP in diabetic nephropathy (both T1DM and T2DM) [220]. Whether or not ET_A receptor antagonists re-establish circadian variation in BP in pre-clinical or clinical T1DM has not been determined, but if demonstrated, it would implicate an inhibitory effect of ET_A receptors on acute pressure natriuresis that can be targeted pharmacologically. Therefore, to determine whether ET_A receptor signalling might be a mechanistic pathway for impairment of acute pressure natriuresis by early

T1DM, the effect of ET_A and ET_B receptor antagonists on 24-hourly BP in early T1DM rats was also measured.

5.1.1 Hypotheses

1. Early T1DM increases BP and disrupts the circadian profile of BP.
2. This is reversed by selective ET_A but not combined ET_A/ET_B receptor antagonism.

5.1.2 Aims

To investigate these hypotheses, radiotelemetric measurement of BP in a rat model of early T1DM was used to answer the following questions:

1) Does early T1DM increase BP and disrupt its circadian variation, and do the effects increase when salt intake increases?
2) Does a selective ET_A receptor antagonist restore normal BP in early T1DM and its circadian variation?
3) Does combined ET_A/ET_B receptor antagonism re-establish increased BP and loss of its circadian variation?

5.2 Methods

5.2.1 Implantation of radiotelemetry units and randomisation

Experiments were performed, single-blinded, in adult male Sprague Dawley rats (Chapter 2.1, page 46). After rats had been acclimatised for six days (Fig. 5.1), pre-calibrated radiotelemetry units (TA11-CA P40; Data Sciences International, 's-Hertogenbosch, Netherlands) were surgically implanted (Chapter 2.7, pages 76-79) over a four-day period in 16 rats. The sensory catheter of the units was implanted into the distal aorta and the transmitter secured to the peritoneal aspect of the body wall. After a minimum of 10 days' recovery, skin staples were removed under brief anaesthesia with isoflurane (IsoFlo; Zoetis Animal Health Limited (Ltd.), Sandwich, United Kingdom (UK)).

Following a further five-to-nine-day recovery period, rats were assigned to early T1DM and control cohorts on Day 20 (Fig. 5.1). Heart rate, and systolic and diastolic BP were acquired at 1kHz for one minute in every hour, for seven days (Randomisation Recording; Fig. 5.1). The beginning of every day was defined as the start of the dark period at 7pm. Data from the middle five days were analysed to ensure that BP and heart rate did not differ between cohorts, by chance, prior to induction of T1DM.

5.2.2 Induction of Type 1 diabetes mellitus

T1DM (blood glucose >12mmol/l) was induced from Day 27 with one or two intraperitoneal (ip.) injections of streptozotocin (STZ); Chapter 2.1, page 46) and healthy control rats received ip. citrate buffer.

5.2.3 Recording blood pressure and circadian variation in blood pressure with radiotelemetry

From Day 41, two weeks after the first ip. injection of STZ/citrate, systolic and diastolic BP, and heart rate were measured continuously by radiotelemetry (Chapter 2.7, page 79) in early T1DM and control rats (Table 5.1) for five more weeks (Fig. 5.1). The first of these weeks confirmed that haemodynamic parameters had reached stability following induction of T1DM. Data from the second week (Diabetes Recording Period, Days 48-55) were analysed to determine the effect of early T1DM. During the third week (Salt Recording Period, Days 55-62), after the 6pm but before the 7pm data acquisition, rats were offered salt supplementation in order to exaggerate any salt-sensitive phenotype. The salt was in the form of an ice-cube (~10ml)-sized gelatin (Dr. Oetker UK Ltd, Leyland, UK) block containing soluble meat extract (80mg sodium chloride/ml; Bovril; Unilever UK Ltd, Leatherhead, UK). The quantity of meat extract was measured so that, for every rat, daily sodium intake was 140mg of sodium/day based on 15g/day daily intake of pelleted food [279]. This equated to a 1% sodium diet, four times the concentration of sodium in the unsupplemented diet. One gelatin block was placed in every rat's cage on top of a cardboard tube used for environmental enrichment, where it could be easily visualised. The block was universally consumed voluntarily and rapidly.

5.2.4 Modification of blood pressure and heart rate with endothelin receptor antagonists

During the fourth week of recording, (Days 62-69, Fig. 5.1), the gelatin block was supplemented with the selective ET_A receptor antagonist, atrasentan (5mg/kg [154]; AbbVie Ltd., Maidenhead, UK). During the fifth and final week (Days 69-76), the gelatin block also contained the selective ET_B receptor antagonist, A-192621 (10mg/kg [154]; AbbVie Ltd.). After the final recording period, rats were euthanased by a Schedule one method (Chapter 2.1, page 46) and examined *post mortem*, to ensure correct placement of the radiotelemetry pressure transducer catheter.

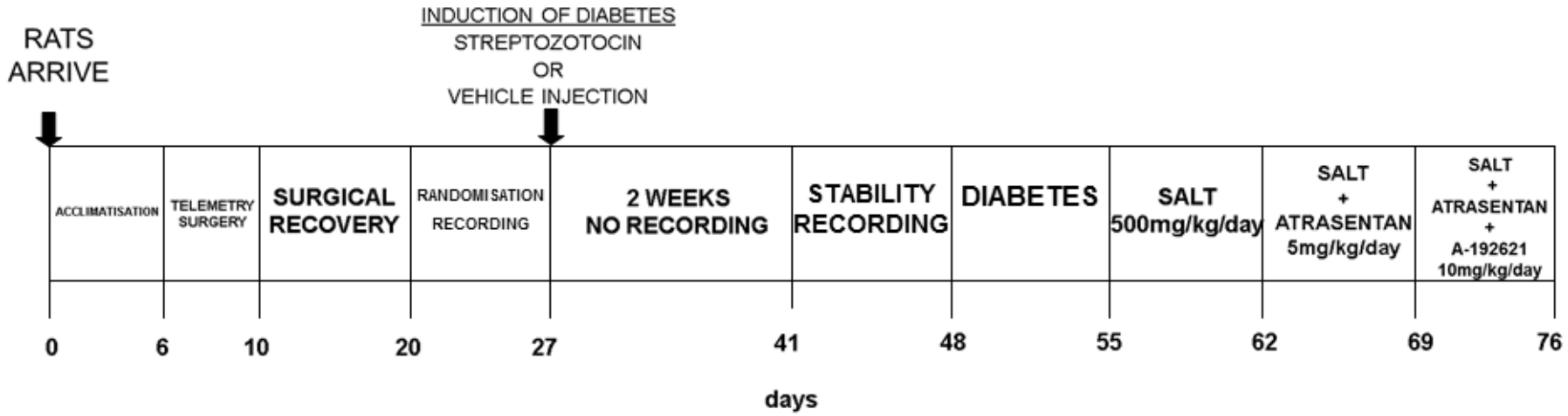

Fig. 5.1. Timeline (days) for radiotelemetry study

Radiotelemetry units were implanted following acclimatisation after purchase. All recording periods were seven days long but only data from the middle five days were analysed.

	Radiotelemetry start		Radiotelemetry end	
	Control	**Diabetic**	**Control**	**Diabetic**
Number	4	4	4	4
Weight (g)	331.0±3.6	**316.8±2.7****	585.5±10.5	**477.3±22.8****
BG (mmol/L)	4.4±0.3	**18.7±1.8****	5.1±0.3	**19.5±1.1****

Table 5.1. Number, weight and blood glucose (BG) in control and diabetic rats that completed the radiotelemetry study.

Data are mean ± standard error of the mean (SEM), **=P<0.05 compared with controls. All comparisons made with two-sample Student's *t*-tests.

5.2.5 Statistical analysis

Studies were designed to obtain a power >80% if cohort sizes were six rats, BP was 3.0±1.5mmHg higher in diabetic rats than in controls, and diurnal dipping in BP was 3.0±1.5% lower in diabetics [280]. Additional rats were included to account for an expected dropout rate of 25% due to experimental mortality and technological malfunction (n=15).

The first and last days of every seven-day recording period were excluded prior to analysis to remove confounding stress effects associated with weekly staff changes and routine husbandry.

Data are expressed as mean values ± standard error of the mean (SEM). Mean values for every phase were the mean of every four-hour period for five days, so

every rat contributed 30 values in total. To illustrate changes in BP and heart rate over time in each cohort, the mean value ± SEM at the same time point in every one of the five days was plotted against 24 individual hours. These data differed slightly from the data from every four-hour period.

Normality of data were determined by the Anderson-Darling test, or if n<6, by visual assessment of data distribution [281]. Single comparisons of BP and heart rate between cohorts were made with two-sample Student's *t*-tests (normal) or Mann Whitney *U*-tests (non-normal) according to normality, while multiple comparisons employed one-way analysis of variance (ANOVA) with Tukey's *post hoc* tests with or without transformation according to normality and equality of variance of residuals. Kruskal Wallis with Dunn's *post hoc* tests was employed only where transformation was unsuccessful.

Circadian variations in BP and heart rate were determined from diurnal dipping, 24-hour-periodicity and cosinor analysis (Chapter 2.7, pages 79-80). Diurnal dipping was defined as the percentage reduction in heart rate or BP at every light-to-dark transition. It was calculated for every rat for every day, from the mean of three four-hourly light periods and three four-hourly dark periods. Every rat contributed one value of dipping per day for five days to the comparisons between cohorts. Twenty-four-hour-periodicity in each cohort was obtained from chi-square analysis of hourly heart rate and BP [237] . Every rat contributed to every mean hourly value, and 24 mean values per day for five days were analysed. Tau was assumed to be between 19 and 27 hours. Cosinor analysis of heart rate and BP was performed in

individual rats and used hourly measurements (24 data points per rat per day) for five days. Welch's *t*-test was used to compare the mean values of mesor, amplitude (amp) and acrophase (acro) in each cohort.

Seven out of 15 rats failed to complete the study. One rat died from intra-operative haemorrhage, one diabetic rat was euthanased due to excessive weight loss, one rat failed to become diabetic, and device malfunction occurred in four rats due to lead migration or thrombus formation over the lead tip. Where applicable, these rats were euthanased. None of the data from these rats is presented.

For all tests, statistical significance was set at $P<0.05$.

5.3 Results

5.3.1 Haemodynamic parameters prior to induction of Type 1 diabetes mellitus (Randomisation Recording Period)

There was no difference in systolic and diastolic BP and heart rate between rats assigned to control and early T1DM cohorts prior to induction of T1DM (Table 5.2; Fig. 5.2).

RRP	Systolic BP		Diastolic BP		Heart rate	
	Control	**Diabetic**	**Control**	**Diabetic**	**Control**	**Diabetic**
Mean (mmHg/bpm)	124.1±0.5	124.2±0.4	93.8±0.4	91.9±0.3	405.1±2.5	406.1±2.4
Dip (%)	4±1	3±1	5±0	5±0	12±1	13±1
Mesor (mmHg/bpm)	123.5±4.5	124.9±3.8	93.8±2.7	91.5±3.2	402.4±13.5	406.6±12.1
Amp (mmHg/bpm)	3.9±0.3	3.2±0.3	3.7±0.9	2.8±0.9	39.9±4.5	42.0±4.7
Acro (radians)	26.7±16.1	20.5±17.0	27.1±11.2	41.7±13.1	11.9±5.7	5.0±4.8

Table 5.2. Means, dips and cosinor analysis values for systolic and diastolic blood pressure (BP) and heart rate in rats assigned to control and diabetic cohorts rats during the Randomisation Recording Period (RRP)

Data are mean ± standard error of the mean (SEM). Comparisons made with two-sample Student's *t*-tests for means and dips, and Welch's *t*-test for cosinor analysis.

bpm=beats per minute, Amp=amplitude, Acro=acrophase

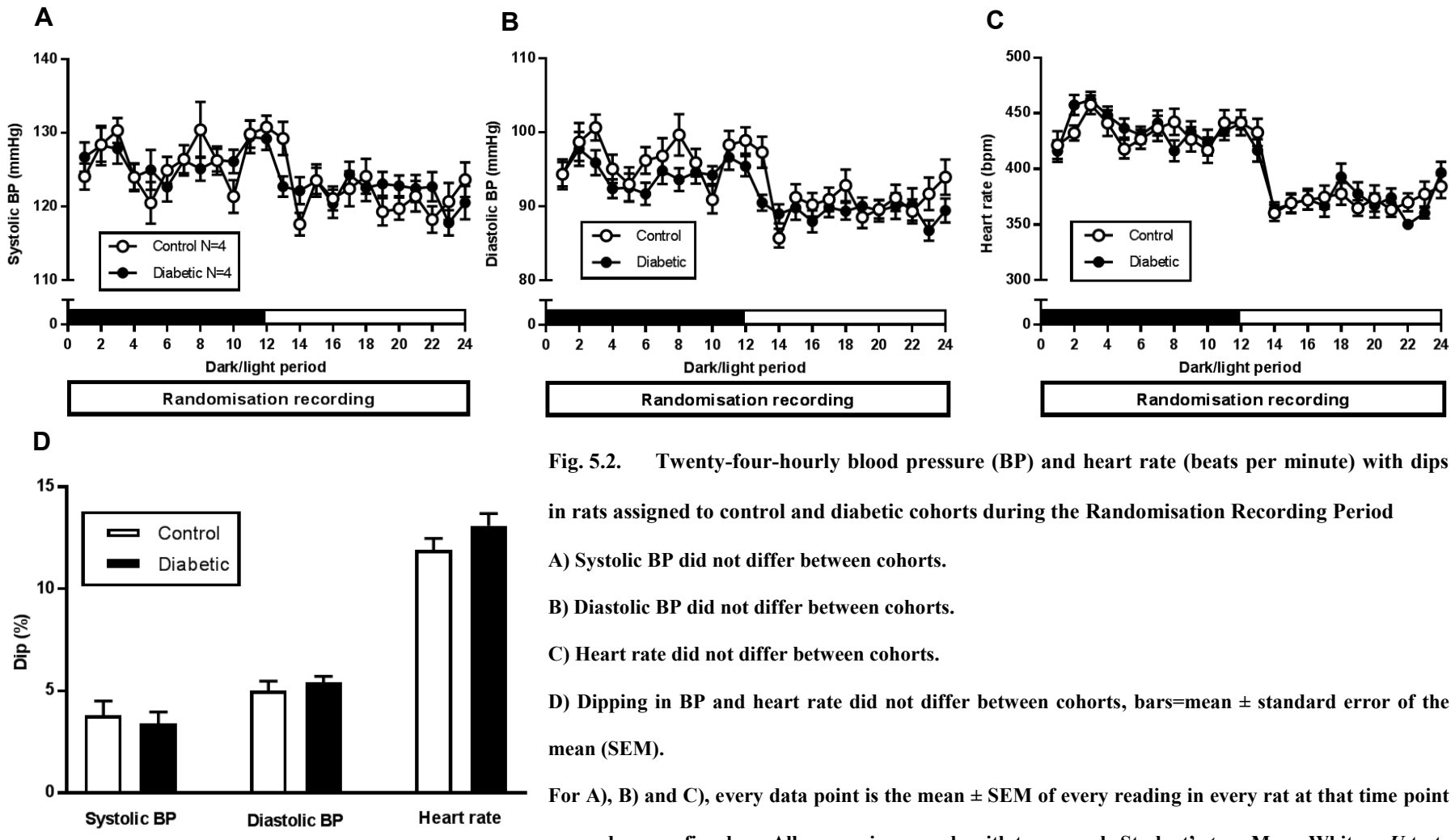

Fig. 5.2. Twenty-four-hourly blood pressure (BP) and heart rate (beats per minute) with dips in rats assigned to control and diabetic cohorts during the Randomisation Recording Period

A) Systolic BP did not differ between cohorts.

B) Diastolic BP did not differ between cohorts.

C) Heart rate did not differ between cohorts.

D) Dipping in BP and heart rate did not differ between cohorts, bars=mean ± standard error of the mean (SEM).

For A), B) and C), every data point is the mean ± SEM of every reading in every rat at that time point every day over five days. All comparisons made with two-sample Student's *t*- or Mann Whitney *U*-tests.

5.3.2 Stability of haemodynamic parameters two weeks after induction of Type 1 diabetes mellitus (Stability Recording Period)

Subjective assessment of graphs of systolic and diastolic BP and heart rate (Fig. 5.3), showed that dark-to-light dipping in all these parameters was established in both cohorts by the second dark-to-light transition of the five-day Stability Recording Period. Differences between cohorts reached stability by the third dark-to-light period, although heart rate decreased in both cohorts during the final two periods.

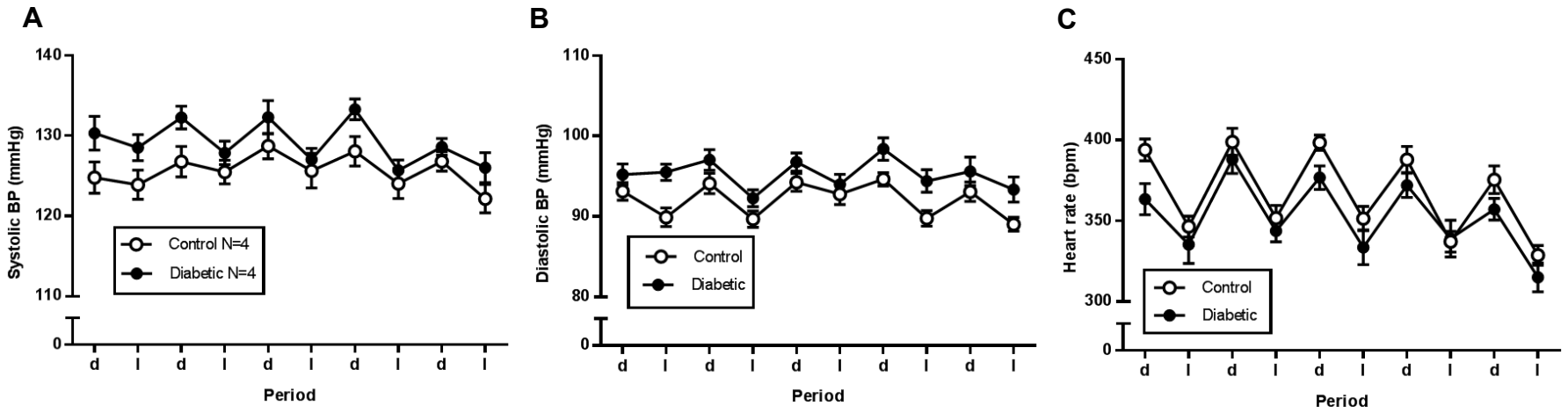

Fig. 5.3. Twelve-hourly blood pressure (BP) and heart rate (beats per minute) in control and diabetic rats during the Stability Recording Period

A) Variation in systolic BP was established in control rats by the second dark-to-light period. The difference between cohorts had narrowed by the end of the recording period.

B) Variation in diastolic BP was established in diabetic rats by the second dark-to-light period. Differences between cohorts were subsequently maintained.

C) Variation in heart rate (beats per minute) was well established in both cohorts throughout the recording period. There was a trend towards a lower heart rate in both cohorts during the final two dark-to-light periods.

Every data point is the mean ± standard error of the mean (SEM) of every reading in every rat during a 12-hourly light or dark period, d= dark period, l=light period.

5.3.3 Effects of Type 1 diabetes mellitus on blood pressure (Diabetes Recording Period)

Twenty-four-hourly systolic BP (Fig. 5.4A) was not different between cohorts (~126mmHg) but 24-hourly diastolic BP (Fig. 5.4B) was 5mmHg higher in early T1DM rats ($P<0.01$; Table 5.3). Mean heart rate was lower in early T1DM rats by ~20 beats/min ($P<0.01$; Table 5.3; Fig. 5.4C).

5.3.4 Effects of Type 1 diabetes mellitus on circadian variation (Diabetes Recording Period)

Circadian variation in systolic BP (dipping ~3%, mesor ~127mmHg, amplitude ~3mmHg and acrophase ~70 radians) and heart rate (dipping ~14%, mesor 350 beats/min, amplitude ~40 beats/min and acrophase ~74 radians) were similar between cohorts (Table 5.3; Figs. 5.4A,C). By contrast, there were abnormalities in the circadian variation in diastolic BP in early T1DM rats. Diastolic dipping was 4% less compared to controls ($P<0.01$; Figs. 5.4B,D) and in agreement with this, early T1DM reduced diastolic amplitude by ~2mmHg. Diastolic mesor and acrophase were unaffected (Table 5.3). Twenty-four-hour-periodicity in systolic and diastolic BP were unaffected by diabetic status (Figs. 5.5A,B). Heart rate in diabetics varied over a cycle length that was three hours shorter than controls (Fig. 5.5C).

DRP	Systolic BP		Diastolic BP		Heart rate	
	Control	**Diabetic**	**Control**	**Diabetic**	**Control**	**Diabetic**
Mean (mmHg/bpm)	126.2±0.5	126.5±0.4	92.2±0.4	**97.1±0.4****	361.7±2.5	**341.5±2.3****
Dip (%)	3±1	3±1	6±1	**2±1****	15±1	12±1
Mesor (mmHg/bpm)	127.4±2.9	126.5±1.1	91.4±1.2	94.0±2.7	362.3±11.1	336.7±17.5
Amp (mmHg/bpm)	2.9±0.5	3.1±0.3	4.1±0.4	**1.8±0.7****	45.8±4.5	35.4±3.8
Acro (radians)	69.3±4.4	71.3±1.7	81.6±2.9	46.2±15.8	71.1±2.6	76.6±6.8

Table 5.3. Means, dips and cosinor analysis values for systolic and diastolic blood pressure (BP) and heart rate (beats per minute) in control and diabetic rats during the Diabetes Recording Period (DRP)

Data expressed as mean ± standard error of the mean (SEM), **=P<0.05 compared with controls. Comparisons made with two-sample Student's *t*-tests for means and dips, and Welch's *t*-test for cosinor analysis.

bpm=beats per minute, Amp=amplitude, Acro=acrophase

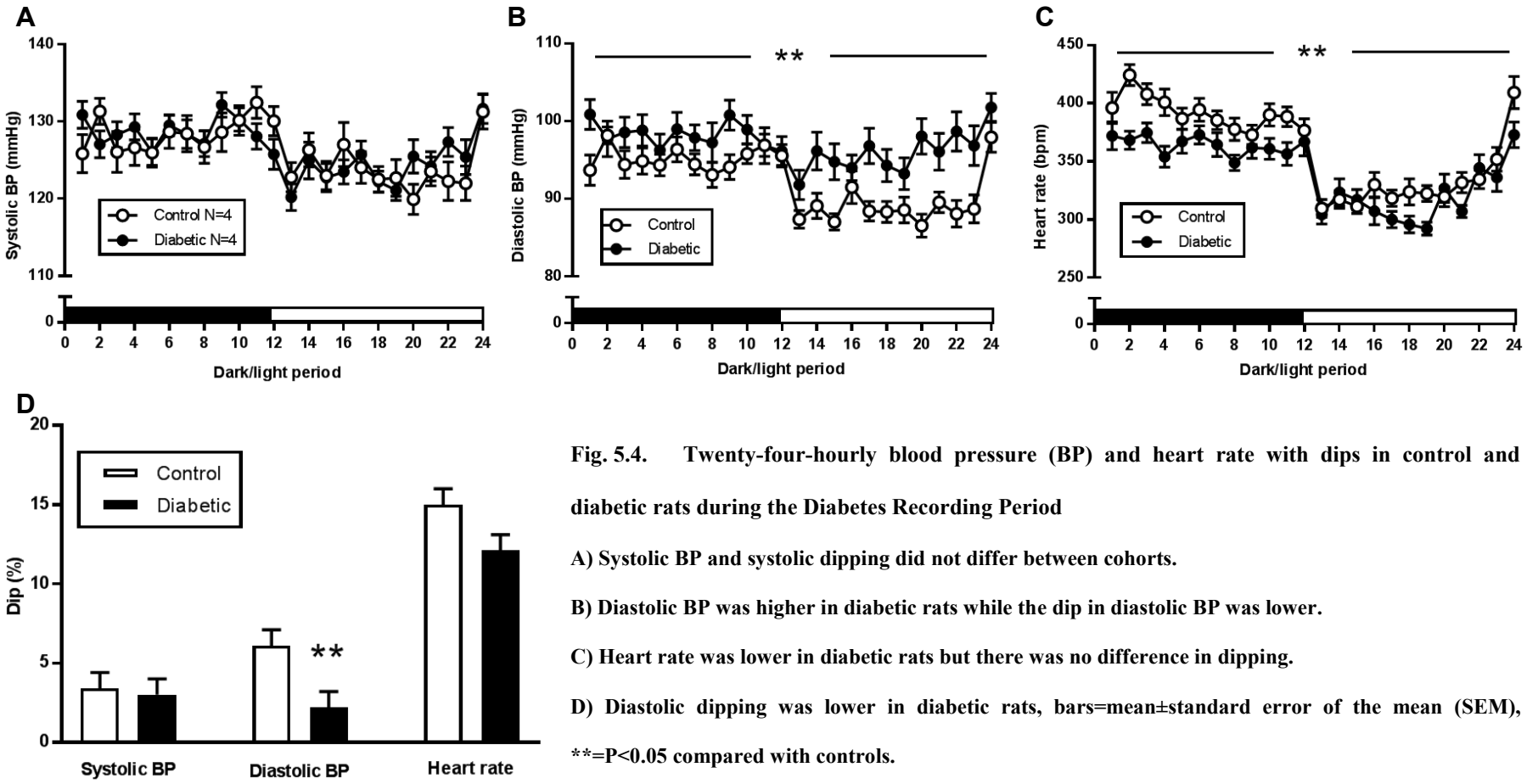

Fig. 5.4. Twenty-four-hourly blood pressure (BP) and heart rate with dips in control and diabetic rats during the Diabetes Recording Period

A) Systolic BP and systolic dipping did not differ between cohorts.

B) Diastolic BP was higher in diabetic rats while the dip in diastolic BP was lower.

C) Heart rate was lower in diabetic rats but there was no difference in dipping.

D) Diastolic dipping was lower in diabetic rats, bars=mean±standard error of the mean (SEM), **=P<0.05 compared with controls.

For A), B) and C), every data point is the mean ± SEM of every reading in every rat at that time point every day over five days, **=P<0.05 for average value over 24 hours in diabetic rats compared with controls. All comparisons made with two-sample Student's *t*- or Mann Whitney *U*-tests.

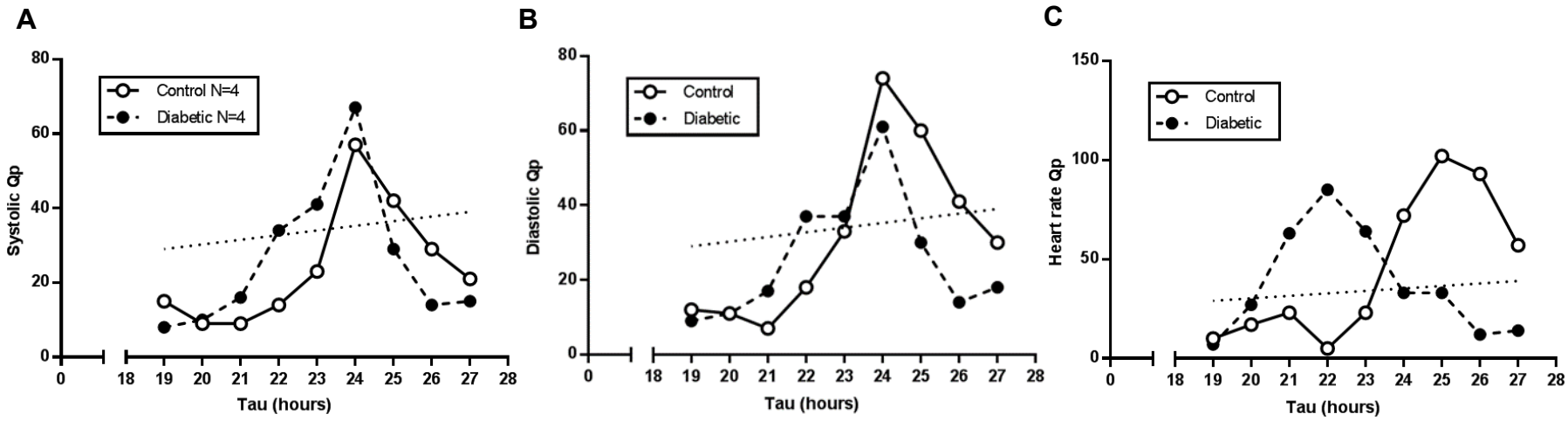

Fig. 5.5. Twenty-four-hour-periodicity (Qp) in blood pressure (BP) in control and diabetic rats during the Diabetes Recording Period

A) Twenty-four-hour-periodicity in systolic BP was present in control and diabetic rats.

B) Twenty-four-hour-periodicity in diastolic BP was present in control and diabetic rats.

C) Heart rate varied around a period of 25 hours in control rats and 22 hours in diabetic rats.

The straight dashed line represents the value above which *Qp* is significant.

5.3.5 Effects of salt supplementation (Salt Recording Period)

Salt supplementation eliminated the differences in diastolic BP and dipping observed during the Diabetes Recording Period. In control rats, systolic (Fig. 5.6A) and diastolic BP (Fig. 5.6B) increased by ~3-5mmHg (both P<0.01; Table 5.4), and diurnal diastolic dipping decreased from 6 to 3% (P=0.03; Fig. 5.6D). Sinusoidal variation and 24-hour periodicity in systolic BP were also both lost in controls (Table 5.4; Fig. 5.7A;). By contrast, BP in the early T1DM rats was relatively unaffected with only a rise of ~2mmHg in systolic BP (Table 5.4; Fig. 5.6A), and sinusoidal variation in systolic and diastolic BP and their 24-hour-periodicity were also maintained (Table 5.4; Figs. 5.7A,B). Heart rate decreased in both cohorts by ~8-15 beats/min but remained lower in the early T1DM rats (Table 5.4; Fig.5.6C) by ~14 beats/min.

SALT	**Systolic BP**		**Diastolic BP**		**Heart rate**	
	Control	**Diabetic**	**Control**	**Diabetic**	**Control**	**Diabetic**
Mean (mmHg/bpm)	**129.7±0.5***	**128.2±0.4***	**97.6±0.6***	96.5±05	**346.9±2.6***	**333.6±2.0*,****
Dip (%)	1±1	3±1	3±1	2±1	10±3	12±3
Mesor (mmHg/bpm)	-	127.8±2.3	94.3±1.0	96.8±6.6	347.9±7.0	328.6±7.5
Amp (mmHg/bpm)	-	3.2±0.8	3.0±0.1	3.0±1.1	34.0±4.5	32.8±3.5
Acro (radians)	-	7.9±9.9	71.3±0.6	74.1±6.7	62.5±9.0	81.8±5.2

Table 5.4. Mean values, dips and cosinor analysis values for systolic and diastolic blood pressure (BP) and heart rate (beats per minute) in control and diabetic rats during the Salt Recording Period. Data are mean ± standard error of the mean (SEM). **=P<0.05 compared with controls, *=P<0.05 compared with Diabetes Recording Period. Comparisons between cohorts made with two-sample Student's *t*-tests for means and dips, and Welch's *t*-test for cosinor analysis, blank boxes denote where sinusoidal variation was absent. Comparisons between recording periods made with one-way analysis of variance (ANOVA) with Tukey's *post hoc* tests, bpm=beats per minute, Amp=amplitude, Acro=acrophase

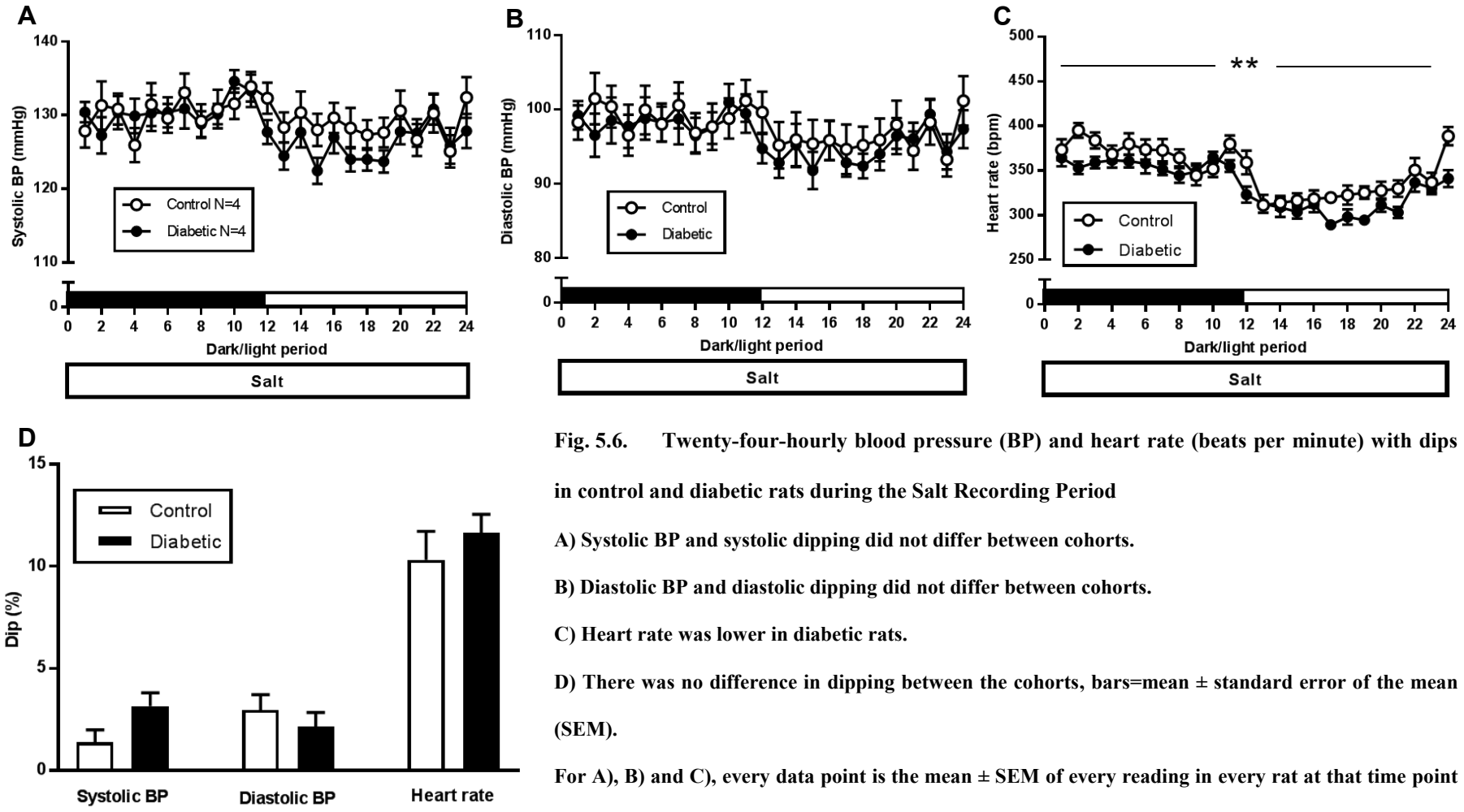

Fig. 5.6. Twenty-four-hourly blood pressure (BP) and heart rate (beats per minute) with dips in control and diabetic rats during the Salt Recording Period

A) Systolic BP and systolic dipping did not differ between cohorts.

B) Diastolic BP and diastolic dipping did not differ between cohorts.

C) Heart rate was lower in diabetic rats.

D) There was no difference in dipping between the cohorts, bars=mean ± standard error of the mean (SEM).

For A), B) and C), every data point is the mean ± SEM of every reading in every rat at that time point every day over five days, **=P<0.05 for average value over 24 hours in diabetic rats compared with controls. All comparisons made with two-sample Student's *t*- or Mann Whitney *U*- tests.

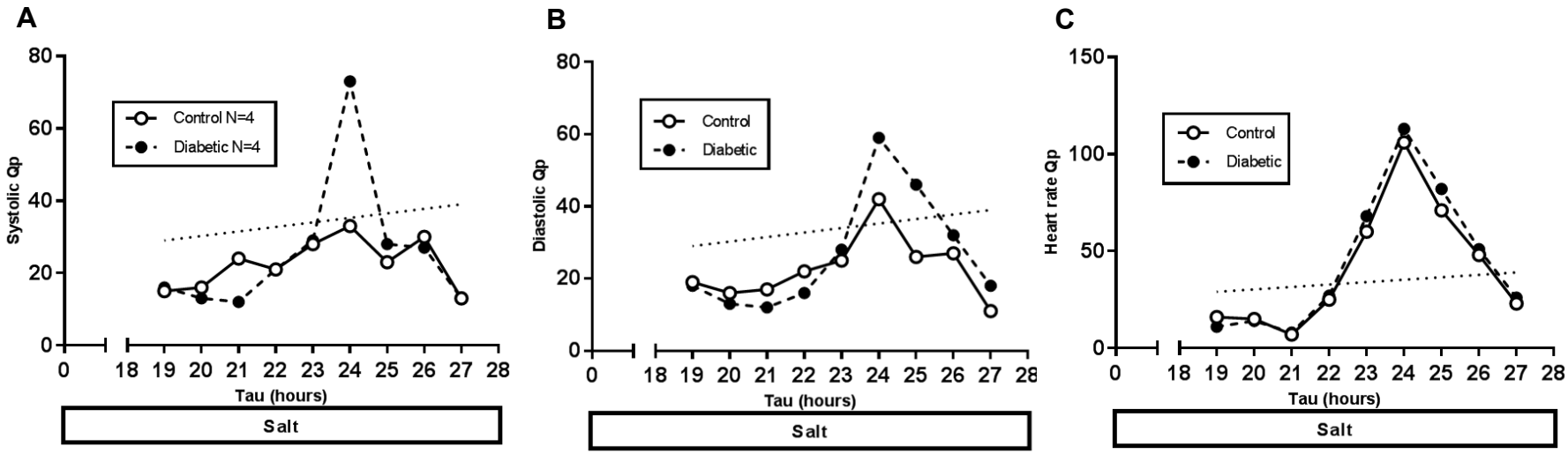

Fig. 5.7. Twenty-four-hour-periodicity (Qp) in blood pressure (BP) in control and diabetic rats during the Salt Recording Period

A) Twenty-four-hour-periodicity in systolic BP was lost in control rats but not diabetics.

B) Twenty-four-hour-periodicity in diastolic BP was present in control rats and diabetics.

C) Twenty-four-hour-periodicity in heart rate was present in control rats and diabetics.

The straight dashed line represents the value above which *Qp* is significant.

5.3.6 Effects of selective endothelin A receptor antagonism (Salt+Atrasentan Recording Period)

Atrasentan, decreased systolic BP and diastolic BP in both control and early T1DM rats (Table 5.5). The effect in controls was ~8mmHg (systolic) and ~11mmHg (diastolic), whereas, in diabetics, the effect was much reduced (~2mmHg systolic, ~5mmHg diastolic). The consequence was that both systolic (Fig. 5.8A) and diastolic BP (Fig. 5.8B) were higher in early T1DM rats by ~5mmHg. Heart rate was unaffected by atrasentan in both cohorts (Table 5.5; Fig. 5.8C).

Atrasentan also induced abnormalities in circadian variation in BP, which were more prevalent in diabetics than controls. In early T1DM rats, atrasentan decreased diastolic dipping to 2% less than in controls (Table 5.5; Fig. 5.9B) and removed 24-hour-periodicity in systolic and diastolic BP (Figs. 5.10A,B). In both cohorts, sinusoidal variation in diastolic BP was also disrupted (Table 5.5) but there was no effect on systolic dipping (Fig. 5.9A), sinusoidal variation in systolic BP or any assessment of circadian variation in heart rate (Table 5.5; Figs. 5.9C, 5.10C).

5.3.7 Effects of combined endothelin receptor antagonism (Salt+Atrasentan+A-192621 Recording Period)

In control rats, addition of A-192621 reversed the effects of atrasentan, by increasing systolic BP (Fig. 5.8A) by ~8mmHg and diastolic BP (Fig. 5.8B) by ~7mmHg. By contrast, there was no effect on BP in early T1DM rats (Table 5.5; Figs. 5.8A,B) so that systolic and diastolic BP were ~2-3mmHg lower than control values. Heart rate did decrease by ~20 beats/min in the early T1DM rats to become ~35 beats/min less

than in controls (Table 5.5; Fig. 5.8C). Using all methods of assessment, circadian variation in systolic and diastolic BP recovered in early T1DM rats to match controls (Table 5.5; Figs. 5.9A,B; 5.10A,B). In control rats, sinusoidal variation in diastolic BP also returned (Table 5.5). Once again, all assessments of circadian variation in heart rate failed to identify an effect of ET receptor antagonism in either cohort (Table 5.5; Figs. 5.9C, 5.10C).

SALT + ATRASENTAN	Systolic BP		Diastolic BP		Heart rate	
	Control	**Diabetic**	**Control**	**Diabetic**	**Control**	**Diabetic**
Mean (mmHg/bpm)	**121.8±0.6***	**126.5±0.4*,****	**86.3±0.4***	**91.1±0.5*,****	350.2±2.3	**332.6±2.0****
Dip (%)	2±1	1±1	3±2	**1±1****	13±3	12±3
Mesor (mmHg/bpm)	120.0±2.8	122.8±0.7	-	-	340.2±19.6	332.5±22.0
Amp (mmHg/bpm)	2.2±1.0	2.0±0.3	-	-	40.9±2.6	34.0±4.9
Acro (radians)	5.2±24.8	49.5±16.1	-	-	70.6±8.6	77.1±4.9
SALT + ATRASENTAN + A-192621	**Systolic BP**		**Diastolic BP**		**Heart rate**	
	Control	**Diabetic**	**Control**	**Diabetic**	**Control**	**Diabetic**
Mean (mmHg/bpm)	**129.1±0.5***	**126.2±0.4****	**93.4±0.4***	**91.0±0.3****	348.1±2.7	**313.1±2.2*,****
Dip (%)	2±1	2±1	3±2	2±1	14±3	12±3
Mesor (mmHg/bpm)	128.4±4	127.9±2.6	92.3±1.9	93.0±2.0	355.3±4.9	315.5±13.1
Amp (mmHg/bpm)	1.5±0.4	2.7±0.3	2.4±0.4	1.9±0.3	41.3±2.3	36.0±6.1
Acro (radians)	68.2±5.3	67.5±7.3	68.1±10.3	65.2±4.8	69.2±1.1	65.9±6.9

Table 5.5. Mean values, dips and cosinor analysis values for systolic and diastolic blood pressure (BP) and heart rate (beats per minute) in control and diabetic rats with salt and endothelin (ET) receptor antagonist supplementation

Data are mean ± standard error of the mean (SEM). **=P<0.05 compared with controls, *=P<0.05 compared with previous recording period. Comparisons between cohorts made with two-sample Student's *t*-tests for means and dips, and Welch's *t*-test for cosinor analysis, blank boxes denote where sinusoidal variation was absent. Comparisons between recording periods made with one-way analysis of variance (ANOVA) with Tukey's *post hoc* tests, bpm=beats per minute, Amp=amplitude, Acro=acrophase

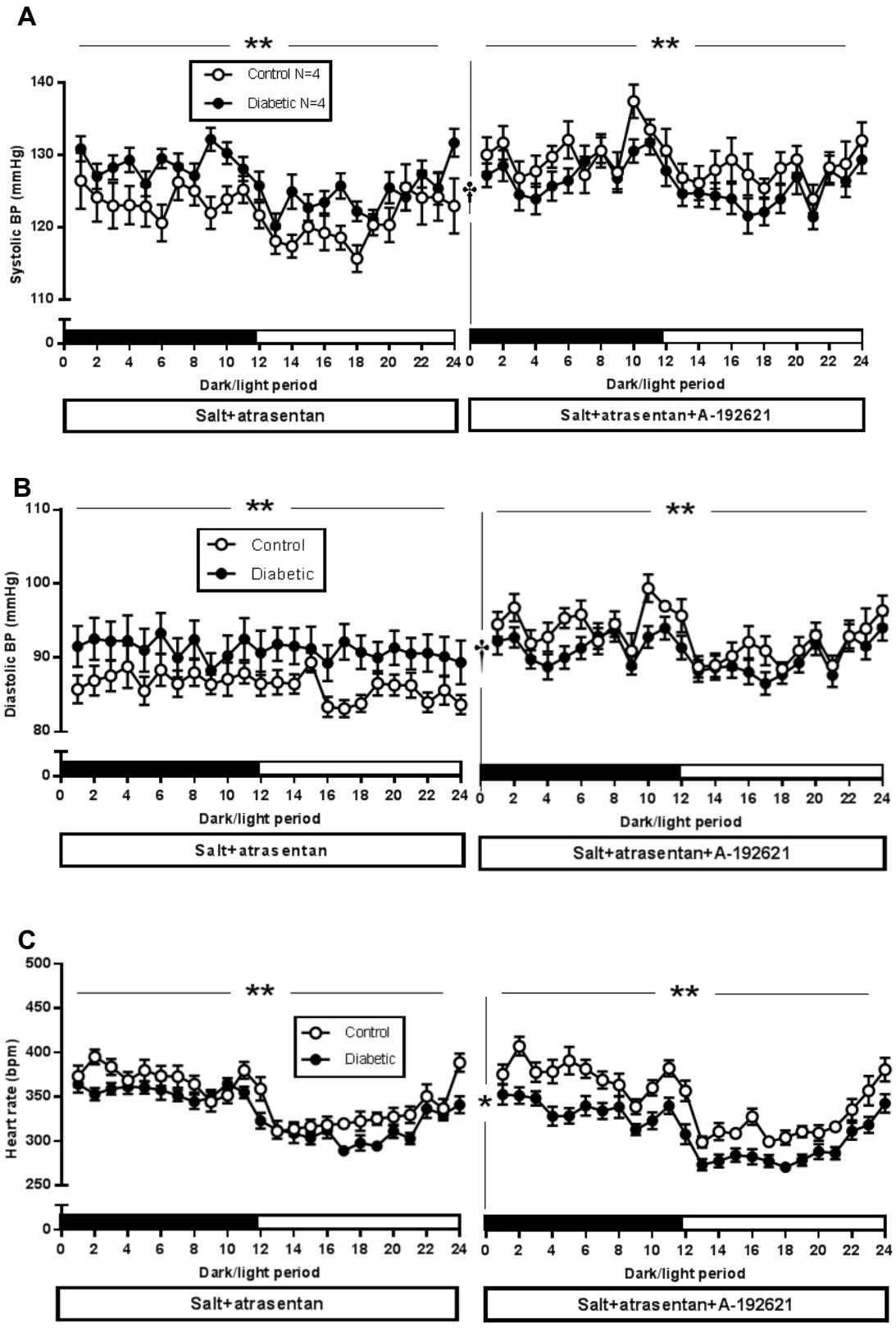
A
**
**
Control N=4
Diabetic N=4
Systolic BP (mmHg)
140
130
120
110
0
0 2 4 6 8 10 12 14 16 18 20 22 24
Dark/light period
Salt+atrasentan
Salt+atrasentan+A-192621
B
Control
Diabetic
Diastolic BP (mmHg)
110
100
90
80
Salt+atrasentan
Salt+atrasentan+A-192621
C
Heart rate (bpm)
500
450
400
350
300
250
*

Fig. 5.8. (page opposite) Twenty-four-hourly systolic and diastolic blood pressure (BP) and heart rate (beats per minute) in control and diabetic rats during endothelin (ET) receptor antagonism

A) Atrasentan decreased systolic BP in controls and diabetics but the effect was less in diabetics. A-192621 increased systolic BP in control rats but not in diabetics.

B) Atrasentan decreased diastolic BP in controls and diabetics but the effect was less in diabetics. A-192621 increased diastolic BP in control rats but not in diabetics.

C) Heart rate was lower in diabetic rats than in controls during atrasentan supplementation. This difference increased with addition of A-192621.

Every data point is the mean ± standard error of the mean (SEM) of every reading at that time point every day over five days, **=P<0.05 for average value over 24 hours in diabetic rats compared with controls. †=increased average value over 24 hours in control rats on addition of A-192621, P<0.05. *=decreased average value over 24 hours in diabetic rats on addition of A-192621. Comparisons between cohorts made with two-sample Student's *t*- or Mann Whitney *U*- tests. Comparisons between recording periods made with one-way analysis of variance (ANOVA) with Tukey's *post hoc* tests.

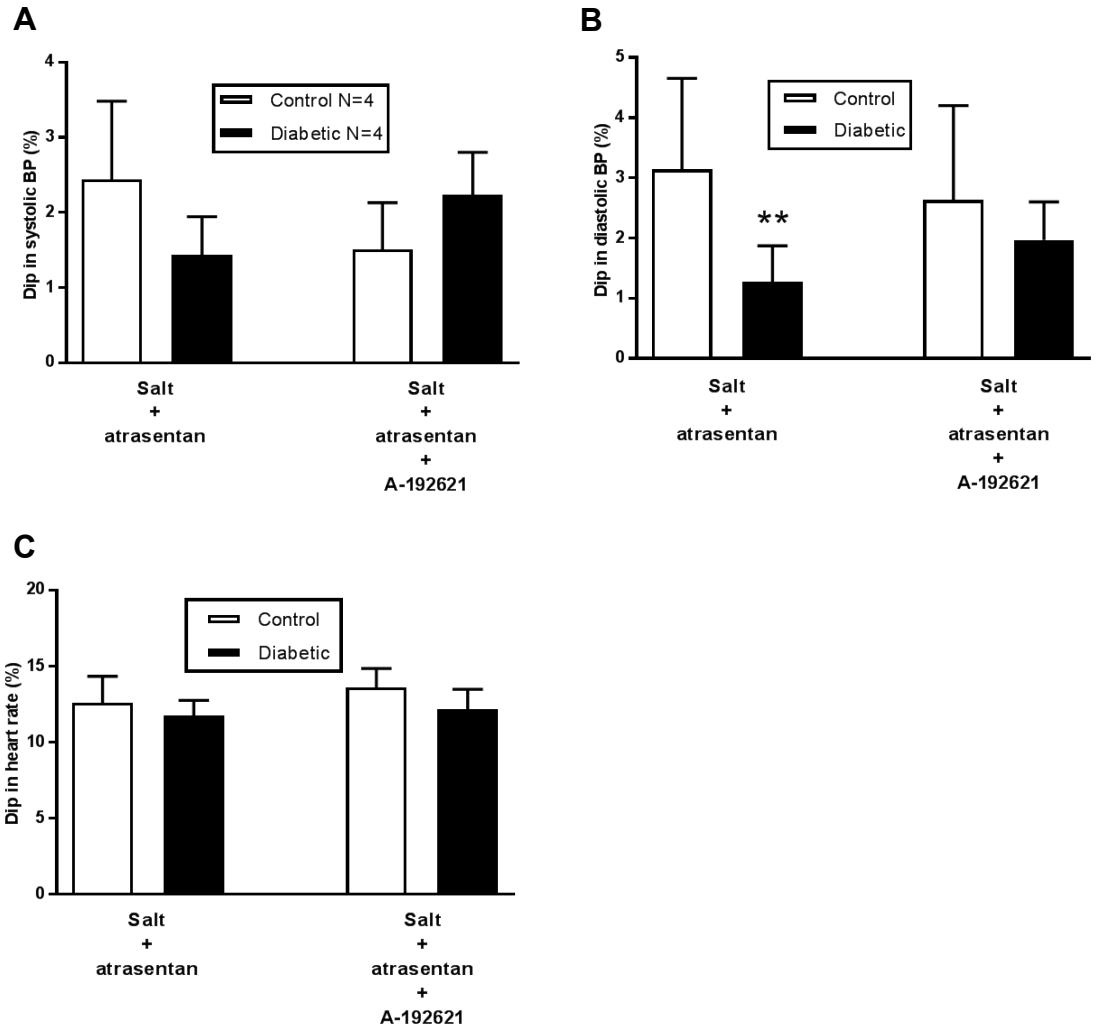

Fig. 5.9. Dipping in systolic and diastolic blood pressure (BP) and heart rate during endothelin (ET) receptor antagonism in control and diabetic rats

A) Neither atrasentan nor A-192621 affected systolic dipping in controls and diabetics.

B) Diastolic dipping in diabetics decreased with atrasentan but recovered with A-192621.

C) Dipping in heart rate was similar in both cohorts during ET receptor antagonism.

Bars=mean ± standard error of the mean (SEM), **=P<0.05 compared with controls. All comparisons made with two-sample Student's *t*- or Mann Whitney *U*-tests.

A

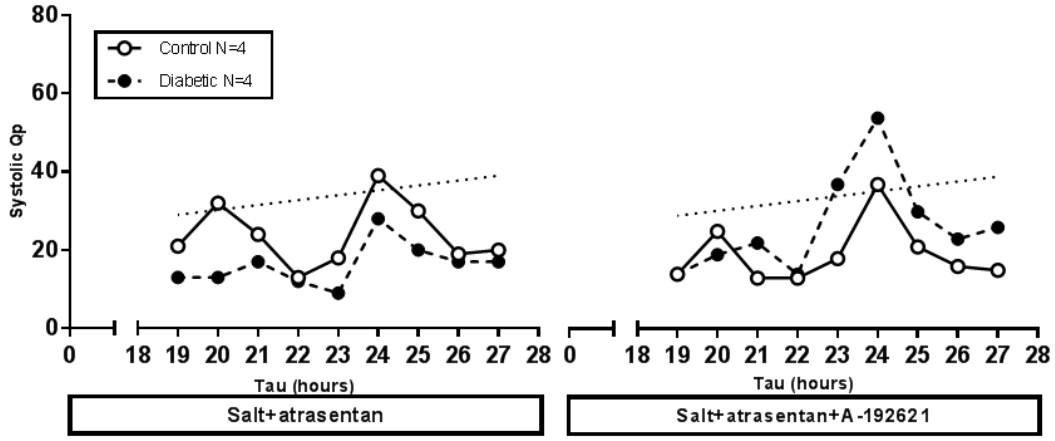
Control N=4
Diabetic N=4
Systolic Qp
Tau (hours)
Salt+atrasentan
Salt+atrasentan+A-192621

B

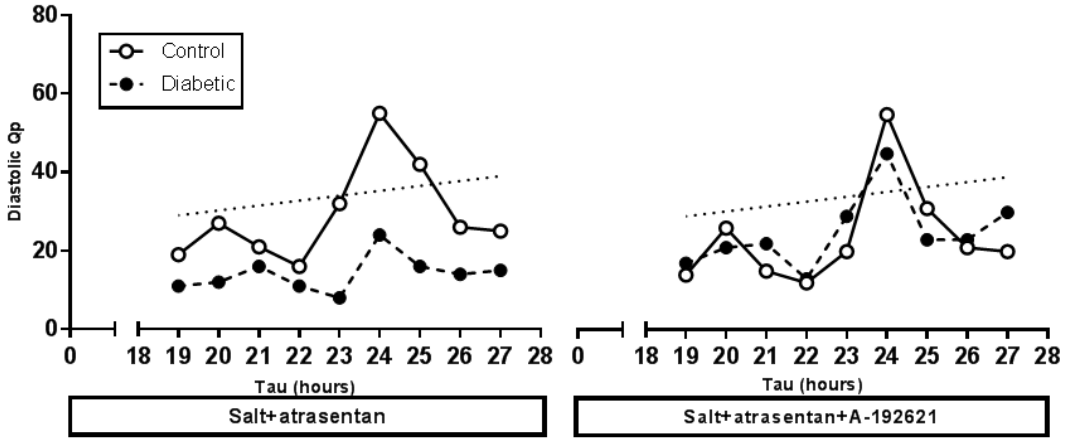
Control
Diabetic
Diastolic Qp
Tau (hours)
Salt+atrasentan
Salt+atrasentan+A-192621

C

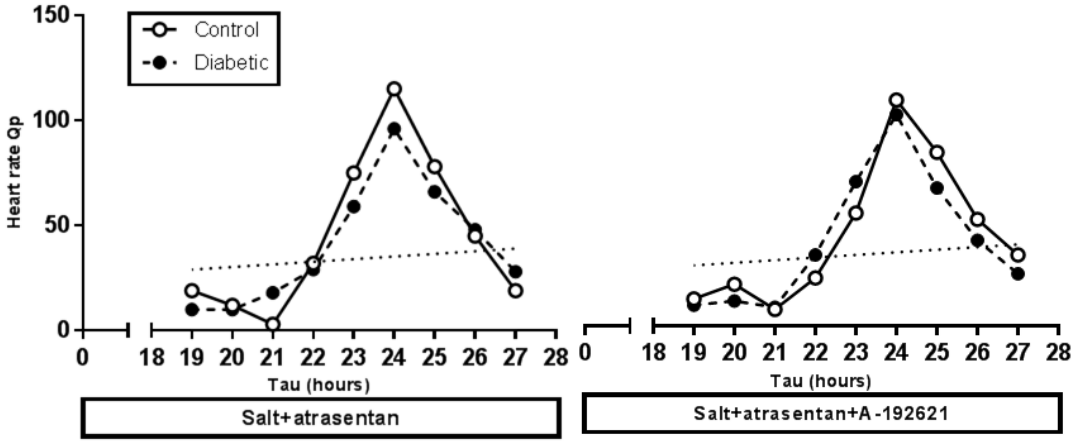
Control
Diabetic
Heart rate Qp
Tau (hours)
Salt+atrasentan
Salt+atrasentan+A-192621

Fig. 5.10. (page opposite) Twenty-four-hour-periodicity (Qp) in systolic and diastolic blood pressure (BP) in control and diabetic rats during endothelin (ET) receptor antagonism

A) Atrasentan restored periodicity in systolic BP in controls. Periodicity corresponded to cycle lengths of either 20 or 24 hours. Twenty-four-hour-periodicity was lost in diabetics. A-192621 maintained 24-hour-periodicity in controls and restored it in diabetics.

B) Twenty-four-hour-periodicity was lost in diabetics with atrasentan but restored with A-192621.

C) Twenty-four-hour-periodicity in heart rate was maintained in both cohorts during ET receptor antagonism.

The straight dashed line represents the value above which *Qp* is significant.

5.4 Discussion

Chapter 4 demonstrated that acute pressure natriuresis is suppressed in a rat model of early T1DM, and that this is associated with reduced urinary ET-1 excretion. In this chapter, radiotelemetry demonstrated that early T1DM increases diastolic BP and disrupts its circadian regulation. Therefore, impaired acute pressure natriuresis and UET-1 excretions are associated with increased diastolic BP and impairment to its circadian variation. Attempts at exaggerating this phenotype with salt were unsuccessful, instead unmasking a degree of salt sensitivity in control rats. Oral supplementation with selective ET_A and then combined ET_A/ET_B receptor antagonists led to predictable reductions (ET_A) and increments (ET_B) in systolic and diastolic BP in controls, but these effects were small or absent in rats with early T1DM.

Surprisingly, ET_A receptor antagonism disrupted circadian variation in BP in diabetic rats whereas additional ET_B receptor antagonism restored it. Circadian variation in BP is regulated by acute pressure natriuresis, and predicts cardiovascular risk [102-104]. It is concluded that impaired acute pressure natriuresis and reduced UET-1 excretion in early T1DM are associated with changes in BP that increase cardiovascular risk. Reduced renal ET_A signalling and increased renal ET_B signalling may underpin this effect.

5.4.1 Early Type 1 diabetes mellitus increases diastolic blood pressure, consistent with impaired acute pressure natriuresis.

In these experiments, radiotelemetry recorded an increase in diastolic BP in rats with early T1DM. Radiotelemetry was used because it allows real-time, direct measurement of BP in fully conscious, unrestrained rats. This is advantageous because every rat contributes multiple data points. This increases statistical power while simultaneously removing the confounding effects associated with stress from indirect oscillometric and Doppler-based methods of BP measurement [280], and associated with direct, arterial measurements during general anaesthesia. This may explain the discrepancy between the increased diastolic BP measured in diabetic rats in these experiments and the anaesthetised diabetic rats in Chapter 4.

The radiotelemetry data are novel because this is the first study to measure both systolic and diastolic BP continuously over several days in rats with early T1DM. There are only a small number of published radiotelemetric studies in T1DM rats and none has measured systolic and diastolic BP simultaneously for more than 24 hours. Two studies [282,283] measured only systolic BP and concluded that BP was unaffected by T1DM. The data in this chapter show that this conclusion should not be made without also measuring diastolic BP, which can increase even when systolic BP is unchanged. One other study, in genetically T1DM-prone rats, showed that early T1DM increases mean BP by ~4mmHg [280] but the relative contributions of systolic and diastolic BP to this increase were not determined. Hicks *et al*. [284] also used radiotelemetry to measure diastolic BP in rats with STZ-induced T1DM but failed to demonstrate the increase in diastolic BP that was recorded in this chapter. This was

despite the same cohort sizes and levels of hyperglycaemia. Hicks *et al.* [284] sampled BP more frequently (every 10 minutes) than in this study, and recorded BP for periods lasting seven days with no intervening gaps. Their protocol did not take into account the potential confounding effects of stress on BP that are associated with the increased husbandry needs of diabetic rats. T1DM causes polyuria and polydipsia. Water bottles must be re-filled and absorbent bedding added over the day. This must be controlled for by performing these tasks for all rats, including controls, at the same time. During recording periods used here, BP was measured over one minute in every hour so that there was sufficient time for the water and bedding needs of all the early T1DM rats (and controls) to be met between sampling periods, leaving a recovery period of tens of minutes before the next BP measurement. After every five-day long recording period, rats had to be transferred to clean cages with fresh bedding. This coincided with staff changes during weekend periods, and gave rats >24 hours to recover before the first measurement of the next recording period. By sampling every 10 minutes with no gap between recording periods, the protocol used by Hicks *et al*. [284] contained no recovery periods and may have acquired data confounded by increases in BP associated with husbandry. If control rats were less acclimatised to husbandry for diabetics, this could lead to an increase in BP that explains the discrepancy in diastolic BP between the two studies. This possibility is reinforced by analysis of circadian variation in diastolic BP, which was not performed by Hicks *et al*. [284].

5.4.2 Early Type 1 diabetes mellitus disrupts circadian variation in diastolic blood pressure, consistent with impaired acute pressure natriuresis.

As well as increasing diastolic BP, early T1DM also disrupted circadian variation in diastolic BP. In mammalian species, BP is controlled by the circadian clock in the hypothalamus but is also highly dependent on salt balance [78,89]. BP in normotensive subjects is usually higher during the day, and dips by ~10-20% at night [285]. Pre-clinical and clinical studies have shown that salt sensitivity disrupts this pattern. For example, a salt challenge in Dahl salt-sensitive (DSS) rats, which have an impaired acute pressure natriuresis response, increases their mean BP during periods of inactivity [286]. Similarly, people with salt sensitivity of different aetiologies excrete less sodium during the day at the expense of increased BP at night [101,287], but can restore their nocturnal dip in BP by restricting their salt intake [287]. Acute pressure natriuresis offsets increases in BP by increasing sodium excretion, so it is now believed that impairment to acute pressure natriuresis underpins the "non-dipper" phenotype [100]. Failure to excrete sodium during periods of peak salt ingestion results in elevated BP and continued acute pressure natriuresis during the night [100]. The "non-dipper" phenotype is clinically relevant because it is associated with increased cardiovascular risk [288] and predicts nephropathy in T1DM [74]. In order to determine the potential consequences of the impairment to acute pressure natriuresis in early T1DM (Chapter 4), circadian variation in systolic and diastolic BP were calculated in this chapter. This analysis has not been performed previously in a rodent model of early T1DM, and three separate methods were used in order to test the consistency of large data sets: diurnal dipping (analogous to nocturnal dipping in people), cosinor analysis (how tightly variation in BP adheres to a

sinusoidal pattern) and 24-hour-periodicity (whether cyclic variation in BP occurs over a 24-hour cycle) [237].

A reduction in diurnal diastolic dipping and in the amplitude of sinusoidal variation in diastolic BP were both identified in the diabetic rats. By contrast, circadian variation in systolic BP was unaffected. BP is dependent on heart rate, stroke volume and peripheral vascular resistance. Heart rate could not explain these effects because it was lower rather than higher in diabetic rats, and experienced minimal disruption to its circadian rhythm throughout the entire study. Age-related changes in systolic and diastolic BP in people suggest that systolic BP is highly dependent on peripheral vascular resistance whereas diastolic BP is associated more with plasma volume [289]. Impaired acute pressure natriuresis leads to elevated plasma volume [89], and so in diabetic rats with impaired acute pressure natriuresis (Chapter 4), the lack of effect on systolic BP in this and previous radiotelemetric studies [282,283], and the disruption to the circadian regulation of diastolic BP, recorded only in this study, were predictable. This has direct relevance to the risk of nephropathy and CVD in patients with T1DM. Even before the onset of office hypertension, diastolic BP in young children with T1DM has a stronger correlation than systolic BP with microalbuminuria and morphometric abnormalities of nephropathy [74,290,291]. Furthermore, daytime diastolic BP, and not systolic BP, increases in adults with T1DM, prior to development of nephropathy. Therefore, the changes to BP in this chapter strongly suggest a link between impaired acute pressure natriuresis in early T1DM, and increased cardiovascular risk.

5.4.3 Salt supplementation identified salt sensitivity in the control rats.

Both cohorts of rats received dietary salt supplementation (Salt Recording Period), equivalent to a moderate salt diet [292]. Since rats with early T1DM had impaired acute pressure natriuresis (Chapter 4), additional salt was expected to exaggerate their sodium retention, and increase systolic and diastolic BP by up to 10mmHg more than controls [292,293]. It was hoped that this would maximise the statistical power of the hypothesised restoration of normal BP in diabetic rats during subsequent selective ET_A receptor antagonism. Unexpectedly, salt supplementation had no effect on BP in rats with early T1DM, but, instead, it disrupted circadian variation in systolic BP in control rats, and increased their diastolic BP so that it matched diabetic levels. This suggested that salt had unmasked a salt sensitivity in the control cohort rather than the diabetic cohort. Why sensitivity to oral salt supplementation was not also observed in rats with early T1DM and impaired acute pressure natriuresis is not clear. One possibility is that glycosuria increased sodium excretion through osmotic diuresis, preventing retention of excess dietary sodium, and increased BP [294]. Salt sensitivity increases BP and reduces circadian variation in BP [101,287], so if salt sensitivity was a confounder for the experiments in this chapter, it would at least decrease rather than increase the differences in BP and circadian variation in BP between control and early T1DM cohorts. Therefore, the conclusions drawn from the Diabetes Recording Period that early T1DM increases diastolic BP and hinders its circadian variation are unchanged.

5.4.4 Endothelin receptor antagonists exerted greater effects on blood pressure in control rats than rats with early Type 1 diabetes mellitus.

Despite the salt sensitivity detected in control rats, addition of the selective ET_A receptor antagonist, atrasentan, still reduced systolic and diastolic BP. These reductions were predicted: atrasentan prevents calcium-dependent vasoconstriction and reduces mean BP by ~15mmHg in ren-2 transgenic rats that are salt sensitive from overexpression of the mouse renin gene [295]. Similarly, the increases in systolic and diastolic BP in controls, following addition of the selective ET_B receptor antagonist, A-192621, were consistent with loss of ET_B receptor-mediated vasodilation [77] and natriuresis [181]. By contrast, ET_A and combined ET_A/ET_B receptor antagonism exerted only minor effects on systolic and diastolic BP in rats with early T1DM. This was unexpected.

T1DM increases endothelial secretion of ET-1 [205] and shifts vascular tone towards increased ET_A receptor-mediated vasoconstriction [257,258] and away from ET_B receptor-mediated vasodilation [259]. Therefore, ET_A receptor antagonism was predicted to lower systolic and diastolic BP to a greater extent in the diabetic rats than the controls, and additional ET_B receptor antagonism was expected to partially reverse these effects. The failure of ET receptor antagonism to modify average systolic and diastolic BP in the diabetic state suggests that ET receptors may play a lesser role than predicted in the regulation of BP in early T1DM. Further insight into the mechanistic basis to these results came from analysis of circadian variation in BP.

5.4.5 Endothelin receptor antagonists exerted greater effects on circadian variation in blood pressure in rats with Type 1 diabetes mellitus than controls.

There was little or no effect of atrasentan or A-192621 on circadian variation in either systolic or diastolic BP in controls. However, in rats with early T1DM, ET receptor antagonism modified circadian variation in both systolic and diastolic BP. Since circadian variation in BP is a marker of acute pressure natriuresis [100], and urinary ET-1 excretion as well as urinary sodium excretion was suppressed in rats with early T1DM (Chapter 4), a greater influence of ET receptor antagonists on circadian variation in BP in early T1DM rats had been predicted. It was also unsurprising that the effects exerted by ET_A and ET_B receptor antagonists were opposite in nature since ET_A and ET_B receptors generally exert opposite vascular effects [77]. What was not expected was that the effects on circadian variation were entirely at odds with the putative roles of each ET receptor subtype.

ET_A receptor antagonism was expected to enhance circadian variation in the rats with early T1DM. This is because ET_A receptor antagonists should have a greater vasodilatory effect in early T1DM [257,258], increasing renal blood flow and acute pressure natriuresis [89]. It would also be consistent with the recovery of nocturnal dipping in both systolic and diastolic BP observed in non-diabetic CKD patients treated with the selective ET_A receptor antagonist, sitaxentan [226]. Instead, atrasentan suppressed circadian variation in BP in the diabetic rats, removing 24-hour-periodicity in systolic and diastolic BP, and reducing diurnal dipping in diastolic BP. Addition of the ET_B receptor antagonist was expected to reduce circadian variation in diabetic systolic and diastolic BP because further loss of ET_B

receptor-mediated vasodilation [259], which would reduce renal blood flow, and loss of inhibition of the renal epithelial sodium channel (ENaC), which would increase sodium reabsorption [181], should both suppress acute pressure natriuresis [89]. Instead, contrary to the hypothesis, addition of A-192621 restored 24-hour-periodicity in both systolic and diastolic BP, and diurnal dipping in diastolic BP

These results would be consistent with a novel pro-natriuretic role for ET_A receptors, and a novel anti-natriuretic role for ET_B receptors that are unmasked by early T1DM. The mechanisms behind these roles, and how they are enhanced by early T1DM, should now be the focus of follow-on experiments because they have significant clinical implications.

5.4.6 Clinical significance of results

Decreased diurnal dipping in diastolic BP recorded in rats with early T1DM during ET_A receptor antagonism, instead of the increased dipping recorded in clinical non-diabetic CKD [226], raises the possibility that clinical outcomes from ET_A receptor antagonists that are associated with reduced cardiovascular risk may not cross over from CKD to diabetic nephropathy. Further investigation of a pro-natriuretic role for ET_A receptors may reveal a candidate mechanism for sodium and water retention, an important adverse effect observed clinically with even highly selective ET_A receptor antagonists [227].

5.5 Conclusions

Diastolic BP is increased and circadian variation in diastolic BP is reduced in rats with early T1DM that also have impaired acute pressure natriuresis and suppressed urinary ET-1 excretion. This is consistent with increased cardiovascular risk in early T1DM as a consequence of impaired acute pressure natriuresis.

ET receptor antagonists modify the disruption to circadian variation in diastolic BP in a manner suggestive of novel pro-natriuretic and anti-natriuretic roles for ET_A and ET_B receptors respectively. These effects are not observed in healthy control rats, suggesting that early T1DM may impair acute pressure natriuresis by modifying renal ET-1 signalling through both receptor subtypes.

5.5.1 Follow-on work

The next set of experiments in rats with early T1DM should investigate whether the contrasting effects of ET receptor antagonists on circadian variation in diastolic BP might be derived from contrasting effects on acute pressure natriuresis. This should be determined by repeating ligature-induced acute pressure natriuresis studies during ET_A and ET_B receptor antagonism. To clarify the roles of ET receptors, the effect of early T1DM, and provide preliminary information on their mechanistic basis, the renal vascular and tubular components of acute pressure natriuresis will also be assessed.

6 The effects of Type 1 diabetes mellitus, insulin and endothelin receptor antagonists on renal blood flow during acute pressure natriuresis

6.1 Introduction

In acute pressure natriuresis, renal vascular and tubular functions combine to transmit increases in blood pressure (BP) into a compensatory natriuresis [89,138]. Previous chapters have demonstrated that early Type 1 diabetes mellitus (T1DM) impairs acute pressure natriuresis (Chapter 4), and disrupts regulation of diastolic BP (Chapter 5). In people, hypertension and nephropathy, which are both risk factors for cardiovascular disease (CVD) in T1DM, are preceded by disruption of regulation of diastolic BP [247-249]. Therefore, Chapters 4 and 5 suggest that restoration of acute pressure natriuresis in early T1DM might reduce cardiovascular risk. In order to identify a pharmacological target that achieves this, the mechanism to the impairment must first be understood.

In the first phase of acute pressure natriuresis, there is an increase in blood flow through the medullary *vasa recta* [138]. Increased medullary perfusion increases medullary interstitial hydrostatic pressure [89,296]. The second phase of acute pressure natriuresis is suppression of tubular reabsorption of sodium [89,296]. The proximal convoluted tubule (PCT), which is responsible for ~70% of sodium reabsorption [90] is especially sensitive to increased interstitial hydrostatic pressure [89]. Sodium reabsorption is impaired through Starling's forces [91] and pressure-sensitive paracrine signalling [92,297-299]. The more distal tubule has the capacity to abrogate this response through increased activity of multiple sodium transporters such as the sodium-chloride co-transporter (NCC) and the epithelial sodium channel (ENaC). Therefore, regulation of these transporters, by paracrine and neurohumoral means [93,95,96,180], may also be sensitive to increase in BP.

Simultaneous measurement of intrarenal blood flow and sodium excretion during acute rises in BP should determine whether early T1DM impairs the vascular or tubular phase of acute pressure natriuresis. Candidate mechanisms can also be tested, such as those regulated by insulin, which restored acute pressure natriuresis in rats with early T1DM in Chapter 4. This is important because, in T2DM, insulin increases rather than decreases sodium reabsorption through NCC and ENaC [238] suggesting that restoration of acute pressure natriuresis is more likely to originate from increased medullary perfusion.

An alternative candidate mechanism is renal endothelin-1 (ET-1) signalling. ET-1 has potent vasoconstrictive and vasodilatory effects via vascular ET_A and ET_B receptors [77], and also promotes sodium reabsorption from the collecting duct by ET_B receptor-mediated inhibition of ENaC [181]. Therefore, ET-1 has the potential to impair both vascular and tubular phases of acute pressure natriuresis. Moreover, T1DM modifies ET-1 signalling in a way that could impair the acute pressure natriuresis response. As well as increasing endothelial ET-1 expression [205] and circulatory ET-1 levels [255], T1DM also promotes vascular dysfunction through decreased expression of vasodilatory endothelial ET_B receptors [259] and increased expression of vasoconstrictive ET_A and ET_B receptors on vascular smooth muscle cells [258,300]. However, the effect of T1DM on the relative expressions of the two receptor subtypes may vary in individual organs, and ET_A receptor expression may be unaffected while ET_B receptor expression increases [301].

A link between ET-1 and impaired acute pressure natriuresis in early T1DM was demonstrated in Chapter 4 when suppression of urinary ET-1 excretion in diabetic rats matched suppression of urinary sodium excretion. This link was reinforced in Chapter 5 when circadian regulation of diastolic BP, a marker of acute pressure natriuresis and cardiovascular risk [74,100,124], was disrupted in diabetic rats by ET_A receptor antagonism and restored by additional ET_B receptor antagonism. However, these results suggest that ET_A receptors promote acute pressure natriuresis in early T1DM, while ET_B receptors impair it- novel roles which must now be confirmed experimentally and compared with changes in renal ET_A and ET_B receptor expression.

6.1.1 Hypotheses

1) Early T1DM impairs acute pressure natriuresis by reducing renal medullary blood flow. This effect is a consequence of downregulation of renal ET_A receptors and upregulation of renal ET_B receptors.
2) Insulin restores acute pressure natriuresis by increasing renal medullary blood flow and reversing the effects of early T1DM on renal ET receptor expression.

6.1.2 Aims

Ligature-induced acute pressure natriuresis was performed in rats with early T1DM with and without insulin treatment. Renal blood flow was measured following administration of selective ET receptor antagonists. The following questions were addressed:

1) Does early T1DM reduce medullary perfusion?
2) Is this effect reversed by insulin?
3) Does ET_A receptor antagonism suppress medullary perfusion and natriuresis?
4) Does ET_B receptor antagonism enhance medullary perfusion and natriuresis?
5) Are the effects of ET receptor antagonism still detectable in early T1DM with and without insulin treatment?

6.2 Methods

6.2.1 Animals

Experiments were performed, single-blinded, in three groups of adult male Sprague Dawley rats: early T1DM (blood glucose >12mmol/l induced with one or two intraperitoneal (ip.) injections of streptozotocin (STZ); Chapter 2.1, page 46), T1DM+insulin (subcutaneous (sc.) insulin implant inserted into early T1DM rats seven days after the first injection of STZ; Chapter 2.1, page 47), and healthy control rats (ip. citrate buffer).

6.2.2 Preparation for ligature-induced acute pressure natriuresis and measurement of renal blood flow

Control, early T1DM and T1DM+insulin rats (Table 6.1) were anaesthetised (Chapter 3.2, page 88) and prepared for ligature-induced acute pressure natriuresis (Fig. 6.1; Chapter 4.2, page 115). Tube cystotomy was not performed. Instead, the left ureter was cannulated for urine collection (Chapter 2.6, page 69; Figs. 2.10A,B). Renal artery flow (ml/min) was measured by a Doppler ultrasound flow probe (Chapter 2.6, page 70; Figs. 2.11A,B). Renal cortical and medullary blood flow were individually measured by laser Doppler spectroscopy (LDS; Chapter 2.6; Figs. 2.12; 2.13A,B). Both laser Doppler probes measured blood flow as flux in tissue perfusion units (TPU; Chapter 2.6, page 71).

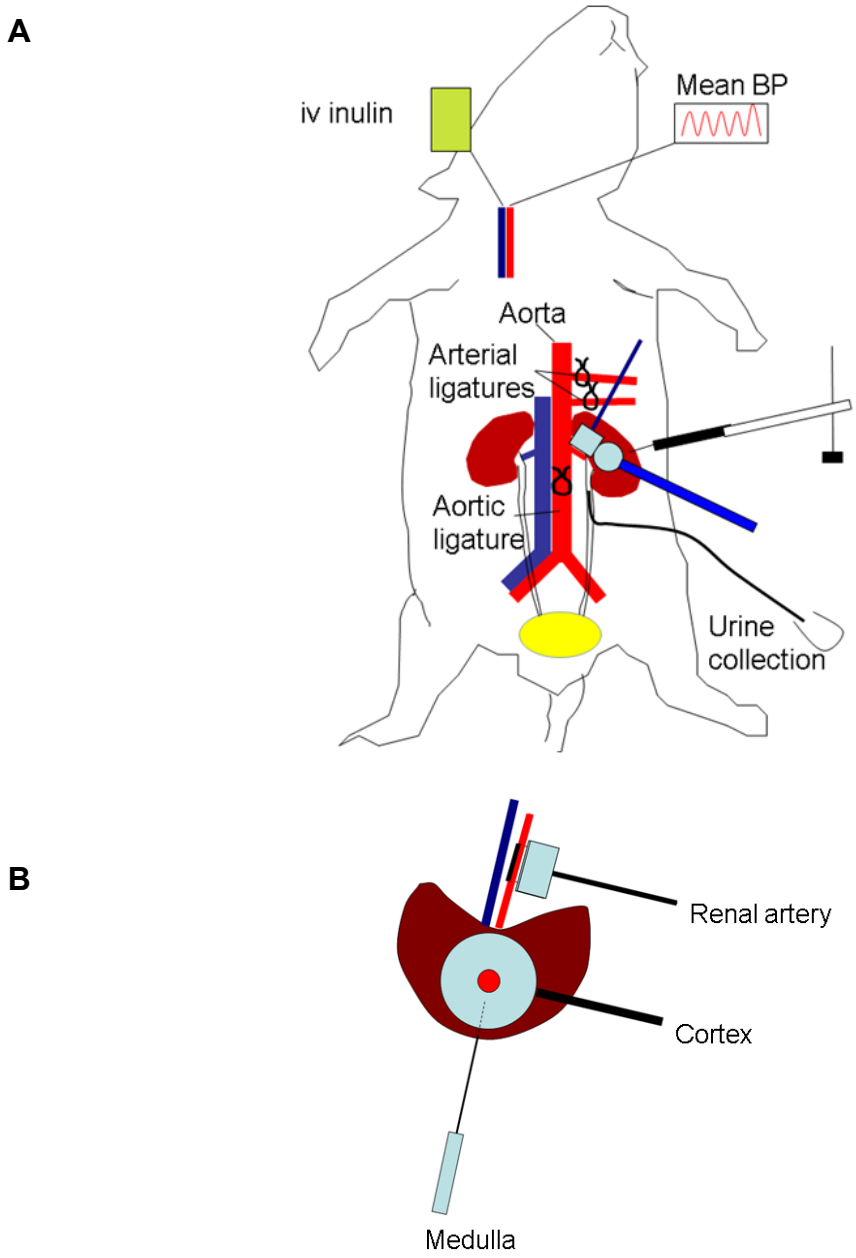

Fig. 6.1. Schematic diagram of measurement of renal blood flow during ligature-induced acute pressure natriuresis

A) Urine is collected from the left ureter while left renal blood flow is measured at three sites. Stepwise increase in mean blood pressure (BP) follow simultaneous tightening of arterial ligatures and, later, the distal aorta.

B) Magnified view of the three renal probes: around the left renal artery, glued to the renal capsule (cortical flux) and inserted into the renal medulla (needle probe, medullary flux)

iv=intravenous

6.2.3 Injection of endothelin receptor antagonists and ligature-induced acute pressure natriuresis

On completion of surgical preparation (~80 minutes), all rats received slow (over five minutes) intravenous (iv.) injection of one of four treatment options: atrasentan (ET_A receptor antagonist, 5mg/kg [302] dissolved in 1ml of vehicle), A-192621 (ET_B receptor antagonist, 10mg/kg [302] dissolved in 1ml of vehicle), combined atrasentan and A-192621, or vehicle (1ml of balanced electrolyte solution, pH 7.4 (Chapter 2.9, page 82), and one drop of 70% ethanol). This created four cohorts within each group of control, early T1DM or T1DM+insulin rats (12 cohorts in total; Table 6.1). All ET receptor antagonists were kindly supplied by AbbVie Limited (Ltd.; Maidenhead, United Kingdom (UK)). Rats then entered a 30-minute equilibration period (Fig. 6.2).

Following equilibration, urine and blood were collected as before (Chapter 4.2, page 115), over three 30-minute periods pre- and post arterial ligation: Baseline, Clearance 1 and Clearance 2. Systolic and diastolic BP, renal artery flow, cortical flux and medullary flux were recorded continuously. Mean BP was calculated post acquisition.

After euthanasia and removal and weighing of the kidneys, the left kidney was sectioned sagittally to confirm correct placement of the needle laser Doppler medullary probe (Fig. 6.3). Urinary sodium concentrations were measured. Glomerular filtration rate (GFR), urine flow rate (UV), urinary sodium excretion rate (UNaV) and fractional excretion of sodium (FENa) were calculated (Chapter 2.6,

pages 74-76). Changes in renal artery flow and in cortical and medullary flux after each arterial ligation were expressed as percentage changes from Baseline, which was set at 100%. Where appropriate, measurements were indexed to kidney weight (kw).

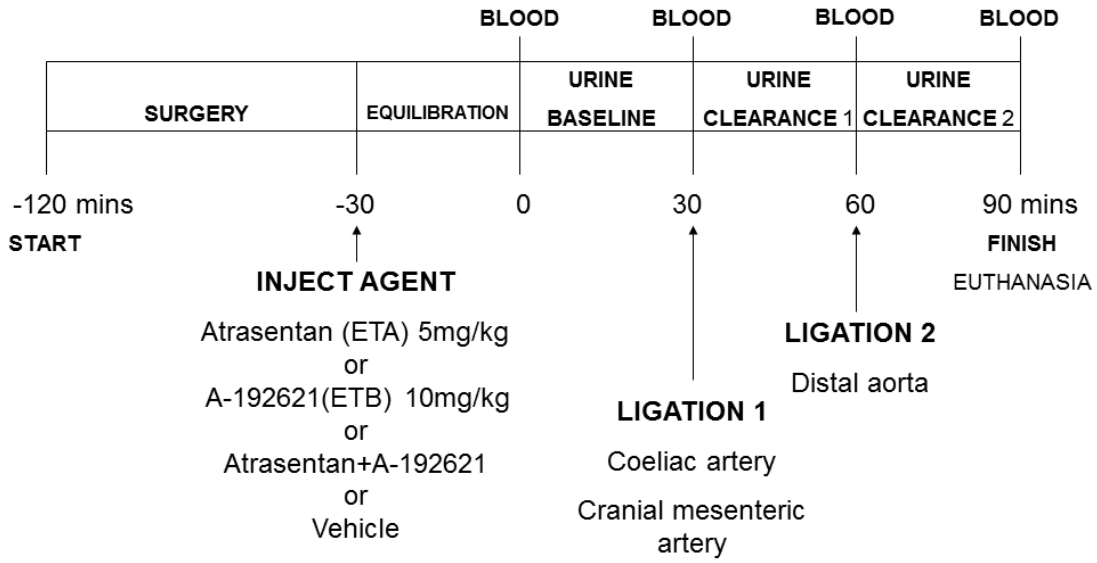

Fig. 6.2. Timeline for ligature-induced acute pressure natriuresis showing time points for antagonist injection, and blood and urine collection.

mins=minutes

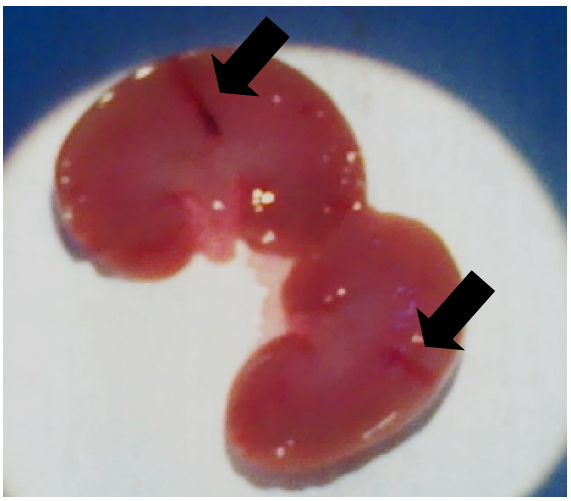

Fig. 6.3. *Post mortem* examination of the left kidney confirmed correct placement of the needle laser Doppler probe into the renal medulla (arrows).

6.2.4 The effect of Type 1 diabetes mellitus on renal endothelin A and endothelin B receptor expression

In a separate experiment, semi-quantitative polymerase chain reaction (qPCR; Chapter 2.4, pages 57-60) of renal tissue (Chapter 2.2, pages 49-51) measured expression of markers of renal ET-1 signalling. Total ribonucleic acid (RNA) was extracted from pulverised snap-frozen renal cortex and medulla from control, T1DM and T1DM+insulin rats. First-strand complementary deoxyribonucleic acid (cDNA) was reverse transcribed and amplified (qPCR) with exon-spanning, unlabelled, rat-specific primers for the genes that code for ET-1, ET_A receptor and ET_B receptor (EDN1, EDRA and EDRB respectively), mixed with a fluorescein amidite (FAM) dye-labelled Taqman probe (ThermoFisher Scientific Inc, Glasgow, UK; Table 6.2). Using the change in cycle threshold (ΔC_T) method, fluorescence of the FAM probes was compared to reference genes 3-phophate dehydrogenase (GAPDH) and thymine-adenine-thymine-adenine (TATA) box binding protein (TBP) [232], which had been previously compared between cohorts to confirm they were unchanged by diabetic status. Where differences were identified, the fold-difference was calculated using the $\Delta\Delta C_T$ method [233].

6.2.5 Statistical analysis

Studies were designed to obtain a power >80% if:

1) cohort sizes were six rats and UNaV in early T1DM rats was 50±25% [262] of the expected value in controls [112].
2) medullary blood flow was 20±5% greater in controls over untreated diabetic rats and half this difference in insulin-treated diabetic rats [138].

A lower value of relative suppression of UNaV (50%) was estimated for early T1DM than that obtained in Chapter 4 (85%), because it was assumed that the additional surgical preparation time for measurement of renal blood flow would lower mean BP and hence natriuresis. Additional rats were included in every cohort to account for an expected dropout rate of 25% due to experimental mortality.

Data were expressed as mean ± standard error of the mean (SEM) and analysed with Minitab 17 (Minitab Ltd, Coventry, UK) and GraphPad Prism 6.0 (GraphPad Software, La Jolla, United States (US)).

For acute pressure natriuresis studies, two-way analysis of variance (ANOVA) with Tukey's *post hoc* tests were used to compare Baseline mean BP and increments (independent variable), and dependent variables between cohorts. Data were transformed by log or square-root transformation according to normality and equality of variance of residuals. Interaction between diabetic status and clearance period was calculated. As additional analyses, dependent variables were plotted against BP, and regression lines were compared by analysis of covariance (ANCOVA) with Tukey's *post hoc* tests (linear) and extra sum of squares F-tests (non-linear).

For comparison of weight, blood glucose and gene expression, multiple comparisons employed one-way ANOVA with Tukey's *post hoc* tests or Kruskal Wallis with Dunn's *post hoc* tests according to normality and equality of variance of residuals.

For all tests, statistical significance was set at $P<0.05$

	Control				Diabetic				Insulin			
	Vehicle	**ET_A**	**ET_B**	**ET_A+ET_B**	**Vehicle**	**ET_A**	**ET_B**	**ET_A+ET_B**	**Vehicle**	**ET_A**	**ET_B**	**ET_A+ET_B**
Number	10	8	9	5	11	7	6	8	5	8	5	8
Weight (g)	363±7	389±14	400±15	381±11	**331±8****	334±9	323±23	341±12	**377±23***	369±13	377±7	315±33
BG (mmol/l)	6.1±0.3	5.7±0.4	5.1±0.7	6.6±0.3	**16.7±1.7****	20.0±1.5	24.6±3.5	21.0±1.6	**7.6±0.5***	8.0±1.0	10.9±2.0	10.3±1.1

Table 6.1. Number, weight, blood glucose (BG) of control, diabetic and insulin-treated diabetic rats, immediately prior to general anaesthesia for ligature-induced acute pressure natriuresis

Data are mean ± standard error of the mean (SEM), **=P<0.05 compared with controls, *=P<0.05 compared with diabetics. All comparisons made with one-way analysis of variance (ANOVA) with Tukey's *post hoc* tests.

Gene	Marker	Manufacturer reference	Exon boundary	Location	Length	Approximate probe sequence
EDN1	ET-1	Rn00561129_m1	1-2	252	88	5'GAGCTCCAGAAACAGCTGTCTTGGGAG3'
EDRA	ET_A receptor	Rn01463848_m1	2-3	715	118	5'ATGTGTTTAAGCTGTTGGCGGGGCGCT3'
EDRB	ET_B receptor	Rn01437681_m1	2-3	741	79	5'CTACAAGCTGCTGGCAGGGGACTGGCC3'
GAPDH	Reference gene	Rn01775763_g1	8-8	1153	174	5'GAGGAGTCCCCATCCCAACTCAGCCCC3'
TBP	Reference gene	Rn01455646_m1	4-5	791	75	5'TAATCCCAAGCGGTTTGCTGCAGTCAT3'

Table 6.2. Semi-quantitative polymerase chain reaction (qPCR) probes selected for determining renal injury

The probe sequence is not released by the manufacturer (ThermoFisher Scientific). The approximate probe sequence within the amplicon is derived from adding 13 nucleotides upstream and downstream of the assay location, using the Reference Sequence Database of the National Center for Biotechnology Information (NCBI, Bethesda, United States (US)), ET and EDN=endothelin, EDRA=ET_A receptor, EDRB=ET_B receptor, GAPDH=glyceraldehyde 3-phosphate dehydrogenase, TBP=TATA (thymine-adenine-thymine-adenine) box binding protein, A=adenine, C=cytosine, G=guanine, T=thymine.

6.3 Results

6.3.1 Impairment of acute pressure natriuresis in rats with Type 1 diabetes mellitus, and recovery with insulin

Following sequential ligation, mean BP rose by ~20mmHg in the three cohorts receiving vehicle ($P<0.01$; Table 6.3; Fig. 6.4A). Although, overall, mean BP was greater in controls than in early T1DM rats ($P=0.03$), there was no difference between cohorts during any of the three individual collection periods (interaction $P=0.97$; Table 6.3; Fig. 6.4A). Mean GFR was similar in all cohorts (control 0.9±0.1ml/min/gkw, early T1DM 1.1±0.2ml/min/gkw, T1DM+insulin 1.5±0.3ml/min/gkw; $P=0.23$) and was unaffected by clearance period ($P=0.73$, interaction $P=0.80$; Table 6.3 Fig. 6.4B).

VEHICLE	Baseline			Clearance 1			Clearance 2		
	Control	**Diabetic**	**Insulin**	**Control**	**Diabetic**	**Insulin**	**Control**	**Diabetic**	**Insulin**
BP (mmHg)	124.0±4.3	116.1±4.2	122.3±5.3	136.0±4.9	127.5±4.1	136.5±4.3	143.9±4.2	137.9±5.1	146.2±2.9
GFR (ml/min/gkw)	0.9±0.1	1.3±0.5	1.8±0.7	1.0±0.1	0.8±0.2	1.4±0.3	1.0±0.1	1.1±0.2	1.3±0.3
UV (µl/min/gkw)	7.2±1.6	8.7±3.2	13.1±4.5	16.3±3.5	8.5±2.5	17.8±5.7	38.6±6.2	**14.0±3.4****	**30.4±12.4***
UNaV (µmol/min/gkw)	2.2±0.6	2.1±0.7	2.6±1.1	6.5±0.8	2.0±0.4	4.3±1.8	16.7±1.4	**4.1±1.1****	**24.9±17.8***
FENa (%)	1.7±0.6	1.9±0.8	1.0±0.4	3.5±0.7	2.8±1.0	2.2±0.5	15.0±2.4	**3.7±1.0****	**9.6±4.9***
Δ RA flow (%)				93.2±7.5	93.2±6.6	102.8±6.9	108.3±11.7	104.0±7.7	113.2±4.5
Δ cortical flux (%)				93.5±4.8	97.6±6.1	94.2±6.1	98.5±6.5	99.6±8.3	79.3±9.0
Δ medullary flux (%)				159.4±20.1	**95.7±12.1****	108.7±6.1	227.2±26.7	**115.4±10.3****	**112.2±6.8****

Table 6.3. Mean blood pressure (BP), glomerular filtration rate (GFR), urine flow rate (UV), urinary sodium excretion rate (UNaV), fractional excretion of sodium (FENa), and changes (Δ) in renal artery (RA) flow, cortical flux and medullary flux in control, diabetic and insulin-treated diabetic rats during Baseline and Clearances 1 and 2, after injection of vehicle

****=P<0.05 compared with control rats during same clearance period, *=P<0.05 compared with diabetic rats receiving vehicle during same clearance period. All data are mean ± standard error of the mean (SEM). All comparisons made with two-way analysis of variance (ANOVA) with Tukey's *post hoc* tests.**

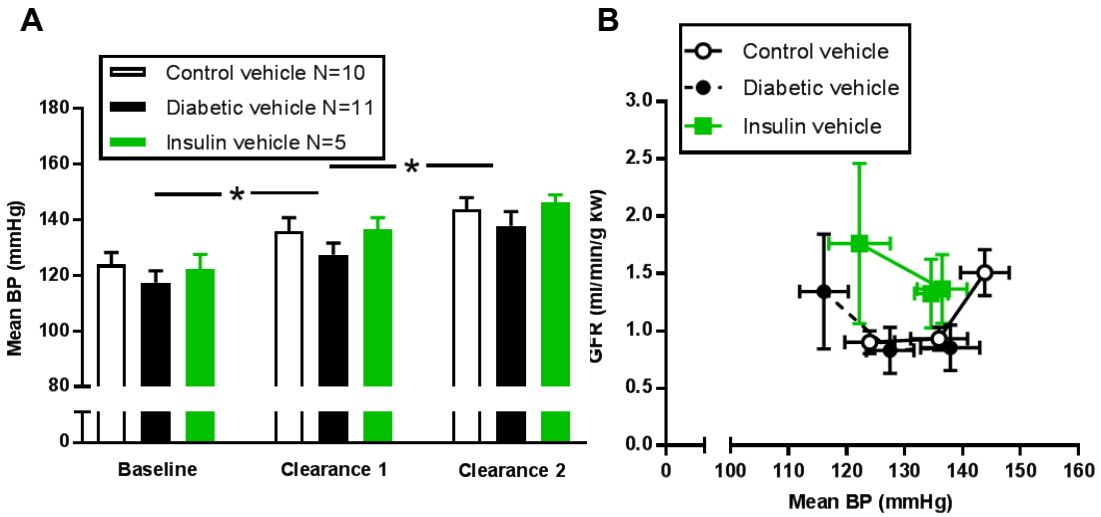

Fig. 6.4. Mean blood pressure (BP) and glomerular filtration rate (GFR) during ligature-induced acute pressure natriuresis in all rats receiving vehicle

A) Baseline mean BP and increments were not significantly different between cohorts, bars=mean ± standard error of the mean (SEM), *=P<0.05 compared with mean BP in previous period. All comparisons made with two-way analysis of variance (ANOVA) with Tukey's *post hoc* tests.

B) GFRs were similar between cohorts during every clearance period. Every data point is the mean value of the dependent variable plotted against mean BP±SEM of both variables, and corresponds to one of three clearance periods.

Pressure diuresis and natriuresis were induced (both P<0.01) but maximum UV and UNaV in controls were only ~50-75% of values in Chapter 4 (Table 6.3; Figs. 6.5A,C). Increases in UV and UNaV were again suppressed in early T1DM rats (both P<0.01 versus controls; Table 6.3), only attaining ~25-35% of control values during Clearance 2 (both P<0.01), and the non-linear (k=0.03) and linear (P<0.01) nature of these relationships was lost (Figs. 6.5B,D). Unlike in Chapter 4, a tight relationship between FENa and mean BP could not be identified in controls (Fig. 6.5F) but there was still a clear suppression of FENa in early T1DM rats (P<0.01, interaction P=0.14), particularly during Clearance 2, by ~75% (P<0.01; Table 6.3; Fig. 6.5E). By contrast, UV (P=0.046 versus early T1DM) and UNaV (P=0.04 versus early T1DM) recovered in T1DM+insulin rats (Table 6.3; Figs. 6.5A,C), although their tight relationships with BP did not (Figs. 6.5B,D).

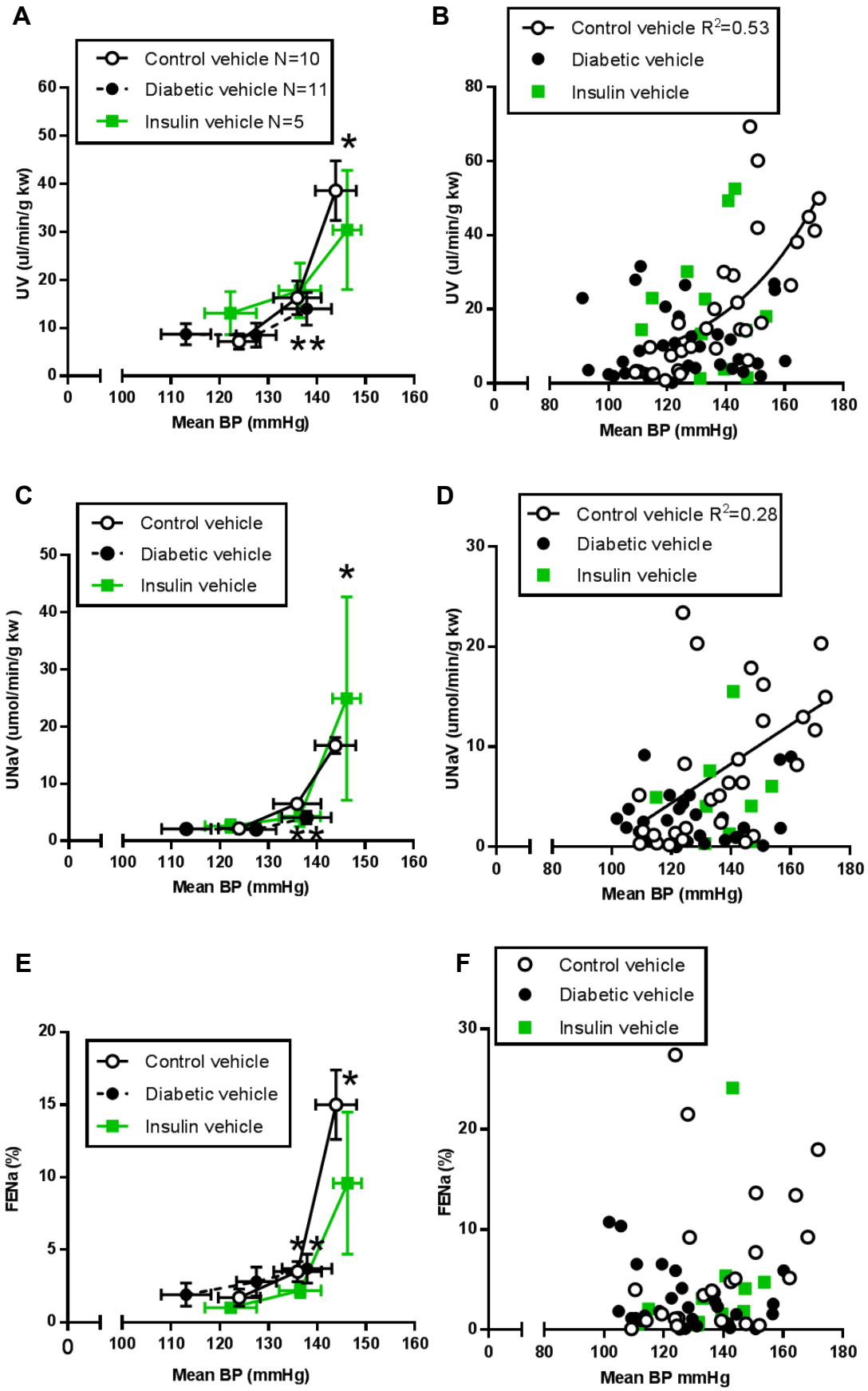
A
Control vehicle N=10
Diabetic vehicle N=11
Insulin vehicle N=5
UV (ul/min/g kw)
Mean BP (mmHg)
B
Control vehicle R2=0.53
Diabetic vehicle
Insulin vehicle
UV (ul/min/g kw)
Mean BP (mmHg)
C
Control vehicle
Diabetic vehicle
Insulin vehicle
UNaV (umol/min/g kw)
Mean BP (mmHg)
D
Control vehicle R2=0.28
Diabetic vehicle
Insulin vehicle
UNaV (umol/min/g kw)
Mean BP (mmHg)
E
Control vehicle
Diabetic vehicle
Insulin vehicle
FENa (%)
Mean BP (mmHg)
F
Control vehicle
Diabetic vehicle
Insulin vehicle
FENa (%)
Mean BP mmHg

Fig. 6.5. (page opposite) Ligature-induced acute pressure natriuresis in control, diabetic and insulin-treated diabetic rats

A) Pressure diuresis responses, with reduced urine flow rate (UV) in diabetic rats during Clearance 2

B) Pressure diuresis responses, with loss of the non-linear relationship with mean blood pressure (BP; k=0.03) in diabetic and insulin-treated diabetic rats

C) Pressure natriuresis responses, with reduced urinary sodium excretion rate (UNaV) in diabetic rats during Clearance 2

D) Pressure natriuresis responses, with loss of the linear relationship with mean BP (0.07-0.32, 95% confidence) in diabetic and insulin-treated diabetic rats

E) Reduced fractional excretion of sodium (FENa) in diabetic rats during Clearance 2

F) No relationship between FENa and mean BP in any of the cohorts

****=P<0.05 compared with controls, *=P<0.05 compared with diabetics**

For A), C) and E), every data point is the mean value of the dependent variable plotted against mean BP ± standard error of the mean (SEM) of both variables, and corresponds to one of three clearance periods. All comparisons made with two-way analysis of variance (ANOVA) with Tukey's *post hoc* tests.

For B) and D), R^2=coefficient of determination

6.3.2 The effects of Type 1 diabetes mellitus and insulin on renal blood flow

In control rats, medullary flux increased with mean BP (Table 6.3; Fig. 6.6A,B). Early T1DM suppressed the rise in medullary perfusion during Clearances 1 and 2 so that, overall, medullary flux was approximately half that measured in controls ($P<0.01$; Table 6.3; Fig. 6.6A). The curvilinear relationship between the percentage rises in medullary flux and mean BP was also lost in the diabetics ($P<0.01$; Fig. 6.6B). The percentage change in medullary flux correlated with the percentage change in UV in control and early T1DM cohorts (control $P<0.01$, early T1DM $P=0.03$; Fig. 6.6C) but although it also correlated in controls with the percentage change in UNaV ($P<0.01$), this was not observed in early T1DM (Fig.6.6D).

Insulin did not reverse suppression of medullary flux in early T1DM during either clearance period ($P<0.01$; interaction between diabetic status and period $P=0.43$; Table 6.3; Fig. 6.6A) but did re-establish a curvilinear relationship with the percentage change in mean BP (Fig. 6.6B). The percentage change in medullary flux with insulin did not correlate with the percentage change in either UV or UNaV (Fig. 6.6C,D).

Cortical and renal artery flux did not change in the three rat cohorts as mean BP rose (Table 6.3; Figs. 6.7A,B). Percentage changes in cortical flux did not correlate with percentage changes in UV or UNaV (Figs. 6.7C,D) in any cohort. In controls only, the percentage change in renal artery flow did correlate with the percentage change in UNaV (P=0.045; Fig. 6.7F), but not UV (Fig.6.7E).

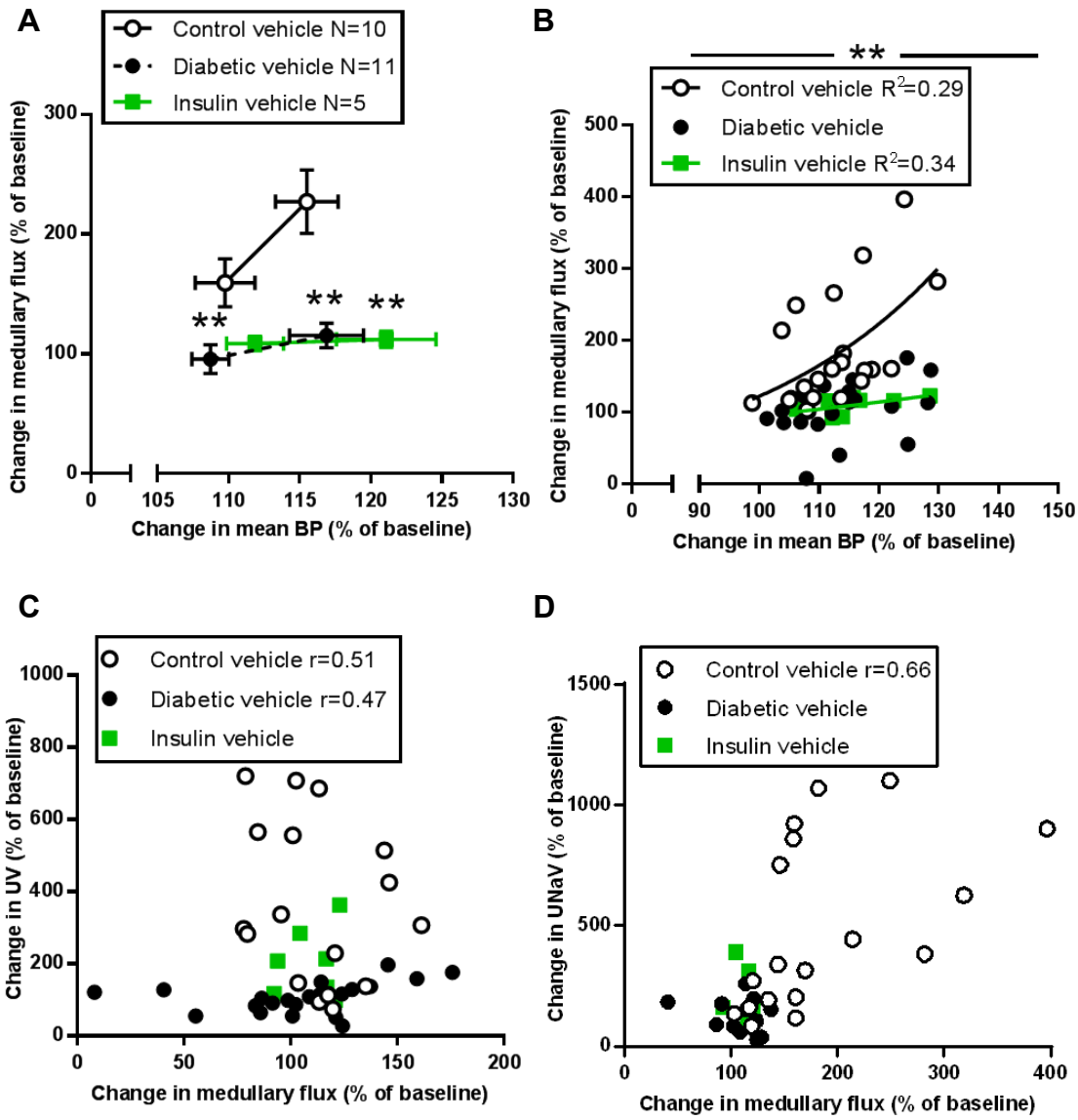
A
Control vehicle N=10
Diabetic vehicle N=11
Insulin vehicle N=5
Change in medullary flux (% of baseline)
Change in mean BP (% of baseline)
**
**
**
B
**
Control vehicle R2=0.29
Diabetic vehicle
Insulin vehicle R2=0.34
Change in medullary flux (% of baseline)
Change in mean BP (% of baseline)
C
Control vehicle r=0.51
Diabetic vehicle r=0.47
Insulin vehicle
Change in UV (% of baseline)
Change in medullary flux (% of baseline)
D
Control vehicle r=0.66
Diabetic vehicle
Insulin vehicle
Change in UNaV (% of baseline)
Change in medullary flux (% of baseline)

Fig. 6.6. (page opposite) Changes in medullary flux with mean blood pressure (BP), urine flow rate (UV) and urinary sodium excretion rate (UNaV) in control, diabetic and insulin-treated diabetic rats

A) Increases in medullary flux were not observed in diabetic and insulin-treated diabetic rats. Every data point is the mean value of the dependent variable plotted against mean BP ± standard error of the mean (SEM) of both variables, and corresponds to Clearance 1 or Clearance 2. All comparisons made with two-way analysis of variance (ANOVA) with Tukey's *post hoc* tests.

B) The curvilinear relationship between changes in medullary flux and mean BP (k=0.02) was lost in diabetics but re-established with insulin at a smaller rate of change (k=0.01), R^2=coefficient of determination.

C) Percentage changes in UV correlated with percentage changes in medullary flux in control and diabetic rats.

D) Correlations between percentage changes in UNaV and medullary flux were lost in diabetics and not re-established with insulin.

For C) and D), correlations made with Pearson's and Spearman's rank tests, r=coefficient of correlation, **=P<0.05 compared with controls

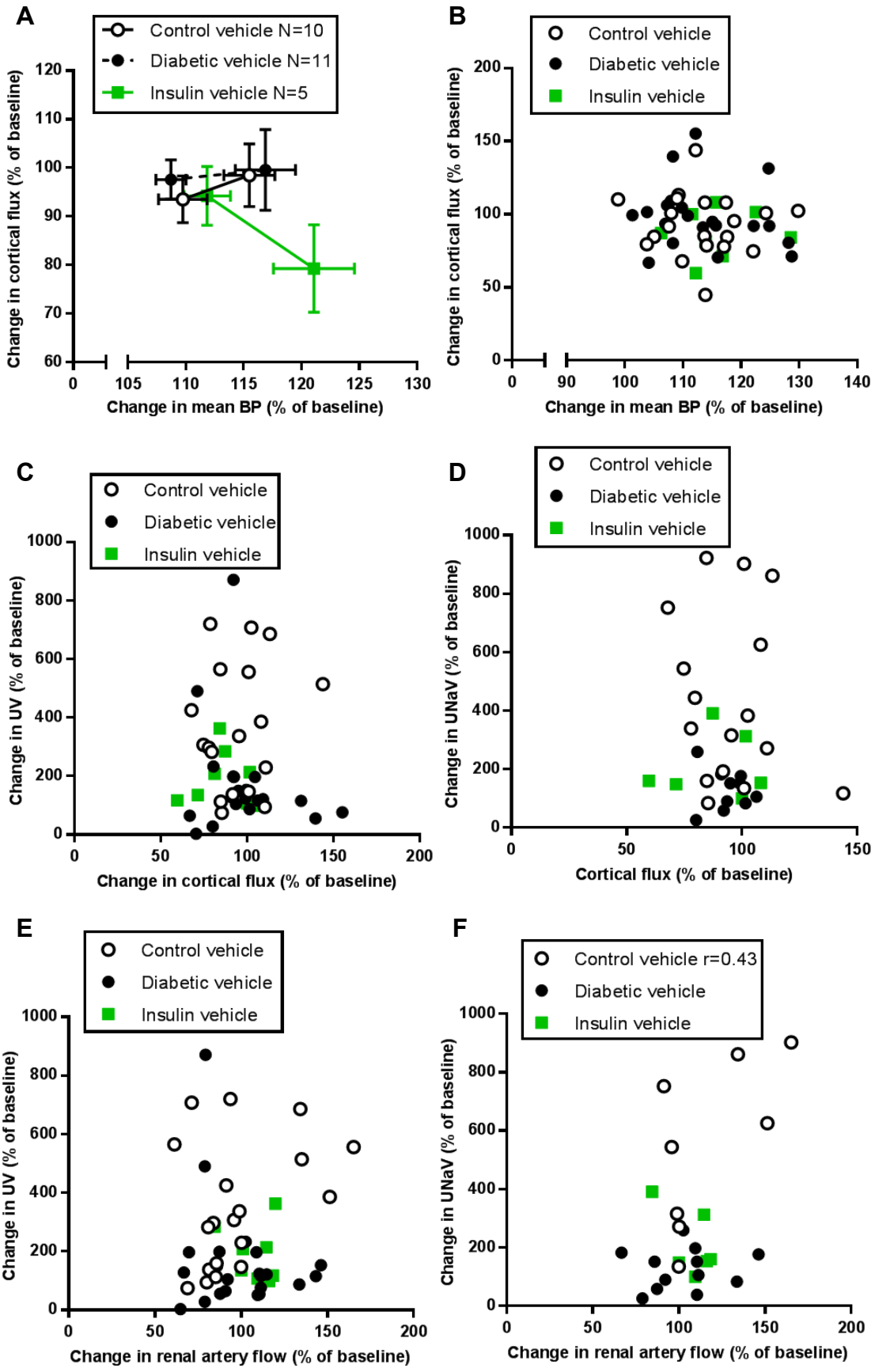
A
Control vehicle N=10
Diabetic vehicle N=11
Insulin vehicle N=5
Change in cortical flux (% of baseline)
Change in mean BP (% of baseline)
B
Control vehicle
Diabetic vehicle
Insulin vehicle
Change in cortical flux (% of baseline)
Change in mean BP (% of baseline)
C
Control vehicle
Diabetic vehicle
Insulin vehicle
Change in UV (% of baseline)
Change in cortical flux (% of baseline)
D
Control vehicle
Diabetic vehicle
Insulin vehicle
Change in UNaV (% of baseline)
Cortical flux (% of baseline)
E
Control vehicle
Diabetic vehicle
Insulin vehicle
Change in UV (% of baseline)
Change in renal artery flow (% of baseline)
F
Control vehicle r=0.43
Diabetic vehicle
Insulin vehicle
Change in UNaV (% of baseline)
Change in renal artery flow (% of baseline)

Fig. 6.7. (page opposite) Changes in cortical flux and renal artery flow with mean blood pressure (BP), urine flow rate (UV) and urinary sodium excretion rate (UNaV) in control, diabetic and insulin-treated diabetic rats

A) Cortical flux did not increase with mean BP in any cohort. Every data point is the mean value of the dependent variable plotted against mean BP ± standard error of the mean (SEM) of both variables, and corresponds to Clearance 1 or Clearance 2. All comparisons made with two-way analysis of variance (ANOVA) with Tukey's *post hoc* tests.

B) There was no relationship between percentage changes in cortical flux and mean BP in any cohort.

C) Percentage changes in UV did not correlate with percentage changes in cortical flux in any cohort.

D) Percentage changes in UNaV did not correlate with percentage changes in cortical flux in any cohort.

E) Percentage changes in UV did not correlate with percentage changes in renal artery flow in any cohort.

F) Correlations between the percentage changes in UNaV and the percentage changes in renal artery flow were lost in diabetics and not re-established with insulin.

For C)-F), correlations made with Pearson's and Spearman's rank tests, r=coefficient of correlation

6.3.3 The effects of endothelin receptor antagonists on acute pressure natriuresis and renal blood flow in healthy control rats

Mean BP rose in control rats receiving ET receptor antagonists by ~25-40mmHg ($P<0.01$, interaction $P=0.61$) and the rise was greatest overall in rats receiving the ET_B receptor antagonist ($P<0.01$; Table 6.4; Fig. 6.8A). However, the only difference in mean BP between agents was a mean BP ~18mmHg higher in ET_B rats compared to ET_A+ET_B rats during Clearance 2 (Table 6.4; Fig. 6.8A). GFR increased by up to 1.4ml/min/gkw ($P<0.01$) but there was no difference in the rise between agents ($P=0.71$, interaction $P=0.12$; Table 6.4; Fig. 6.8B).

ET_A receptor antagonism with atrasentan markedly suppressed acute pressure diuresis and natriuresis. Maximum UV was reduced by ~60% ($P=0.02$ overall, $P<0.01$ during Clearance 2, interaction $P=0.291$; Table 6.4; Fig. 6.9A), UNaV was reduced by ~90% ($P<0.01$ overall and during Clearance 2, interaction $P=0.339$; Fig. 6.9C), and FENa by ~80% ($P=0.04$ overall and during Clearance 2, interaction $P=0.219$; Fig. 6.9E), and their relationships with mean BP were disrupted (Fig. 6.9B,D,F). This was accompanied by suppression of medullary flux which increased by only ~20% so that medullary perfusion was approximately half of that with vehicle ($P<0.01$ overall and during Clearance 2; Table 6.4; Fig. 6.10A). Relationships between medullary flux and mean BP (Fig. 6.10B), UV (Fig. 6.10C) and UNaV (Fig. 6.10D) that had all been observed with vehicle, were lost with atrasentan. Cortical flux (Fig. 6.10E) and renal artery flow (Fig. 6.12F) remained close to Baseline levels, matching values obtained with vehicle (Table 6.4).

By contrast, the ET_B receptor antagonist, A-192621, increased UNaV (P=0.03 overall, P=0.02 during Clearance 2; Fig. 6.9C) and FENa (P=0.04 overall, P=0.046 during Clearance 2; Fig. 6.9E) by ~40-60% more than maximum vehicle values but without a corresponding increase in UV (Table 6.4; Fig. 6.9A). These effects were accompanied by the same doubling of medullary flux that was observed with vehicle (Table 6.4; Fig. 6.10A) so that the relationships between medullary flux and mean BP (Fig. 6.10B), UV (Fig. 6.10C) and UNaV (Fig. 6.10D) that were observed with vehicle were again disrupted.

Combined ET_A+ET_B receptor antagonism gave a similar pattern of results to ET_A receptor antagonism (Table 6.4). It suppressed UNaV (P=0.04 overall and during Clearance 2; Fig. 6.9C) and FENa (P=0.03 overall, P=0.048 during Clearance 2; Fig.6.9E) by~70-90% without changing UV (Fig. 6.9A). This effect was accompanied by a failure in medullary flux to rise (P=0.01 overall, P<0.01 during Clearance 2; Fig. 6.10A) and an increase in cortical flux during Clearance 2 (P=0.03; Fig. 6.10E) so that cortical perfusion was 40% greater than with vehicle.

CONTROL	Baseline				Clearance 1				Clearance 2			
	Vehicle	**ET_A**	**ET_B**	**ET_A+ET_B**	**Vehicle**	**ET_A**	**ET_B**	**ET_A+ET_B**	**Vehicle**	**ET_A**	**ET_B**	**ET_A+ET_B**
BP (mmHg)	124.0±4.3	109.6±5.2	116.0±4.7	108.4±7.0	136.0±4.9	124.3±4.1	134.5±3.7	123.4±3.9	143.9±4.2	135.0±3.8	155.9±4.6	137.9±5.1
GFR (ml/min/gkw)	0.9±0.1	0.9±0.3	0.8±0.1	0.3±0.1	1.0±0.1	1.2±0.2	1.3±0.2	1.3±0.3	1.0±0.1	0.9±0.2	1.3±0.2	1.5±0.3
UV (µl/min/gkw)	7.2±1.6	3.8±0.7	13.8±4.1	3.0±0.6	16.3±3.5	6.1±0.6	28.3±7.3	5.9±1.3	38.6±6.2	**15.7±4.9****	47.4±12.4	19.6±4.2
UNaV (µmol/min/gkw)	2.2±0.6	0.8±0.2	7.6±3.5	0.9±0.4	6.5±0.8	1.4±0.5	21.9±6.8	3.1±0.8	16.7±1.4	**1.7±0.5****	**26.6±6.9****	**5.0±2.4****
FENa (%)	1.7±0.6	0.5±0.1	5.6±3.0	1.4±0.3	3.5±0.7	1.7±0.8	10.0±4.0	3.1±2.0	15.0±2.4	**3.4±1.4****	**21.6±3.4****	**1.6±1.1****
Δ RA flow (%)					93.2±7.5	94.4±4.4	97.8±4.1	102.4±4.6	108.3±11.7	107.1±3.3	97.7±8.7	114.2±12.1
Δ cortical flux (%)					93.5±4.8	103.3±3.2	96.1±4.3	122.6±14.4	98.5±6.5	112.8±4.2	83.6±11.8	**143.9±24.1****
Δ medullary flux (%)					159.4±20.1	108.8±10.3	150.0±9.7	109.4±9.8	227.2±26.7	**122.2±26.7****	206.8±31.5	**105.9±12.9****

Table 6.4. Mean blood pressure (BP), glomerular filtration rate (GFR), urine flow rate (UV), urinary sodium excretion rate (UNaV), fractional excretion of sodium (FENa), and changes (Δ) in renal artery (RA) flow, cortical flux and medullary flux in healthy control rats during Baseline and Clearances 1 and 2, after endothelin (ET) receptor antagonism

****=P<0.05 compared with vehicle during same clearance period. All data are mean ± standard error of the mean (SEM). All comparisons made with two-way analysis of variance (ANOVA) with Tukey's *post hoc* tests.**

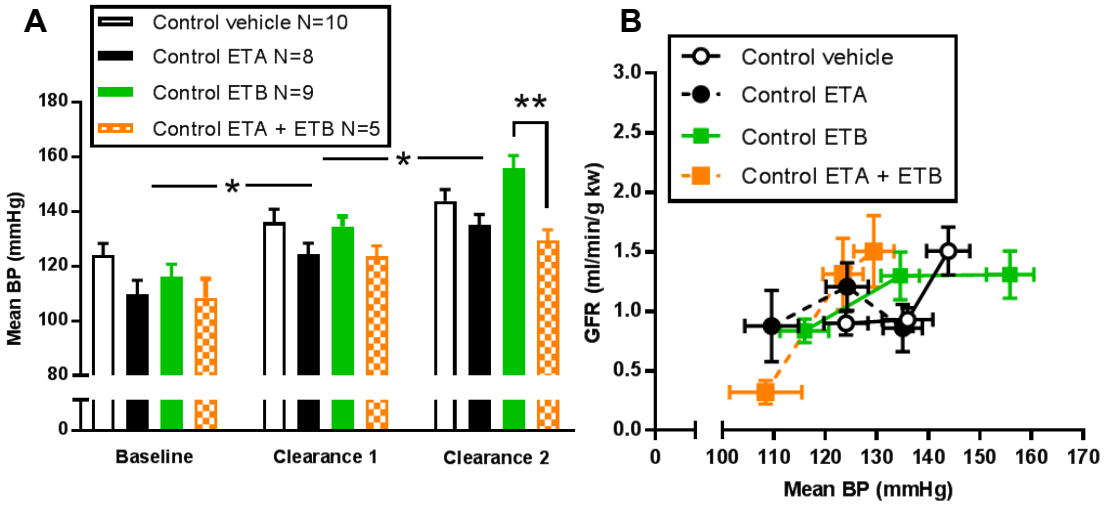

Fig. 6.8. Mean blood pressure (BP) and glomerular filtration rate (GFR) during ligature-induced acute pressure natriuresis in healthy control rats after endothelin (ET) receptor antagonism

A) Baseline mean BP and increments were not significantly different between cohorts except for a higher BP in ET_B rats compared to ET_A+ET_B rats during Clearance 2. Bars=mean ± standard error of the mean (SEM), *=P<0.05 compared with mean BP in previous period, **=P<0.05 compared with other cohort. All comparisons made with two-way analysis of variance (ANOVA) with Tukey's *post hoc* tests.

B) GFRs were similar between cohorts during every clearance period. Every data point is the mean value of the dependent variable plotted against mean BP±SEM of both variables, and corresponds to one of three clearance periods.

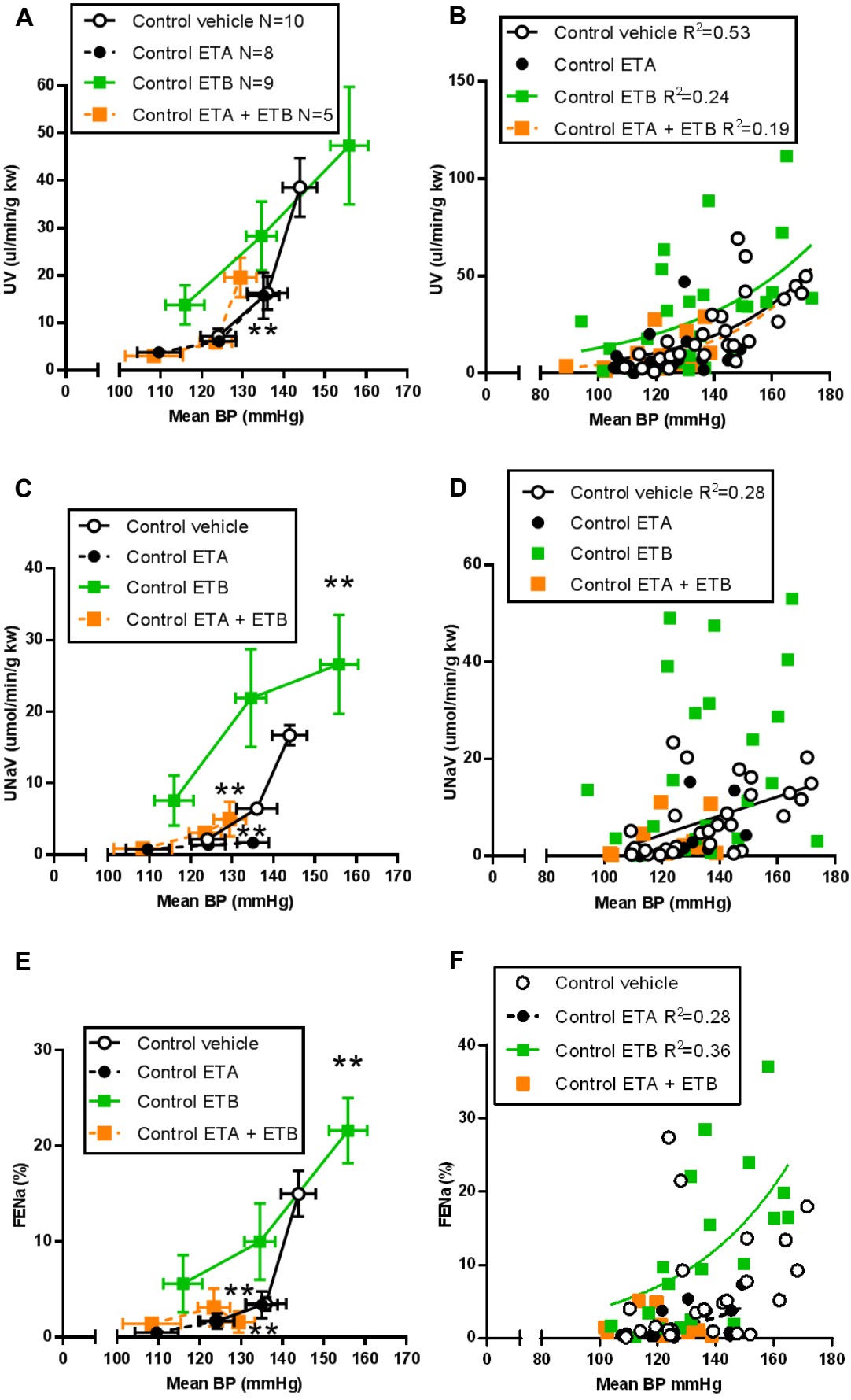
A
Control vehicle N=10
Control ETA N=8
Control ETB N=9
Control ETA + ETB N=5
UV (ul/min/g kw)
Mean BP (mmHg)
**
B
Control vehicle R2=0.53
Control ETA
Control ETB R2=0.24
Control ETA + ETB R2=0.19
UV (ul/min/g kw)
Mean BP (mmHg)
C
Control vehicle
Control ETA
Control ETB
Control ETA + ETB
UNaV (umol/min/g kw)
Mean BP (mmHg)
**
D
Control vehicle R2=0.28
Control ETA
Control ETB
Control ETA + ETB
UNaV (umol/min/g kw)
Mean BP (mmHg)
E
Control vehicle
Control ETA
Control ETB
Control ETA + ETB
FENa (%)
Mean BP (mmHg)
**
F
Control vehicle
Control ETA R2=0.28
Control ETB R2=0.36
Control ETA + ETB
FENa (%)
Mean BP mmHg

Fig. 6.9. (page opposite) Ligature-induced acute pressure natriuresis in healthy control rats after endothelin (ET) receptor antagonism

A) Pressure diuresis responses, with reduced urine flow rate (UV) during Clearance 2 in ET_A receptor antagonist-treated rats

B) Pressure diuresis responses with loss of the non-linear relationship with mean blood pressure (BP, growth constant (k)=0.03) in ET_A receptor antagonist-treated rats. A curvilinear relationship was present in ET_B (k=0.02) and ETA+ETB (k=0.03) receptor antagonist-treated rats.

C) Pressure natriuresis responses, with reduced urinary sodium excretion rate (UNaV) in ET_A receptor antagonist-treated rats and increased UNaV in ET_B receptor antagonist-treated rats during Clearance 2

D) Pressure natriuresis responses, with loss of the linear relationship with mean BP (0.07-0.32, 95% confidence) with ET receptor antagonism

E) Reduced fractional excretion of sodium (FENa) in ET_A receptor antagonist-treated rats and increased FENa in ET_B receptor antagonist-treated rats during Clearance 2

F) A curvilinear relationship between FENa and mean BP was established in ET_A (k=0.02) and ET_B (k=0.01) receptor antagonist-treated rats.

****=P<0.05 compared with vehicle**

For A), C) and E), every data point is the mean value of the dependent variable plotted against mean BP ± standard error of the mean (SEM) of both variables, and corresponds to one of three clearance periods. All comparisons made with two-way analysis of variance (ANOVA) with Tukey's *post hoc* tests.

For B), D) and F), R^2=coefficient of determination

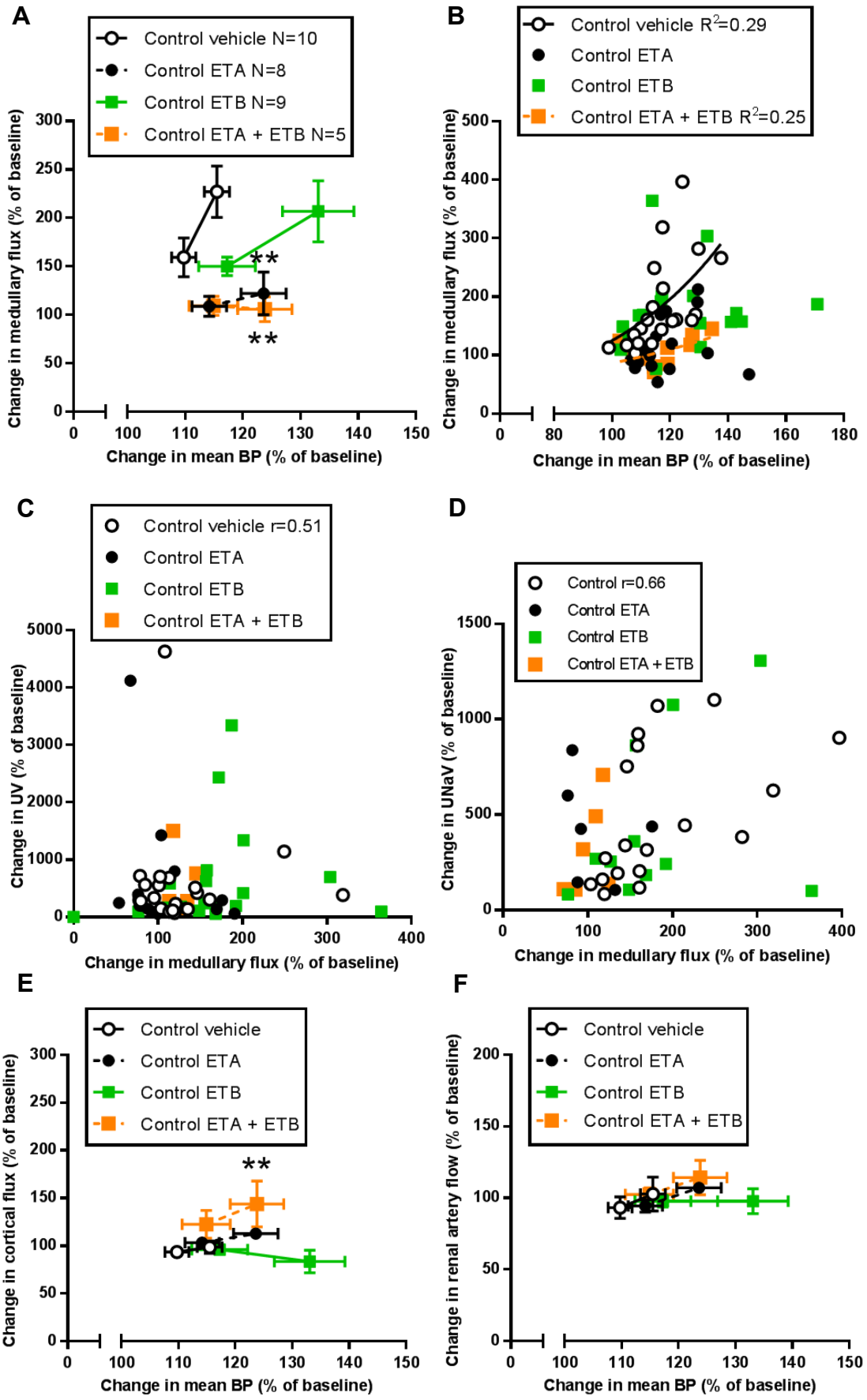
A
Control vehicle N=10
Control ETA N=8
Control ETB N=9
Control ETA + ETB N=5
Change in medullary flux (% of baseline)
Change in mean BP (% of baseline)
**
**
B
Control vehicle R2=0.29
Control ETA
Control ETB
Control ETA + ETB R2=0.25
Change in medullary flux (% of baseline)
Change in mean BP (% of baseline)
C
Control vehicle r=0.51
Control ETA
Control ETB
Control ETA + ETB
Change in UV (% of baseline)
Change in medullary flux (% of baseline)
D
Control r=0.66
Control ETA
Control ETB
Control ETA + ETB
Change in UNaV (% of baseline)
Change in medullary flux (% of baseline)
E
Control vehicle
Control ETA
Control ETB
Control ETA + ETB
**
Change in cortical flux (% of baseline)
Change in mean BP (% of baseline)
F
Control vehicle
Control ETA
Control ETB
Control ETA + ETB
Change in renal artery flow (% of baseline)
Change in mean BP (% of baseline)

Fig. 6.10. (page opposite) Changes in medullary flux, cortical flux and renal artery flow with mean blood pressure (BP), urine flow rate (UV) and urinary sodium excretion rate (UNaV) in healthy control rats after endothelin (ET) receptor antagonism

A) Medullary flux failed to rise in ET_A and ET_A+ET_B receptor antagonist-treated rats.

B) The curvilinear relationship between changes in medullary flux and mean BP (k=0.02) was lost in ET_A and in ET_B receptor antagonist-treated rats but was maintained in ET_A+ET_B receptor antagonist-treated rats, with a smaller rate of change (k=0.01).

C) The correlation between percentage changes in UV and medullary flux was lost with ET receptor antagonism.

D) The correlation between percentage changes in UNaV and medullary flux was lost with ET receptor antagonism.

E) Cortical flux increased in ET_A+ET_B receptor antagonist-treated rats during Clearance 2.

F) Renal artery flow was autoregulated in all control rats.

****=P<0.05 compared with controls**

For A), E) and F), every data point is the mean value of the dependent variable plotted against mean BP ± standard error of the mean (SEM) of both variables, and corresponds to Clearance 1 or Clearance 2. All comparisons made with two-way analysis of variance (ANOVA) with Tukey's *post hoc* tests, R^2=coefficient of determination.

For C) and D), correlations made by Pearson's and Spearman's rank tests, r=coefficient of correlation

6.3.4 The effects of endothelin receptor antagonists on acute pressure natriuresis and renal blood flow in diabetic and insulin-treated diabetic rats

Mean BP rose in the early T1DM and T1DM+insulin rats by ~20-30mmHg (both $P<0.01$) but did not differ between ET receptor antagonists (T1DM P=0.20, interaction P=0.979; T1DM+insulin P=0.11, interaction P=0.98; Tables 6.5, 6.6; Figs. 6.11A,C). GFR (early T1DM P=0.32; T1DM+insulin P=0.24; Figs. 6.11B,D) did not increase from Baseline values and did not differ within the early T1DM and T1DM+insulin cohorts (Tables 6.5, 6.6).

Despite marked effects on pressure diuresis/natriuresis in healthy control rats, ET receptor antagonists had no effect on its suppression in early T1DM rats nor its recovery in T1DM+insulin rats (Tables 6.5, 6.6; Figs. 6.12A-F). There were trends in the data that had a similar pattern to the effects of ET receptor antagonists in healthy controls: suppression with ET_A receptor antagonism, enhancement with ET_B receptor antagonism, and combined ET_A+ET_B receptor antagonism giving similar results to ET_A alone. However, the data spread was wide so that these trends did not reach statistical significance

ET receptor antagonists had no effect on the suppression of medullary flux in early T1DM and T1DM+insulin rats (Tables 6.5, 6.6; Figs. 6.13A,C), although the ET_A receptor antagonist, atrasentan, re-established relationships between percentage changes in medullary flux and UNaV in early T1DM rats (P=0.049; Fig. 6.14B), while atrasentan and the ET_B receptor antagonist, A-192621, each individually

re-established linear relationships between percentage changes in mean BP and medullary flux in T1DM+insulin rats (both P<0.01; Fig. 6.13D).

Cortical flux (T1DM P=0.42; T1DM+insulin P=0.34; Figs. 6.15A,B) remained at Baseline levels in all the ET receptor antagonist cohorts. Overall, renal artery flow increased in both early T1DM and T1DM+insulin rats by ~10-15% (both P<0.01) but there was no difference between agents (early T1DM P=0.37, interaction P=0.66; T1DM+insulin P=0.25, interaction P=0.78) within either diabetic group (Tables 6.5, 6.6; Figs. 6.15C,D).

DIABETIC	Baseline				Clearance 1				Clearance 2			
	Vehicle	ET_A	ET_B	ET_A+ET_B	Vehicle	ET_A	ET_B	ET_A+ET_B	Vehicle	ET_A	ET_B	ET_A+ET_B
BP (mmHg)	116.1±4.2	110.9±6.8	122.0±7.2	116.3±6.1	127.5±4.1	126.1±8.4	135.4±8.1	135.4±8.1	137.9±5.1	133.4±8.5	149.9±7.7	137.4±6.7
GFR (ml/min/gkw)	1.3±0.5	0.7±0.3	0.6±0.1	0.7±0.2	0.8±0.2	1.3±0.6	0.6±0.2	0.9±0.2	1.1±0.2	1.2±0.4	1.3±0.3	1.1±0.2
UV (µl/min/gkw)	8.7±3.2	3.2±0.9	5.0±1.1	4.1±0.6	8.5±2.5	5.4±1.5	7.9±3.3	4.5±0.8	**14.0±3.4****	7.9±2.5	17.7±6.0	11.0±1.8
UNaV (µl/min/gkw)	2.1±0.7	1.6±0.8	2.0±0.7	1.4±0.5	2.0±0.4	2.4±0.9	4.5±2.0	1.4±0.4	**4.1±1.1****	3.2±1.4	7.0±3.4	2.6±1.4
FENa (%)	1.9±0.8	0.8±0.3	1.2±0.4	1.7±0.6	2.8±1.0	1.0±0.4	1.8±1.1	1.1±0.2	**3.7±1.0****	2.0±0.7	7.8±6.0	0.7±0.2
Δ RA flow (%)					93.2±6.6	97.2±2.8	97.3±7.7	96.2±1.9	104.0±7.7	113.2±5.0	132.0±16.2	109.6±3.4
Δ cortical flux (%)					97.6±6.1	93.8±5.8	96.6±4.4	97.7±3.8	99.6±8.3	98.7±3.3	99.8±8.2	107.4±7.1
Δ medullary flux (%)					**95.7±12.1****	101.8±9.3	85.4±9.6	108.4±10.4	**115.4±10.3****	89.3±9.6	146.6±19.4	120.2±14.8

Table 6.5. Mean blood pressure (BP), glomerular filtration rate (GFR), urine flow rate (UV), urinary sodium excretion rate (UNaV), fractional excretion of sodium (FENa), and changes (Δ) in renal artery (RA) flow, cortical flux and medullary flux in diabetic rats during Baseline and Clearances 1 and 2, after endothelin (ET) receptor antagonism

****=P<0.05 compared with vehicle-treated controls. All data are mean ± standard error of the mean (SEM). All comparisons made with two-way analysis of variance (ANOVA) with Tukey's *post hoc* tests.**

INSULIN	Baseline				Clearance 1				Clearance 2			
	Vehicle	ET_A	ET_B	ET_A+ET_B	Vehicle	ET_A	ET_B	ET_A+ET_B	Vehicle	ET_A	ET_B	ET_A+ET_B
BP (mmHg)	122.3±5.3	112.0±6.8	122.7±8.4	111.5±2.6	136.5±4.3	129.5±8.7	134.3±10.9	127.4±3.1	146.2±2.9	141.6±7.8	155.7±13.4	135.4±2.3
GFR (ml/min/gkw)	1.8±0.7	0.6±0.2	0.8±0.2	0.9±0.2	1.4±0.3	1.5±0.6	1.3±0.6	1.2±0.2	1.3±0.3	1.9±0.6	1.7±0.5	1.4±0.2
UV (µl/min/gkw)	13.1±4.5	2.5±0.5	6.4±3.7	3.8±0.8	17.8±5.7	7.0±1.9	13.6±9.8	5.9±1.3	**30.4±12.4***	22.5±4.3	37.0±14.2	14.4±2.9
UNaV (µmol/min/gkw)	2.6±1.1	0.9±0.4	4.7±3.8	1.3±0.5	4.3±1.8	1.8±0.6	9.9±8.5	2.6±1.0	**24.9±17.8***	8.6±3.0	21.9±9.8	6.1±2.0
FENa (%)	1.0±0.4	0.9±0.2	3.4±2.4	1.2±0.4	2.2±0.5	1.1±0.3	4.6±3.1	1.4±0.4	**9.6±4.9***	5.8±2.2	8.5±3.3	2.9±0.3
Δ RA flow (%)					102.8±6.9	107.9±6.5	85.2±6.1	97.6±3.4	113.2±4.5	121.2±9.3	112.0±13.6	117.3±6.5
Δ cortical flux (%)					94.2±6.1	102.7±2.5	82.1±13.6	89.2±10.1	79.3±9.0	117.7±6.4	91.9±4.3	103.5±13.3
Δ medullary flux (%)					108.7±6.1	104.2±9.2	85.8±21.2	111.1±8.7	**112.2±6.8****	110.2±10.5	116.8±32.7	125.1±9.4

Table 6.6. Mean blood pressure (BP), glomerular filtration rate (GFR), urine flow rate (UV), urinary sodium excretion rate (UNaV), fractional excretion of sodium (FENa), and changes (Δ) in renal artery (RA) flow, cortical flux and medullary flux in insulin-treated diabetic rats during Baseline and Clearances 1 and 2, after endothelin (ET) receptor antagonism

****=P<0.05 compared with vehicle-treated controls and *=P<0.05 compared with vehicle-treated diabetic rats during same clearance period. All data are mean ± standard error of the mean (SEM). All comparisons made with two-way analysis of variance (ANOVA) with Tukey's *post hoc* tests.**

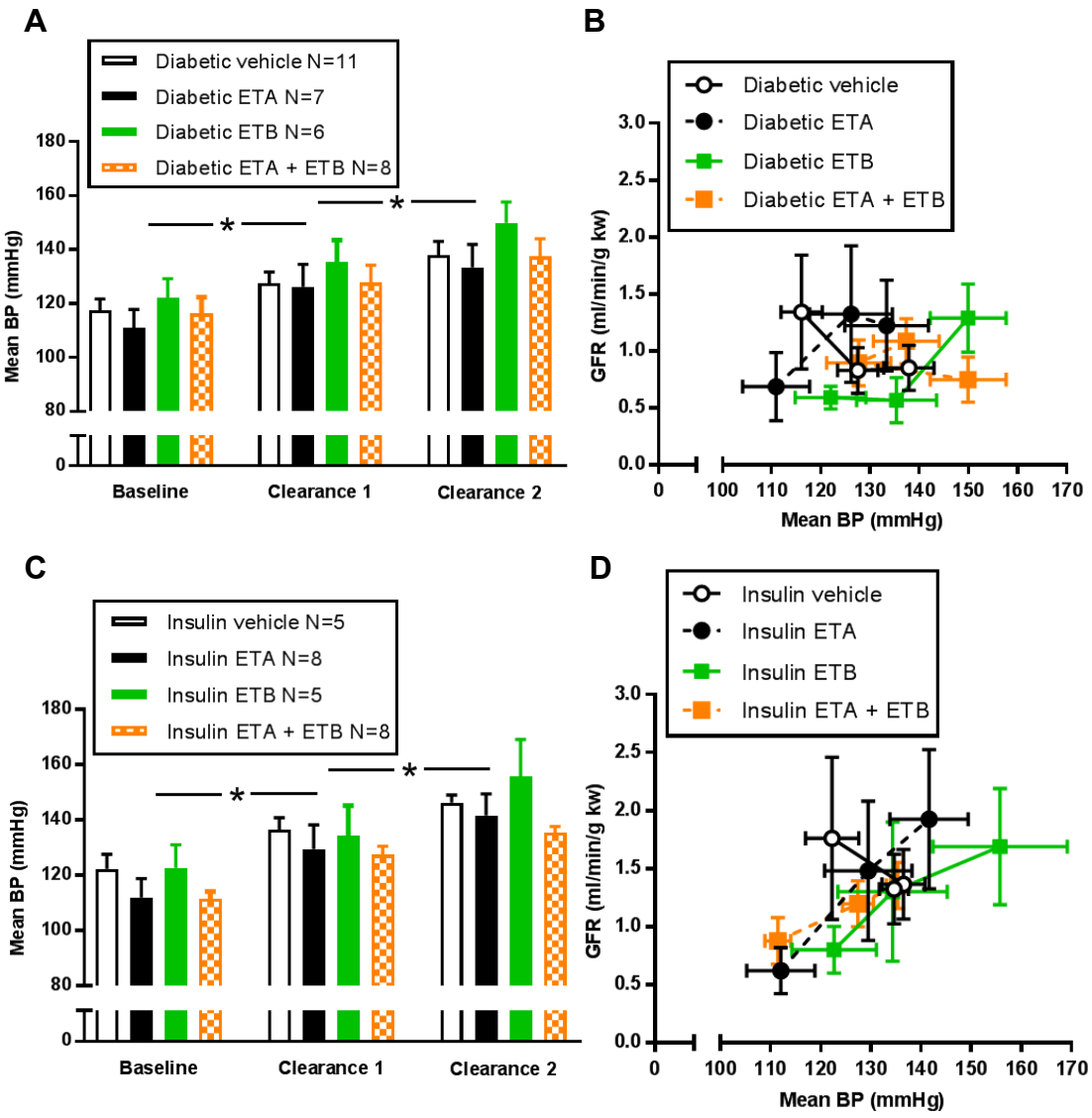
A
Diabetic vehicle N=11
Diabetic ETA N=7
Diabetic ETB N=6
Diabetic ETA + ETB N=8
Mean BP (mmHg)
180
160
140
120
100
80
0
Baseline
Clearance 1
Clearance 2
*
*
B
Diabetic vehicle
Diabetic ETA
Diabetic ETB
Diabetic ETA + ETB
GFR (ml/min/g kw)
3.0
2.5
2.0
1.5
1.0
0.5
0.0
0
100
110
120
130
140
150
160
170
Mean BP (mmHg)
C
Insulin vehicle N=5
Insulin ETA N=8
Insulin ETB N=5
Insulin ETA + ETB N=8
Mean BP (mmHg)
180
160
140
120
100
80
0
Baseline
Clearance 1
Clearance 2
*
*
D
Insulin vehicle
Insulin ETA
Insulin ETB
Insulin ETA + ETB
GFR (ml/min/g kw)
3.0
2.5
2.0
1.5
1.0
0.5
0.0
0
100
110
120
130
140
150
160
170
Mean BP (mmHg)

Fig. 6.11. (page opposite) Mean blood pressure (BP) and glomerular filtration rate (GFR) during ligature-induced acute pressure natriuresis in diabetic and insulin-treated diabetic rats after endothelin (ET) receptor antagonism

A) Baseline mean BP and increments were not significantly different between diabetic cohorts.

B) GFRs were similar between diabetic cohorts during every clearance period.

C) Baseline mean BP and increments were not significantly different between cohorts.

D) GFRs were similar between cohorts during every clearance period

For A) and C), bars=mean ± standard error of the mean (SEM). All comparisons made with two-way analysis of variance (ANOVA) with Tukey's *post hoc* tests, *=P<0.05 compared with mean BP in previous period.

For, B) and D), every data point is the mean value of the dependent variable plotted against mean BP±SEM of both variables, and corresponds to one of three clearance periods.

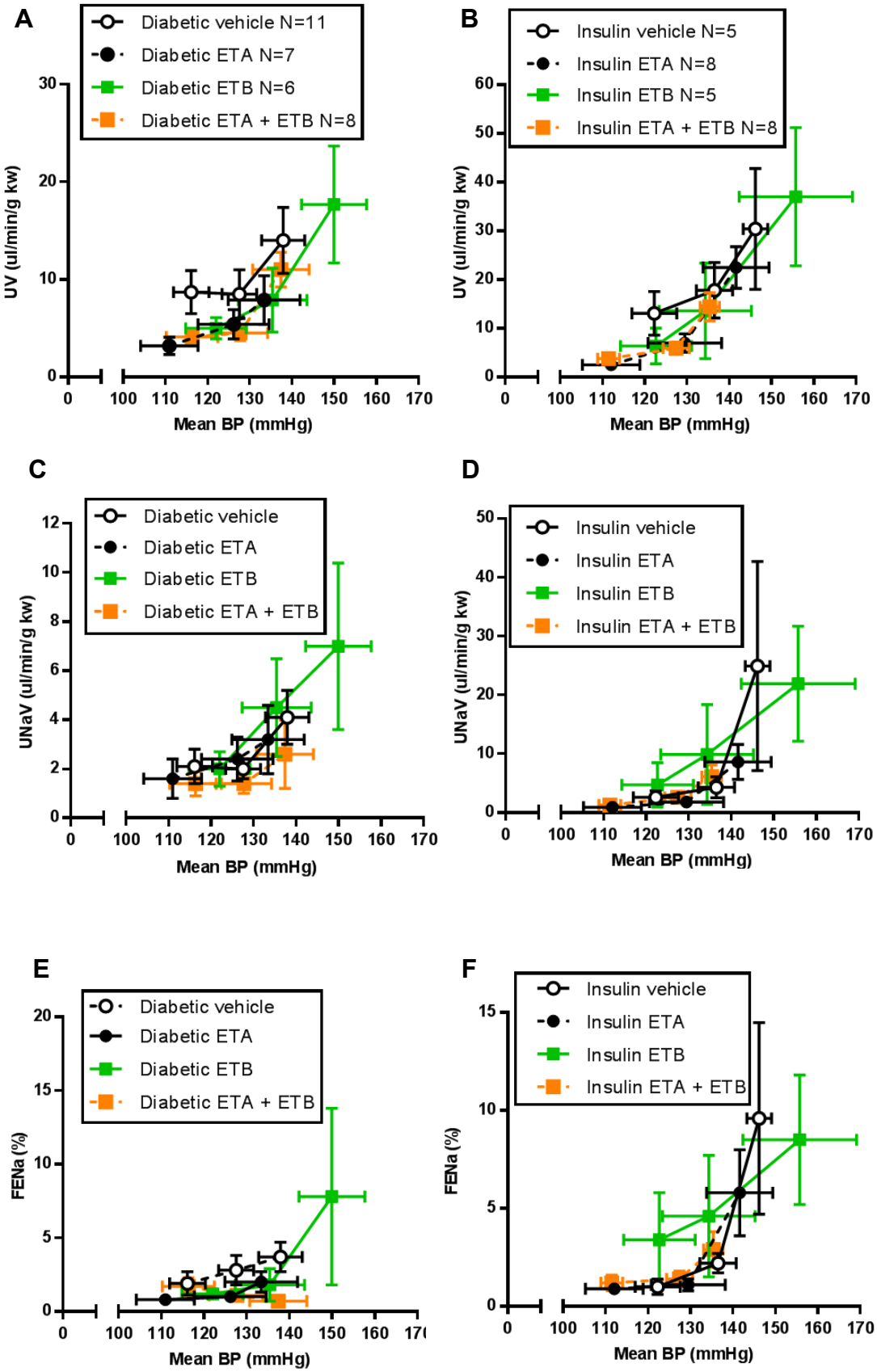
A
Diabetic vehicle N=11
Diabetic ETA N=7
Diabetic ETB N=6
Diabetic ETA + ETB N=8
UV (ul/min/g kw)
Mean BP (mmHg)
B
Insulin vehicle N=5
Insulin ETA N=8
Insulin ETB N=5
Insulin ETA + ETB N=8
UV (ul/min/g kw)
Mean BP (mmHg)
C
Diabetic vehicle
Diabetic ETA
Diabetic ETB
Diabetic ETA + ETB
UNaV (ul/min/g kw)
Mean BP (mmHg)
D
Insulin vehicle
Insulin ETA
Insulin ETB
Insulin ETA + ETB
UNaV (ul/min/g kw)
Mean BP (mmHg)
E
Diabetic vehicle
Diabetic ETA
Diabetic ETB
Diabetic ETA + ETB
FENa (%)
Mean BP (mmHg)
F
Insulin vehicle
Insulin ETA
Insulin ETB
Insulin ETA + ETB
FENa (%)
Mean BP (mmHg)

Fig. 6.12. (page opposite) Ligature-induced acute pressure natriuresis in diabetic and insulin-treated diabetic rats after endothelin (ET) receptor antagonism

A) Suppression of pressure diuresis was unaffected by ET receptor antagonists in diabetic rats.

B) Recovery of pressure diuresis was unaffected by ET receptor antagonists in insulin-treated diabetic rats.

C) Suppression of pressure natriuresis was unaffected by ET receptor antagonists in diabetic rats.

D) Recovery of pressure natriuresis was unaffected by ET receptor antagonists in insulin-treated diabetic rats.

E) Reductions in FENa were unaffected by ET receptor antagonists in diabetic rats.

F) Recovery of FENa was unaffected by ET receptor antagonists in insulin-treated diabetic rats.

Every data point is the mean value of the dependent variable plotted against mean blood pressure (BP) ± standard error of the mean (SEM) of both variables, and corresponds to one of three clearance periods. All comparisons made with two-way analysis of variance (ANOVA) with Tukey's *post hoc* tests.

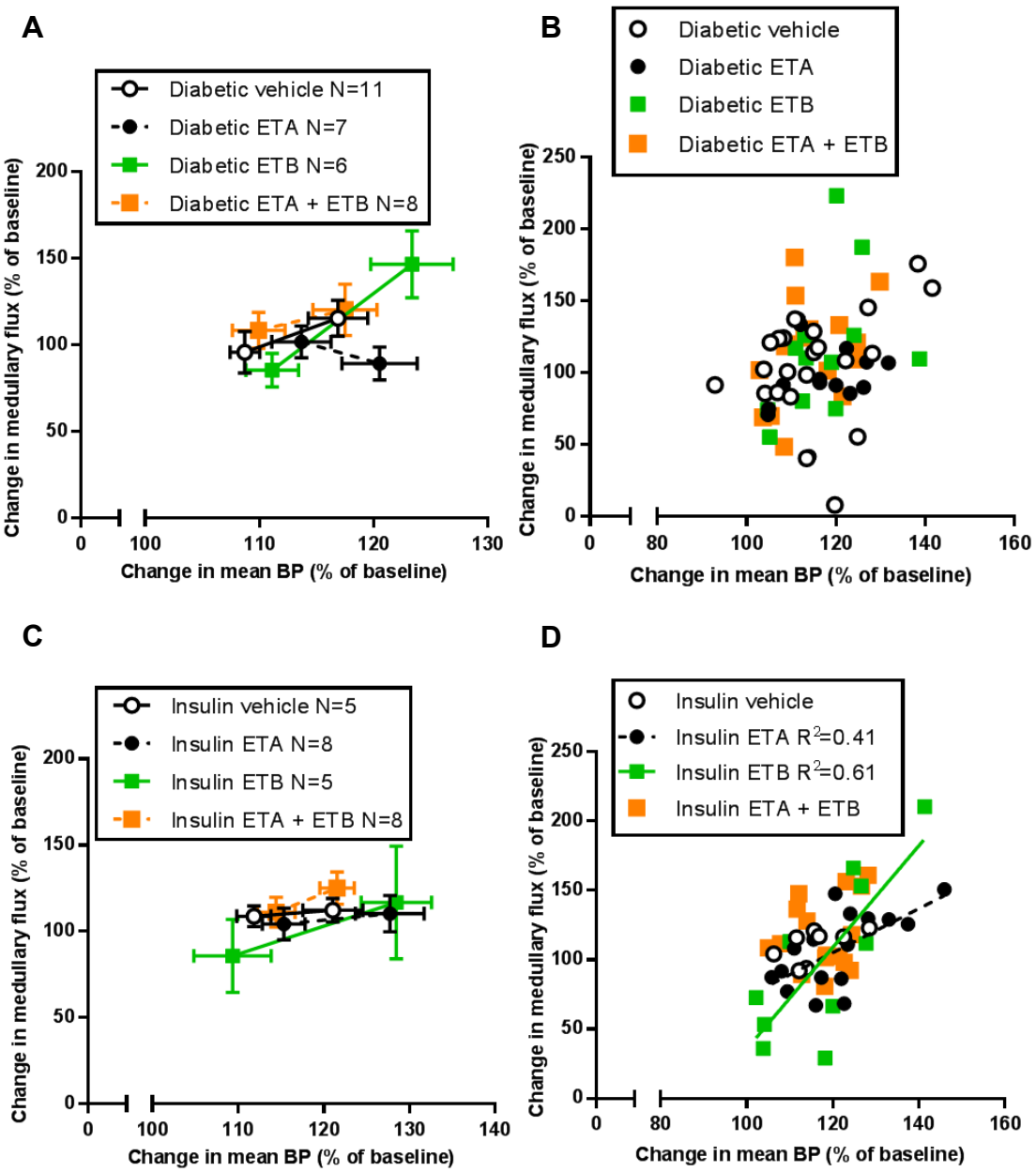
A
Diabetic vehicle N=11
Diabetic ETA N=7
Diabetic ETB N=6
Diabetic ETA + ETB N=8
Change in medullary flux (% of baseline)
Change in mean BP (% of baseline)
B
Diabetic vehicle
Diabetic ETA
Diabetic ETB
Diabetic ETA + ETB
Change in medullary flux (% of baseline)
Change in mean BP (% of baseline)
C
Insulin vehicle N=5
Insulin ETA N=8
Insulin ETB N=5
Insulin ETA + ETB N=8
Change in medullary flux (% of baseline)
Change in mean BP (% of baseline)
D
Insulin vehicle
Insulin ETA R2=0.41
Insulin ETB R2=0.61
Insulin ETA + ETB
Change in medullary flux (% of baseline)
Change in mean BP (% of baseline)

Fig. 6.13. (page opposite) Changes in medullary flux with mean blood pressure (BP) in diabetic and insulin-treated diabetic rats after endothelin (ET) receptor antagonism

A) Suppression of medullary flux was unaffected by ET receptor antagonists in diabetic rats.

B) There was no relationship between percentage changes in medullary flux and mean BP in any diabetic cohort.

C) Suppression of medullary flux was unaffected by ET receptor antagonists in insulin-treated diabetic rats.

D) Linear relationships between percentage changes in medullary flux and mean BP were re-established in insulin-treated diabetic rats receiving ET_A and ET_B receptor antagonists, R^2=coefficient of determination.

For A) and C), every data point is the mean value of the dependent variable plotted against mean BP ± standard error of the mean (SEM) of both variables, and corresponds to Clearance 1 or Clearance 2. All comparisons made with two-way analysis of variance (ANOVA) with Tukey's *post hoc* tests.

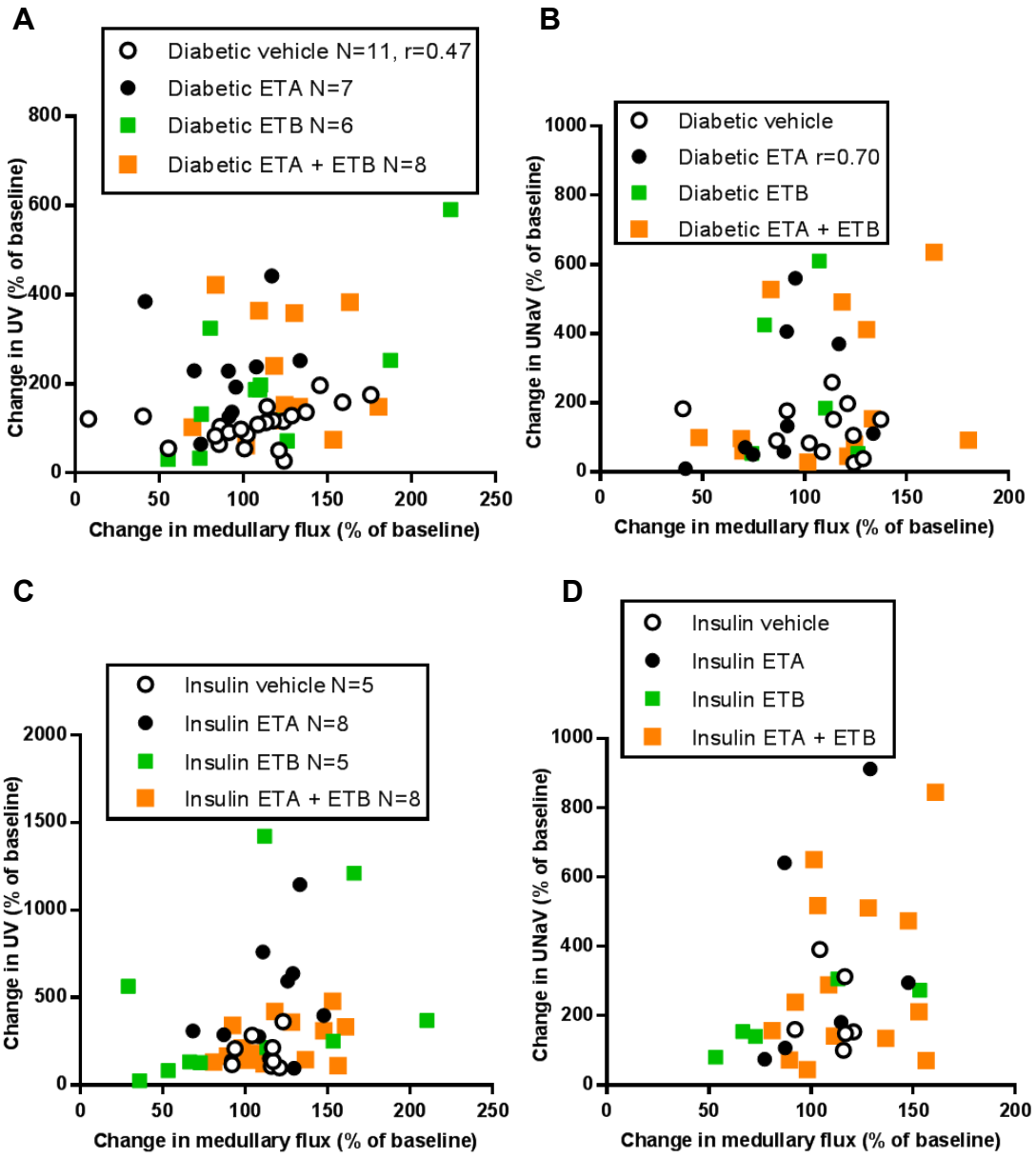
A
Diabetic vehicle N=11, r=0.47
Diabetic ETA N=7
Diabetic ETB N=6
Diabetic ETA + ETB N=8
Change in UV (% of baseline)
Change in medullary flux (% of baseline)
B
Diabetic vehicle
Diabetic ETA r=0.70
Diabetic ETB
Diabetic ETA + ETB
Change in UNaV (% of baseline)
Change in medullary flux (% of baseline)
C
Insulin vehicle N=5
Insulin ETA N=8
Insulin ETB N=5
Insulin ETA + ETB N=8
Change in UV (% of baseline)
Change in medullary flux (% of baseline)
D
Insulin vehicle
Insulin ETA
Insulin ETB
Insulin ETA + ETB
Change in UNaV (% of baseline)
Change in medullary flux (% of baseline)

Fig. 6.14. (page opposite) Changes in medullary flux with urine flow rate (UV) and urinary sodium excretion rate (UNaV) in diabetic and insulin-treated diabetic rats after endothelin (ET) receptor antagonism

A) Correlations between percentage changes in medullary flux and UV were lost with ET receptor antagonists in diabetic rats.

B) Correlations between percentage changes in medullary flux and UNaV were re-established in diabetic rats receiving ET_A receptor antagonist.

C) Lack of correlation between percentage changes in medullary flux and UV was unaffected by ET receptor antagonists in insulin-treated diabetic rats.

D) Lack of correlation between percentage changes in medullary flux and UNaV was unaffected by ET receptor antagonists in insulin-treated diabetic rats.

Correlations made with Pearson's and Spearman's rank tests, r=coefficient of correlation

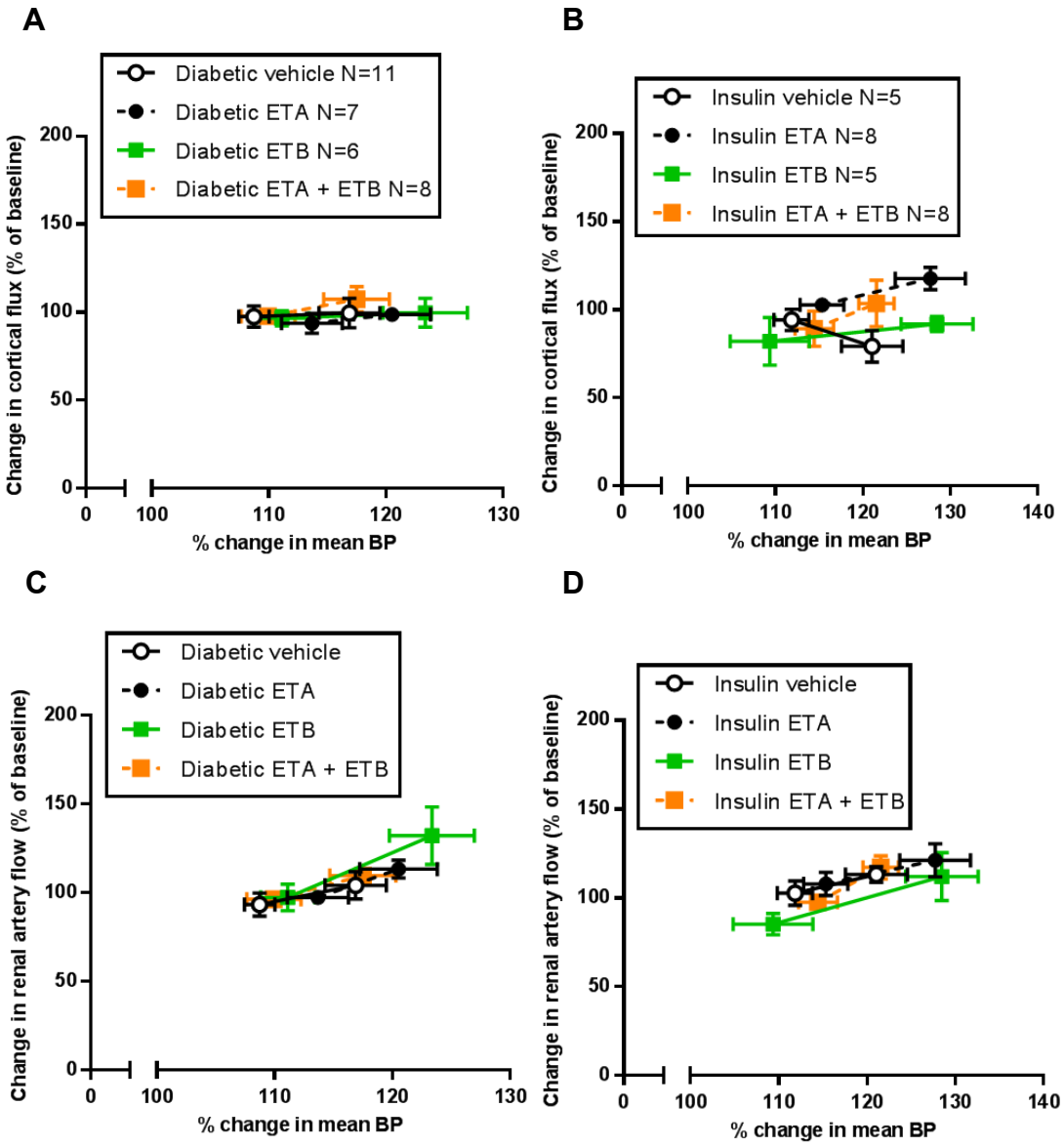
A
Diabetic vehicle N=11
Diabetic ETA N=7
Diabetic ETB N=6
Diabetic ETA + ETB N=8
Change in cortical flux (% of baseline)
% change in mean BP
B
Insulin vehicle N=5
Insulin ETA N=8
Insulin ETB N=5
Insulin ETA + ETB N=8
Change in cortical flux (% of baseline)
% change in mean BP
C
Diabetic vehicle
Diabetic ETA
Diabetic ETB
Diabetic ETA + ETB
Change in renal artery flow (% of baseline)
% change in mean BP
D
Insulin vehicle
Insulin ETA
Insulin ETB
Insulin ETA + ETB
Change in renal artery flow (% of baseline)
% change in mean BP

Fig. 6.15. (page opposite) Changes in cortical flux and renal artery flow with mean blood pressure (BP) in diabetic and insulin-treated diabetic rats after endothelin (ET) receptor antagonism

A) Cortical flux did not change from Baseline levels in all diabetic cohorts.

B) Cortical flux did not change from Baseline levels in all insulin-treated diabetic cohorts.

C) Renal artery flow increased overall during Clearance 2 but did not differ between individual diabetic cohorts.

D) Renal artery flow increased overall during Clearance 2 but did not differ between individual insulin-treated diabetic cohorts.

Every data point is the mean value of the dependent variable plotted against mean BP ± standard error of the mean (SEM) of both variables, and corresponds to Clearance 1 or Clearance 2. All comparisons made with two-way analysis of variance (ANOVA) with Tukey's *post hoc* tests

6.3.5 Changes in expression of the renal endothelin-1 system

Renal expression of EDN1, EDRA and EDRB in the cortex and medulla was not different in early T1DM and T1DM+insulin rats compared to controls (Figs. 6.16A,B).

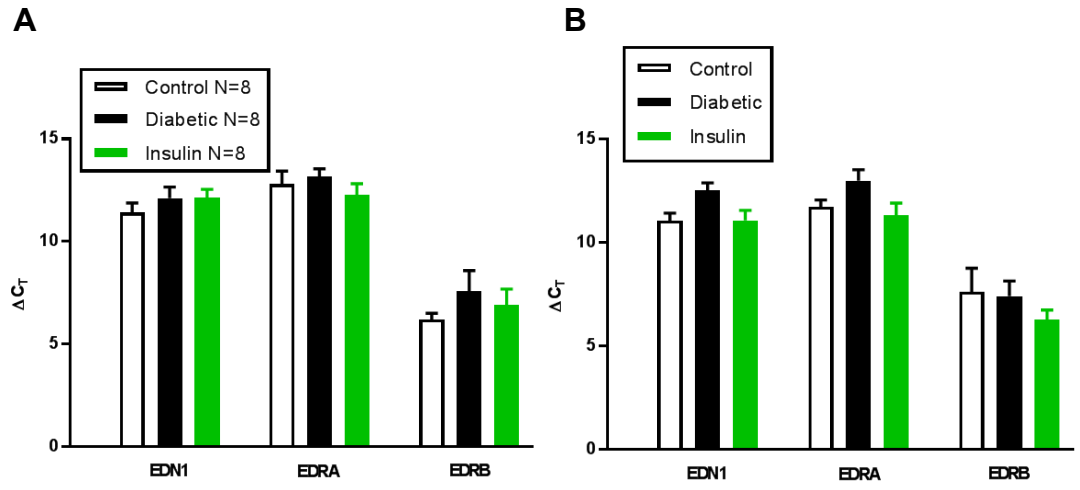

Fig. 6.16. Expression of the renal endothelin (ET) system in control, diabetic and insulin-treated diabetic rats

A) Cortical expression of EDN1 and both EDRA and EDRB was no different in diabetic and insulin-treated diabetic rats compared to controls.

B) Medullary expression of EDN1 and both EDRA and EDRB was no different in diabetic and insulin-treated diabetic rats compared to controls.

ΔC_T refers to the cycle threshold referenced to glyceraldehyde 3-phosphate dehydrogenase (GAPDH), bars=mean ± standard error of the mean (SEM). All comparisons made with one-way analysis of variance (ANOVA) or Kruskal Wallis with Tukey's or Dunn's *post hoc* tests.

6.4 Discussion

In these experiments, measurement of renal blood flow has demonstrated that early T1DM has profound consequences for the renal handling of salt at higher BP. Early T1DM suppresses the rise in medullary perfusion that is the vascular phase of acute pressure natriuresis. Whether this is the physiological mechanism responsible for the impairment of acute pressure natriuresis that was demonstrated in Chapter 4 remains unclear because insulin restores natriuresis without restoring medullary perfusion. It is concluded that normalising blood glucose with insulin does not restore the uncoupling of BP and medullary perfusion, but is sufficient to restore natriuresis.

An additional major finding from these experiments is that ET-1 regulates acute pressure natriuresis through a balance of opposing ET receptor-mediated effects. Use of selective ET receptor antagonists has shown that ET_A receptors increase medullary perfusion and are pro-natriuretic whereas ET_B receptors enhance tubular sodium reabsorption directly and are anti-natriuretic. These effects are unexpected because they contradict many of the putative roles of ET receptors. However, they are consistent with the disruption to the circadian variation in diastolic BP recorded in rats during ET_A receptor antagonism in Chapter 5 and its restoration with additional ET_B receptor antagonism. Whereas the effects on BP were recorded in rats with early T1DM, modification of acute pressure natriuresis by ET receptor antagonists was only recorded in healthy controls and not diabetics. One explanation for this discrepancy comes from the spread of data in this chapter that suggest that experiments may have been underpowered to demonstrate treatment effects in the untreated and insulin-treated diabetic cohorts.

Chapter 5 demonstrated that impaired acute pressure natriuresis in early T1DM is associated with changes in diastolic BP that relate to increased cardiovascular risk. Combined with this chapter's data, it is concluded that if the clinical goal of tight blood glucose control with insulin is not achievable, reversing suppression of renal medullary perfusion might contribute to restoring acute pressure natriuresis in early T1DM, and may confer reductions in cardiovascular risk. They also raise the possibility of obtaining reductions in cardiovascular risk even when control of blood glucose is optimal. However, it is unlikely this would be achieved with highly selective ET_A receptor antagonists, because they prevent ET_A receptor-mediated increases in renal medullary perfusion and natriuresis.

6.4.1 Renal blood flow was measured by further adaptation of ligature-induced acute pressure natriuresis.

The experimental protocol to induce acute pressure natriuresis was the same as the one developed in Chapter 3 and used in Chapter 4. Similar stepwise increases in mean BP were generated by arterial ligation across the control, early T1DM and T1DM+insulin cohorts. Mean GFR was not a confounding variable because it remained within a range of mean GFRs measured during baseline clearance studies (Chapter 3). An additional adaptation from the Chapter 4 protocol was to place three probes for measuring renal blood flow, and to cannulate the left ureter rather than perform a tube cystotomy. These adaptations did not prevent the induction of acute pressure natriuresis, its impairment in rats with early T1DM, and its recovery in T1DM+insulin rats.

A combination of ultrasound and laser Doppler spectroscopy (LDS) was used to measure simultaneous shifts in total and regional renal blood flow during acute pressure natriuresis. LDS has been used previously to measure fluctuations in cortical and medullary blood flow [185,225,303-307]. It follows the Doppler principle [235,236] and has been validated against other real-time (electromagnetic) and *in vitro* (microspheres) methods [236].

6.4.2 Impairment of acute pressure natriuresis in early Type 1 diabetes mellitus is associated with suppressed medullary perfusion.

Roman and Cowley [138] were the first to demonstrate an increase in medullary blood flow, but not cortical or renal artery flow, when mean BP or renal perfusion pressure increase. In this chapter, by using a similar protocol to Roman and Cowley [112], a similar increase in medullary perfusion was demonstrated in healthy controls. Increasing medullary perfusion leads to the increase in interstitial hydrostatic pressure that suppresses pressure-sensitive sodium reabsorption and results in natriuresis [89,308,309]. Therefore, these data would suggest that early T1DM impairs acute pressure natriuresis by preventing transmission of increased mean BP to the medullary circulation.

Renal artery flow failed to increase, consistent with an autoregulatory response [138] that suggests there is a proportionate increase in renal vascular resistance downstream of the renal artery when mean BP increases. Therefore, an increase in renal perfusion pressure rather than just renal artery flow is required to sustain the increase in medullary perfusion that leads to acute pressure natriuresis.

Renal perfusion pressure has been studied previously in rats with early T1DM but more in terms of glomerular rather than medullary haemodynamics [310-312]. Glomerular hyperperfusion is a major contributor to the glomerular hyperfiltration that initiates diabetic nephropathy [44]. Studies in STZ-induced T1DM rats have shown that increased glucose levels within the renal filtrate promote sodium reabsorption from the PCT [52]. This exposes the *macula densa* downstream to lower concentrations of sodium, blunting the influence of tubuloglomerular feedback (TGF) on the myogenic response of the afferent arteriole [99]. The consequence is inappropriate afferent arteriodilation that drives glomerular hyperperfusion [99,310]. In this chapter, Baseline renal artery flow and GFR were not increased in rats with early T1DM. This may, in part, have been a consequence of general anaesthesia lowering mean BP in the diabetic rats to control levels. This may also have occurred in Chapter 4, despite the impairment to acute pressure natriuresis caused by early T1DM.

Less is known about the impact of early T1DM on efferent arteriolar flow than on afferent arteriolar flow. Blood exits the glomerulus through the efferent arteriole and perfuses the post glomerular peritubular network, including the medullary *vasa recta* [305]. Therefore, increased efferent arteriolar flow initiates acute pressure natriuresis [313]. Both the renal cortex and the medulla contain elements of the peritubular vascular network but the majority is contained within the medulla, while the cortex also contains glomerular and preglomerular components. Therefore, by measuring the differences in cortical and medullary perfusion, the experiments of

this chapter are the first to quantify the post glomerular effects of early T1DM and the consequences for the vascular component of acute pressure natriuresis.

Cortical flow was also autoregulated while medullary flow increased, even though all medullary blood flow is derived from the cortex. The cortex contains the glomeruli of two different types of nephrons: cortical nephrons, which have short loops of Henle and *vasa recta*, and juxtamedullary nephrons, whose loops of Henle and *vasa recta* are long and penetrate the inner medulla [305]. During acute pressure natriuresis, there is a shift from perfusion of cortical nephrons towards juxtamedullary nephrons [305]. This allows overall cortical perfusion to remain unchanged while medullary perfusion increases. The shift from cortical to juxtamedullary nephrons is based on relative changes in vascular resistance [305]. The mechanism for this should be investigated in future experiments (Chapter 7.2, page 276) as it may underpin the impairment of medullary perfusion and acute pressure natriuresis demonstrated in early T1DM in this chapter.

6.4.3 Changes in renal perfusion in Type 1 diabetes mellitus are similar to those observed in models of hypertension.

The failure of medullary blood flow to rise in rats with early T1DM, despite increases in renal perfusion pressure, is common to other rodent models of hypertension such as rats chronically infused with the nitric oxide synthase (NOS) inhibitor N-nitro L-arginine methyl ester (L-NAME) [314] or angiotensin II (AngII) [315], and deoxycorticosterone acetate (DOCA) salt-sensitive [316], and AngII receptor type II knockout (AngII RII KO) [317] mice . Not only does this show that different

rodent models may share common pathways that drive hypertension through dysregulation of medullary perfusion, but it is also consistent with the concept that the state of hypertension can only be maintained if there is a concurrent dysfunction in acute pressure natriuresis [89]. This has clinical significance for two reasons. First, suppressed medullary perfusion following increases in BP has also been recorded in Fischer (F344) rats that are prone to hypertensive renal damage [123], offering a potential link between impaired medullary perfusion in early T1DM and the development of nephropathy, an important contributor to cardiovascular risk. Second, non-diabetic rodent models of hypertension could provide mechanistic insight and reveal pharmacological targets that enhance medullary perfusion and acute pressure natriuresis in early T1DM, and hence reduce cardiovascular risk. Such mechanisms include upregulation of the purinergic receptor P2X7 [123,315], reduced arachidonic acid hydroxylase activity [317] and impaired nitric oxide (NO) signalling [306].

NO signalling is of particular interest because it has profound effects on both vascular and tubular phases of acute pressure natriuresis. It is discussed below in relation to its interactions with insulin.

6.4.4 Insulin does not fully restore acute pressure natriuresis in early Type 1 diabetes mellitus.

Chapter 4 demonstrated that sodium excretion during acute pressure natriuresis recovered in early T1DM following treatment with insulin. The experiments in this chapter provided further mechanistic insight into this recovery. Restoration of

natriuresis in the T1DM+insulin cohort was accompanied by an increase in fractional sodium excretion even though medullary perfusion remained suppressed. The data show that replacement insulin therapy elicits a compensatory natriuresis without completely restoring the renal vasculotubular interactions of acute pressure natriuresis. It is concluded that medullary perfusion and tubular sodium transport are tightly linked to blood glucose and insulin levels but that tubular sodium transport is more sensitive to the effects of glycaemic control with insulin.

6.4.5 The role of insulin in sodium transport may vary with the form of diabetes mellitus.

What is not clear is whether the compensatory natriuresis from insulin therapy is a consequence of a direct inhibitory effect of insulin on tubular sodium reabsorption or because lowering blood glucose with insulin reverses increased tubular sodium reabsorption that is driven by hyperglycaemia. The latter would appear more plausible since hyperglycaemia is already known to increase sodium reabsorption through increased activity of the sodium-glucose co-transporter-2 (SGLT2) [318]. Evidence that this was responsible might have come from higher glomerular filtration rates in untreated early T1DM rats compared to their insulin-treated counterparts, as a consequence of reduced TGF and glomerular hyperperfusion [312,318]. However, GFR did not vary with diabetic status. Therefore, a direct effect of insulin on sodium transport should be considered.

If insulin reduces tubular sodium transport directly, then it would contradict the increase in tubular sodium transport by which insulin is thought to contribute to

hypertension in T2DM [267], and which is targeted by SGLT2 inhibitors [268]. Clinical trials in T2DM have shown that by preventing sodium-glucose co-transport in the PCT, SGLT2 inhibitors promote weight loss, reducing insulin resistance and additional sodium reabsorption due to hyperinsulinaemia [319]. In my experiments, however, restoration of natriuresis, but not medullary blood flow, suggests that low levels of insulin sufficient to normalise blood glucose also directly inhibit tubular sodium transport. This is in agreement with studies in renal insulin receptor KO mice in which sodium excretion is reduced and BP is increased [146]. Thus, the contrasting pro-natriuretic role of low levels of insulin and anti-natriuretic role of insulin in hyperinsulinaemia may represent fundamental differences between the pathogeneses of hypertension in T1DM and T2DM.

One potential mechanism for insulin-induced natriuresis is insulin-induced release of NO [146,269]. T1DM is known to interfere with NO signalling but, multiple *in vitro* and *in vivo* studies have generated contradictory data that suggest NO bioavailability within the kidney is both enhanced and suppressed [137]. All three isoforms of NOS are expressed within the kidney, and T1DM has been shown to increase the activity of them all [320,321]. However, this does not always equate to increased NOS expression. Instead, T1DM can increase NOS activity through post-translational modifications [322]. The resulting increase in production of vasodilatory NO has been implicated in the afferent arteriodilation and glomerular hyperfiltration thought to initiate diabetic nephropathy [310]. In the medulla, the situation is less clear. NOS1 and NOS3 activity are increased [322] but T1DM also increases production of reactive oxygen species (ROS) and advanced glycosylation products that quench NO and

counteract increased NO production [137]. NO in the medulla plays an important role in recruiting *vasa recta* to increase medullary perfusion and initiate acute pressure natriuresis [306,323]. However, in this chapter, medullary perfusion was not restored with insulin, suggesting that any effect on NO signalling was more likely to occur in the renal tubules. Insulin is known to increase NO production in renal collecting duct cells [269], which is the same site for ET_B-receptor mediated NO release and inhibition of ENaC [260]. Therefore, an interaction between insulin and ET_B receptor-mediated release of NO was investigated during the same series of experiments by challenging the restoration of natriuresis in T1DM+insulin rats with an ET_B receptor antagonist.

Regardless of whether lowering blood glucose or increasing insulin can induce natriuresis, how this allows BP to bridge the suppression of medullary perfusion and couple it to tubular sodium reabsorption is not apparent. Furthermore, whether this can be sustained in the long term to maintain adequate sodium excretion to offset varying increments in BP is also not known. It is, perhaps, not surprising that with the large number of regulatory mechanisms for sodium excretion, that the tubules were able to mount a natriuretic response to extreme increases in mean BP. However, since Chapter 5 showed that early T1DM disrupts regulation of diastolic BP and because suppressed medullary perfusion has also been demonstrated in various models of hypertension, the data in this chapter suggest that restoration of medullary perfusion should be considered the therapeutic goal when attempting to reduce cardiovascular risk in early T1DM, especially if control of blood glucose levels with insulin is not tight. Exploration of a mechanistic link between suppression of

medullary perfusion and impaired acute pressure natriuresis attempted to confirm this, by assessing the potent vascular effects of ET_A and ET_B receptor antagonists during acute pressure natriuresis.

6.4.6 Endothelin receptor antagonism modifies the acute pressure natriuresis response in healthy rats and has clinical significance.

In healthy control rats, selective ET_A (atrasentan) and ET_B (A-192621) receptor antagonists modified acute pressure natriuresis, inducing marked, opposing effects on sodium excretion. ET_A receptor antagonism impaired acute pressure natriuresis and suppressed the pressure-induced increase in renal medullary perfusion. There was a trend towards a lower mean BP in the ET_A receptor antagonist cohort, most likely as a consequence of systemic arteriodilation [77]. Therefore, the possibility that medullary perfusion and natriuresis had been suppressed by a lower mean BP compared to controls was analysed.

There was good evidence that the ET_A receptor antagonist had interfered with the transmission of increased BP to the renal tubules. The curvilinear and linear relationships of mean BP with UV and UNaV, both of which were observed with vehicle, were disrupted by atrasentan, and atrasentan also decreased UNaV at similar mean BPs to the vehicle cohort. Furthermore, for similar proportionate increases in mean BP, the proportionate increase in medullary perfusion was reduced by atrasentan compared to vehicle. It is concluded that suppression of medullary perfusion and natriuresis by the ET_A receptor antagonist was independent of the antagonist's effects on mean BP.

By contrast to ET_A receptor antagonism, ET_B receptor antagonism with A-192621 enhanced pressure natriuresis but this occurred without a corresponding increase in medullary perfusion. This was consistent with direct inhibition of tubular sodium reabsorption. Similar to atrasentan, the effects of A-192621 could not be explained by the agent's systemic vasodilatory properties [77]. Following injection, mean BP was similar to mean BP in vehicle-treated rats, there was a clear leftward shift in the pressure diuresis curve, and values of UNaV at similar mean BPs to the vehicle cohort were greater.

Combined ET receptor antagonism mirrored the effects of ET_A receptor antagonism. The contribution made by ET_B receptor antagonism may have been reduced by the lower mean BP in this cohort, suggesting that the natriuresis observed during selective ET_B receptor antagonism was dependent on intact ET_A receptor signalling or an increase in medullary blood flow. The implication is that improved glycaemic control with insulin, and ET_B receptor antagonism promote natriuresis through separate mechanisms: insulin-induced natriuresis was observed when medullary perfusion was still suppressed, while A-192621-mediated natriuresis was only observed when medullary perfusion was at vehicle levels.

Together, these data from healthy rats support the hypothesis of a pro-natriuretic role for ET_A receptors, by increasing medullary perfusion, and an anti-natriuretic role for ET_B receptors by enhancing tubular sodium reabsorption. This is not consistent with many of the effects ascribed to these receptors. ET_A receptors are generally regarded

as mediating pathological effects such as powerful vasoconstriction [77] which is implicated in vascular dysfunction [258,300], and promotion of inflammation [154,188-195], cell damage and fibrosis [50,196-198]. They have also been shown to promote rather than prevent sodium and water retention by potentiating the activity of vasopressin and the anti-diuretic/anti-natriuretic effects of sympathetic activation on the kidney [324,325]. ET_B receptors, on the other hand, have well-established diuretic and natriuretic roles centred around inhibition of sodium reabsorption through ENaC and water reabsorption through aquaporin-2 (AQP2) in the collecting duct [181,260]. However, these effects were observed *in vitro*, in animal models during resting states with carefully controlled sodium intakes, or in animal models with deletion of ET-1 signalling targeted to discrete regions of the nephron [122]. In two studies where sodium loading was mimicked by alternative strategies to arterial ligation (rapid iv. infusion of physiological saline [262], and intramedullary injection of hyperosmolar saline [302]), and renal ET-1 signalling was manipulated by ET receptor antagonists, ET-1 appeared to take on a different role. In both studies, ET_A receptor antagonism reduced urinary sodium excretion, and ET_B receptor antagonism (either alone or in combination with ET_A receptor antagonism) increased sodium excretion. Neither of these studies attempted to identify a mechanism, and changes in renal blood flow were not measured, but when combined with the data in this chapter, they suggest that these apparently novel roles for ET receptors are not apparent during the resting state and only become active following acute rises in BP or sodium intake.

One study of ligature-induced acute pressure natriuresis contradicts this concept. Vassileva *et al.* [225] administered the same ET_B receptor antagonist, A-192621, to

healthy rats and demonstrated reductions in both medullary perfusion and sodium excretion. However, there are a number of differences between Vassileva *et al.'s* study and the experiments in this chapter. First, Vassileva *et al.* measured only resting medullary blood flow. They did not measure the change in medullary perfusion when mean BP was increased. Second, they measured medullary blood flow only during infusion of Big ET-1, and after rats had been placed on a high salt diet. A high salt diet, which is known to upregulate renal ET_B receptors [326], combined with higher than physiologically normal levels of ET-1, may have elicited an increase in sodium excretion that was not representative of the acute pressure natriuresis response. Third, they exposed rats to much lower mean BPs (80-144mmHg) compared to this chapter (110-156mmHg).

A weak pro-natriuretic role for renal ET_A receptors has also been identified in experiments in which acute salt loading was not modelled. KO mouse models suggest that the ET_A receptors involved are located within the collecting duct [327]. However, suppression of medullary perfusion during ET_A receptor antagonism, as shown in this chapter, and reduced fluid retention in smooth muscle ETA receptor KO mice during ET_A receptor antagonism [327] would both suggest that they lie within the renal vasculature. The exact location of these ET_A receptors is open to speculation. Vascular ET_A receptors on *vasa recta* pericytes promote constriction [183] which would reduce rather than increase medullary blood flow. This would make a location within the cortex rather than the medulla more likely. One potential source of ET_A receptors is in the afferent arteriole where they contribute to glomerular autoregulation. Intravital microscopy of cortical and medullary afferent and efferent

arterioles during infusion with ET-1 and the selective ET_A receptor antagonist, BQ123, suggest a greater vasoconstrictive response in the afferent arterioles of cortical glomeruli [139] that could promote diversion of flow through juxtamedullary glomeruli and into medullary *vasa recta*. Furthermore, ET_A receptors in juxtamedullary afferent arterioles appear to interact with ET_B receptors to promote arteriodilation [328] which could also promote medullary perfusion.

If vascular ET_A receptors are considered as coupling medullary perfusion to BP, and the conflicting data sets for ET_B receptor antagonism from this chapter and Vassileva *et al.'s* study are considered, a dynamic role for ET-1 emerges in which novel effects on sodium excretion only become active once a threshold of mean BP is exceeded.

Regardless of the mechanistic basis, a role for ET_A receptors in promoting medullary perfusion and acute pressure natriuresis has clinical significance as it would explain the sodium and water retention observed clinically with even highly selective ET_A receptor antagonists [218,219,223,329]. Reductions in proteinuria in diabetic nephropathy [218,219,329] and non-diabetic CKD [330], and improved nocturnal dipping in non-diabetic CKD [226] have been demonstrated clinically. The results in this chapter suggest that this may be a consequence of the anti-inflammatory and anti-fibrotic effects of ET_A receptor antagonists [150] rather than their effects on renal salt handling.

6.4.7 The effects of ET receptor antagonists on acute pressure natriuresis are consistent with their effects on blood pressure.

A pro-natriuretic role for ET_A receptors and an anti-natriuretic for ET_B receptors were proposed following continuous measurement of BP during ET receptor challenge in rats with early T1DM (Chapter 5).

Circadian regulation of BP can be used as a marker of acute pressure natriuresis, and circadian regulation of diastolic BP was suppressed with atrasentan and restored with A-192621. However, these effects on diastolic BP were recorded only in the diabetic rat cohort, and in this chapter, despite marked effects in healthy control rats, neither ET receptor antagonist modified the effects of early T1DM or insulin on the vascular or tubular phases of acute pressure natriuresis. So, although the roles of ET receptors were correctly predicted, there is a clear disconnect between their effects in early T1DM during small rises in BP following oral salt and water ingestion, and acute, severe rises in BP under general anaesthesia. However, there was a striking similarity in the pattern of results for UV, UNaV and FENa across all cohorts during ET receptor antagonism: suppression with ET_A receptor antagonism, enhancement with ET_B receptor antagonism, and combined ET receptor antagonism matching ET_A receptor antagonism. The spread of data in the early T1DM and T1DM+insulin cohorts was wide, and so these trends did not achieve statistical significance, but the pattern of the data raises the possibility that the study was underpowered for demonstrating effects of ET receptor antagonism in these cohorts.

Although the study was powered for the proportionate suppression of diuresis and natriuresis that was demonstrated, the absolute values of UV and UNaV following arterial ligation were far less than in the experiments in Chapter 4. This, and the uncoupling of the relationship between FENa and rising BP (Chapter 4), suggest that the additional adaptations made to the protocol disrupted the acute pressure natriuresis response. One could speculate that the surgical preparation time (20% longer than in Chapter 4) and manipulation of abdominal organs required to place three probes and a ureteral cannula may have contributed to reduced urinary sodium and water excretion because, subjectively, they increased fluid loss into the abdomen (Chapter 3). It is concluded that the protocol used in this chapter was operating at its experimental limits, which could have reduced the effect size of ET receptor antagonists on medullary perfusion and sodium excretion in early T1DM and T1DM+insulin, and introduced Type 2 errors.

The risk of Type 2 errors could have been reduced by supplementing the study with additional rats, following unblinding. However, by this stage the study had already used >100 rats over a period of one year, and prolonging the study posed practical difficulties relating to time, resources and finance. Alternatively, the study could be repeated without measuring renal blood flow and ureteral cannulation. Similar cohort sizes should provide adequate power for demonstrating additional diuretic and natriuretic effects of ET receptor antagonists in both diabetic cohorts but would not provide any insight into the physiological mechanisms responsible.

6.4.8 The response to endothelin receptor antagonists is not reflected in the expression of genes that code for endothelin-1 and its receptors.

These data suggest that both early T1DM and ET_A receptor antagonism suppress acute pressure natriuresis by suppressing medullary perfusion. Additional experiments (Chapter 7) would be required to confirm the mechanistic link between suppression of medullary perfusion and suppression of acute pressure natriuresis, but the possibility that early T1DM suppresses medullary perfusion by interfering with ET_A receptor signalling was partially explored by qPCR. A link between increased sodium excretion via insulin and impaired ET_B receptor signalling was also investigated at the transcriptional level. However, no association between diabetic status and levels of EDN1, EDRA and EDRB mRNA in the renal cortex and medulla could be demonstrated.

These results were perhaps surprising because upregulation of genes that code for ET-1, and ET_A and ET_B receptors have been demonstrated previously in T1DM [255,258,259,300]. There are a number of possible explanations for these results. It could be that the rat model used in this thesis is at too early a stage of T1DM to demonstrate increased expression of genes coding for the ET system. Studies of expression in blood vessels, for example, have been performed after 10-14 weeks of T1DM [255,258,259,300] compared to two-to-three weeks in these experiments. Chapter 4 failed to demonstrate an increase in expression of markers of renal pathology, including 24-hourly urinary ET-1 excretion [261], and it may be that increased expression of ET signalling components is only measurable after the onset of structural renal changes. This would not be incompatible with early T1DM and

insulin exerting functional effects by modifying EDN1 expression because ET-1 mRNA has a short half-life of ~15 minutes [77] and ET-1 is usually secreted as soon as translation is complete [77]. Tissue was not collected during acute pressure natriuresis and, therefore, it is possible that early T1DM and insulin influence rapid transcription of EDN1 in response to acute changes in BP and that this would not be detected by qPCR performed on tissue collected when BP is stable. As an alternative explanation, any interference from early T1DM and insulin on ET-1 signalling could be downstream of EDN1 and EDRA and EDRB expression. This is known to occur in other key regulatory mechanisms in T1DM, such as post-translational modification of NOS enhancing NO signalling with no change in NOS expression [322]. As a final possibility, sections of cortex that were collected will have included both cortical and juxtamedullary glomeruli. Therefore, while there may have been changes in the relative expression of elements of ET signalling within these glomerular types, sufficient to increase blood flow through the medulla, the overall expression in the cortex may have been unchanged.

Combined with the failure of the ET_B receptor antagonist to prevent insulin-induced natriuresis, these qPCR data provide additional evidence that recovery of natriuresis by insulin does not involve ET_B receptor-mediated inhibition of ENaC by NO. Therefore, future experiments attempting to identify the causative mechanism should focus on sodium transport more proximally within the nephron.

6.5 Conclusions

These data show that suppression of acute pressure natriuresis by early T1DM may be a consequence of suppression of medullary perfusion. This does not recover completely with insulin, which restores natriuresis through direct inhibition of tubular sodium reabsorption. Renal ET-1 regulates acute pressure natriuresis and both receptor subtypes play key roles. ET_A receptor signalling increases renal medullary perfusion and natriuresis. ET_B receptor signalling increases sodium reabsorption and inhibits natriuresis.

Semi-quantitative PCR failed to demonstrate that the effects of early T1DM and insulin on acute pressure natriuresis result from changes in cortical or medullary expression of genes that encode ET-1 and its receptors. ET receptor antagonists also failed to modify the effects of early T1DM and insulin on acute pressure natriuresis but the study may have been underpowered for demonstrating a drug effect downstream of receptor expression.

ET_A receptors are pro-natriuretic and ET_B receptors can be anti-natriuretic, which is contrary to their putative roles. These roles may only become active at higher BPs, and may explain sodium and water retention with highly selective ET_A receptor antagonists.

Although the mechanistic basis to these results has not been determined, the data support developing therapies that increase renal medullary perfusion in early T1DM to confer additional reductions in cardiovascular risk to those obtained with insulin

alone. This is unlikely to be achieved by highly selective ET_A receptor antagonism. This is because ET_A receptor antagonists impair rather than promote medullary perfusion and acute pressure natriuresis, and off-target ET_B receptor effects can enhance as well as impair natriuresis.

7 Final conclusions and future directions

7.1 Introduction

The experiments described in this thesis have investigated the contribution that impaired renal handling of salt makes to the regulation of blood pressure (BP) in early Type 1 diabetes mellitus (T1DM), the implications for cardiovascular risk, and the potential for reducing this risk by pharmacologically targeting the role played by renal ET-1.

T1DM is one of the most common endocrine disorders in children [7], and increases their risk of cardiovascular disease (CVD) in later life [16-18]. Tight control of blood glucose with insulin, within a crucial early window after diagnosis, reduces but does not eliminate cardiovascular risk [24,29], and also increases the risk of life-threatening hypoglycaemia [34], especially in young patients. There is, therefore, a great unmet need to target and treat risk factors for CVD in early T1DM, in order to complement the clinical benefits from lowering blood glucose with insulin.

Major cardiovascular risk factors in T1DM are hypertension and nephropathy [247-249]. They are tightly linked, since elevated BP, in the presence of hyperglycaemia, is key to the development of diabetic nephropathy [72]. Acute pressure natriuresis within the kidney regulates BP [79-81,89]: rapid rises in BP increase renal medullary blood flow, inhibit tubular sodium reabsorption and increase urinary sodium excretion, normalising BP. This would suggest that hypertension, nephropathy and increased cardiovascular risk in T1DM must be preceded by disruption to acute pressure natriuresis [89]. This thesis used a rodent model to investigate key functional changes

in acute pressure natriuresis in early T1DM, and the role played by the endothelin (ET) system.

The ET system is of interest because it is highly expressed within the kidney [77] and it is already known to play a key role in the development of diabetic nephropathy. The principal ligand is ET-1, and T1DM increases its transcription and release [205]. In the glomerulus, ET-1 binds to its receptor subtype, ET_A, to promote inflammation, mesangial expansion, fibrosis and proteinuria [50,154,188-198,331], all hallmarks of diabetic nephropathy. ET-1 has potent vasoactive effects, and T1DM shifts its vascular influence towards vasoconstriction via enhanced smooth muscle ET_A and ET_B receptor signalling, and reduced vasodilation via impaired endothelial ET_B receptor signalling [258,259,300]. However, ET-1 also has potent pro-natriuretic properties via ET_B receptors that inhibit the epithelial sodium channel (ENaC) in the renal collecting duct [180,181,260]. Since acute pressure natriuresis consists of both vascular and tubular phases, increased renal ET-1 activity in T1DM has the potential to modify acute pressure natriuresis, BP and hence cardiovascular risk profoundly.

Selective ET_A receptor antagonists are already at an advanced stage of clinical development, and have been shown to reduce BP and proteinuria in established diabetic nephropathy [218,219,329]. Therefore, experiments were conducted not only to determine the degree to which early T1DM impairs acute pressure natriuresis and regulation of BP, but also the contribution that ET-1 makes to acute pressure natriuresis and BP, and whether this is modified by early T1DM. Inflammatory and fibrotic effects, which are mediated by ET-1, were removed by using rats at a very

early stage of T1DM, before the development of nephropathy. This also modelled the early window of opportunity within which insulin reduces cardiovascular risk and addressed the question of whether selective ET_A receptor antagonists might have a clinical application in reducing cardiovascular risk in T1DM prior to the onset of nephropathy.

7.1.1 Acute pressure natriuresis in Type 1 diabetes mellitus.

In the first series of experiments (Chapter 4), I induced acute pressure natriuresis in a streptozotocin (STZ) rat model of early T1DM. I modified the protocol of Roman and Cowley [112] (Chapter 3), in which stepwise increases in mean BP were obtained by serial ligation of major abdominal arteries and the distal aorta.

The suppression of acute pressure natriuresis in early T1DM rats was striking. Maximum urine flow and sodium excretion rates (UV and UNaV) failed to reach 25% of control levels, despite maintaining glomerular filtration rate (GFR). Fractional excretion of sodium (FENa) matched the suppression of UNaV, indicating that impairment of natriuresis by early T1DM was a consequence of inappropriate tubular sodium reabsorption. Biochemical and molecular analysis of renal tissue and urine confirmed that these were functional effects that preceded activation of the renin-angiotensin-aldosterone system (RAAS) and the development of structural nephropathy.

When rats with early T1DM were treated with insulin to normalise blood glucose (T1DM+insulin), UV, UNaV and FENa were restored. Urinary ET-1 excretion rate

(UET-1V), a marker of renal ET-1 activity [209], was tightly correlated with UV and UNaV, regardless of diabetic status. The causative nature of these relationships was not determined, but a role for ET-1 in regulating the suppression of acute pressure natriuresis in early T1DM, and its recovery with insulin, was implicated.

Together, the experiments in Chapter 4 demonstrated that T1DM disrupts a key regulatory mechanism for BP, very early on in the course of the disease, prior to the development of nephropathy. Furthermore, this functional effect can be reversed with insulin without disrupting the tight relationships between urinary sodium and water excretion and renal ET-1 activity.

7.1.2 Blood pressure and its circadian variation in Type 1 diabetes mellitus

In order to justify further investigation into the mechanistic basis to these results, I first explored the implications for cardiovascular risk of a link between impaired acute pressure natriuresis in early T1DM and ET-1 signalling. BP was measured by radiotelemetry and used as a surrogate marker for cardiovascular risk because hypertension is a consequence of impaired acute pressure natriuresis, and is associated with increased cardiovascular risk in T1DM [247,248].

Early T1DM increased diastolic BP by ~5mmHg and circadian regulation of diastolic BP was also disrupted. Normally, circadian variation in BP mirrors circadian variation in sodium excretion: BP and sodium excretion are usually higher during the day and dip at night. BP at night increases when daytime acute pressure natriuresis is inadequate [100], and in people, this predicts nephropathy in T1DM and

cardiovascular risk [102-104]. In the diabetic rats, diurnal dipping in diastolic BP was 4% less than in controls over a 24-hour cycle. Increased diastolic BP has a higher correlation than increased systolic BP with the risk of developing nephropathy [290,291]. Therefore, combined, the data generated from acute pressure natriuresis and radiotelemetry studies provided strong evidence for a contemporaneous relationship between impaired acute pressure natriuresis in early T1DM and increased risk of nephropathy and CVD.

In order to determine whether manipulation of the tight relationship between sodium and urinary ET-1 excretion translated into quantifiable effects on BP, I also measured BP in the same rats during supplementation with salt, an ET_A receptor antagonist and then combined ET_A and ET_B receptor antagonism. ET_A receptors mediate powerful vasoconstriction [77,163] and so the reduction in systolic and diastolic BP recorded in control and early T1DM cohorts during ET_A receptor antagonism was expected. However, the effect size was smaller in the diabetic rats, despite a degree of salt sensitivity in the control rats. Increased circadian variation in BP was also expected during ET_A receptor antagonism because antagonising vasoconstriction should increase renal medullary blood flow and activate acute pressure natriuresis. Instead, surprisingly, circadian variation in diastolic BP was reduced in the rats with early T1DM. Together the results suggested that ET_A receptor antagonism impairs rather than enhances acute pressure natriuresis.

The addition of the ET_B receptor antagonist also led to unexpected results. ET_B receptors mediate vasodilation [77] and inhibit ENaC [181] which should promote both

the vascular and tubular components of acute pressure natriuresis. Antagonising these effects was expected to increase BP and decrease circadian variation in BP. Instead, diastolic BP in the early T1DM rats did not rise, and circadian variation in diastolic BP was restored, suggesting that ET_B receptors impair rather than promote acute pressure natriuresis in early T1DM.

Overall, the effects of the ET receptor antagonists on diastolic BP were suggestive of novel pro-natriuretic (ET_A) and anti-natriuretic (ET_B) roles for ET receptors. It was clear that further *in vivo* investigation into the mechanism of impairment and recovery of acute pressure natriuresis by early T1DM and insulin, should include manipulation with ET_A and ET_B receptor antagonists.

7.1.3 Renal blood flow in Type 1 diabetes mellitus

In acute pressure natriuresis, acute rises in BP shift renal perfusion to the medulla, which increases interstitial hydrostatic pressure, and inhibits tubular sodium reabsorption [89,138,296]. Suppression and recovery of acute pressure natriuresis could either result from changes to medullary blood flow or changes to tubular sodium reabsorption. Therefore, the effects of early T1DM, insulin and ET receptor antagonists on the vascular and tubular components of acute pressure natriuresis were determined (Chapter 6). This work shows that sodium excretion is dependent on a series of complex interactions in the kidney between BP, medullary blood flow, blood and urinary glucose, and insulin.

Early T1DM prevented a rise in renal medullary perfusion when BP was increased, suggesting that uncoupling of medullary blood flow from BP was the physiological mechanism driving impaired acute pressure natriuresis in early T1DM. However, in a T1DM+insulin cohort, natriuresis was restored without restoring the rise in medullary blood flow. One explanation would be that medullary blood flow in treated or untreated early T1DM is not as crucial to coupling BP to inhibition of sodium reabsorption as normalising blood glucose and insulin levels. However, this would be inconsistent with many rodent models of hypertension in which suppression of medullary perfusion is a consistent feature. An alternative explanation would be that lowering blood glucose with insulin elicits a compensatory natriuresis by a different mechanism that is independent of medullary blood flow. Such a mechanism could be activated by lowering blood glucose or by insulin directly. For the latter to apply, insulin would have to have a bidirectional relationship with tubular sodium reabsorption that varies according to insulin levels, because in T2DM, high levels of insulin promote rather than inhibit retention of sodium. This would represent a fundamental difference in the aetiology of hypertension in T1DM and T2DM.

Whether a compensatory natriuresis, as observed in the T1DM+insulin cohort, is adequate to tightly regulate BP over a range of values and over prolonged periods is beyond the scope of my thesis. However, I believe that the data in Chapters 5 and 6 suggest that a therapeutic goal for reducing cardiovascular risk could be to ensure adequate coupling of BP to sodium excretion by restoring regulation of medullary blood flow. This is an attractive prospect because it might confer additional

reductions in cardiovascular risk to patients whose blood glucose is tightly controlled with insulin, as well as those patients with poor blood glucose control. Furthermore, there is the potential for it to be applicable to T2DM as well as T1DM patients, despite the differing aetiologies of those diseases. This is because it would be independent of the effects of insulin on tubular sodium reabsorption, although medullary perfusion during acute pressure natriuresis in rodent models of T2DM has not been measured.

7.1.4 Renal blood flow during endothelin receptor antagonism

In Chapter 5, radiotelemetry data had suggested, surprisingly, that ET_A receptor antagonism suppresses acute pressure natriuresis. I confirmed this in Chapter 6, in which ET_A receptor antagonism also suppressed medullary perfusion in healthy rats. I conclude from these results that ET_A receptors play a significant role in promoting acute pressure natriuresis in the healthy state, by coupling BP to medullary perfusion. This pro-natriuretic effect has not been described previously but it provides an explanation for the tight relationship between UET-1 excretion and both UV and UNaV identified in Chapter 4. UET-1 is an overspill of renal ET-1 [209], so an increase in ET-1/ET_A signalling, might increase UV, UNaV and UET-1 simultaneously.

Studies have suggested that ET_A receptor antagonists inhibit natriuresis by off-target inhibition of collecting duct ET_B receptors [181,227], or by inhibiting the small number of collecting duct ET_A receptors that enhance collecting duct ET_B receptor-mediated natriuresis [332]. Instead, it would appear that renal vascular ET_A receptors are

responsible. ET_A receptors exert potent long-lasting vasoconstriction [77,163] so the key ET_A receptors would have to be upstream of the medullary *vasa recta*. Potential sites are the afferent and efferent arterioles of the cortical nephrons or their supplying arteries, since vasoconstriction here would divert blood flow to the juxtamedullary arterioles that supply the medulla.

I believe that these results are highly relevant to the single biggest physiological obstacle to the licensing of ET_A receptor antagonists for hypertension and renal disease: sodium and water retention [227]. The conclusion is that there will always be a risk of this adverse effect even when a highly selective ET_A antagonist is used, unless medullary perfusion can be protected by an alternative agent.

In contrast to the selective ET_A receptor antagonist, radiotelemetry data in Chapter 5 had suggested that ET_B receptor antagonism enhances acute pressure natriuresis. I also confirmed this in Chapter 6, when an ET_B receptor antagonist enhanced acute pressure natriuresis in healthy rats without modifying the normal rise in medullary blood flow. This evidence for an anti-natriuretic role for ET_B receptors is perhaps more surprising than a pro-natriuretic role for ET_A receptors. Pre-clinical data, including from knockout (KO) mouse models [180,181], demonstrate that ET_B receptors in the collecting duct, where they are most highly expressed [333], inhibit ENaC, and the effect increases when dietary salt content is increased [260,270]. Furthermore, off-target blockade of collecting duct ET_B receptors has long been implicated as underpinning sodium and water retention with ET_A receptor antagonists [223,227].

However, two previous studies, both mimicking acute salt loading, have also supported an anti-natriuretic role for renal ET_B receptors [262,302]. The data from Chapter 6 provide additional insight into a novel role for ET_B receptors when BP or sodium intake is increased acutely: the mechanism does not appear to involve vascular ET_B receptor signalling, but it is possibly dependent on increased medullary perfusion. Increased medullary perfusion exerts its greatest influence on tubular sodium reabsorption [89] in the proximal convoluted tubule (PCT), so anti-natriuretic ET_B receptors might be located here. This is supported by a range of *in vitro* studies that have demonstrated ET_B receptor-mediated increased sodium transport through the sodium-glucose transporter-2 (SGLT2) [334], the sodium-hydrogen anti-porter-3 (NHE3) [335] and the sodium-potassium adenosine triphosphatase (ATPase) pump [336], all located within the PCT.

The effects of ET-1 and its receptors in regulating sodium excretion would now appear to be more dependent on BP and medullary perfusion than previously recognised. My data suggest that elevations in BP above a certain threshold initiate a sequence of events that excrete sodium according to a balance of pro-natriuretic ET_A and anti-natriuretic ET_B receptor-mediated effects that are inactive during the steady state.

Even greater effects of ET receptor antagonists on acute pressure natriuresis were expected with early T1DM or T1DM+insulin. This was because it was in early T1DM that the ET receptor antagonists had exerted effects on circadian rhythm in

diastolic BP (Chapter 5) that had correctly predicted effects on acute pressure natriuresis in healthy controls in Chapter 6.

Surprisingly, in these cohorts, my experiments failed to demonstrate an influence of ET receptor antagonism on either renal medullary blood flow or tubular sodium reabsorption. However, there were trends in UV, UNaV and FENa that were strikingly similar to the effects of ET receptor antagonists in healthy controls, and the study may have been underpowered to demonstrate an effect in addition to the ones that early T1DM and insulin had caused. An alternative explanation is that early T1DM exerts its effects by inhibiting ET_A receptor signalling, and insulin inhibits ET_B receptor signalling. However, the transcriptomics work I undertook in Chapter 6 failed to identify a difference in the relative expressions of genes encoding cortical or medullary ET-1, ET_A receptors and ET_B receptors. I conclude that if early T1DM and insulin modify ET-1 signalling at this very early stage of the disease, it is downstream of ET receptor expression.

7.1.5 The role of endothelin-1 in the renal handling of salt in early Type 1 diabetes mellitus

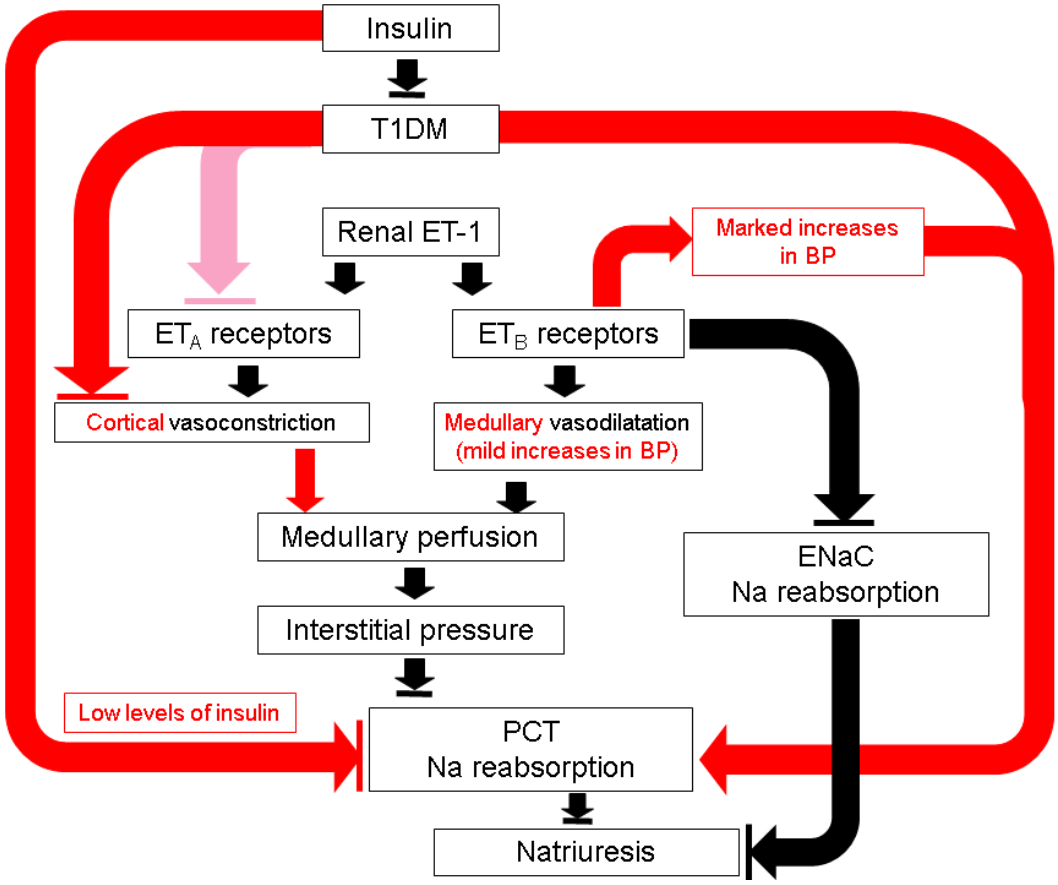

Fig. 7.1 Algorithm of proposed mechanisms by which early Type 1 diabetes mellitus (T1DM) and insulin modify regulation of acute pressure natriuresis by endothelin-1 (ET-1).

Red arrows and text are modifications of the pathways proposed in Fig. 4.10 (page 147). The pink arrow is a potential pathway with less supporting evidence. Lines blocking arrows represent inhibition. PCT=proximal convoluted tubule, ENaC=epithelial sodium channel, BP=blood pressure

Overall, from the work in this thesis, a more dynamic role for ET-1 in the long term regulation of BP emerges (Fig. 7.1).

It is already accepted that ET-1 plays a key role in regulating sodium excretion and BP. It is released from the renal collecting duct in response to increased flow of filtrate [271] and sodium delivery [270], and it binds in an autocrine or paracrine manner to inhibit sodium and water reabsorption [77]. The implication is that a gradient of less and less sodium reabsorption is established along the length of the collecting duct. Having flow and sodium delivery as the main stimuli to its release, limits the ability of collecting duct ET-1 to match increased BP with an appropriate diuresis and natriuresis because it suggests that there is a preceding step more proximally within the nephron that has already established increased flow and sodium delivery to the collecting duct. This is consistent with the known physiology of acute pressure natriuresis in which the PCT is the part of the nephron most sensitive to increases in BP and medullary blood flow [89]. Therefore, the role of collecting duct ET-1 would appear to be to offset small fluctuations in BP by providing additional diuresis and natriuresis as required. The consequence would be that where BP-to-medullary perfusion coupling is lost, collecting duct ET-1 can mediate a diuresis and natriuresis which may not fully match an increase in BP.

However, my thesis also suggests that renal ET-1 has an additional role in the regulation of sodium excretion and it is to couple large increases in BP to medullary perfusion. This is mediated by ET_A receptors, and because ET_A receptors promote vasoconstriction, I would speculate that they lie within the cortex, upstream of the

medullary *vasa recta*. Published data [225] have shown that ET_B receptors may be important in promoting medullary perfusion at lower BPs, but in this thesis ET_B receptors also appear to promote sodium reabsorption and inhibit natriuresis at higher BPs, countering some of the natriuretic effects of collecting duct ET_B receptors downstream. An anti-natriuretic effect from renal ET_B receptors has been suggested previously [262,302] but the mechanism has never been explored. My work suggests that ET_B receptors located in the tubules are responsible. An increase in sodium reabsorption when BP is increased appears counter-intuitive to the concept of acute pressure natriuresis. However, a gradient of decreasing sodium reabsorption that is mediated by collecting duct ET-1 and is activated by increased flow and sodium delivery, as occurs during acute pressure natriuresis, runs the risk of leading to a runaway natriuretic effect. An increase in sodium reabsorption more proximally when BP is markedly elevated would serve to "brake" an excessive natriuretic response. My data also suggest that ET_B receptor-mediated sodium reabsorption is dependent on large increases in medullary perfusion resulting from large increases in BP. This might explain the discrepancy between the marked effects of ET receptor antagonism on acute pressure natriuresis in healthy controls rats when BP was acutely and severely increased experimentally (Chapter 6), and the lack of effect on BP and circadian regulation of BP that I recorded in healthy control rats (Chapter 5) during the small daily fluctuations in BP associated with salt and water ingestion.

In early T1DM, the situation is less clear. The acute pressure natriuresis studies in Chapter 6 suggest that the role played by ET_A receptors in coupling of BP to medullary perfusion is lost, either because early T1DM blocks signalling

downstream of ET_A receptor expression or because an alternative mechanism overwhelms the response. The role of ET_B receptors in balancing sodium reabsorption and sodium excretion is also limited. My study may have been underpowered for demonstrating a residual anti-natriuretic effect, but there was no evidence during ET_B receptor antagonism or from semi-quantitative polymerase chain reaction (PCR) of renal cortex and medulla to suggest that the relative contributions of pro- and anti-natriuretic ET_B receptors to sodium excretion were modified. Despite these results, ET_A receptor antagonism reduced circadian variation in diastolic BP, and ET_B receptor antagonism had the opposite effect, leading me to conclude that there is a role for ET-1 in mediating acute pressure natriuresis in early T1DM when fluctuations in BP are less marked than those induced experimentally.

ET-1 may mediate inflammation and fibrosis in diabetic nephropathy, but, prior to nephropathy, it has an important role in regulating acute pressure natriuresis and BP. The recent premature termination of SONAR [162] means that Phase 3 clinical trial data that demonstrate the clinical benefits of ET_A receptor antagonism in T2DM, once nephropathy has developed, remain elusive. Frustratingly, this is not as a consequence of sodium and water retention but rather of study design. Unfortunately, the pre-clinical data I have generated show that it is precisely because of promoting sodium and water retention that ET_A receptor antagonism in T1DM, prior to nephropathy, could limit reductions in cardiovascular risk obtained by tightly controlling blood glucose with insulin. Therefore, my thesis does not support selective ET_A receptor antagonism in early T1DM. However, it does support a

therapeutic strategy of increasing renal medullary blood flow to reduce cardiovascular risk in early T1DM, as well as tight control of blood glucose with insulin. Further investigation of the mechanisms responsible for coupling BP to renal medullary flow, and tubular sodium reabsorption, the novel roles played by ET_A and ET_B receptors and the influences of early T1DM is indicated and outlined below.

7.2 Limitations and additional experiments

The experiments described in my thesis have clarified aspects of early T1DM that promote sodium and water retention, and their association with increased cardiovascular risk. I have shown that lowering blood glucose with insulin does not reverse key events in the kidney that match sodium excretion to BP. I have also identified novel roles for renal ET-1 in the regulation of BP and sodium excretion that may explain an important adverse effect observed clinically from ET_A receptor antagonists.

However, the relationship between BP and tubular sodium reabsorption when medullary perfusion is suppressed requires additional clarification and although physiological mechanisms have been identified, mechanisms at a molecular level have not. Several key questions remain unanswered and should be addressed by future research.

7.2.1 Does restoration of renal medullary perfusion restore acute pressure natriuresis in rats with Type 1 diabetes mellitus?

It should be confirmed that suppression of renal medullary perfusion is the cause of impaired acute pressure natriuresis in early T1DM. It could be achieved by cannulating the renal artery in rats with early T1DM undergoing ligature-induced pressure natriuresis. Injection of vasoactive agents, such as phenylephrine and acetylcholine, directly into the renal artery has been shown to modify medullary perfusion, without exerting systemic effects [303,306]. Pre-implanted polyethylene matrices, connected to pressure transducers, would confirm that increases in medullary blood flow were linked to corresponding increases in renal interstitial hydrostatic pressure [337].

7.2.2 What is the mechanism by which Type 1 diabetes mellitus suppresses renal medullary blood flow as blood pressure rises?

Answering this question will require a systematic assessment of the regulation of medullary blood flow at pre-glomerular, glomerular and post glomerular (pericyte) levels, using a combination of *in vitro* and *in vivo* approaches.

In vitro, wire and pressure myographic studies have been applied to resistance vessels from diabetic animal models [338], but less frequently to small resistance vessels from the kidney. These techniques are limited by vessel size but are feasible in arcuate arteries and interlobular arteries from rats [339]. Interlobular arteries are immediately upstream of afferent arterioles, so can be studied to measure pre-glomerular regulation of renal blood flow. Stereomicroscopy would allow

discrimination and dissection of cortical from juxtaglomerular interlobular nephrons [340], so that regional differences in pre-glomerular vascular resistance that determine medullary blood flow could be quantified.

More distally, the role that the pericytes that surround *vasa recta* play in regulating medullary perfusion has recently been uncovered by live kidney-slice microscopy. Although this technique has been applied more to juxtamedullary nephrons, with their longer *vasa recta* and greater numbers of pericytes [182], functional comparisons with pericytes of cortical nephrons, and whether differences are modified by early T1DM could be made *in situ* [182,341]. Pericyte constriction of *vasa recta* is modified by renal tubules through tubulovascular crosstalk, and offers a post glomerular level of regulation of medullary perfusion [184]. The influence of early T1DM could be explored through light microscopy of micro-dissected and perfused *vasa recta* bundles with and without their attached thick ascending limb of the loop of Henle [184].

In vivo, micropuncture techniques would measure changes in capillary pressures downstream of the interlobular arteries or upstream of the *vasa recta* pericytes [340], but would be limited to the study of cortical nephrons. Using stereomicroscopy, changes in afferent and efferent arteriolar and peritubular capillary hydrostatic pressures can be measured before and after arterial ligation [340], and this technique could be readily applied to the rat model of early T1DM since the surgical preparation required is very similar to that used for laser Doppler spectroscopy (LDS; Chapter 6).

Direct imaging of renal perfusion pre- and post arterial ligation is an attractive technique for identifying shifts in renal blood flow because it allows real-time visualisation of regional changes in perfusion and the immediate response to pharmacological manipulation, in a setting that could be applied to patients clinically. Indeed, magnetic resonance imaging (MRI) perfusion studies using arterial spin-labelling, and positron emission tomography computed tomography (PET CT) using $H_2{}^{15}O$ as a tracer have already mapped changes in cortical and medullary flow in people [342,343]. However, to image differences in the perfusion of cortical and juxtamedullary nephrons, and the effect of early T1DM in rats would require a resolution capable of differentiating inner and outer layers of the cortex as well as the cortex and medulla. This would be at the extreme limits of current technology. As an adjunct to this technique, additional information could be obtained using blood oxygen level-dependent (BOLD) MRI which uses the paramagnetic properties of deoxyhaemoglobin to map changes in the renal corticomedullary oxygen gradient [344]. This could be used as a surrogate marker of changes in the relative resistances of the vasculature of cortical and juxtamedullary nephrons.

7.2.3 Does insulin or normalising blood glucose decrease tubular sodium reabsorption?

This question is important because it addresses a key difference in the role of insulin in sodium balance and the development of hypertension in T1 and T2DM. It could be answered by performing ligature-induced acute pressure natriuresis in insulin-treated rats with early T1DM in which blood glucose is clamped to a range of blood glucose values by a controlled glucose-saline intravenous (iv.) infusion.

Semi-quantitative PCR analysis of the tissue samples collected in Chapter 4 would measure the effects of early T1DM and insulin on expression of key renal sodium transporters along the length of the nephron (SGLT2, NHE3, sodium-potassium ATPase pump, sodium-potassium-chloride co-transporter-2 (NKCC2), sodium-chloride co-transporter (NCC) and ENaC). Western blotting of the same tissue would identify post-translational modification including transporter phosphorylation, which is a marker of transporter activity. This work is currently being conducted by colleagues as part of a post-doctoral programme of research.

7.2.4 Which pool of endothelin A receptors increase renal medullary blood flow as blood pressure rises?

This question addresses the mechanism behind the pro-natriuretic role of ET_A receptors and the sodium and water retention observed clinically with ET_A receptor antagonists [227]. Immunofluorescence has already identified the cortical and medullary distributions of ET receptor subtypes within the kidney, and the presence of ET_A receptors in arcuate and lobular arteries [333]. Therefore, it has the potential to identify whether vascular ET_A receptor density varies between cortical and juxtamedullary nephrons, and whether this is modified by early T1DM. Semi-quantitative PCR and Western blotting from carefully dissected outer and inner cortices would validate these findings, and their functional significance would be reinforced by myography of intact and endothelium-denuded arcuate and interlobular arteries, and their response to ET-1.

7.2.5 Which pool of endothelin B receptors take on an anti-natriuretic role as blood pressure rises?

Answering this question should reveal the mechanism behind the natriuresis observed with ET_B receptor antagonists (Chapter 6) and could identify targets for enhancing natriuresis in early T1DM that are independent of changes to renal perfusion. Investigations should focus on sodium transport in the PCT because this plays the greatest role in the tubular response to acute pressure natriuresis [89]. ET_B receptors have already been identified in the PCT where they promote sodium reabsorption via sodium-potassium ATPase, NHE3 and SGLT2 [334-336].

Building on the results from Western blot analysis suggested earlier, the interaction between ET_B receptors and sodium transporters could be investigated further *in vitro*, using an Ussing chamber to measure electrogenic ion transport [345] through the sodium channels of cultured PCT cells. This experimental set-up is currently available on-site and has the advantage of allowing quantification of changes in sodium reabsorption in response to ET_B receptor agonists and antagonists, and inhibitors of SGLT2. *In vitro* responses could then be tested *in vivo* using the protocol for ligature-induced acute pressure natriuresis. This would have clinical relevance because SGLT2 inhibitors are currently used in clinical T2DM [346], and offer the prospect of blocking ET_B receptor-mediated sodium reabsorption in early T1DM, without the loss of collecting duct ET_B receptor-mediated natriuresis [181].

7.3 Summary of conclusions

- Early T1DM severely impairs acute pressure natriuresis prior to the onset of structural nephropathy. Suppression of renal medullary blood flow is a possible mechanism. These effects are accompanied by changes in BP associated with increased cardiovascular risk.
- Lowering blood glucose with insulin restores natriuresis when BP is increased, but does not restore medullary blood flow. Whether restoration of natriuresis is mediated directly by insulin or by euglycaemia, and whether the natriuresis can adequately compensate for increases in BP remain unclear.
- Renal ET-1 regulates sodium excretion and BP by multiple mechanisms. In health, novel effects of ET_A and ET_B receptors become apparent at higher BPs: ET_A receptors mediate an increase in medullary perfusion while ET_B receptors dampen the natriuretic response.
- In early T1DM, these novel effects of ET receptors are less apparent during acute severe increases in BP. However, they appear to contribute to the circadian regulation of BP.
- Pharmacological targeting of medullary blood flow in early T1DM may confer reductions in cardiovascular risk in addition to those obtained by lowering blood glucose with insulin. This is unlikely to be achieved with selective ET_A receptor antagonists which, prior to nephropathy, may impair acute pressure natriuresis and regulation of BP, and reduce the clinical benefits of tight blood glucose control.

References

1. Atkinson MA, Eisenbarth GS. Type 1 diabetes: new perspectives on disease pathogenesis and treatment. *Lancet.* 2001;358(9277):221-229.
2. Stylianou C, Kelnar C. The introduction of successful treatment of diabetes mellitus with insulin. *J R Soc Med.* 2009;102(7):298-303.
3. Zajac J, Shrestha A, Patel P, Poretsky L. The main events in the history of diabetes mellitus. In: Poretsky L. ed. *Principles of Diabetes Mellitus.* 2nd ed. New York, United States: Springer Verlag; 2010: 3-16.
4. Minkowski O. Historical development of the theory of pancreatic diabetes by Oscar Minkowski, 1929: introduction and translation by Rachmiel Levine. *Diabetes.* 1989;38(1):1-6.
5. Banting FG, Best CH, Collip JB, Campbell WR, Fletcher AA. Pancreatic extracts in the treatment of diabetes mellitus. *Can Med Assoc J.* 1922;12(3):141-146.
6. Banting FG, Campbell WR, Fletcher AA. Further clinical experience with insulin (pancreatic extracts) in the treatment of diabetes mellitus. *Br Med J.* 1923;1(3236):8-12.
7. Atkinson MA, Eisenbarth GS, Michels AW. Type 1 diabetes. *Lancet.* 2014;383(9911):69-82.
8. Collaboration NCDRF. Worldwide trends in diabetes since 1980: a pooled analysis of 751 population-based studies with 4.4 million participants. *Lancet.* 2016;387(10027):1513-1530.

9. Holman N, Young B, Gadsby R. Current prevalence of Type 1 and Type 2 diabetes in adults and children in the UK. *Diabet Med.* 2015;32(9):1119-1120.

10. Patterson CC, Dahlquist GG, Gyurus E, Green A, Soltesz G, Group ES. Incidence trends for childhood type 1 diabetes in Europe during 1989-2003 and predicted new cases 2005-20: a multicentre prospective registration study. *Lancet.* 2009;373(9680):2027-2033.

11. Dahlquist GG, Nystrom L, Patterson CC, Swedish Childhood Diabetes Study G, Diabetes Incidence in Sweden Study G. Incidence of type 1 diabetes in Sweden among individuals aged 0-34 years, 1983-2007: an analysis of time trends. *Diabetes Care.* 2011;34(8):1754-1759.

12. Hex N, Bartlett C, Wright D, Taylor M, Varley D. Estimating the current and future costs of Type 1 and Type 2 diabetes in the UK, including direct health costs and indirect societal and productivity costs. *Diabet Med.* 2012;29(7):855-862.

13. Ziegler AG, Hummel M, Schenker M, Bonifacio E. Autoantibody appearance and risk for development of childhood diabetes in offspring of parents with type 1 diabetes: the 2-year analysis of the German BABYDIAB Study. *Diabetes.* 1999;48(3):460-468.

14. Willcox A, Richardson SJ, Bone AJ, Foulis AK, Morgan NG. Analysis of islet inflammation in human type 1 diabetes. *Clin Exp Immunol.* 2009;155(2):173-181.

15. Livingstone SJ, Levin D, Looker HC, Lindsay RS, Wild SH, Joss N, et al. Estimated life expectancy in a Scottish cohort with type 1 diabetes, 2008-2010. *JAMA.* 2015;313(1):37-44.

16. Soedamah-Muthu SS, Fuller JH, Mulnier HE, Raleigh VS, Lawrenson RA, Colhoun HM. High risk of cardiovascular disease in patients with type 1 diabetes in the U.K.: a cohort study using the general practice research database. *Diabetes Care.* 2006;29(4):798-804.

17. Orchard TJ, Costacou T, Kretowski A, Nesto RW. Type 1 diabetes and coronary artery disease. *Diabetes Care.* 2006;29(11):2528-2538.

18. Deckert T, Poulsen JE, Larsen M. Prognosis of diabetics with diabetes onset before the age of thirty-one. I. Survival, causes of death, and complications. *Diabetologia.* 1978;14(6):363-370.

19. Thiruvoipati T, Kielhorn CE, Armstrong EJ. Peripheral artery disease in patients with diabetes: Epidemiology, mechanisms, and outcomes. *World J Diabetes.* 2015;6(7):961-969.

20. Laing SP, Swerdlow AJ, Carpenter LM, Slater SD, Burden AC, Botha JL, et al. Mortality from cerebrovascular disease in a cohort of 23 000 patients with insulin-treated diabetes. *Stroke.* 2003;34(2):418-421.

21. Harding S. Extracts from "concise clinical evidence". Diabetic retinopathy. *BMJ.* 2003;326(7397):1023-1025.

22. Martin CL, Albers JW, Pop-Busui R, Group DER. Neuropathy and related findings in the diabetes control and complications trial/epidemiology of diabetes interventions and complications study. *Diabetes Care.* 2014;37(1):31-38.

23. Locatelli F, Canaud B, Eckardt KU, Stenvinkel P, Wanner C, Zoccali C. The importance of diabetic nephropathy in current nephrological practice. *Nephrol Dial Transplant.* 2003;18(9):1716-1725.

24. Nathan DM, Cleary PA, Backlund JY, Genuth SM, Lachin JM, Orchard TJ, et al. Intensive diabetes treatment and cardiovascular disease in patients with type 1 diabetes. *N Engl J Med.* 2005;353(25):2643-2653.

25. Wiltshire EJ, Gent R, Hirte C, Pena A, Thomas DW, Couper JJ. Endothelial dysfunction relates to folate status in children and adolescents with type 1 diabetes. *Diabetes.* 2002;51(7):2282-2286.

26. Urbina EM, Wadwa RP, Davis C, Snively BM, Dolan LM, Daniels SR, et al. Prevalence of increased arterial stiffness in children with type 1 diabetes mellitus differs by measurement site and sex: the SEARCH for Diabetes in Youth Study. *J Pediatr.* 2010;156(5):731-737, 737 e731.

27. Harjutsalo V, Sjoberg L, Tuomilehto J. Time trends in the incidence of type 1 diabetes in Finnish children: a cohort study. *Lancet.* 2008;371(9626):1777-1782.

28. Johansen K, Svendsen PA, Lorup B. Variations in renal threshold for glucose in Type 1 (insulin-dependent) diabetes mellitus. *Diabetologia.* 1984;26(3):180-182.

29. The effect of intensive treatment of diabetes on the development and progression of long-term complications in insulin-dependent diabetes mellitus. The Diabetes Control and Complications Trial Research Group. *N Engl J Med.* 1993;329(14):977-986.

30. Goldstein DE, Little RR, Lorenz RA, Malone JI, Nathan DM, Peterson CM, et al. Tests of glycemia in diabetes. *Diabetes Care.* 2003;26 Suppl 1:S106-108.

31. Nathan DM, Group DER. The diabetes control and complications trial/epidemiology of diabetes interventions and complications study at 30 years: overview. *Diabetes Care.* 2014;37(1):9-16.

32. Nathan DM, Lachin J, Cleary P, Orchard T, Brillon DJ, Backlund JY, et al. Intensive diabetes therapy and carotid intima-media thickness in type 1 diabetes mellitus. *N Engl J Med.* 2003;348(23):2294-2303.

33. Cleary PA, Orchard TJ, Genuth S, Wong ND, Detrano R, Backlund JY, et al. The effect of intensive glycemic treatment on coronary artery calcification in type 1 diabetic participants of the Diabetes Control and Complications Trial/Epidemiology of Diabetes Interventions and Complications (DCCT/EDIC) Study. *Diabetes.* 2006;55(12):3556-3565.

34. Risk factors for development of microalbuminuria in insulin dependent diabetic patients: a cohort study. Microalbuminuria Collaborative Study Group, United Kingdom. *BMJ.* 1993;306(6887):1235-1239.

35. Jones TW, Borg WP, Borg MA, Boulware SD, McCarthy G, Silver D, et al. Resistance to neuroglycopenia: an adaptive response during intensive insulin treatment of diabetes. *J Clin Endocrinol Metab.* 1997;82(6):1713-1718.

36. Levey AS, Eckardt KU, Tsukamoto Y, Levin A, Coresh J, Rossert J, et al. Definition and classification of chronic kidney disease: a position statement from Kidney Disease: Improving Global Outcomes (KDIGO). *Kidney Int.* 2005;67(6):2089-2100.

37. Eckardt KU, Coresh J, Devuyst O, Johnson RJ, Kottgen A, Levey AS, et al. Evolving importance of kidney disease: from subspecialty to global health burden. *Lancet.* 2013;382(9887):158-169.

38. Hallan SI, Coresh J, Astor BC, Asberg A, Powe NR, Romundstad S, et al. International comparison of the relationship of chronic kidney disease prevalence and ESRD risk. *J Am Soc Nephrol.* 2006;17(8):2275-2284.

39. Thompson S, James M, Wiebe N, Hemmelgarn B, Manns B, Klarenbach S, et al. Cause of death in patients with reduced kidney function. *J Am Soc Nephrol.* 2015;26(10):2504-2511.

40. Sarnak MJ, Levey AS, Schoolwerth AC, Coresh J, Culleton B, Hamm LL, et al. Kidney disease as a risk factor for development of cardiovascular disease: a statement from the American Heart Association Councils on Kidney in Cardiovascular Disease, High Blood Pressure Research, Clinical Cardiology, and Epidemiology and Prevention. *Circulation.* 2003;108(17):2154-2169.

41. Levey AS, Beto JA, Coronado BE, Eknoyan G, Foley RN, Kasiske BL, et al. Controlling the epidemic of cardiovascular disease in chronic renal disease: what do we know? What do we need to learn? Where do we go from here? National Kidney Foundation Task Force on Cardiovascular Disease. *Am J Kidney Dis.* 1998;32(5):853-906.

42. Kerr M, Bray B, Medcalf J, O'Donoghue DJ, Matthews B. Estimating the financial cost of chronic kidney disease to the NHS in England. *Nephrol Dial Transplant.* 2012;27 Suppl 3:iii73-80.

43. Gilg J, Rao A, Fogarty D. UK Renal Registry 16th annual report: chapter 1 UK renal replacement therapy incidence in 2012: national and centre-specific analyses. *Nephron Clin Pract.* 2013;125(1-4):1-27.

44. Mogensen CE, Osterby R, Gundersen HJ. Early functional and morphologic vascular renal consequences of the diabetic state. *Diabetologia.* 1979;17(2):71-76.

45. Loutzenhiser R, Griffin K, Williamson G, Bidani A. Renal autoregulation: new perspectives regarding the protective and regulatory roles of the underlying mechanisms. *Am J Physiol Regul Integr Comp Physiol.* 2006;290(5):R1153-1167.

46. Navar LG, Bell PD. Romancing the macula densa at UAB. *Kidney Int Suppl.* 2004(91):S34-40.

47. Fligny C, Barton M, Tharaux PL. Endothelin and podocyte injury in chronic kidney disease. *Contrib Nephrol.* 2011;172:120-138.

48. Remuzzi G, Bertani T. Pathophysiology of progressive nephropathies. *N Engl J Med.* 1998;339(20):1448-1456.

49. Abbate M, Remuzzi G. Proteinuria as a mediator of tubulointerstitial injury. *Kidney Blood Press Res.* 1999;22(1-2):37-46.

50. Chatziantoniou C, Dussaule JC. Insights into the mechanisms of renal fibrosis: is it possible to achieve regression? *Am J Physiol Renal Physiol.* 2005;289(2):F227-234.

51. Hillege HL, Fidler V, Diercks GF, van Gilst WH, de Zeeuw D, van Veldhuisen DJ, et al. Urinary albumin excretion predicts cardiovascular and

noncardiovascular mortality in general population. *Circulation.* 2002;106(14):1777-1782.

52. Vallon V, Richter K, Blantz RC, Thomson S, Osswald H. Glomerular hyperfiltration in experimental diabetes mellitus: potential role of tubular reabsorption. *J Am Soc Nephrol.* 1999;10(12):2569-2576.

53. Vallon V, Kirschenmann D, Wead LM, Lortie MJ, Satriano J, Blantz RC, et al. Effect of chronic salt loading on kidney function in early and established diabetes mellitus in rats. *J Lab Clin Med.* 1997;130(1):76-82.

54. Vallon V, Wead LM, Blantz RC. Renal hemodynamics and plasma and kidney angiotensin II in established diabetes mellitus in rats: effect of sodium and salt restriction. *J Am Soc Nephrol.* 1995;5(10):1761-1767.

55. Miller JA. Renal responses to sodium restriction in patients with early diabetes mellitus. *J Am Soc Nephrol.* 1997;8(5):749-755.

56. Luik PT, Hoogenberg K, Van Der Kleij FG, Beusekamp BJ, Kerstens MN, De Jong PE, et al. Short-term moderate sodium restriction induces relative hyperfiltration in normotensive normoalbuminuric Type I diabetes mellitus. *Diabetologia.* 2002;45(4):535-541.

57. Lambers Heerspink HJ, Navis G, Ritz E. Salt intake in kidney disease--a missed therapeutic opportunity? *Nephrol Dial Transplant.* 2012;27(9):3435-3442.

58. Sima CA, Koeners MP, Joles JA, Braam B, Magil AB, Cupples WA. Increased susceptibility to hypertensive renal disease in streptozotocin-treated diabetic rats is not modulated by salt intake. *Diabetologia.* 2012;55(8):2246-2255.

59. Thomas MC, Moran J, Forsblom C, Harjutsalo V, Thorn L, Ahola A, et al. The association between dietary sodium intake, ESRD, and all-cause mortality in patients with type 1 diabetes. *Diabetes Care.* 2011;34(4):861-866.

60. O'Donnell MJ, Yusuf S, Mente A, Gao P, Mann JF, Teo K, et al. Urinary sodium and potassium excretion and risk of cardiovascular events. *JAMA.* 2011;306(20):2229-2238.

61. Romero CA, Orias M, Weir MR. Novel RAAS agonists and antagonists: clinical applications and controversies. *Nat Rev Endocrinol.* 2015;11(4):242-252.

62. Zatz R, Dunn BR, Meyer TW, Anderson S, Rennke HG, Brenner BM. Prevention of diabetic glomerulopathy by pharmacological amelioration of glomerular capillary hypertension. *J Clin Invest.* 1986;77(6):1925-1930.

63. Lewis EJ, Hunsicker LG, Bain RP, Rohde RD. The effect of angiotensin-converting-enzyme inhibition on diabetic nephropathy. The Collaborative Study Group. *N Engl J Med.* 1993;329(20):1456-1462.

64. Denton KM, Fennessy PA, Alcorn D, Anderson WP. Morphometric analysis of the actions of angiotensin II on renal arterioles and glomeruli. *Am J Physiol.* 1992;262(3 Pt 2):F367-372.

65. Sowers JR, Epstein M, Frohlich ED. Diabetes, hypertension, and cardiovascular disease: an update. *Hypertension.* 2001;37(4):1053-1059.

66. Iwanami J, Mogi M, Iwai M, Horiuchi M. Inhibition of the renin-angiotensin system and target organ protection. *Hypertens Res.* 2009;32(4):229-237.

67. Amiel SA, Pursey N, Higgins B, Dawoud D, Guideline Development G. Diagnosis and management of type 1 diabetes in adults: summary of updated NICE guidance. *BMJ.* 2015;351:h4188.

68. Mancia G, Fagard R, Narkiewicz K, Redon J, Zanchetti A, Bohm M, et al. 2013 ESH/ESC guidelines for the management of arterial hypertension: the Task Force for the Management of Arterial Hypertension of the European Society of Hypertension (ESH) and of the European Society of Cardiology (ESC). *Eur Heart J.* 2013;34(28):2159-2219.

69. Lim SS, Vos T, Flaxman AD, Danaei G, Shibuya K, Adair-Rohani H, et al. A comparative risk assessment of burden of disease and injury attributable to 67 risk factors and risk factor clusters in 21 regions, 1990-2010: a systematic analysis for the Global Burden of Disease Study 2010. *Lancet.* 2012;380(9859):2224-2260.

70. Collins AJ, Foley RN, Chavers B, Gilbertson D, Herzog C, Ishani A, et al. US Renal Data System 2013 annual data report. *Am J Kidney Dis.* 2014;63(1 Suppl):A7.

71. Freedman BI, Sedor JR. Hypertension-associated kidney disease: perhaps no more. *J Am Soc Nephrol.* 2008;19(11):2047-2051.

72. Conway BR, Rennie J, Bailey MA, Dunbar DR, Manning JR, Bellamy CO, et al. Hyperglycemia and renin-dependent hypertension synergize to model diabetic nephropathy. *J Am Soc Nephrol.* 2012;23(3):405-411.

73. Cooper ME, Allen TJ, Macmillan P, Bach L, Jerums G, Doyle AE. Genetic hypertension accelerates nephropathy in the streptozotocin diabetic rat. *Am J Hypertens.* 1988;1(1):5-10.

74. Lurbe E, Redon J, Kesani A, Pascual JM, Tacons J, Alvarez V, et al. Increase in nocturnal blood pressure and progression to microalbuminuria in type 1 diabetes. *N Engl J Med.* 2002;347(11):797-805.

75. Laitinen T, Hartikainen J, Niskanen L, Geelen G, Lansimies E. Sympathovagal balance is major determinant of short-term blood pressure variability in healthy subjects. *Am J Physiol.* 1999;276(4 Pt 2):H1245-1252.

76. Hall JE, Granger JP, do Carmo JM, da Silva AA, Dubinion J, George E, et al. Hypertension: physiology and pathophysiology. *Compr Physiol.* 2012;2(4):2393-2442.

77. Kohan DE, Rossi NF, Inscho EW, Pollock DM. Regulation of blood pressure and salt homeostasis by endothelin. *Physiol Rev.* 2011;91(1):1-77.

78. Guyton AC. Renal function curve--a key to understanding the pathogenesis of hypertension. *Hypertension.* 1987;10(1):1-6.

79. Dahl LK, Heine M, Thompson K. Genetic influence of renal homografts on the blood pressure of rats from different strains. *Proc Soc Exp Biol Med.* 1972;140(3):852-856.

80. Dahl LK, Heine M, Thompson K. Genetic influence of the kidneys on blood pressure. Evidence from chronic renal homografts in rats with opposite predispositions to hypertension. *Circ Res.* 1974;34(1):94-101.

81. Dahl LK, Heine M. Primary role of renal homografts in setting chronic blood pressure levels in rats. *Circ Res.* 1975;36(6):692-696.

82. Rettig R, Folberth C, Stauss H, Kopf D, Waldherr R, Unger T. Role of the kidney in primary hypertension: a renal transplantation study in rats. *Am J Physiol.* 1990;258(3 Pt 2):F606-611.

83. Kopf D, Waldherr R, Rettig R. Source of kidney determines blood pressure in young renal transplanted rats. *Am J Physiol.* 1993;265(1 Pt 2):F104-111.

84. Frey BA, Grisk O, Bandelow N, Wussow S, Bie P, Rettig R. Sodium homeostasis in transplanted rats with a spontaneously hypertensive rat kidney. *Am J Physiol Regul Integr Comp Physiol.* 2000;279(3):R1099-1104.

85. Graf C, Maser-Gluth C, de Muinck Keizer W, Rettig R. Sodium retention and hypertension after kidney transplantation in rats. *Hypertension.* 1993;21(5):724-730.

86. Grisk O, Heukaufer M, Steinbach A, Gruska S, Rettig R. Analysis of arterial pressure regulating systems in renal post-transplantation hypertension. *J Hypertens.* 2004;22(1):199-207.

87. Crowley SD, Gurley SB, Oliverio MI, Pazmino AK, Griffiths R, Flannery PJ, et al. Distinct roles for the kidney and systemic tissues in blood pressure regulation by the renin-angiotensin system. *J Clin Invest.* 2005;115(4):1092-1099.

88. Coffman TM, Crowley SD. Kidney in hypertension: guyton redux. *Hypertension.* 2008;51(4):811-816.

89. Ivy JR, Bailey MA. Pressure natriuresis and the renal control of arterial blood pressure. *J Physiol.* 2014;592(Pt 18):3955-3967.

90. Guyton AC, Hall JE. Regulation of extracellular fluid osmolarity and sodium concentration. In: Guyton AC, Hall JE, eds. *Textbook of Medical Physiology.* 11th ed. Philadelphia, United States: Elsevier Saunders; 2006:348-364.

91. Schafer JA. Transepithelial osmolality differences, hydraulic conductivities, and volume absorption in the proximal tubule. *Annu Rev Physiol.* 1990;52:709-726.

92. Magyar CE, McDonough AA. Molecular mechanisms of sodium transport inhibition in proximal tubule during acute hypertension. *Curr Opin Nephrol Hypertens.* 2000;9(2):149-156.

93. Ashek A, Menzies RI, Mullins LJ, Bellamy CO, Harmar AJ, Kenyon CJ, et al. Activation of thiazide-sensitive co-transport by angiotensin II in the cyp1a1-Ren2 hypertensive rat. *PLoS One.* 2012;7(4):e36311.

94. Dautzenberg M, Keilhoff G, Just A. Modulation of the myogenic response in renal blood flow autoregulation by NO depends on endothelial nitric oxide synthase (eNOS), but not neuronal or inducible NOS. *J Physiol.* 2011;589(Pt 19):4731-4744.

95. Burnstock G, Evans LC, Bailey MA. Purinergic signalling in the kidney in health and disease. *Purinergic Signal.* 2014;10(1):71-101.

96. Garvin JL, Herrera M, Ortiz PA. Regulation of renal NaCl transport by nitric oxide, endothelin, and ATP: clinical implications. *Annu Rev Physiol.* 2011;73:359-376.

97. Hall JE, Granger JP, Smith MJ, Jr., Premen AJ. Role of renal hemodynamics and arterial pressure in aldosterone "escape". *Hypertension.* 1984;6(2 Pt 2):I183-192.

98. Wang XY, Masilamani S, Nielsen J, Kwon TH, Brooks HL, Nielsen S, et al. The renal thiazide-sensitive Na-Cl cotransporter as mediator of the aldosterone-escape phenomenon. *J Clin Invest.* 2001;108(2):215-222.

99. Stockand JD, Mironova E, Bugaj V, Rieg T, Insel PA, Vallon V, et al. Purinergic inhibition of ENaC produces aldosterone escape. *J Am Soc Nephrol.* 2010;21(11):1903-1911.

100. Fukuda M, Goto N, Kimura G. Hypothesis on renal mechanism of non-dipper pattern of circadian blood pressure rhythm. *Med Hypotheses.* 2006;67(4):802-806.

101. Bankir L, Bochud M, Maillard M, Bovet P, Gabriel A, Burnier M. Nighttime blood pressure and nocturnal dipping are associated with daytime urinary sodium excretion in African subjects. *Hypertension.* 2008;51(4):891-898.

102. Schwartz GL, Bailey KR, Mosley T, Knopman DS, Jack CR, Jr., Canzanello VJ, et al. Association of ambulatory blood pressure with ischemic brain injury. *Hypertension.* 2007;49(6):1228-1234.

103. Cuspidi C, Macca G, Sampieri L, Fusi V, Severgnini B, Michev I, et al. Target organ damage and non-dipping pattern defined by two sessions of ambulatory blood pressure monitoring in recently diagnosed essential hypertensive patients. *J Hypertens.* 2001;19(9):1539-1545.

104. Henskens LH, van Oostenbrugge RJ, Kroon AA, de Leeuw PW, Lodder J. Brain microbleeds are associated with ambulatory blood pressure levels in a hypertensive population. *Hypertension.* 2008;51(1):62-68.

105. Standards of medical care in diabetes--2015: summary of revisions. *Diabetes Care.* 2015;38 Suppl:S4.

106. Hermida RC. Sleep-time ambulatory blood pressure as a prognostic marker of vascular and other risks and therapeutic target for prevention by hypertension

chronotherapy: Rationale and design of the Hygia Project. *Chronobiol Int.* 2016;33(7):906-936.

107. O'Hare JP, Roland JM, Walters G, Corrall RJ. Impaired sodium excretion in response to volume expansion induced by water immersion in insulin-dependent diabetes mellitus. *Clin Sci (Lond).* 1986;71(4):403-409.

108. Tang D, Yu T, Khraibi AA. Cardiovascular and renal characteristics, and responses to acute volume expansion of a rat model of diabetic pregnancy. *Life Sci.* 2004;74(23):2909-2918.

109. Patel KP, Zhang PL. Reduced renal responses to volume expansion in streptozotocin-induced diabetic rats. *Am J Physiol.* 1989;257(3 Pt 2):R672-679.

110. O'Hare JP, Anderson JV, Millar ND, Dalton N, Tymms DJ, Bloom SR, et al. Hormonal response to blood volume expansion in diabetic subjects with and without autonomic neuropathy. *Clin Endocrinol (Oxf).* 1989;30(5):571-579.

111. Kunau RT, Jr., Lameire NH. The effect of an acute increase in renal perfusion pressure on sodium transport in the rat kidney. *Circ Res.* 1976;39(5):689-695.

112. Roman RJ, Cowley AW, Jr. Characterization of a new model for the study of pressure-natriuresis in the rat. *Am J Physiol.* 1985;248(2 Pt 2):F190-198.

113. Dresser TP, Lynch RE, Schneider EG, Knox FG. Effect of increases in blood pressure on pressure and reabsorption in the proximal tubule. *Am J Physiol.* 1971;220(2):444-447.

114. Williams JM, Sarkis A, Lopez B, Ryan RP, Flasch AK, Roman RJ. Elevations in renal interstitial hydrostatic pressure and 20-

hydroxyeicosatetraenoic acid contribute to pressure natriuresis. *Hypertension.* 2007;49(3):687-694.

115. Gross V, Lippoldt A, Yagil C, Yagil Y, Luft FC. Pressure natriuresis in salt-sensitive and salt-resistant Sabra rats. *Hypertension.* 1997;29(6):1252-1259.

116. Roman RJ. Abnormal renal hemodynamics and pressure-natriuresis relationship in Dahl salt-sensitive rats. *Am J Physiol.* 1986;251(1 Pt 2):F57-65.

117. Gross V, Lippoldt A, Luft FC. Pressure diuresis and natriuresis in DOCA-salt mice. *Kidney Int.* 1997;52(5):1364-1368.

118. Furchgott RF, Zawadzki JV. The obligatory role of endothelial cells in the relaxation of arterial smooth muscle by acetylcholine. *Nature.* 1980;288(5789):373-376.

119. Palmer RM, Ferrige AG, Moncada S. Nitric oxide release accounts for the biological activity of endothelium-derived relaxing factor. *Nature.* 1987;327(6122):524-526.

120. Guarasci GR, Kline RL. Pressure natriuresis following acute and chronic inhibition of nitric oxide synthase in rats. *Am J Physiol.* 1996;270(2 Pt 2):R469-478.

121. Hyndman KA, Boesen EI, Elmarakby AA, Brands MW, Huang P, Kohan DE, et al. Renal collecting duct NOS1 maintains fluid-electrolyte homeostasis and blood pressure. *Hypertension.* 2013;62(1):91-98.

122. Schneider MP, Ge Y, Pollock DM, Pollock JS, Kohan DE. Collecting duct-derived endothelin regulates arterial pressure and Na excretion via nitric oxide. *Hypertension.* 2008;51(6):1605-1610.

123. Menzies RI, Unwin RJ, Dash RK, Beard DA, Cowley AW, Jr., Carlson BE, et al. Effect of P2X4 and P2X7 receptor antagonism on the pressure diuresis relationship in rats. *Front Physiol.* 2013;4:305.

124. Fukuda M, Munemura M, Usami T, Nakao N, Takeuchi O, Kamiya Y, et al. Nocturnal blood pressure is elevated with natriuresis and proteinuria as renal function deteriorates in nephropathy. *Kidney Int.* 2004;65(2):621-625.

125. Crisa L, Mordes JP, Rossini AA. Autoimmune diabetes mellitus in the BB rat. *Diabetes Metab Rev.* 1992;8(1):4-37.

126. Shoda LK, Young DL, Ramanujan S, Whiting CC, Atkinson MA, Bluestone JA, et al. A comprehensive review of interventions in the NOD mouse and implications for translation. *Immunity.* 2005;23(2):115-126.

127. Shultz LD, Ishikawa F, Greiner DL. Humanized mice in translational biomedical research. *Nat Rev Immunol.* 2007;7(2):118-130.

128. Mazzone T, Chait A, Plutzky J. Cardiovascular disease risk in type 2 diabetes mellitus: insights from mechanistic studies. *Lancet.* 2008;371(9626):1800-1809.

129. Tesch GH, Allen TJ. Rodent models of streptozotocin-induced diabetic nephropathy. *Nephrology (Carlton).* 2007;12(3):261-266.

130. Betz B, Conway BR. An Update on the Use of Animal Models in Diabetic Nephropathy Research. *Curr Diab Rep.* 2016;16(2):18.

131. Lenzen S. The mechanisms of alloxan- and streptozotocin-induced diabetes. *Diabetologia.* 2008;51(2):216-226.

132. Oelze M, Knorr M, Schuhmacher S, Heeren T, Otto C, Schulz E, et al. Vascular dysfunction in streptozotocin-induced experimental diabetes strictly depends on insulin deficiency. *J Vasc Res.* 2011;48(4):275-284.

133. Benter IF, Yousif MH, Hollins AJ, Griffiths SM, Akhtar S. Diabetes-induced renal vascular dysfunction is normalized by inhibition of epidermal growth factor receptor tyrosine kinase. *J Vasc Res.* 2005;42(4):284-291.

134. Nacci C, Tarquinio M, De Benedictis L, Mauro A, Zigrino A, Carratu MR, et al. Endothelial dysfunction in mice with streptozotocin-induced type 1 diabetes is opposed by compensatory overexpression of cyclooxygenase-2 in the vasculature. *Endocrinology.* 2009;150(2):849-861.

135. Shibata R, Ueda S, Yamagishi S, Kaida Y, Matsumoto Y, Fukami K, et al. Involvement of asymmetric dimethylarginine (ADMA) in tubulointerstitial ischaemia in the early phase of diabetic nephropathy. *Nephrol Dial Transplant.* 2009;24(4):1162-1169.

136. Koya D, Hayashi K, Kitada M, Kashiwagi A, Kikkawa R, Haneda M. Effects of antioxidants in diabetes-induced oxidative stress in the glomeruli of diabetic rats. *J Am Soc Nephrol.* 2003;14(8 Suppl 3):S250-253.

137. Komers R, Anderson S. Paradoxes of nitric oxide in the diabetic kidney. *Am J Physiol Renal Physiol.* 2003;284(6):F1121-1137.

138. Roman RJ, Cowley AW, Jr., Garcia-Estan J, Lombard JH. Pressure-diuresis in volume-expanded rats. Cortical and medullary hemodynamics. *Hypertension.* 1988;12(2):168-176.

139. Endlich K, Hoffend J, Steinhausen M. Localization of endothelin ETA and ETB receptor-mediated constriction in the renal microcirculation of rats. *J Physiol.* 1996;497 (Pt 1):211-218.

140. Bank N, Aynedjian HS. Progressive increases in luminal glucose stimulate proximal sodium absorption in normal and diabetic rats. *J Clin Invest.* 1990;86(1):309-316.

141. Sallstrom J, Eriksson T, Fredholm BB, Persson AE, Palm F. Inhibition of sodium-linked glucose reabsorption normalizes diabetes-induced glomerular hyperfiltration in conscious adenosine A(1)-receptor deficient mice. *Acta Physiol (Oxf).* 2014;210(2):440-445.

142. Sallstrom J, Carlsson PO, Fredholm BB, Larsson E, Persson AE, Palm F. Diabetes-induced hyperfiltration in adenosine A(1)-receptor deficient mice lacking the tubuloglomerular feedback mechanism. *Acta Physiol (Oxf).* 2007;190(3):253-259.

143. Harris RC, Brenner BM, Seifter JL. Sodium-hydrogen exchange and glucose transport in renal microvillus membrane vesicles from rats with diabetes mellitus. *J Clin Invest.* 1986;77(3):724-733.

144. Albertoni Borghese MF, Majowicz MP, Ortiz MC, Passalacqua Mdel R, Sterin Speziale NB, Vidal NA. Expression and activity of SGLT2 in diabetes induced by streptozotocin: relationship with the lipid environment. *Nephron Physiol.* 2009;112(3):p45-52.

145. Song J, Knepper MA, Verbalis JG, Ecelbarger CA. Increased renal ENaC subunit and sodium transporter abundances in streptozotocin-induced type 1 diabetes. *Am J Physiol Renal Physiol.* 2003;285(6):F1125-1137.

146. Tiwari S, Sharma N, Gill PS, Igarashi P, Kahn CR, Wade JB, et al. Impaired sodium excretion and increased blood pressure in mice with targeted deletion of renal epithelial insulin receptor. *Proc Natl Acad Sci U S A.* 2008;105(17):6469-6474.

147. Qi Z, Fujita H, Jin J, Davis LS, Wang Y, Fogo AB, et al. Characterization of susceptibility of inbred mouse strains to diabetic nephropathy. *Diabetes.* 2005;54(9):2628-2637.

148. Zheng S, Huang Y, Yang L, Chen T, Xu J, Epstein PN. Uninephrectomy of diabetic OVE26 mice greatly accelerates albuminuria, fibrosis, inflammatory cell infiltration and changes in gene expression. *Nephron Exp Nephrol.* 2011;119(1):e21-32.

149. Zhao HJ, Wang S, Cheng H, Zhang MZ, Takahashi T, Fogo AB, et al. Endothelial nitric oxide synthase deficiency produces accelerated nephropathy in diabetic mice. *J Am Soc Nephrol.* 2006;17(10):2664-2669.

150. Gagliardini E, Corna D, Zoja C, Sangalli F, Carrara F, Rossi M, et al. Unlike each drug alone, lisinopril if combined with avosentan promotes regression of renal lesions in experimental diabetes. *Am J Physiol Renal Physiol.* 2009;297(5):F1448-1456.

151. Sugimoto H, Shikata K, Hirata K, Akiyama K, Matsuda M, Kushiro M, et al. Increased expression of intercellular adhesion molecule-1 (ICAM-1) in diabetic rat glomeruli: glomerular hyperfiltration is a potential mechanism of ICAM-1 upregulation. *Diabetes.* 1997;46(12):2075-2081.

152. Kato S, Luyckx VA, Ots M, Lee KW, Ziai F, Troy JL, et al. Renin-angiotensin blockade lowers MCP-1 expression in diabetic rats. *Kidney Int.* 1999;56(3):1037-1048.

153. Conway BR, Betz B, Sheldrake TA, Manning JR, Dunbar DR, Dobyns A, et al. Tight blood glycaemic and blood pressure control in experimental diabetic nephropathy reduces extracellular matrix production without regression of fibrosis. *Nephrology (Carlton).* 2014;19(12):802-813.

154. Saleh MA, Pollock JS, Pollock DM. Distinct actions of endothelin A-selective versus combined endothelin A/B receptor antagonists in early diabetic kidney disease. *J Pharmacol Exp Ther.* 2011;338(1):263-270.

155. Reiser J, Mundel P. Dual effects of RAS blockade on blood pressure and podocyte function. *Curr Hypertens Rep.* 2007;9(5):403-408.

156. Johnson RJ, Alpers CE, Yoshimura A, Lombardi D, Pritzl P, Floege J, et al. Renal injury from angiotensin II-mediated hypertension. *Hypertension.* 1992;19(5):464-474.

157. Sharma K, Ziyadeh FN, Alzahabi B, McGowan TA, Kapoor S, Kurnik BR, et al. Increased renal production of transforming growth factor-beta1 in patients with type II diabetes. *Diabetes.* 1997;46(5):854-859.

158. Lopez B, Salom MG, Arregui B, Valero F, Fenoy FJ. Role of superoxide in modulating the renal effects of angiotensin II. *Hypertension.* 2003;42(6):1150-1156.

159. Mauer M, Zinman B, Gardiner R, Suissa S, Sinaiko A, Strand T, et al. Renal and retinal effects of enalapril and losartan in type 1 diabetes. *N Engl J Med.* 2009;361(1):40-51.

160. Bilous R, Chaturvedi N, Sjolie AK, Fuller J, Klein R, Orchard T, et al. Effect of candesartan on microalbuminuria and albumin excretion rate in diabetes: three randomized trials. *Ann Intern Med.* 2009;151(1):11-20, W13-14.

161. Randomised placebo-controlled trial of lisinopril in normotensive patients with insulin-dependent diabetes and normoalbuminuria or microalbuminuria. The EUCLID Study Group. *Lancet.* 1997;349(9068):1787-1792.

162. Schievink B, de Zeeuw D, Smink PA, Andress D, Brennan JJ, Coll B, et al. Prediction of the effect of atrasentan on renal and heart failure outcomes based on short-term changes in multiple risk markers. *Eur J Prev Cardiol.* 2016;23(7):758-768.

163. Yanagisawa M, Kurihara H, Kimura S, Tomobe Y, Kobayashi M, Mitsui Y, et al. A novel potent vasoconstrictor peptide produced by vascular endothelial cells. *Nature.* 1988;332(6163):411-415.

164. Inoue A, Yanagisawa M, Kimura S, Kasuya Y, Miyauchi T, Goto K, et al. The human endothelin family: three structurally and pharmacologically distinct isopeptides predicted by three separate genes. *Proc Natl Acad Sci U S A.* 1989;86(8):2863-2867.

165. Imig JD, Pham BT, LeBlanc EA, Reddy KM, Falck JR, Inscho EW. Cytochrome P450 and cyclooxygenase metabolites contribute to the endothelin-1 afferent arteriolar vasoconstrictor and calcium responses. *Hypertension.* 2000;35(1 Pt 2):307-312.

166. Inscho EW, Imig JD, Cook AK, Pollock DM. ETA and ETB receptors differentially modulate afferent and efferent arteriolar responses to endothelin. *Br J Pharmacol.* 2005;146(7):1019-1026.

167. D'Orleans-Juste P, Plante M, Honore JC, Carrier E, Labonte J. Synthesis and degradation of endothelin-1. *Can J Physiol Pharmacol.* 2003;81(6):503-510.

168. Haynes WG, Webb DJ. Contribution of endogenous generation of endothelin-1 to basal vascular tone. *Lancet.* 1994;344(8926):852-854.

169. Ozaka T, Doi Y, Kayashima K, Fujimoto S. Weibel-Palade bodies as a storage site of calcitonin gene-related peptide and endothelin-1 in blood vessels of the rat carotid body. *Anat Rec.* 1997;247(3):388-394.

170. Gasic S, Wagner OF, Vierhapper H, Nowotny P, Waldhausl W. Regional hemodynamic effects and clearance of endothelin-1 in humans: renal and peripheral tissues may contribute to the overall disposal of the peptide. *J Cardiovasc Pharmacol.* 1992;19(2):176-180.

171. Dupuis J, Stewart DJ, Cernacek P, Gosselin G. Human pulmonary circulation is an important site for both clearance and production of endothelin-1. *Circulation.* 1996;94(7):1578-1584.

172. Abassi ZA, Tate JE, Golomb E, Keiser HR. Role of neutral endopeptidase in the metabolism of endothelin. *Hypertension.* 1992;20(1):89-95.

173. Bohm F, Pernow J, Lindstrom J, Ahlborg G. ETA receptors mediate vasoconstriction, whereas ETB receptors clear endothelin-1 in the splanchnic and renal circulation of healthy men. *Clin Sci (Lond).* 2003;104(2):143-151.

174. Parvanova A, van der Meer IM, Iliev I, Perna A, Gaspari F, Trevisan R, et al. Effect on blood pressure of combined inhibition of endothelin-converting enzyme and neutral endopeptidase with daglutril in patients with type 2 diabetes who have albuminuria: a randomised, crossover, double-blind, placebo-controlled trial. *Lancet Diabetes Endocrinol.* 2013;1(1):19-27.

175. Shindo T, Kurihara H, Maemura K, Kurihara Y, Ueda O, Suzuki H, et al. Renal damage and salt-dependent hypertension in aged transgenic mice overexpressing endothelin-1. *J Mol Med (Berl).* 2002;80(2):105-116.

176. Hocher B, Thone-Reineke C, Rohmeiss P, Schmager F, Slowinski T, Burst V, et al. Endothelin-1 transgenic mice develop glomerulosclerosis, interstitial fibrosis, and renal cysts but not hypertension. *J Clin Invest.* 1997;99(6):1380-1389.

177. Kitamura K, Tanaka T, Kato J, Ogawa T, Eto T, Tanaka K. Immunoreactive endothelin in rat kidney inner medulla: marked decrease in spontaneously hypertensive rats. *Biochem Biophys Res Commun.* 1989;162(1):38-44.

178. Kuc R, Davenport AP. Comparison of endothelin-A and endothelin-B receptor distribution visualized by radioligand binding versus immunocytochemical localization using subtype selective antisera. *J Cardiovasc Pharmacol.* 2004;44 Suppl 1:S224-226.

179. Pupilli C, Brunori M, Misciglia N, Selli C, Ianni L, Yanagisawa M, et al. Presence and distribution of endothelin-1 gene expression in human kidney. *Am J Physiol.* 1994;267(4 Pt 2):F679-687.

180. Ahn D, Ge Y, Stricklett PK, Gill P, Taylor D, Hughes AK, et al. Collecting duct-specific knockout of endothelin-1 causes hypertension and sodium retention. *J Clin Invest.* 2004;114(4):504-511.

181. Ge Y, Bagnall A, Stricklett PK, Strait K, Webb DJ, Kotelevtsev Y, et al. Collecting duct-specific knockout of the endothelin B receptor causes hypertension and sodium retention. *Am J Physiol Renal Physiol.* 2006;291(6):F1274-1280.

182. Crawford C, Kennedy-Lydon T, Sprott C, Desai T, Sawbridge L, Munday J, et al. An intact kidney slice model to investigate vasa recta properties and function in situ. *Nephron Physiol.* 2012;120(3):p17-31.

183. Silldorff EP, Yang S, Pallone TL. Prostaglandin E2 abrogates endothelin-induced vasoconstriction in renal outer medullary descending vasa recta of the rat. *J Clin Invest.* 1995;95(6):2734-2740.

184. O'Connor PM, Cowley AW, Jr. Medullary thick ascending limb buffer vasoconstriction of renal outer-medullary vasa recta in salt-resistant but not salt-sensitive rats. *Hypertension.* 2012;60(4):965-972.

185. Ahmeda AF, Johns EJ. The regulation of blood perfusion in the renal cortex and medulla by reactive oxygen species and nitric oxide in the anaesthetised rat. *Acta Physiol (Oxf).* 2012;204(3):443-450.

186. Schneider MP, Inscho EW, Pollock DM. Attenuated vasoconstrictor responses to endothelin in afferent arterioles during a high-salt diet. *Am J Physiol Renal Physiol.* 2007;292(4):F1208-1214.

187. Hocher B, Rohmeiss P, Zart R, Diekmann F, Vogt V, Metz D, et al. Significance of endothelin receptor subtypes in the kidneys of spontaneously hypertensive rats: renal and hemodynamic effects of endothelin receptor antagonists. *J Cardiovasc Pharmacol.* 1995;26 Suppl 3:S470-472.

188. Cui P, Tani K, Kitamura H, Okumura Y, Yano M, Inui D, et al. A novel bioactive 31-amino acid endothelin-1 is a potent chemotactic peptide for human neutrophils and monocytes. *J Leukoc Biol.* 2001;70(2):306-312.

189. Achmad TH, Rao GS. Chemotaxis of human blood monocytes toward endothelin-1 and the influence of calcium channel blockers. *Biochem Biophys Res Commun.* 1992;189(2):994-1000.

190. Javeshghani D, Barhoumi T, Idris-Khodja N, Paradis P, Schiffrin EL. Reduced macrophage-dependent inflammation improves endothelin-1-induced vascular injury. *Hypertension.* 2013;62(1):112-117.

191. Bacon CR, Cary NR, Davenport AP. Endothelin peptide and receptors in human atherosclerotic coronary artery and aorta. *Circ Res.* 1996;79(4):794-801.

192. Ehrenreich H, Anderson RW, Fox CH, Rieckmann P, Hoffman GS, Travis WD, et al. Endothelins, peptides with potent vasoactive properties, are produced by human macrophages. *J Exp Med.* 1990;172(6):1741-1748.

193. Helset E, Sildnes T, Seljelid R, Konopski ZS. Endothelin-1 stimulates human monocytes in vitro to release TNF-alpha , IL-1beta and IL-6. *Mediators Inflamm.* 1993;2(6):417-422.

194. Ruetten H, Thiemermann C. Endothelin-1 stimulates the biosynthesis of tumour necrosis factor in macrophages: ET-receptors, signal transduction and inhibition by dexamethasone. *J Physiol Pharmacol.* 1997;48(4):675-688.

195. Foschi M, Sorokin A, Pratt P, McGinty A, La Villa G, Franchi F, et al. PreproEndothelin-1 expression in human mesangial cells: evidence for a p38 mitogen-activated protein kinase/protein kinases-C-dependent mechanism. *J Am Soc Nephrol.* 2001;12(6):1137-1150.

196. Ong AC, Jowett TP, Firth JD, Burton S, Kitamura M, Fine LG. Human tubular-derived endothelin in the paracrine regulation of renal interstitial fibroblast function. *Exp Nephrol.* 1994;2(2):134.

197. Gomez-Garre D, Largo R, Liu XH, Gutierrez S, Lopez-Armada MJ, Palacios I, et al. An orally active ETA/ETB receptor antagonist ameliorates proteinuria and glomerular lesions in rats with proliferative nephritis. *Kidney Int.* 1996;50(3):962-972.

198. Simonson MS, Ismail-Beigi F. Endothelin-1 increases collagen accumulation in renal mesangial cells by stimulating a chemokine and cytokine autocrine signaling loop. *J Biol Chem.* 2011;286(13):11003-11008.

199. Barton M, Shaw S, d'Uscio LV, Moreau P, Luscher TF. Angiotensin II increases vascular and renal endothelin-1 and functional endothelin converting enzyme activity in vivo: role of ETA receptors for endothelin regulation. *Biochem Biophys Res Commun.* 1997;238(3):861-865.

200. Matsumura Y, Nakase K, Ikegawa R, Hayashi K, Ohyama T, Morimoto S. The endothelium-derived vasoconstrictor peptide endothelin inhibits renin release in vitro. *Life Sci.* 1989;44(2):149-157.

201. Otsuka A, Mikami H, Katahira K, Tsunetoshi T, Minamitani K, Ogihara T. Changes in plasma renin activity and aldosterone concentration in response to endothelin injection in dogs. *Acta Endocrinol (Copenh).* 1989;121(3):361-364.

202. Kawaguchi H, Sawa H, Yasuda H. Endothelin stimulates angiotensin I to angiotensin II conversion in cultured pulmonary artery endothelial cells. *J Mol Cell Cardiol.* 1990;22(8):839-842.

203. Schiffrin EL. The angiotensin-endothelin relationship: does it play a role in cardiovascular and renal pathophysiology? *J Hypertens.* 2003;21(12):2245-2247.

204. Fukui M, Nakamura T, Ebihara I, Osada S, Tomino Y, Masaki T, et al. Gene expression for endothelins and their receptors in glomeruli of diabetic rats. *J Lab Clin Med.* 1993;122(2):149-156.

205. Yamauchi T, Ohnaka K, Takayanagi R, Umeda F, Nawata H. Enhanced secretion of endothelin-1 by elevated glucose levels from cultured bovine aortic endothelial cells. *FEBS Lett.* 1990;267(1):16-18.

206. Morigi M, Buelli S, Zanchi C, Longaretti L, Macconi D, Benigni A, et al. Shigatoxin-induced endothelin-1 expression in cultured podocytes autocrinally mediates actin remodeling. *Am J Pathol.* 2006;169(6):1965-1975.

207. Morigi M, Buelli S, Angioletti S, Zanchi C, Longaretti L, Zoja C, et al. In response to protein load podocytes reorganize cytoskeleton and modulate endothelin-1 gene: implication for permselective dysfunction of chronic nephropathies. *Am J Pathol.* 2005;166(5):1309-1320.

208. Ortmann J, Amann K, Brandes RP, Kretzler M, Munter K, Parekh N, et al. Role of podocytes for reversal of glomerulosclerosis and proteinuria in the aging kidney after endothelin inhibition. *Hypertension.* 2004;44(6):974-981.

209. Goddard J, Johnston NR, Cumming AD, Webb DJ. Fractional urinary excretion of endothelin-1 is reduced by acute ETB receptor blockade. *Am J Physiol Renal Physiol.* 2007;293(5):F1433-1438.

210. Lenoir O, Milon M, Virsolvy A, Henique C, Schmitt A, Masse JM, et al. Direct action of endothelin-1 on podocytes promotes diabetic glomerulosclerosis. *J Am Soc Nephrol.* 2014.

211. Fukui M, Nakamura T, Ebihara I, Makita Y, Osada S, Tomino Y, et al. Effects of enalapril on endothelin-1 and growth factor gene expression in diabetic rat glomeruli. *J Lab Clin Med.* 1994;123(5):763-768.

212. Kassab S, Miller MT, Novak J, Reckelhoff J, Clower B, Granger JP. Endothelin-A receptor antagonism attenuates the hypertension and renal injury in Dahl salt-sensitive rats. *Hypertension.* 1998;31(1 Pt 2):397-402.

213. Nagase M, Shibata S, Yoshida S, Nagase T, Gotoda T, Fujita T. Podocyte injury underlies the glomerulopathy of Dahl salt-hypertensive rats and is reversed by aldosterone blocker. *Hypertension.* 2006;47(6):1084-1093.

214. Saleh MA, Boesen EI, Pollock JS, Savin VJ, Pollock DM. Endothelin-1 increases glomerular permeability and inflammation independent of blood pressure in the rat. *Hypertension.* 2010;56(5):942-949.

215. Opocensky M, Kramer HJ, Backer A, Vernerova Z, Eis V, Cervenka L, et al. Late-onset endothelin-A receptor blockade reduces podocyte injury in homozygous Ren-2 rats despite severe hypertension. *Hypertension.* 2006;48(5):965-971.

216. Trenkner J, Priem F, Bauer C, Neumayer HH, Raschak M, Hocher B. Endothelin receptor A blockade reduces proteinuria and vascular hypertrophy in spontaneously hypertensive rats on high-salt diet in a blood-pressure-independent manner. *Clin Sci (Lond).* 2002;103 Suppl 48:385S-388S.

217. de Zeeuw D, Coll B, Andress D, Brennan JJ, Tang H, Houser M, et al. The endothelin antagonist atrasentan lowers residual albuminuria in patients with Type 2 diabetic nephropathy. *J Am Soc Nephrol.* 2014.

218. Andress DL, Coll B, Pritchett Y, Brennan J, Molitch M, Kohan DE. Clinical efficacy of the selective endothelin A receptor antagonist, atrasentan, in patients with diabetes and chronic kidney disease (CKD). *Life Sci.* 2012;91(13-14):739-742.

219. Kohan DE, Pritchett Y, Molitch M, Wen S, Garimella T, Audhya P, et al. Addition of atrasentan to renin-angiotensin system blockade reduces albuminuria in diabetic nephropathy. *J Am Soc Nephrol.* 2011;22(4):763-772.

220. Wenzel RR, Littke T, Kuranoff S, Jurgens C, Bruck H, Ritz E, et al. Avosentan reduces albumin excretion in diabetics with macroalbuminuria. *J Am Soc Nephrol.* 2009;20(3):655-664.

221. Hoeper MM, Olsson KM, Schneider A, Golpon H. Severe hepatitis associated with sitaxentan and response to glucocorticoid therapy. *Eur Respir J.* 2009;33(6):1518-1519.

222. Battistini B, Berthiaume N, Kelland NF, Webb DJ, Kohan DE. Profile of past and current clinical trials involving endothelin receptor antagonists: the novel "-sentan" class of drug. *Exp Biol Med (Maywood).* 2006;231(6):653-695.

223. Mann JF, Green D, Jamerson K, Ruilope LM, Kuranoff SJ, Littke T, et al. Avosentan for overt diabetic nephropathy. *J Am Soc Nephrol.* 2010;21(3):527-535.

224. Smolander J, Vogt B, Maillard M, Zweiacker C, Littke T, Hengelage T, et al. Dose-dependent acute and sustained renal effects of the endothelin receptor

antagonist avosentan in healthy subjects. *Clin Pharmacol Ther.* 2009;85(6):628-634.

225. Vassileva I, Mountain C, Pollock DM. Functional role of ETB receptors in the renal medulla. *Hypertension.* 2003;41(6):1359-1363.

226. Dhaun N, Moorhouse R, MacIntyre IM, Melville V, Oosthuyzen W, Kimmitt RA, et al. Diurnal Variation in Blood Pressure and Arterial Stiffness in Chronic Kidney Disease: The Role of Endothelin-1. *Hypertension.* 2014.

227. Kohan DE, Cleland JG, Rubin LJ, Theodorescu D, Barton M. Clinical trials with endothelin receptor antagonists: what went wrong and where can we improve? *Life Sci.* 2012;91(13-14):528-539.

228. Coyle K, Coyle D, Blouin J, Lee K, Jabr MF, Tran K, et al. Cost effectiveness of first-line oral therapies for pulmonary arterial hypertension: a modelling study. *Pharmacoeconomics.* 2016;34(5):509-520.

229. Gage GJ, Kipke DR, Shain W. Whole animal perfusion fixation for rodents. *J Vis Exp.* 2012(65).

230. Borner U, Szasz G, Bablok W, Busch EW. [A specific fully enzymatic method for creatinine: reference values in serum (author's transl)]. *J Clin Chem Clin Biochem.* 1979;17(11):679-682.

231. Al-Dujaili EA, Mullins LJ, Bailey MA, Kenyon CJ. Development of a highly sensitive ELISA for aldosterone in mouse urine: validation in physiological and pathophysiological states of aldosterone excess and depletion. *Steroids.* 2009;74(4-5):456-462.

232. Cabiati M, Raucci S, Caselli C, Guzzardi MA, D'Amico A, Prescimone T, et al. Tissue-specific selection of stable reference genes for real-time PCR normalization in an obese rat model. *J Mol Endocrinol.* 2012;48(3):251-260.

233. Schmittgen TD, Livak KJ. Analyzing real-time PCR data by the comparative C(T) method. *Nat Protoc.* 2008;3(6):1101-1108.

234. Rodriguez-Iturbe B, Quiroz Y, Shahkarami A, Li Z, Vaziri ND. Mycophenolate mofetil ameliorates nephropathy in the obese Zucker rat. *Kidney Int.* 2005;68(3):1041-1047.

235. Stern MD, Lappe DL, Bowen PD, Chimosky JE, Holloway GA, Jr., Keiser HR, et al. Continuous measurement of tissue blood flow by laser-Doppler spectroscopy. *Am J Physiol.* 1977;232(4):H441-448.

236. Stern MD, Bowen PD, Parma R, Osgood RW, Bowman RL, Stein JH. Measurement of renal cortical and medullary blood flow by laser-Doppler spectroscopy in the rat. *Am J Physiol.* 1979;236(1):F80-87.

237. Refinetti R, Lissen GC, Halberg F. Procedures for numerical analysis of circadian rhythms. *Biol Rhythm Res.* 2007;38(4):275-325.

238. Brands MW, Manhiani MM. Sodium-retaining effect of insulin in diabetes. *Am J Physiol Regul Integr Comp Physiol.* 2012;303(11):R1101-1109.

239. Roman RJ, Smits C. Laser-Doppler determination of papillary blood flow in young and adult rats. *Am J Physiol.* 1986;251(1 Pt 2):F115-124.

240. Roman RJ, Cowley AW, Jr. Abnormal pressure-diuresis-natriuresis response in spontaneously hypertensive rats. *Am J Physiol.* 1985;248(2 Pt 2):F199-205.

241. Liu KL, Lo M, Grouzmann E, Mutter M, Sassard J. The subtype 2 of angiotensin II receptors and pressure-natriuresis in adult rat kidneys. *Br J Pharmacol.* 1999;126(3):826-832.

242. Chamienia AL, Johns EJ. The cardiovascular and renal functional responses to the 5-HT1A receptor agonist flesinoxan in two rat models of hypertension. *Br J Pharmacol.* 1996;118(8):1891-1898.

243. Suzuki H, Ikenaga H, Hayashida T, Otsuka K, Kanno Y, Ohno Y, et al. Sodium balance and hypertension in obese and fatty rats. *Kidney Int Suppl.* 1996;55:S150-153.

244. Ikenaga H, Suzuki H, Ishii N, Itoh H, Saruta T. Role of NO on pressure-natriuresis in Wistar-Kyoto and spontaneously hypertensive rats. *Kidney Int.* 1993;43(1):205-211.

245. Fujiwara K, Hayashi K, Matsuda H, Kubota E, Honda M, Ozawa Y, et al. Altered pressure-natriuresis in obese Zucker rats. *Hypertension.* 1999;33(6):1470-1475.

246. Gross V, Lippoldt A, Schneider W, Luft FC. Effect of captopril and angiotensin II receptor blockade on pressure natriuresis in transgenic TGR(mRen-2)27 rats. *Hypertension.* 1995;26(3):471-479.

247. Jensen T, Borch-Johnsen K, Deckert T. Changes in blood pressure and renal function in patients with type I (insulin-dependent) diabetes mellitus prior to clinical diabetic nephropathy. *Diabetes Res.* 1987;4(4):159-162.

248. Jensen T, Borch-Johnsen K, Kofoed-Enevoldsen A, Deckert T. Coronary heart disease in young type 1 (insulin-dependent) diabetic patients with and

without diabetic nephropathy: incidence and risk factors. *Diabetologia.* 1987;30(3):144-148.

249. de Ferranti SD, de Boer IH, Fonseca V, Fox CS, Golden SH, Lavie CJ, et al. Type 1 diabetes mellitus and cardiovascular disease: a scientific statement from the American Heart Association and American Diabetes Association. *Circulation.* 2014;130(13):1110-1130.

250. Valdorf-Hansen F, Jensen T, Borch-Johnsen K, Deckert T. Cardiovascular risk factors in type I (insulin-dependent) diabetic patients with and without proteinuria. *Acta Med Scand.* 1987;222(5):439-434.

251. Shankar A, Klein R, Klein BE, Nieto FJ, Moss SE. Relationship between low-normal blood pressure and kidney disease in type 1 diabetes. *Hypertension.* 2007;49(1):48-54.

252. Feldt-Rasmussen B, Mathiesen ER, Deckert T, Giese J, Christensen NJ, Bent-Hansen L, et al. Central role for sodium in the pathogenesis of blood pressure changes independent of angiotensin, aldosterone and catecholamines in type 1 (insulin-dependent) diabetes mellitus. *Diabetologia.* 1987;30(8):610-617.

253. American Diabetes Association. Standards of medical care in diabetes-2015 abridged for primary care providers. *Clin Diabetes.* 2015;33(2):97-111.

254. Hargrove GM, Dufresne J, Whiteside C, Muruve DA, Wong NC. Diabetes mellitus increases endothelin-1 gene transcription in rat kidney. *Kidney Int.* 2000;58(4):1534-1545.

255. Makino A, Kamata K. Elevated plasma endothelin-1 level in streptozotocin-induced diabetic rats and responsiveness of the mesenteric arterial bed to endothelin-1. *Br J Pharmacol.* 1998;123(6):1065-1072.

256. Haak T, Jungmann E, Felber A, Hillmann U, Usadel KH. Increased plasma levels of endothelin in diabetic patients with hypertension. *Am J Hypertens.* 1992;5(3):161-166.

257. Wang Z, Yadav AS, Leskova W, Harris NR. Attenuation of streptozotocin-induced microvascular changes in the mouse retina with the endothelin receptor A antagonist atrasentan. *Exp Eye Res.* 2010;91(5):670-675.

258. Matsumoto T, Yoshiyama S, Kobayashi T, Kamata K. Mechanisms underlying enhanced contractile response to endothelin-1 in diabetic rat basilar artery. *Peptides.* 2004;25(11):1985-1994.

259. Leo CH, Hart JL, Woodman OL. Impairment of both nitric oxide-mediated and EDHF-type relaxation in small mesenteric arteries from rats with streptozotocin-induced diabetes. *Br J Pharmacol.* 2011;162(2):365-377.

260. Hyndman KA, Pollock JS. Nitric oxide and the A and B of endothelin of sodium homeostasis. *Curr Opin Nephrol Hypertens.* 2013;22(1):26-31.

261. Sasser JM, Sullivan JC, Hobbs JL, Yamamoto T, Pollock DM, Carmines PK, et al. Endothelin A receptor blockade reduces diabetic renal injury via an anti-inflammatory mechanism. *J Am Soc Nephrol.* 2007;18(1):143-154.

262. Wongmekiat O, Johns EJ. Endothelin as a causative factor of blunted volume reflex in diabetic rats. *Br J Pharmacol.* 2003;138(8):1403-1410.

263. Vallon V, Huang DY, Deng A, Richter K, Blantz RC, Thomson S. Salt-sensitivity of proximal reabsorption alters macula densa salt and explains the paradoxical effect of dietary salt on glomerular filtration rate in diabetes mellitus. *J Am Soc Nephrol.* 2002;13(7):1865-1871.

264. Slaughter TN, Paige A, Spires D, Kojima N, Kyle PB, Garrett MR, et al. Characterization of the development of renal injury in Type-1 diabetic Dahl salt-sensitive rats. *Am J Physiol Regul Integr Comp Physiol.* 2013;305(7):R727-734.

265. Oxlund CS, Buhl KB, Jacobsen IA, Hansen MR, Gram J, Henriksen JE, et al. Amiloride lowers blood pressure and attenuates urine plasminogen activation in patients with treatment-resistant hypertension. *J Am Soc Hypertens.* 2014;8(12):872-881.

266. Wongmekiat O, Johns E. Contribution of endothelial nitric oxide synthase in the blunted renal responses to volume expansion in diabetic rats. *Exp Physiol.* 2001;86(4):481-488.

267. Song J, Hu X, Riazi S, Tiwari S, Wade JB, Ecelbarger CA. Regulation of blood pressure, the epithelial sodium channel (ENaC), and other key renal sodium transporters by chronic insulin infusion in rats. *Am J Physiol Renal Physiol.* 2006;290(5):F1055-1064.

268. Liu XY, Zhang N, Chen R, Zhao JG, Yu P. Efficacy and safety of sodium-glucose cotransporter 2 inhibitors in type 2 diabetes: a meta-analysis of randomized controlled trials for 1 to 2years. *J Diabetes Complications.* 2015;29(8):1295-1303.

269. Pandey G, Makhija E, George N, Chakravarti B, Godbole MM, Ecelbarger CM, et al. Insulin regulates nitric oxide production in the kidney collecting duct cells. *J Biol Chem.* 2015;290(9):5582-5591.

270. Pandit MM, Strait KA, Matsuda T, Kohan DE. Na delivery and ENaC mediate flow regulation of collecting duct endothelin-1 production. *Am J Physiol Renal Physiol.* 2012;302(10):F1325-1330.

271. Lyon-Roberts B, Strait KA, van Peursem E, Kittikulsuth W, Pollock JS, Pollock DM, et al. Flow regulation of collecting duct endothelin-1 production. *Am J Physiol Renal Physiol.* 2011;300(3):F650-656.

272. Hyndman KA, Bugaj V, Mironova E, Stockand JD, Pollock JS. NOS1-dependent negative feedback regulation of the epithelial sodium channel in the collecting duct. *Am J Physiol Renal Physiol.* 2015;308(3):F244-251.

273. Wong NL, Tsui JK. Angiotensin regulates endothelin-B receptor in rat inner medullary collecting duct. *Metabolism.* 2001;50(6):661-666.

274. Wong NL, Wong BP, Tsui JK. Vasopressin regulates endothelin-B receptor in rat inner medullary collecting duct. *Am J Physiol Renal Physiol.* 2000;278(3):F369-374.

275. Edwards RM, Stack EJ, Pullen M, Nambi P. Endothelin inhibits vasopressin action in rat inner medullary collecting duct via the ETB receptor. *J Pharmacol Exp Ther.* 1993;267(3):1028-1033.

276. Hughes AK, Stricklett PK, Kishore BK, Kohan DE. Adenosine triphosphate inhibits endothelin-1 production by rat inner medullary collecting duct cells. *Exp Biol Med (Maywood).* 2006;231(6):1006-1009.

277. Gohar EY, Speed JS, Kasztan M, Jin C, Pollock DM. Activation of purinergic receptors (P2) in the renal medulla promotes endothelin-dependent natriuresis in male rats. *Am J Physiol Renal Physiol.* 2016;311(2):F260-267.

278. Pallone TL, Silldorff EP. Pericyte regulation of renal medullary blood flow. *Exp Nephrol.* 2001;9(3):165-170.

279. . *Nutrient Requirements of Laboratory Animals: Fourth Revised Edition, 1995*. Washington (DC)1995.

280. Anigbogu CN, Williams DT, Brown DR, Silcox DL, Speakman RO, Brown LC, et al. Circadian variations in blood pressure, heart rate, and HR-BP cross-correlation coefficient during progression of diabetes mellitus in rat. *Int J Hypertens.* 2011;2011:1-8.

281. Ghasemi A, Zahediasl S. Normality tests for statistical analysis: a guide for non-statisticians. *Int J Endocrinol Metab.* 2012;10(2):486-489.

282. Bidani AK, Griffin KA. Pathophysiology of hypertensive renal damage: implications for therapy. *Hypertension.* 2004;44(5):595-601.

283. Lau C, Sudbury I, Thomson M, Howard PL, Magil AB, Cupples WA. Salt-resistant blood pressure and salt-sensitive renal autoregulation in chronic streptozotocin diabetes. *Am J Physiol Regul Integr Comp Physiol.* 2009;296(6):R1761-1770.

284. Hicks KK, Seifen E, Stimers JR, Kennedy RH. Effects of streptozotocin-induced diabetes on heart rate, blood pressure and cardiac autonomic nervous control. *J Auton Nerv Syst.* 1998;69(1):21-30.

285. Centonza L, Castoldi G, Chianca R, Busca G, Golin R, Zanchetti A, et al. Short-term analysis of the relationship between blood pressure and urinary sodium excretion in normotensive subjects. *Clin Sci (Lond).* 2000;98(4):495-500.

286. Sufiun A, Rafiq K, Fujisawa Y, Rahman A, Mori H, Nakano D, et al. Effect of dipeptidyl peptidase-4 inhibition on circadian blood pressure during the development of salt-dependent hypertension in rats. *Hypertens Res.* 2015;38(4):237-243.

287. Fujii T, Uzu T, Nishimura M, Takeji M, Kuroda S, Nakamura S, et al. Circadian rhythm of natriuresis is disturbed in nondipper type of essential hypertension. *Am J Kidney Dis.* 1999;33(1):29-35.

288. Verdecchia P, Porcellati C, Schillaci G, Borgioni C, Ciucci A, Battistelli M, et al. Ambulatory blood pressure. An independent predictor of prognosis in essential hypertension. *Hypertension.* 1994;24(6):793-801.

289. Franklin SS, Gustin Wt, Wong ND, Larson MG, Weber MA, Kannel WB, et al. Hemodynamic patterns of age-related changes in blood pressure. The Framingham Heart Study. *Circulation.* 1997;96(1):308-315.

290. Drummond K, Mauer M, International Diabetic Nephropathy Study G. The early natural history of nephropathy in type 1 diabetes: II. Early renal structural changes in type 1 diabetes. *Diabetes.* 2002;51(5):1580-1587.

291. Kordonouri O, Danne T, Hopfenmuller W, Enders I, Hovener G, Weber B. Lipid profiles and blood pressure: are they risk factors for the development of early background retinopathy and incipient nephropathy in children with insulin-dependent diabetes mellitus? *Acta Paediatr.* 1996;85(1):43-48.

292. Nakamura K, Cowley AW, Jr. Sequential changes of cerebrospinal fluid sodium during the development of hypertension in Dahl rats. *Hypertension.* 1989;13(3):243-249.

293. Gu JW, Bailey AP, Tan W, Shparago M, Young E. Long-term High Salt Diet Causes Hypertension and Decreases Renal Expression of Vascular Endothelial Growth Factor in Sprague-Dawley Rats. *J Am Soc Hypertens.* 2008;2(4):275-285.

294. Majewski C, Bakris GL. Blood pressure reduction: an added benefit of sodium-glucose cotransporter 2 inhibitors in patients with type 2 diabetes. *Diabetes Care.* 2015;38(3):429-430.

295. Vaneckova I, Rezacova L, Kunes J, Zicha J. Moderate additive effects of endothelin receptor A blockade in Ren-2 transgenic rats subjected to various types of RAS blockade. *Life Sci.* 2016;159:127-134.

296. Roman RJ. Pressure-diuresis in volume-expanded rats. Tubular reabsorption in superficial and deep nephrons. *Hypertension.* 1988;12(2):177-183.

297. McDonough AA. Mechanisms of proximal tubule sodium transport regulation that link extracellular fluid volume and blood pressure. *Am J Physiol Regul Integr Comp Physiol.* 2010;298(4):R851-861.

298. Bailey MA. Inhibition of bicarbonate reabsorption in the rat proximal tubule by activation of luminal P2Y1 receptors. *Am J Physiol Renal Physiol.* 2004;287(4):F789-796.

299. Bailey MA, Shirley DG. Effects of extracellular nucleotides on renal tubular solute transport. *Purinergic Signal.* 2009;5(4):473-480.

300. Kelly-Cobbs AI, Harris AK, Elgebaly MM, Li W, Sachidanandam K, Portik-Dobos V, et al. Endothelial endothelin B receptor-mediated prevention of cerebrovascular remodeling is attenuated in diabetes because of up-regulation

of smooth muscle endothelin receptors. *J Pharmacol Exp Ther.* 2011;337(1):9-15.

301. Ikeda K, Wada Y, Sanematsu H, Foster HE, Jr., Shin D, Weiss RM, et al. Regulatory effect of experimental diabetes on the expression of endothelin receptor subtypes and their gene transcripts in the rat adrenal gland. *J Endocrinol.* 2001;168(1):163-175.

302. Boesen EI, Pollock DM. Cooperative role of ETA and ETB receptors in mediating the diuretic response to intramedullary hyperosmotic NaCl infusion. *Am J Physiol Renal Physiol.* 2010;299(6):F1424-1432.

303. Sarkis A, Liu KL, Lo M, Benzoni D. Angiotensin II and renal medullary blood flow in Lyon rats. *Am J Physiol Renal Physiol.* 2003;284(2):F365-372.

304. Sarkis A, Liu KL, Lo M, Benzoni D. Renal medullary blood flow and salt load in Lyon hypertensive rats. *Am J Hypertens.* 2002;15(3):212-216.

305. Mattson DL. Importance of the renal medullary circulation in the control of sodium excretion and blood pressure. *Am J Physiol Regul Integr Comp Physiol.* 2003;284(1):R13-27.

306. Mattson DL, Roman RJ, Cowley AW, Jr. Role of nitric oxide in renal papillary blood flow and sodium excretion. *Hypertension.* 1992;19(6 Pt 2):766-769.

307. Ahmeda AF, Rae MG, Al Otaibi MF, Anweigi LM, Johns EJ. Effect of tempol and tempol plus catalase on intra-renal haemodynamics in spontaneously hypertensive stroke-prone (SHSP) and Wistar rats. *J Physiol Biochem.* 2017;73(2):207-214.

308. Garcia-Estan J, Roman RJ. Role of renal interstitial hydrostatic pressure in the pressure diuresis response. *Am J Physiol.* 1989;256(1 Pt 2):F63-70.

309. Komolova M, Adams MA. Moment-to-moment characteristics of the relationship between arterial pressure and renal interstitial hydrostatic pressure. *Hypertension.* 2010;56(4):650-657.

310. Bell TD, DiBona GF, Biemiller R, Brands MW. Continuously measured renal blood flow does not increase in diabetes if nitric oxide synthesis is blocked. *Am J Physiol Renal Physiol.* 2008;295(5):F1449-1456.

311. Brands MW, Bell TD, Fleming C, Labazi H, Sturgis LC. Lack of blood pressure salt-sensitivity supports a preglomerular site of action of nitric oxide in Type I diabetic rats. *Clin Exp Pharmacol Physiol.* 2007;34(5-6):475-479.

312. Vallon V, Blantz RC, Thomson S. Homeostatic efficiency of tubuloglomerular feedback is reduced in established diabetes mellitus in rats. *Am J Physiol.* 1995;269(6 Pt 2):F876-883.

313. Harrison-Bernard LM, Carmines PK. Juxtamedullary microvascular responses to arginine vasopressin in rat kidney. *Am J Physiol.* 1994;267(2 Pt 2):F249-256.

314. Mattson DL, Lu S, Nakanishi K, Papanek PE, Cowley AW, Jr. Effect of chronic renal medullary nitric oxide inhibition on blood pressure. *Am J Physiol.* 1994;266(5 Pt 2):H1918-1926.

315. Menzies RI, Howarth AR, Unwin RJ, Tam FW, Mullins JJ, Bailey MA. Inhibition of the purinergic P2X7 receptor improves renal perfusion in angiotensin-II-infused rats. *Kidney Int.* 2015;88(5):1079-1087.

316. Gross V, Lippoldt A, Bohlender J, Bader M, Hansson A, Luft FC. Cortical and medullary hemodynamics in deoxycorticosterone acetate-salt hypertensive mice. *J Am Soc Nephrol.* 1998;9(3):346-354.

317. Gross V, Schunck WH, Honeck H, Milia AF, Kargel E, Walther T, et al. Inhibition of pressure natriuresis in mice lacking the AT2 receptor. *Kidney Int.* 2000;57(1):191-202.

318. Vallon V, Blantz R, Thomson S. The salt paradox and its possible implications in managing hypertensive diabetic patients. *Curr Hypertens Rep.* 2005;7(2):141-147.

319. Butler J, Hamo CE, Filippatos G, Pocock SJ, Bernstein RA, Brueckmann M, et al. The potential role and rationale for treatment of heart failure with sodium-glucose co-transporter 2 inhibitors. *Eur J Heart Fail.* 2017;19(11):1390-1400.

320. Choi KC, Kim NH, An MR, Kang DG, Kim SW, Lee J. Alterations of intrarenal renin-angiotensin and nitric oxide systems in streptozotocin-induced diabetic rats. *Kidney Int Suppl.* 1997;60:S23-27.

321. Shin SJ, Lai FJ, Wen JD, Hsiao PJ, Hsieh MC, Tzeng TF, et al. Neuronal and endothelial nitric oxide synthase expression in outer medulla of streptozotocin-induced diabetic rat kidney. *Diabetologia.* 2000;43(5):649-659.

322. Lee DL, Sasser JM, Hobbs JL, Boriskie A, Pollock DM, Carmines PK, et al. Posttranslational regulation of NO synthase activity in the renal medulla of diabetic rats. *Am J Physiol Renal Physiol.* 2005;288(1):F82-90.

323. Fenoy FJ, Ferrer P, Carbonell L, Garcia-Salom M. Role of nitric oxide on papillary blood flow and pressure natriuresis. *Hypertension.* 1995;25(3):408-414.

324. Kopp UC, Cicha MZ, Smith LA. Differential effects of endothelin on activation of renal mechanosensory nerves: stimulatory in high-sodium diet and inhibitory in low-sodium diet. *Am J Physiol Regul Integr Comp Physiol.* 2006;291(5):R1545-1556.

325. Ge Y, Stricklett PK, Hughes AK, Yanagisawa M, Kohan DE. Collecting duct-specific knockout of the endothelin A receptor alters renal vasopressin responsiveness, but not sodium excretion or blood pressure. *Am J Physiol Renal Physiol.* 2005;289(4):F692-698.

326. Jin C, Speed JS, Pollock DM. High salt intake increases endothelin B receptor function in the renal medulla of rats. *Life Sci.* 2016;159:144-147.

327. Stuart D, Chapman M, Rees S, Woodward S, Kohan DE. Myocardial, smooth muscle, nephron, and collecting duct gene targeting reveals the organ sites of endothelin A receptor antagonist fluid retention. *J Pharmacol Exp Ther.* 2013;346(2):182-189.

328. Fellner RC, Guan Z, Cook AK, Pollock DM, Inscho EW. Endothelin contributes to blunted renal autoregulation observed with a high-salt diet. *Am J Physiol Renal Physiol.* 2015;309(8):F687-696.

329. de Zeeuw D, Coll B, Andress D, Brennan JJ, Tang H, Houser M, et al. The endothelin antagonist atrasentan lowers residual albuminuria in patients with type 2 diabetic nephropathy. *J Am Soc Nephrol.* 2014;25(5):1083-1093.

330. Dhaun N, Macintyre IM, Melville V, Lilitkarntakul P, Johnston NR, Goddard J, et al. Blood pressure-independent reduction in proteinuria and arterial stiffness after acute endothelin-a receptor antagonism in chronic kidney disease. *Hypertension.* 2009;54(1):113-119.

331. Gomez-Garre D, Ruiz-Ortega M, Ortego M, Largo R, Lopez-Armada MJ, Plaza JJ, et al. Effects and interactions of endothelin-1 and angiotensin II on matrix protein expression and synthesis and mesangial cell growth. *Hypertension.* 1996;27(4):885-892.

332. Ge Y, Bagnall A, Stricklett PK, Webb D, Kotelevtsev Y, Kohan DE. Combined knockout of collecting duct endothelin A and B receptors causes hypertension and sodium retention. *Am J Physiol Renal Physiol.* 2008;295(6):F1635-1640.

333. Wendel M, Knels L, Kummer W, Koch T. Distribution of endothelin receptor subtypes ETA and ETB in the rat kidney. *J Histochem Cytochem.* 2006;54(11):1193-1203.

334. Majowicz MP, Gonzalez Bosc LV, Albertoni Borghese MF, Delgado MF, Ortiz MC, Sterin Speziale N, et al. Atrial natriuretic peptide and endothelin-3 target renal sodium-glucose cotransporter. *Peptides.* 2003;24(12):1971-1976.

335. Laghmani K, Sakamoto A, Yanagisawa M, Preisig PA, Alpern RJ. A consensus sequence in the endothelin-B receptor second intracellular loop is required for NHE3 activation by endothelin-1. *Am J Physiol Renal Physiol.* 2005;288(4):F732-739.

336. Yu C, Yang Z, Ren H, Zhang Y, Han Y, He D, et al. D3 dopamine receptor regulation of ETB receptors in renal proximal tubule cells from WKY and SHRs. *Am J Hypertens.* 2009;22(8):877-883.

337. Khraibi AA, Haas JA, Knox FG. Effect of renal perfusion pressure on renal interstitial hydrostatic pressure in rats. *Am J Physiol.* 1989;256(1 Pt 2):F165-170.

338. Khavandi K, Greenstein AS, Sonoyama K, Withers S, Price A, Malik RA, et al. Myogenic tone and small artery remodelling: insight into diabetic nephropathy. *Nephrol Dial Transplant.* 2009;24(2):361-369.

339. Ochodnicky P, Henning RH, Buikema HJ, de Zeeuw D, Provoost AP, van Dokkum RP. Renal vascular dysfunction precedes the development of renal damage in the hypertensive Fawn-Hooded rat. *Am J Physiol Renal Physiol.* 2010;298(3):F625-633.

340. Vallon V. Micropuncturing the nephron. *Pflugers Arch.* 2009;458(1):189-201.

341. Crawford C, Kennedy-Lydon TM, Callaghan H, Sprott C, Simmons RL, Sawbridge L, et al. Extracellular nucleotides affect pericyte-mediated regulation of rat in situ vasa recta diameter. *Acta Physiol (Oxf).* 2011;202(3):241-251.

342. Li LP, Tan H, Thacker JM, Li W, Zhou Y, Kohn O, et al. Evaluation of Renal Blood Flow in Chronic Kidney Disease Using Arterial Spin Labeling Perfusion Magnetic Resonance Imaging. *Kidney Int Rep.* 2017;2(1):36-43.

343. Alpert NM, Rabito CA, Correia DJ, Babich JW, Littman BH, Tompkins RG, et al. Mapping of local renal blood flow with PET and H(2)(15)O. *J Nucl Med.* 2002;43(4):470-475.

344. Menzies RI, Zammit-Mangion A, Hollis LM, Lennen RJ, Jansen MA, Webb DJ, et al. An anatomically unbiased approach for analysis of renal BOLD magnetic resonance images. *Am J Physiol Renal Physiol.* 2013;305(6):F845-852.

345. Mansley MK, Neuhuber W, Korbmacher C, Bertog M. Norepinephrine stimulates the epithelial Na+ channel in cortical collecting duct cells via alpha2-adrenoceptors. *Am J Physiol Renal Physiol.* 2015;308(5):F450-458.

346. Shyangdan DS, Uthman OA, Waugh N. SGLT-2 receptor inhibitors for treating patients with type 2 diabetes mellitus: a systematic review and network meta-analysis. *BMJ Open.* 2016;6(2):e009417.

Appendices

Appendix 1: Presentations

Oral abstracts

Changes in urinary endothelin-1 excretion in response to changes in renal perfusion pressure

Culshaw GJ, Bailey MA, Binnie D, Hadoke PWF, Webb DJ.

University of Edinburgh/British Heart Foundation Symposium Day

Edinburgh, United Kingdom, June 2013

Changes in urinary endothelin-1 excretion in response to changes in renal perfusion pressure

Culshaw GJ, Bailey MA, Hadoke PWF, Webb DJ.

The Thirteenth International Conference on Endothelin

Tokyo, Japan, September 2013

Impaired pressure natriuresis and urinary ET-1 excretion in a rat model of Type I diabetes mellitus

Culshaw GJ, Bailey MA, Hadoke PWF, Webb DJ.

International Society of Nephrology Forefronts Symposium: Intrinsic Regulation of Renal Function

Charleston, United States of America, March, 2014

The role of endothelin-1 in the regulation of blood pressure in early diabetes mellitus

Culshaw GJ, Bailey MA, Hadoke PWF, Webb DJ.

The Fourteenth International Conference on Endothelin

Savannah, United States of America, September 2015

Endothelin receptor antagonism during pressure natriuresis in a rat model of Type 1 diabetes mellitus

Culshaw GJ, Bailey MA, Binnie D, Dhaun N, Hadoke PWF, Webb DJ.

Scottish Cardiovascular Forum

Glasgow, United Kingdom, January 2017

The roles of endothelin receptors in pressure natriuresis in early experimental Type 1 diabetes mellitus

Culshaw GJ, Bailey MA, Binnie D, Dhaun N, Hadoke PWF, Webb DJ.

The Fifteenth International Conference on Endothelin

Prague, Czech Republic, October 2017

Poster presentations

Impaired pressure natriuresis and urinary ET-1 excretion in a rat model of Type I diabetes mellitus

Culshaw GJ, Bailey MA, Hadoke PWF, Webb DJ.

International Society of Nephrology Forefronts Symposium: Intrinsic Regulation of Renal Function

Charleston, United States of America, March, 2014

The role of endothelin-1 in the regulation of blood pressure in early diabetes

Culshaw GJ, Bailey MA, Hadoke PWF, Webb DJ.

Scottish Cardiovascular Forum

Edinburgh, United Kingdom, February, 2015

The role of endothelin-1 in the regulation of blood pressure in early diabetes mellitus

Culshaw GJ, Bailey MA, Hadoke PWF, Webb DJ.

The Fourteenth International Conference on Endothelin

Savannah, United States of America, September 2015

Type 1 diabetes mellitus impairs pressure natriuresis and medullary flux but only pressure natriuresis recovers with insulin

Culshaw GJ, Bailey MA, Binnie D, Hadoke PWF, Webb DJ.

University of Edinburgh/British Heart Foundation Symposium Day

Edinburgh, United Kingdom, June 2016

Appendix 2: Training record

The University of Edinburgh
Personal Licence Holder Training Record

Name of PIL holder: George Cushnan

Procedure No	Technique	Anaesthesia	Competent to perform supervised				Competent to perform unsupervised				Competent to supervise			
			Supervisor to initial and date											
			Mouse	Rat	Other		Mouse	Rat	Other		Mouse	Rat	Other	
Standard, basic procedures														
1.	Induction and maintenance of local or general anaesthesia using													
	Injectable agents	AB AC		GB 13/12				GB				GB		
	Inhalational agents	AB AC		GB 29/11/12				GB				GB		
	Topical agents	AA		GB 29/11/12				GB				GB		
2.	Administration of substances													
	Orally by gavage	AA												
	Subcutaneously	AA AB AC		GB 13/12				GB				GB		
	Intraperitoneally	AA AB AC		GB 13/12				GB				GB		
	Intradermally	AA AB AC												
	Intravenously	AA AB AC		GB 13/12				GB				GB		
	By topical application	AA AB AC												
3.	Withdrawal of blood by:													
	Venepuncture	AA AB AC												
	Venesection	AA AB AC												
	Arterial puncture	AA AB AC		GB 13/12				GB				GB		
	Cardiac puncture	AC only												

The University of Edinburgh
Personal Licence Holder Training Record

Name of PIL holder: GEOFF CUSHAN

Procedure No	Technique	Competent to perform supervised			Competent to perform unsupervised			Competent to supervise		
		Supervisor to initial and date								
		Mouse	Rat	Other	Mouse	Rat	Other	Mouse	Rat	Other
Schedule 1 Methods (foetal, larval and embryonic forms)										
12.	Overdose of an anaesthetic using a route and an anaesthetic agent appropriate for the size and species of animal [all animals]									
13.	Exposure to carbon dioxide gas in a rising concentration (a)		GB 12/3/12			GB			GB	
14.	Dislocation of the neck (b)		GB 12/3/12			GB			GB	
15.	Concussion of the brain by striking the cranium (c)									

(a) Suitable for rodents, rabbits and birds up to 1.5 kg
(b) Suitable for rodents up to 500 g; rabbits up to 1kg;and birds up to 3kg
(c) Suitable for rodents and rabbits up to 1kg; birds up to 250g; amphibians and reptiles (with destruction of the brain before the return of consciousness) up to 1kg; fishes (with destruction of the brain before the return of consciousness)

The University of Edinburgh
Personal Licence Holder Training Record

Name of PIL holder: GEOFF CUSHAN

Procedure No	Technique	Anaesthesia	Competent to perform supervised			Competent to perform unsupervised			Competent to supervise		
			Supervisor to initial and date								
			Mouse	Rat	Other	Mouse	Rat	Other	Mouse	Rat	Other
22.	IMPLANT TELEMETRY DEVICE	AB		✓ GB 29/7/14			✓ GB 29/7/14			✓ GB 29/7/14	
23.	PRESSURE NATRIURESIS	AC		13/3/12 MAB			13/3/12 MHB			13/3/12. MHB	
24.											
25.											
26.											
27.											
28.											
29.											
30.											
31.											
32.											